ASSESSING THE EFFECTS OF PERFLUOROALKYL SUBSTANCE EXPOSURE USING TRANSDISCIPLINARY SCIENCE

Bevin Ellen Blake

A dissertation submitted to the faculty at the University of North Carolina at Chapel Hill in partial fulfillment of the requirements for the degree of Doctor of Philosophy in Toxicology and Environmental Medicine in the Curriculum in Toxicology.

Chapel Hill
2020

Approved by:

Suzanne Fenton

Rebecca Fry

Bernard Weissman

Beverly Koller

Kelly Ferguson

William Coleman

ABSTRACT

Bevin Ellen Blake: Assessing the Effects of Perfluoroalkyl Substance Exposure Using Transdisciplinary Science
(Under the direction of Suzanne Fenton & Rebecca Fry)

Per- and polyfluoroalkyl substances (PFAS) are ubiquitous drinking water contaminants of concern due to mounting evidence implicating adverse health outcomes associated with exposure, including reduced kidney function, metabolic syndrome, thyroid disruption, and adverse pregnancy outcomes. In an 18-year longitudinal repeated measures study of adult humans (N = 210), an interquartile (IQR) increase in serum perfluorononanoate (PFNA), perfluorohexane sulfonate (PFHxS), and perfluorodecanoate (PFDeA) was associated with a -1.62% (95% CI= -3.02, -0.23), -1.95% (95% CI= -3.41, -0.49), and -2.47% (95% CI= -4.48, -0.45) decrease in estimated glomerular filtration rate, respectively, and an IQR increase in serum perfluorooctanesulfonate (PFOS) was associated with a 10.21% increase in serum TSH (95% CI: 2.29, 18.74). Adverse pregnancy outcomes were studied in pregnant CD-1 mice exposed to perfluorooctanoic acid (PFOA: 0, 1, or 5 mg/kg/day) or a PFOA replacement (GenX: 0, 2, or 10 mg/kg/day) from embryonic day (E) 0.5 to E11.5 or E17.5. Generally, effects induced by GenX occurred with shorter latency or at lower internal concentrations than PFOA. Exposure to GenX or PFOA resulted in increased gestational weight gain. Embryo weight was 9.4% lower relative to controls after exposure to 5 mg/kg/day PFOA. Effect sizes for several outcomes were similar for higher doses (5 mg/kg/day PFOA and 10 mg/kg/day GenX) and lower doses (1 mg/kg/day PFOA and 2 mg/kg/day GenX), including higher maternal liver weights, abnormal liver

histopathology, higher placental weights and embryo-placental weight ratios, and greater incidence of placental abnormalities relative to controls. Transcriptome-wide gene expression analysis of placentas revealed significant enrichment of pathways involved in cholesterol and lipid transport (e.g. liver X receptor activation), innate immune response/inflammation (e.g. acute phase response signaling), and hemostasis (e.g. atherosclerosis signaling). Human-derived placental trophoblasts were utilized in an *in vitro* high-throughput toxicity (HTTS) screen to evaluate the effect of 42 unique PFAS on trophoblast viability and function, and dose-response models were applied to determine EC50 values for viability (27/42, 66%), proliferation (28/42, 68%), and mitochondrial membrane potential (19/42, 45%). Collectively, these data highlight adverse health outcomes associated with PFAS exposure, demonstrate the placenta is a susceptible target tissue, and propose potential molecular mechanisms of placental toxicity.

To all whose lives, health, and well-being have been impacted by PFAS.

ACKNOWLEDGEMENTS

It is difficult to convey the amount of support I have been so fortunate to receive throughout this journey. I deeply thank my mentors, Suzanne Fenton and Rebecca Fry, for providing extensive scientific guidance, challenging me to reach my full potential, and inspiring me through being amazing role models as powerful and successful women in science. Thank you to my doctoral committee for challenging me and guiding me over the past four years.

Thank you to the incredible support staff at NIEHS, especially Louise Harris and Gordon Caviness, whose "behind the scenes" work makes research possible. Thank you to the scientists of the NTP and for the core facility personnel at NIEHS for your enthusiastic support.

I am grateful to my labmates, who have selflessly donated time and energy to my projects to help make the work successful. Thank you for going above and beyond the expectations of coworkers. You have been indispensable as teammates and have helped make the lab feel like an extended family. I especially thank Harlie Cope for spending countless hours in necropsy with me, through both tears and dark humor, Vesna Chappell for being both a scientific and emotional sounding board throughout the day but especially during lunch, Deirdre Tucker for sharing timely advice and encouragement, Sagi Gillera for making my first rotation experience endlessly entertaining, Adam Filgo for reminding me to not take things so seriously, Charlotte Love and Trina Phan for re-energizing my excitement for lab work when I needed it most, and Veronica Godfrey for keeping the lab running like a well-oiled machine.

I am thankful for the friends who have supported me throughout this work, especially Leland Black, Kelsey Noll, and Sloane Tilley, whose friendship is more like a sisterhood. Thank

you for being there for me when things were good but especially when things were bad. Thank you to Coach Dave, who helped inspire me to push not only my academic limits, but also my athletic limits. Thank you for teaching me so many important life lessons through the sport of triathlon. Thank you for helping me learn to believe in myself and for teaching me to always be happy, but never satisfied. To my therapist, who provided the necessary care to help me overcome personal struggles that would have certainly prevented me from completing my work.

Thank you to my family, who has been unwaveringly supportive of me throughout graduate school. I would not have had the strength to get through this without your encouragement and love. Just hearing your voices on the phone, getting a card in the mail, or simply texting back and forth helped to keep me moving forward more than you probably realized at the time. A very special thanks to my loyal canine companion, Finn, who accompanied me on countless walks and jogs while I brainstormed experiments and ideas and kept me company on the couch while writing my dissertation.

Last but far from least, I would like to thank my husband, Jonathan Burg, who should probably receive an honorary degree for everything he has done to support me. Honestly, give this man a medal. Jon, I love you so much. Thank you for being there for me virtually every step of the way. Thank you for encouraging me, consoling me, supporting me, celebrating with me, and believing in me. Thank you for selflessly shouldering a greater burden at home to give me more time and energy to do my research. Thank you for your genuine interest in my work and for providing scientific feedback on my ideas, presentations, posters, and writing. Finding true

love is quite rare but finding it in someone who you consider a deeply respected and highly valued scientific colleague is statistically improbable. I could not have done this without you. Thank you for being my rock and my best friend.

PREFACE

Two published manuscripts comprise Chapter 2 (Blake et al. 2018) and Chapter 3 (Blake et. al 2020) and would not have been possible without the contributions of co-authors. For Chapter 2, Suzanne Fenton stewarded this project; recruited collaborators, identified and supported access to the datasets used for the study, and helped develop the study aims. Kelly Ferguson provided training on appropriate epidemiologic statistical analyses and provided epidemiology expertise, which led to completion of a Translational Medicine training certification through UNC Chapel Hill. Susan Pinney provided access to the dataset and explanation of how data were collected, including repeated measures of serum chemical exposure and clinical measures of chronic health conditions. Erin Hines provided expertise and assisted with interpretation of the kidney function data. Bevin Blake wrote code for and performed the statistical analyses, generated figures and tables, and wrote the manuscript.

For Chapter 3, Heather Stapleton and Samantha Hall conducted analyses of mouse placental thyroid hormones. Robert Keys provided expertise with evaluating microscopic alterations to mouse liver samples using transmission electron microscopy (TEM). Harlie Cope assisted with routine data collection (e.g. gestational weights) and general mouse husbandry. Harlie Cope, Beth Mahler, and Brittany Scott assisted with mouse necropsy procedures and sample preparation for histopathology. Beth Mahler created labeled histopathology and TEM figures for the manuscript. Susan Elmore provided expert pathology diagnoses and led multiple pathology working groups to evaluate histopathological changes to maternal liver, maternal kidney, and placentas. Mark Strynar and James McCord provided expertise in sample

preparation for internal dosimetry analyses on mouse samples and shared instruments and resources required for these measurements. Bevin Blake and Suzanne Fenton designed and developed proposals for Animal Care and Use Committee approval of these experiments, and Bevin Blake coordinated all animal housing, dosing, and data collection procedures. Bevin Blake collected all animal data and samples (with the assistance of H. Cope, B. Mahler, and B. Scott), and collaborated with National Toxicology Program contractors (with the help of Georgia Roberts) for a full data audit of the study. Bevin Blake wrote code for and performed all statistical analyses, generated tables and figures, and wrote the manuscript.

TABLE OF CONTENTS

LIST OF TABLES

LIST OF FIGURES

LIST OF ABBREVIATIONS

17β-HSD1	17β-Hydroxysteroid dehydrogenase 1
ABC	ATP-binding cassette
AFFF	Aqueous film-forming foam
ALB	Albumin
ALP	Alkaline phosphatase
ALT	Alanine aminotransferase
AOX1	Aldehyde oxidase 1
AST	Aspartate aminotransferase
BMI	Body mass index
BUN	Blood urea nitrogen
C8	Perfluorooctanoic acid
CDK-EPI	Chronic kidney disease epidemiology collaboration
Chol	Cholesterol
CI	Confidence interval
CKD	Chronic kidney disease
Cre	Serum creatinine

CVD	Cardiovascular disease
E	Embryonic day
EC50	Half maximal effective concentration
eGFR	Estimated glomerular filtration rate
FXR	Farnesoid X receptor
GD	Gestational diabetes
GenX	Hexafluoropropylene oxide dimer acid
GFR	Glomerular filtration rate
Glu	Glucose
GM	Geometric mean
GPER1	G protein-coupled estrogen receptor 1
GPX1	Glutathione peroxidase 1
GWG	Gestational weight gain
H&E	Hemolysin and eosin
HAL	Health advisory level
HDL	High density lipoprotein
HDP	Hypertensive disorders of pregnancy

HELLP syndrome	Hemolysis, elevated liver enzymes, and low platelets
HFPO-DA	Hexafluoropropylene oxide dimer acid (GenX)
ICC	Intraclass correlation coefficient
IQR	Interquartile range
LDL	Low density lipoprotein
LME	Linear mixed effects
LOAEL	Lowest observed adverse effect level
LOD	Limit of detection
LXR	Liver X receptor
MCL	Maximum contaminant limit
MDL	Method detection limit
MMP	Mitochondrial membrane potential
NHANES	National Health and Nutrition Examination Survey
NOAEL	No observed adverse effect level
OAT	Organic anion transporter
OR	Odds ratio
PE	Preeclampsia

PFAS	Per- and polyfluoroalkyl substances
PFC	Perfluorinated chemical
PFDA, PFDeA	Perfluorodecanoic acid
PFHxS	Perfluorohexane sulfonic acid
PFNA	Perfluorononanoic acid
PFOA	Perfluorooctanoic acid
PFOS	Perfluorooctane sulfonic acid
PI	Placental insufficiency
PIH	Pregnancy induced hypertension
PPAR	Peroxisome proliferator-activated receptor
PTFE	Polytetrafluoroethylene
QC	Quality control
RER	Rough endoplasmic reticulum
RfD	Reference dose
rT3	Reverse triiodothyronine
RXR	Retinoid X receptor
SDH	Sorbitol dehydrogenase

SOD1	Superoxide dismutase 1
SST-RMA	Signal space transformation robust multi-array average
T3	Triiodothyronine
T4	Thyroxine
TBA	Total bile acid
TEM	Transmission electron microscopy
TH	Thyroid hormone
TP	Total protein
Trig	Triglyceride
TSH	Thyroid stimulating hormone
Ucrea	Urinary creatinine
US EPA	United States Environmental Protection Agency
VC	Vehicle control
WNL	Within normal limits

CHAPTER 1: ADVERSE HEALTH OUTCOMES ASSOCIATED WITH EXPOSURE TO PERFLUOROALKYL SUBSTANCES

1.1 Introduction

Per- and polyfluoroalkyl substances (PFAS) comprise a diverse universe of compounds used in a wide variety of industrial processes and the production of consumer goods (ITRC 2017). Since their genesis in the 1940s, PFAS have been detected in the ambient environment, wildlife, and human serum around the globe (Calafat et al. 2007; Domingo and Nadal 2019; Hanssen et al. 2013; Olsen et al. 2017). The environmentally and biologically persistent qualities of PFAS have raised concerns, further heightened by mounting scientific and medical evidence associating PFAS exposure to multiple adverse health outcomes across all life stages.

1.1.1 Physicochemical Properties and Characterization of PFAS

Naming conventions for PFAS have evolved over time due in part to the increasing complexity and number of unique congeners, leading to inconsistencies and confusion across the scientific literature. For example, the term perfluorinated chemical (PFC) has been widely used in the scientific literature, but it is inaccurate as it does not describe polyfluorinated substances, which are an important component of the PFAS family (ITRC 2017). Additionally, many PFAS exist in multiple ionic states (e.g. acids, cations, anions), with different names (e.g. perfluorooctane sulfonic acid and perfluorooctane sulfonate) and different physicochemical properties. Consistent and unified naming conventions for PFAS are necessary to provide clarity, consistency, and improved scientific communication.

PFAS contain 1 or more carbon atoms with fluorine atoms in place of hydrogen atoms, such that the compound contains the moiety C_nF_{2n+1}-R, where R represents additional functional groups (e.g. sulfonate, carboxylic acid; Figure 1-1) (ITRC 2017). The perfluoroalkyl moiety is highly chemically and thermally stable with extremely strong carbon-fluorine bonds, and it exhibits both lipophilic and hydrophilic properties (ITRC 2017). Together, these physical and chemical properties make PFAS ideal as surfactants and surface protection products.

PFAS can be broadly divided into polymers and non-polymers. PFAS polymers are thought to pose less of a risk to human health and the environment and include fluoropolymers, polymeric perfluoropolyethers, and side-chain fluorinated polymers (ITRC 2017). However, the production of PFAS polymers contributes to the release of non-polymers into the environment, and polymers break down into non-polymers in the environment (e.g. PTFE forms PFOA and *N*-methyl perfluorooctane sulfonamide and *N*-ethyl perfluorooctane form PFOS; ITRC 2017). Non-polymer PFAS can be further separated into perfluorinated (fully fluorinated) and polyfluorinated (partially fluorinated) chemicals.

PFAS can be characterized by carbon chain length and side group structure as well as their history of use. PFAS with a longstanding history of use are referred to as "legacy" PFAS whereas replacement and alternative chemistry PFAS are generally referred to as "alternative PFAS" or "replacement PFAS". However, certain legacy PFAS are now substituted for longer chain compounds to comply with regulatory standards, hence such PFAS could be considered both a legacy and a replacement compound (e.g. PFBS; Table 1-1 & Figure 1-2).

1.1.2 History of PFAS Usage in the US

The earliest PFAS compound in the U.S. was first synthesized in the 1930s as a fluoropolymer, called polytetrafluoroethylene (PTFE). Roy J. Plunkett is credited with the discovery of PTFE, although it was an accidental byproduct of Plunkett's attempt to synthesize a

novel chlorofluorocarbon refrigerant in 1938 while employed by DuPont de Nemours Inc (Plunkett 1986). DuPont patented the discovery under the company Kinetic Chemicals in 1941 (Plunkett 1941) and registered the trademarked name, Teflon, in 1945 (Plunkett 1986). By 1948, DuPont was producing over 900 tons of PTFE per year at their facility in Parkersburg, West Virginia and another company, 3M, had begun producing PFAS in production at their plant in Minnesota (Funderburg 2010). Between the 1940s and 1950s, perfluorooctane sulfonic acid (PFOS) and perfluorooctanoic acid (PFOA) started to be used in the manufacturing of PTFE-based non-stick coatings. From the 1950s to the 1960s, PFOS and PFOA were also used to manufacture stain- and water-resistant products as well as protective coatings. By 1961, PTFE was applied to commercial cookware. From the 1960s to the 1970s, PFOS-based fire-fighting foam was manufactured, although it was later voluntarily phased out of Class A fire-fighting foams beginning in 2000 (US DOD 2000; 3M 2000). PFAS have since been utilized in numerous industrial and consumer product manufacturing applications, including: grease-resistant papers (e.g. fast food containers/wrappers, microwave popcorn bags, pizza boxes, candy wrappers); stain resistant coatings applied to carpets, upholstery, and other fabrics; water-resistant clothing and footwear, cleaning products, personal care products (e.g. shampoo, dental floss, cosmetics such as nail polish and eye makeup); paints, varnishes, ski wax and sealants; and Class B aqueous film forming foams (AFFF), which are implemented at airports and military bases for firefighting and training; and many others (ATSDR 2019).

1.1.3 PFAS Usage in North Carolina

In 1968, DuPont began construction of a plant near Fayetteville, NC which was completed by 1971. The facility began producing fluoropolymers and plastics, and byproducts such as hexafluoropropylene oxide dimer acid (HFPO-DA, commonly referred to as GenX) were discharged into the Cape Fear River beginning in 1980. By 2002, the plant began producing

PFOA but began replacing it with GenX between 2008-2009. In 2017, North Carolina Governor Roy Cooper and the North Carolina Department of Environmental Quality (NC DEQ) revoked the permit previously allowing Chemours (formerly DuPont) plant to discharge waste into the Cape Fear River (NC DEQ 2017). Later that year, NC DEQ confirmed that the Chemours plant was no longer discharging GenX into the Cape Fear River.

1.1.4 Sources of PFAS Exposure

Humans are exposed to PFAS through a variety of pathways, including through drinking water, air (both indoor and outdoor), diet, dust, through maternal to fetal transfer *in utero*, and through breastfeeding as neonates (Figure 1-3) (Sunderland et al. 2019). For adults, diet and drinking water are the main sources of exposure, however this likely varies greatly by lifestyle, dietary behaviors, proximity to contamination point sources such as manufacturing facilities or their waste dumping sites, and local drinking water contamination levels. Formula-fed infants are thought to be the most highly exposed members of the human population due to the high water to body weight ratio. Drinking water may be the largest sources of PFAS exposure for communities impacted by high levels of PFAS contamination. Public and private drinking water contamination by PFAS was first reported in the US in 1998 in Washington, West Virginia, a small town located downstream of a manufacturing facility operated by DuPont.

1.2 Adverse Health Effects Associated with PFAS

The desirable chemical properties of PFAS paradoxically impart environmentally and biologically undesirable properties, including indefinite environmental persistence and long half lives in many living organisms, especially humans. Unlike other common environmental pollutants, such as organochlorine pesticides, PFAS do not bioaccumulate in adipose tissue (Pérez et al. 2013). PFAS primarily accumulate in the serum, lungs, kidneys, liver, and brain (Pérez et al. 2013). Human exposure to PFAS has been associated with adverse effects on the

immune (NTP 2016), endocrine, metabolic, and reproductive systems (including fertility and pregnancy outcomes), and increased risk for cancer. However, the weight of evidence supporting these associations varies by both outcome and specific PFAS.

1.2.1 History of PFAS-related Human Health Concerns

Concerns regarding the toxicity of PFAS were first communicated in 1961 in an internal memo at DuPont by Chief Toxicologist Dorothy Hood (EWG 2019). By 1980, PFAS were measured in the serum of occupationally exposed workers and in 1981 concerns were raised internally at DuPont regarding birth defects in children born from occupationally exposed women (EWG 2019). Industrial and occupational exposure studies have since shown increased incidence of cancer including bladder (Alexander et al. 2003), kidney (Consonni et al. 2013), prostate (Gilliland and Mandel 1993; Lundin et al. 2009), and liver (Consonni et al. 2013), leukemia (Consonni et al. 2013), kidney disease (Steenland and Woskie 2012), and elevated cholesterol (Costa et al. 2009; Sakr et al. 2007).

Community-based exposure concerns in the US were first raised in 1998 by Wilbur Tennant, a cattle farmer whose land was downstream from and bordered a landfill used by the DuPont Washington Works plant near Parkersburg, WV (Rich 2016). Tennant enlisted legal counsel from Rob Bilott after documenting unusual phenomenon, such as foamy, discolored water in the creek from which Tennant's cattle drank, atypical behavior of the cattle, and a wide array of physical abnormalities in the cattle including black teeth, skin lesions and tumors, discolored organs, malformed hooves, and calves born with profound birth defects (Rich 2016). One hundred and fifty-three of Tennant's original herd of two hundred cattle died, and Tennant believed the pollution dumped by DuPont into the landfill upstream of his cattle farm was the cause (Rich 2016). What began as a legal case on behalf of private citizen ultimately led to a larger class-action lawsuit filed by Bilott on behalf of over 70,000 citizens in the Mid-Ohio

Valley whose drinking water sources were affected by the contamination stemming from DuPont's plant (Rich 2016).

The class-action lawsuit resulted in a settlement that funded a biomonitoring effort of unprecedented size and scale, called the C8 Health Study (Frisbee et al. 2009). The results of the C8 Health Study identified a probable link between exposure to PFOA and increased cholesterol, kidney cancer, testicular cancer, ulcerative colitis, thyroid disease, and pregnancy-induced hypertension (C8 Science Panel). Since the genesis of the C8 Health Study, numerous epidemiological studies of the adverse health effects associated with PFAS exposure have been conducted across the globe, including many other regions in the US, Europe, and China.

Multiple organizations and regulatory agencies in the US have also generated statements regarding the most well-supported human health effects associated with PFAS. The Center for Disease Control (CDC)/Agency for Toxic Substances and Disease Registry (ATSDR) states that PFAS might increase the risk of cancer, affect the immune system, increase cholesterol levels, act as endocrine disruptors, reduce female fertility, and adversely impact infant/early childhood growth and development (ATSDR 2019). The US EPA states that elevated cholesterol in adults is the most consistent health effect associated with PFAS, but less consistent data suggest PFAS might be associated with low infant birth weight (Johnson et al. 2014; Koustas et al. 2014; Lam et al. 2014), effects on the immune system, increased risk for cancer (specific to PFOA), and disrupted thyroid hormones (specific to PFOS) (822-R-16-005 2016). The World Health Organization (WHO)/International Agency for Research on Cancer (IARC) states that PFOA is possibly carcinogenic to humans. The National Toxicology Program (NTP) states that PFAS might have effects on metabolism, pregnancy, neurodevelopment, and the immune system, with both PFOA and PFOS presumed to be immune hazards (NTP 2016). Such statements only

address the possible health effects associated with legacy PFAS as there are extremely limited data on health outcomes associated with replacement and alternative chemistry PFAS.

Although many biological systems are adversely impacted by PFAS, this dissertation focuses primarily on adverse pregnancy outcomes, metabolic dyshomeostasis, thyroid disruption, and kidney effects (Figure 1-4).

1.2.2 Challenges of Studying PFAS-related Human Health Effects

The challenges presented by PFAS exposure likely contribute to inconsistencies across epidemiologic studies. First, humans are exposed to PFAS as complex mixtures that differ based on the source of exposure (e.g. a military base or an industrial site) and differ temporally within the same geographic location (e.g. an industrial site phasing out PFOA and PFOS and utilizing alternative PFAS instead; seasonal patterns in rainfall/drought affecting the extent to which PFAS in water systems are diluted or concentrated). Very little is known regarding the potential synergistic effects of PFAS mixtures. Human exposure to PFAS also varies by demographic factors, and such demographic factors likely differ by individual PFAS congener within a given population. Lifelong exposure, combined with variable exposure to temporally stochastic mixtures and congener-specific demographic factors, presents a complex set of challenges to understanding the relationship between PFAS exposure and adverse health outcomes.

A second challenge in epidemiologic studies of PFAS-related health effects is the lack of a control population. All humans born after the year 1950, when PFAS were first introduced at the industrial scale, have potentially been exposed to PFAS their entire lives, including *in utero*. This precludes the ability to design and conduct cohort studies with a no-exposure comparison group. Instead, such cohort studies of PFAS must make comparisons between low and high exposure groups to estimate disease risk based on exposure status.

Third, it is possible that PFAS-related adverse health outcomes observed in adulthood are latent manifestations of perturbations during sensitive periods of development. It is also possible that some PFAS-related adverse health outcomes observed in adulthood are due to chronic, lifelong exposure. In order to address these hypotheses, a population of humans without PFAS exposure during early development would be required. However, such a population only existed prior to 1950, making such a study extremely difficult if not impossible.

1.2.3 The Placenta as a Target of PFAS and Critical Driver of Adverse Pregnancy Outcomes

Adverse pregnancy outcomes associated with PFAS exposure in humans include increased time to pregnancy (Bach et al. 2016; Lum et al. 2017), hypertensive disorders of pregnancy (which includes pregnancy induced hypertension [PIH] (Huang et al. 2019; Savitz et al. 2012b), and preeclampsia [PE] (Stein et al. 2009; Wikström et al. 2019)), gestational diabetes (GD) (Matilla-Santander et al. 2017; Zhang et al. 2015), excess gestational weight gain (Ashley-Martin et al. 2016), and low birth weight of the infant (Johnson et al. 2014; Koustas et al. 2014; Lam et al. 2014). Independent of PFAS exposure, deficiencies in placental development and/or function are involved in the etiology of many of these adverse pregnancy outcomes. Thus, I hypothesize the placenta is a target of PFAS, and PFAS-induced reductions in placental function significantly contribute to adverse pregnancy and birth outcomes.

The placenta is a critical organ that exists exclusively during pregnancy and serves as a conduit between mother and developing offspring, mediating the maternal-fetal transfer of nutrients, oxygen, blood, waste, and xenobiotics. The healthy development and function of the placenta is paramount to not only the healthy development of the fetus, but also the health of the mother. Indeed, many adverse pregnancy outcomes are due to placental insufficiency (PI), a condition in which the functional capacity of the placenta is limited or deteriorates, resulting in

reduced transplacental transfer of oxygen and nutrients to the fetus (Gagnon 2003). Previous studies have demonstrated that the placenta is vulnerable to environmental insults (Leclerc et al. 2014; Pedersen et al. 2014), and the placenta shares key biological features with other established target tissues of PFAS such as kidney and liver.

The placenta is a plausible target of PFAS as it plays a role in the etiology of pregnancy disorders related to PFAS exposure, is exposed to PFAS via maternal circulation, and shares biologic features in common with other known target tissues of PFAS. It is well documented in humans and animal models that PFAS readily pass from maternal serum to the developing embryo via the placenta (Chen et al. 2017b; Yang et al. 2016a; Yang et al. 2016b) and that PFOA transplacentally transfers to the mouse offspring (Fenton et al. 2009). During early stages of development, the placenta serves as the liver, lungs, and kidneys for the embryo; the placenta is responsible for xenobiotic metabolism, supplying oxygen, and eliminating waste from embryonic/fetal circulation. Placental trophoblasts express multiple types of ATP-binding cassette (ABC) and organic anion transporter (OAT) proteins in order to shuttle nutrients, xenobiotics, and waste between the maternal and fetal compartments. Many of the transporter proteins expressed in placental trophoblasts are also expressed in liver or kidney, where they excrete substrates into the bile or urine, respectively (Joshi et al. 2016). An *ex vivo* study of human placenta showed the involvement of OAT4 in the placental transport of PFOA and PFOS.

There is limited evidence of the mechanisms of PFAS toxicity towards the placenta. A study in mice showed dose-dependent necrotic changes in placenta after gestational exposure to 10 mg/kg/day and 25 mg/kg/day PFOA (Suh et al. 2011). I have more recently demonstrated gestational exposure to either PFOA or GenX induced placental lesions in CD-1 mice (Blake et al. 2020). *In vitro* studies of JEG-3 human placental trophoblasts showed PFOS, PFOA, and

PFBS inhibit aromatase (CYP19) activity and an exposure to a mixture of eight different PFAS caused an increase in certain lipid classes (Gorrochategui et al. 2014), and that JEG-3 cell exposure to PFAS altered expression of genes vital to placental function (Bangma et al. 2020, *in review*).

Improper development or function of the placenta is associated with a wide array of adverse pregnancy outcomes (including hypertensive disorders of pregnancy), many of which are also associated with maternal exposure to PFAS. I hypothesize that adverse pregnancy outcomes associated with PFAS exposure are mediated in part by the negative impact of PFAS on the development and function of the placenta. Understanding the risk of environmental insults on the health and development of the placenta is critical for protecting both short and long-term maternal and offspring health outcomes; the placenta is a driver of latent disease risk for both postpartum women and their offspring.

1.2.3.1 PFAS Exposure, Hypertensive Disorders of Pregnancy, and the Placenta

Hypertensive disorders of pregnancy (HDP) are a family of disorders that include PE, eclampsia, HELLP (haemolysis, elevated liver enzymes and low platelets) syndrome, and PIH, all of which are related to deficiencies in placental development and/or function (Pijnenborg et al. 1991). This family of disorders not only endangers the health of both the mother and developing fetus during pregnancy, but also increases the risk of post-pregnancy hypertension, heart disease, and stroke in affected women as well as increased risk for adverse cardiometabolic outcomes in adult offspring (Pinheiro et al. 2016).

During normal pregnancy, at 13 weeks gestation the placental cytotrophoblasts begin to invade the maternal uterine wall and remodel the maternal spiral arteries to establish blood flow to the growing embryo (Shah 2020). This process of vasculogenesis and angiogenesis by placental cytotrophoblasts remodels maternal spiral arteries to become low-resistance, low-

capacitance vessels in order to increase blood flow to the growing embryo and supply sufficient nutrients and oxygen (Shah 2020). This carefully coordinated process requires an appropriate balance of proangiogenic and antiangiogenic signals (Shah 2020). Disruption of this process can lead to abnormal placental vascularization, resulting in suboptimal pregnancy hemodynamics which can give rise to HDP as well as impaired fetal growth (Shah 2020).

There is growing evidence from human studies implicating maternal PFAS exposure in the development of HDP. Multiple epidemiologic studies have found positive associations between maternal exposure to PFAS and PE (Huang et al. 2019; Savitz et al. 2012a; Savitz et al. 2012b; Stein et al. 2009; Wikström et al. 2019a) as well as PFAS and PIH (C8 Science Panel; Darrow et al. 2013). It is possible that reduced or impaired placental function as a consequence of PFAS exposure results in or significantly contributes to the development of HDP.

Furthermore, it is well documented that the placenta itself is strongly associated with cardiometabolic disease risk in adults. Indeed, the size of the placenta is strongly associated with both perinatal and adult outcomes. In a study of 87,600 Canadian singleton births, fetuses with abnormally large placentas were at increased risk for adverse neonatal outcomes, including seizures, respiratory morbidity, and low Apgar score (odds ratio [OR] 1.4, 95% confidence interval [CI] 1.2-1.7) while fetuses with abnormally small placentas were at increased risk for stillbirth (OR 2.0, 95% CI 1.4-2.6) (Hutcheon et al. 2012). Bigger is not necessarily better; it has been hypothesized that an enlarged placenta is a biomarker for impaired nutrient supply to the fetus. This reduced capacity could be explained by restricted or impaired blood flow through the placenta. It is possible that impaired blood flow, which would in turn disrupt the normal flow of nutrients, oxygen, and waste between maternal and fetal compartments, during critical windows of *in utero* development may result in long-term adverse function of the cardiometabolic system.

A US cohort study of nearly 30,000 births showed that large placenta relative to birth weight, but not birth weight itself, is associated with high blood pressure in childhood (OR, 1.04) (Hemachandra et al. 2006). In a study of 31,307 Norwegian adults, disproportionately large placentas at birth were associated with increased risk of death associated with cardiovascular disease (CVD), and this association remained positive when considering placenta weight alone (Risnes et al 2009).

While mounting epidemiologic evidence suggests PFAS exposure as a risk factor for the development of HDP, a specific mechanism has yet to be validated in experimental settings. Such experimental systems are critical in addressing the hypothesis that maternal exposure to PFAS increases the risk of developing HDP via disruption of the placenta. Due to the complex and multifactorial nature of HDPs, and interspecies differences in maternal spiral artery structure and formation, current animal models are unable to adequately recapitulate the multiple manifestations of this complex group of disorders (Cushen and Goulopoulou 2017; Marshall et al. 2017). Indeed, there is no "standard" or preferred animal model of HDP, and it is unlikely that such an animal model will ever exist (Cushen and Goulopoulou 2017; Marshall et al. 2017). Thus, the development of sensitive laboratory tools for assessing clinically relevant biomarkers of HDPs in animal model is a necessary next step towards determining mechanisms of PFAS toxicity.

1.2.3.2 PFAS Exposure and Low Birth Weight

Low birth weight is the most consistently reported adverse pregnancy outcome associated with gestational exposure to PFAS in human epidemiologic and animal studies. It is also well established in the literature that placental insufficiency contributes to the etiology of low birth weight (Audette and Kingdom 2018; Cuffe et al. 2017; Henriksen and Clausen 2002). What

remains unaddressed by the current body of literature is the relationship between gestational exposure to PFAS, placental function, and birth weight.

In 2014, a three-paper series performed systematic reviews of the existing human and animal literature on the relationship between *in utero* exposure to PFOA and low birth weight (Johnson et al. 2014; Koustas et al. 2014; Lam et al. 2014). After gathering primary data sets and detailed descriptions of study designs from numerous research teams, the authors were able to calculate estimates corresponding to the predicted reduction in birth weight in humans [-18.9 g birth weight per 1 ng PFOA/mL maternal serum, 95% CI: -29.8, -7.9; (Johnson et al. 2014)] and in mice [-23.0 mg birth weight per 1 mg PFOA/kg maternal body weight/day, 95% CI: -29.0, -16.0; (Koustas et al. 2014)]. The authors concluded from their systematic analyses of the literature that PFOA is indeed associated with reduced birth weight in both humans and mice.

Since the publication of these systematic reviews in 2014, the human epidemiologic literature on the relationship between PFAS and birth weight has expanded to include less well studied PFAS. In a recent report, an analysis of 3,535 mother-infant pairs in the Danish National Birth Cohort examined six different PFAS and reported increased risk for preterm birth associated with maternal serum levels of PFOA, PFOS, PFNA, PFDA, and perfluoroheptane sulfonate (Meng et al. 2018). Low birth weight risk was also elevated, but estimates were less precise in this analysis (Meng et al. 2018). In a study of 1,533 Swedish mother-infant pairs, increased maternal exposure to PFOS, PFOA, PFNA, PFDA, and perfluoroundecanoic acid were associated with lower birth weight and size, but associations were only significant in girls (Wikstrom et al. 2019). Conversely, a study of 457 British mother-son dyads showed inverse associations between maternal PFOS and measures of both birth weight and size (Marks et al. 2019), which had previously been shown in mother-daughter dyads in the same cohort (Maisonet

et al. 2012). A study of 1,645 mother-infant pairs in Massachusetts showed that PFOS and PFNA were weakly inversely associated with birth weight and positively associated with higher odds of preterm birth (Sagiv et al. 2018). In another US cohort, maternal serum PFOA and PFNA was inversely associated with birth weight in an analysis of 628 mother-infant pairs (Starling et al. 2017). A smaller study of 98 Chinese mother-infant pairs also found PFOS was negatively associated with birth weight, and that both PFOS and PFHxS were negatively associated with birth size (small for gestational age, SGA) (Xu et al. 2019). Taken together, these epidemiological studies further underscore the potential for PFAS other than PFOA to adversely affect fetal growth *in utero*.

There are limited animal studies supporting the association between PFAS, other than PFOA and PFOS, and reduced birth weight. Studies of both mice (Chang et al. 2018) and rats (Ramhøj et al. 2018) have shown reduced offspring body weight after developmental exposure to PFHxS. In rats, developmental exposure to perfluoroundecanoic acid has been shown to reduce offspring weight (Takahashi et al. 2014). Previous animal studies of the developmental effects of PFNA have reported adverse neonatal outcomes, but did not report effects on birth weight (Das et al. 2015; Wolf et al. 2010). Similarly, a previous study of the developmental toxicity of PFDA in mice found no reductions in birth weight (Harris and Birnbaum 1989).

The association between PFAS exposure and low birth weight is well supported in humans, as is the causal link between placental insufficiency and low birth weight. This, in combination with the biologically plausible proposed mechanisms of PFAS toxicity towards the placenta, further underscores the need to test the hypothesis that the PFAS-mediated placental effects are a critical driver of adverse pregnancy and birth outcomes.

1.2.4 PFAS Exposure and Metabolic Effects

Metabolic syndrome (also referred to as cardiometabolic syndrome) describes a group of disorders that include obesity, dyslipidemia, elevated blood pressure, and impaired glucose tolerance, and it affects approximately one third of the US adult population (Eckel et al. 2005; Ervin 2009). The liver a central hub in the regulation of pathways controlling systemic metabolic homeostasis, and liver dysfunction is a major component of metabolic syndrome (D'Amore et al. 2014).

A recent review of the literature examined 69 epidemiological studies evaluating the association between PFAS exposure and a variety of metabolic outcomes, including lipid homeostasis, diabetes, overweight/obesity, and cardiovascular disease (Sunderland et al. 2019). Across the human literature, Sunderland et al. (2019) reported relatively consistent and modest positive associations between PFAS exposure and serum lipids, such as total cholesterol and triglycerides. Although associations were less consistent across studies, Sunderland et al. (2019) also reviewed epidemiologic studies examining the adverse effect of PFAS exposure on insulin resistance, diabetes, hypertension, vascular disease, and stroke. Across these health outcomes, adverse effects were most consistently reported in association with exposure to PFOA (Sunderland et al. 2019).

More recently, additional studies of humans have explored the association between PFAS exposure and metabolic syndrome. Christensen et al. (2019) leveraged the National Health and Nutrition Examination Survey (NHANES) to investigate the relationship between PFAS exposure and metabolic syndrome in the general US population between years 2007-2014 and found PFNA was consistently associated with increased risk of metabolic syndrome, while the highest levels of PFHxS exposure were associated with elevated triglycerides (Christensen et al.

2019). This suggests that PFAS other than PFOA and PFOS may contribute to adverse metabolic health outcomes in humans.

The vast majority of animal studies investigating the effect of PFAS exposure on metabolic syndrome have focused on PFOA. Previous work in mice has shown developmental exposure to PFOA disrupts weight gain, leptin, and insulin later in life (Abbott et al. 2012; Hines et al. 2009). While data from animals initially suggested that peroxisome proliferator-activated receptor alpha (PPARα) was the mechanism through which PFOA exerted deleterious effects on the liver and metabolic system (Elcombe et al. 2012; Kennedy et al. 2004; Klaunig et al. 2003; Rosen et al. 2007), later work using mice null for PPARα revealed adverse liver effects persisted, suggesting PFOA can induce toxicity (e.g. tumor development) in the liver via PPARα-independent mechanisms (Filgo et al. 2014). However, more recently PFOA, PFOS, PFNA, and PFHxS were evaluated in mice and found to induce expression of hepatic genes involved in fatty acid and triglyceride synthesis, potentially causing steatosis through disruption of the balance between fatty acid accumulation and oxidation (Das et al. 2017). Similarly, in primary human and rat hepatocytes, PFOA and PFOS were shown to activate multiple nuclear receptors and the metabolic response shifted from carbohydrate metabolism to fatty acid accumulation and oxidation (Bjork et al. 2011). In an *in vitro* 3D spheroid model of mouse liver AML12 cells, PFOA, GenX, and another PFOA alternative, 3,5,7,9-tetraoxadecanoic perfluoro acid (PFO4DA), were shown to induce PPARα targets, oxidative stress, lactate dehydrogenase (LDH) leakage, suggesting PFOA alternatives have the potential to induce liver injury (Sun et al. 2019). Across the human, animal, and *in vitro* literature, there is consistent evidence to suggest PFAS disrupt metabolic homeostasis through damaging the liver.

1.2.5 PFAS Exposure and Thyroid Effects

PFAS are hypothesized to target the thyroid by influencing multiple biological mechanisms involved in thyroid homeostasis, including thyroid hormone biosynthesis, transport, metabolism, and interfering with thyroid receptors in target tissues (Boas et al. 2009). Proposed mechanisms of action of thyroid disruption by PFAS include reduced circulating levels of thyroxine (T4) due to competitive binding to thyroid hormone transport proteins (Weiss et al. 2009), increased T4 metabolism in the thyroid and liver (Chang et al. 2009; Yu et al. 2009; Yu et al. 2011), reduced thyroid production of T4 (Webster et al. 2014), or reduced thyroid peroxidase (TPO) activity (Coperchini et al. 2015).

Previous epidemiologic studies have examined the association between exposure to PFAS and thyroid hormones, with inconsistent findings across the literature. Several studies leveraged the NHANES database and showed positive associations between PFOA and total triiodothyronine (T3) (Jain 2013; Webster et al. 2016; Wen et al. 2013), TSH (Jain 2013; Lewis et al. 2015), and self-reports of current thyroid disease (Melzer et al. 2010). PFHxS has been associated with increases in total T4 across the general US population (Jain 2013) as well as with sex-specific positive associations in women (Wen et al. 2013). A recent meta-analysis of twelve epidemiologic studies found that PFAS are generally negatively associated with T4, but certain associations may be non-monotonic (Kim et al. 2018). For example, PFOS was positively associated with T4 and TSH only in the intermediate exposure group (Kim et al. 2018). Positive associations between serum PFOS and TSH were similarly reported in a longitudinal study of adults with serum levels of PFOS within the range of the general US population (Blake et al. 2018), and PFAS were generally found to be positively associated with TSH in pregnant women in a systematic review (Ballesteros et al. 2017). However, it is possible that inconsistencies across the human literature are attributable to differences in the overall range of PFAS

contamination and exposure across populations studied, which may help explain the non-monotonic dose-response described in Kim et al. (2018).

Pregnant women and their developing offspring are particularly sensitive to disruptions in thyroid hormones due to their critical role in early neurodevelopment (de Escobar et al. 2004; Porterfield 1994). PFAS have been documented as thyroid disrupters in pregnant women in some epidemiologic studies (Ballesteros et al. 2017; Berg et al. 2015; Wang et al. 2014; Webster et al. 2014). Generally, maternal PFAS levels during pregnancy are associated with shifts in thyroid hormone levels consistent with hypothyroidism (e.g. elevated TSH), which is associated with increased risk for low birth weight (Alexander et al. 2017). A recent study in rats reported maternal serum total T3 and T4 were reduced after gestational exposure to HFPO-DA (GenX) (Conley et al. 2019).

Due to the critical role that thyroid hormones play in human health and development, disruptions at any life stage warrant further study to understand potential underlying mechanisms. Both hyperthyroidism and hypothyroidism are suboptimal health outcomes and increase risk for adverse effects on the function of thyroid hormone-responsive tissues, such as kidney and the cardiovascular system. Therefore, continued study of the effects of PFAS on thyroid function are warranted.

1.2.6 PFAS Exposure and Kidney Effects

The kidney is considered a target tissue of PFAS, evidenced by a growing body of human epidemiologic data further supported by animal studies and *in vitro* models. In humans, PFAS exposure has been associated with adverse kidney outcomes such as reduced kidney function, chronic kidney disease (CKD), and kidney cancer, including mortality from kidney cancer.

The primary elimination route for PFAS is via urinary excretion. Given that the most well-studied PFAS do not undergo biotransformation prior to urinary excretion, one

hypothesized mechanism of PFAS-induced kidney injury is via reabsorption of PFAS across the renal tubules which causes localized damage, potentially through oxidative stress (Han et al., 2011). It has been demonstrated in humans that once absorbed, PFAS distribute primarily to serum, liver, and kidney (Fabrega et al. 2014; Perez et al. 2013). It is yet to be determined if the kidney is a sensitive target of PFAS due to high accumulation of PFAS within the renal tissue, creating a high internal dose in kidney, or if the kidney is particularly sensitive to PFAS-induced effects. The extent to which PFAS distribute and/or accumulate in different tissues likely varies by individual congener. For example, perfluorododecanoic acid (PFDoA), perfluorodecanoic acid (PFDeA), and perfluorobutyrate have been shown to highly accumulate in kidney relative to other tissues (Perez et al. 2013).

Elimination rates also vary widely by individual congener with human serum half-lives spanning from about 24 hours to ~15 years which generally (though not always) corresponds to carbon chain length and functional groups (ITRC 2017). Such differences in elimination rate and serum half-life are hypothesized to result from different rates of secretion and reabsorption by the kidney proximal tubules. This process, driven by renal tubule efflux transporters, actively transports PFAS back into systemic circulation, thus contributing to their long half-lives in the human body (Han et al., 2011). Uptake of PFAS into proximal tubules, both apically and basolaterally, is mediated by solute-carrier protein family transporters such as organic anion transporters (OAT). OAT1 and OAT3 have been shown to transport PFAS basolaterally in proximal tubules with apical transport mediated by OAT4 and urate transporter 1 (URAT1) (Worley et al. 2017; Yang et al. 2010; Zhang et al. 2013).

In a recent scoping review of the effect of PFAS on kidney health, Stanifer et al. (2018) identified 74 studies comprised of epidemiologic, pharmacokinetic, and toxicological studies of

humans, animals, and *in vitro* models (Stanifer et al. 2018). Across 21 epidemiologic studies of occupationally and non-occupationally exposed populations, Stanifer et al. (2018) reported consistent associations between PFAS exposure and adverse kidney outcomes, which included reduced kidney function and kidney cancer (Stanifer et al. 2018). Studies published since this scoping review have similarly provided evidence suggesting human exposure to PFAS is detrimental to kidney health. I have demonstrated negative associations between kidney function and serum concentrations of perfluorononanoic acid (PFNA), pefluorodecanoic acid (PFDeA), and perfluorohexane sulfonic acid (PFHxS) in a retrospective longitudinal study (Blake et al. 2018).

In addition to concerns over reduced kidney function, compensatory increases in kidney function (e.g. glomerular filtration rate) are associated with increased risk for cardiovascular morbidity and mortality. Such hyperfiltration has been observed in patients with pre-diabetes and prehypertension (Palatini 2012; Shastri and Sarnak 2011). Blake et al. (2018) reported a positive association between methyl-perfluorosulfonic acid (Me-PFOSA) and increased kidney filtration (Blake et al. 2018). Indeed, the relationship between PFAS exposure and kidney function (glomerular filtration rate) is nonmonotonic (Jain and Ducatman 2019a). It has been hypothesized that altered balance between glomerular secretion of PFAS into the urine for excretion (e.g. via OAT1 and OAT3) and renal reabsorption (e.g. via OAT4) with increasing severity of kidney disease progression may explain the inverse U-shaped relationship. Based on these findings, Jain and Ducatman (2019a) hypothesized that PFAS reabsorption in renal tubules decreases with advancing stages of renal failure. In a follow up study, Jain and Ducatman (2019b) demonstrated that increased albuminuria may provide further explanation for decreasing serum PFAS concentrations with increasing kidney failure. Excessive albumin proteins in the

urine may essentially off-load the body burden of PFAS with high binding affinity to albumin proteins (Jain and Ducatman 2019b). However, these studies were conducted using cross-sectional data from NHANES and the reported findings would be greatly strengthened if validated in longitudinal cohorts.

Animal studies and *in vitro* models have provided further evidence for the adverse effect of PFAS on kidney health (Stanifer et al. 2018). Studies conducted in rats and mice have reported increased kidney weight (Butenhoff et al. 2012; Curran et al. 2008; Ladics et al. 2005), increased blood urea nitrogen (BUN) (Butenhoff et al. 2012; Seacat et al. 2003; Takahashi et al. 2014), renal tubular atrophy (Klaunig et al. 2015) or hypertrophy (Ladics et al. 2005), and tubular epithelial hyperplasia (Kim et al. 2011), among other adverse kidney findings (see Stanifer et al. 2018 for a comprehensive review). *In vitro* systems have provided further evidence to suggest oxidative stress as a mechanism of PFAS-induced kidney damage (Chung 2015; Wen et al. 2016). A recent study by Gong et al. (2019) used rat mesangial cells as an *in vitro* model of diabetic kidney disease to determine the effect of PFAS exposure in the diabetic condition, and similarly reported PFOA or PFOS exposure resulted in increased oxidative stress, fibrosis, and inflammation in this *in vitro* model (Gong et al. 2019). Studies using rats must be interpreted with some caution due to interspecies differences in PFAS elimination rates, with PFAS excretion rates being much higher in rats (especially female rats) compared to mice (Loccisano et al. 2013; Lou et al. 2007; Pizzurro et al. 2019; Russell et al. 2013).

Overall, there is consistent evidence across human epidemiologic, animal, and *in vitro* studies to support the claim that PFAS are damaging to kidney health.

1.2.7 The Interplay Between Biologic Systems Affected by PFAS Exposure

The adverse health effects of PFAS exposure on human metabolic homeostasis, thyroid function, kidney function, and pregnancy outcomes are likely interrelated due to the extensive

overlap between these biologic systems. For example, the liver is responsible for thyroid hormone metabolism and transport, both kidney and liver express type 1 deiodinase (an enzyme that converts T4 to T3) (Sanders et al. 1997), and both the liver and placenta express enzymes of the type 3 deiodinase system, which converts active T4 to inactive rT3, and/or active T3 or inactive rT3 to inactive T2 (Bianco et al. 2002; Darras et al. 1999). During pregnancy, the placenta regulates the degree to which maternal thyroid hormones pass to the developing fetus and maintains the optimal balance of thyroid hormones throughout *in utero* development (Chan et al. 2009).

There is human clinical evidence to suggest shared pathogenic mechanisms for non-alcoholic fatty liver disease and chronic kidney disease (Musso et al. 2016), thyroid disease (both hyperthyroidism and hypothyroidism) and liver injury (Malik and Hodgson 2002), and hypothyroidism and chronic kidney disease (Rhee 2016). The proposed shared pathogenic mechanisms for these overlapping biologic systems also coincide with the hypothesized mechanisms of PFAS toxicity, including disruption of lipid metabolism (e.g. cholesterol and triglycerides), nuclear receptor activation (e.g. peroxisome proliferator-activated receptors, retinoid X receptor), and oxidative stress (Malik and Hodgson 2002; Musso et al. 2016; Rhee 2016), among others. In the context of pregnancy, chronic kidney disease increases the risk of preeclampsia and low birth weight (Fischer 2007), non-alcoholic fatty liver disease increases risk of gestational diabetes and pregnancy-induced hypertension (Hershman et al. 2019).

The clinical evidence underscores the careful balance between multiple biologic systems, and the shared pathogenic mechanisms affecting these systems coincides with toxicologic mechanisms through which PFAS affect these same systems. The complex interplay between the liver, kidney, and thyroid is further complicated by the physiological demands of pregnancy.

Thus, pregnant women and their developing offspring should continue to be considered the most sensitive populations when conducting PFAS health and risk assessments.

1.3 Regulatory Actions Against PFAS in the US

The first actions taken to limit the use and emission of PFAS began in 2000 when the company 3M voluntarily phased PFOS out of production and use. Then in 2006, the US EPA invited eight major fluoropolymer and fluorotelomer manufacturing companies to participate in a global stewardship program to commit to a 95% reduction of PFOA emissions and product by the year 2010 and a complete elimination by 2015 (EPA 2006). To meet these program goals, companies ceased manufacturing and importation of long-chain PFAS and/or transitioned to alternative chemicals while some companies exited the PFAS industry altogether. The impact of this phaseout can be appreciated by temporal declines in human serum PFOA and PFOS concentrations in datasets such as the NHANES; between 1999 and 2014, average PFOA and PFOS serum levels in the general US population declined by ~60% and ~80%, respectively (ATSDR 2017).

In 2016, Hu et al. found that drinking water levels of PFOS and/or PFOA exceeded the US EPA 2016 health advisory level in public water supplies serving approximately six million US citizens (Hu et al. 2016). That same year, the US EPA issued a lifetime drinking water Health Advisory Level (HAL) for PFOA alone or in combination with PFOS (70 parts per trillion, ppt) (822-R-16-005). This HAL represents a non-enforceable exposure level under which no adverse health outcomes would be expected given a lifetime of exposure, based on the US EPA's risk assessment of PFOA, which used a weight of evidence approach to examine existing human epidemiologic and animal toxicity studies. The developmental and reproductive toxicity study conducted by Lau et al. (2006) was selected to obtain the reference dose (RfD) used in

calculation of the lifetime HAL, in order to generate the most protective exposure level (822-R-16-005; Lau et al. 2006).

Despite the reduction in serum burden of PFOA and PFOS since the genesis of the stewardship program, a recent biomonitoring effort determined that drinking water sources for as many as six million US citizens exceed the HAL of 70 ppt (Hu et al. 2016). However, this number likely underestimates the number of US citizens with drinking water exposure above the PFOA/PFOS HAL as the sampling method used by Hu et al. (2016) was conducted under the scope of the third Unregulated Contaminant Monitoring Rule (UCMR3), which limits drinking water PFAS measurements to public systems serving over 10,000 people. The exposure levels for US citizens on private well water or public water systems serving under 10,000 people have yet to characterized.

The lack of federally enforceable regulations on any PFAS in the US, as well as increasing concerns over local contamination levels has led several states to implement their own regulatory actions (Figure 1-5). The states of California, Connecticut, Massachusetts, Michigan, Minnesota, New Hampshire, New Jersey, New York, North Carolina, and Vermont have each proposed various drinking water actions to address PFAS contamination (ASDWA 2020). New Hampshire and New Jersey have formally adopted statewide regulations, mandating drinking water levels for PFOA (NH: 12 ppt), PFOS (NH: 15 ppt), PFHxS (NH: 18 ppt), and PFNA (NH: 11 ppt; NJ: 13 ppt) substantially lower than the US EPA HAL of 70 ppt for PFOA alone or combined with PFOS (ASDWA 2020). Other states, such as North Carolina and Michigan, have proposed health advisories or maximum contaminant levels (MCLs) for replacement PFAS, such as GenX (NC: 140 ppt; MI: 370 ppt) (ASDWA 2020) while Ohio and Washington are in the

process of developing draft health advisories for various PFAS (OH EPA 2019; WA DOH 2020).

PFAS contamination in the environment and drinking water is driven by point sources of pollution, such as industrial/manufacturing sites, airports, biosolids fields, and military training bases. At each site, different levels of a multitude of PFAS are used in complex mixtures, depending on the application. The heterogeneity of the exposure mixture as well as relative concentrations of individual PFAS adds to the complexity of both studying PFAS effects of human health and setting appropriate standards to adequately protect the most vulnerable members of society. There is little to no toxicity data for the vast majority of PFAS currently in use, therefore there is great need for efficient methods to evaluate these compounds.

1.4 Conclusions

The complex universe of PFAS compounds presents unique challenges to toxicologists and risk assessors. The effects of PFAS on human health differ based on compound, impact multiple overlapping biological systems, affect health outcomes at all life stages, and exposure levels (and mixtures) differ temporally and geographically. Importantly, early life PFAS insults may in fact increase susceptibility for later life chronic health conditions, which may be further exacerbated by lifelong PFAS exposure. Thus, it is critical to improve our understanding of the adult health consequences associated with PFAS exposure over time, identify emerging PFAS threats to the most vulnerable members of society, and develop tools to efficiently evaluate and characterize PFAS toxicity. This dissertation examines each of these themes by (1) analyzing the association between PFAS exposure and biomarkers of chronic disease in a cohort of adults with 18 years of longitudinal exposure and outcome data, (2) comparing the developmental and reproductive toxicity of a well-studied PFAS, PFOA, with its replacement, GenX, with a special

focus on the placenta as a target tissue, and (3) developing a high-throughput toxicity screen using human-derived placental trophoblasts *in vitro* to efficiently evaluate a panel of 42 individual PFAS and provide critical baseline toxicity data to inform future studies.

Table 1-1. Common legacy per- and polyfluoroalkyl substances.

Chemical name	CAS	Abbr	Family	# Carbons w/fluorine	Carbon chain length	Type
Perfluorooctanoic acid	335-67-1	PFOA	PFCA	7	8	Legacy
Perfluorohexanoic acid	307-24-4	PFHxA	PFCA	5	6	Legacy
Perfluoropentanoic acid	2706-90-3	PFPeA	PFCA	4	5	Legacy
Perfluoroheptanoic acid	375-85-9	PFHpA	PFCA	6	7	Legacy
Perfluorononanoic acid	375-95-1	PFNA	PFCA	8	9	Legacy
Perfluorodecanoic acid	335-76-2	PFDA	PFCA	9	10	Legacy
Perfluorobutanoic acid	375-22-4	PFBA	PFCA	3	4	Legacy & replacement
Perfluorobutane sulfonic acid	375-73-5	PFBS	PFSA	4	4	Legacy & replacement
Perfluorohexane sulfonic acid	355-46-4	PFHxS	PFSA	6	6	Legacy
Perfluorooctane sulfonic acid	1763-23-1	PFOS	PFSA	8	8	Legacy
Perfluorooctane sulfonamide	754-91-6	PFOSA	PFSA	8	8	Legacy

Abbr: Perfluorocarboxylic acid = PFCA, perfluorosulfonic acid or amide = PFSA

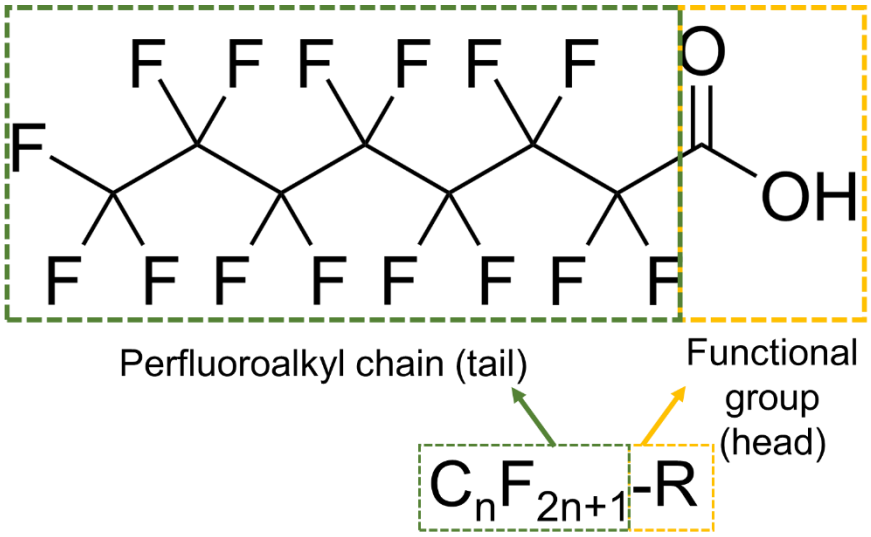

Figure 1-1. Basic structural features of a perfluoroalkyl substance (PFAS). The compound perfluorooctanoic acid (PFOA) is shown here as an example. The perfluoroalkyl chain (tail) is indicated by a dashed green outline, while the functional group (head) is indicated by a dashed yellow outline. Legacy PFAS share these structural features while replacement, or "alternative chemistry" PFAS, contain substitutions along the carbon tail.

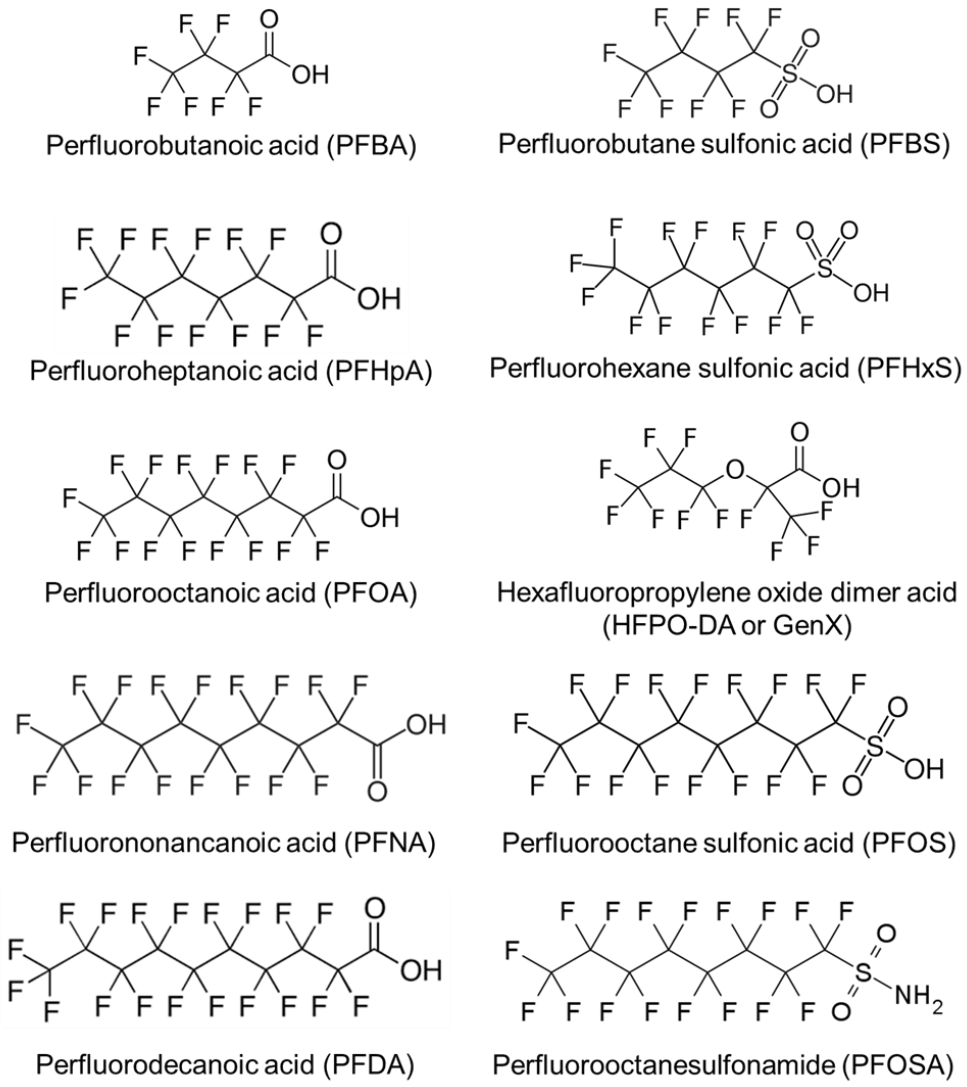

Figure 1-2. Structures of common legacy perfluoroalkyl substances (PFAS) and replacement PFAS. The ether substitution in the carbon tail of hexafluoropropylene oxide dimer acid (HFPO-DA, or GenX) is thought to favorably alter the toxicokinetic profile of the compound. Perfluorobutane sulfonic acid (PFBS) has classic structural features but has been selected as a replacement compound for longer-chain PFAS.

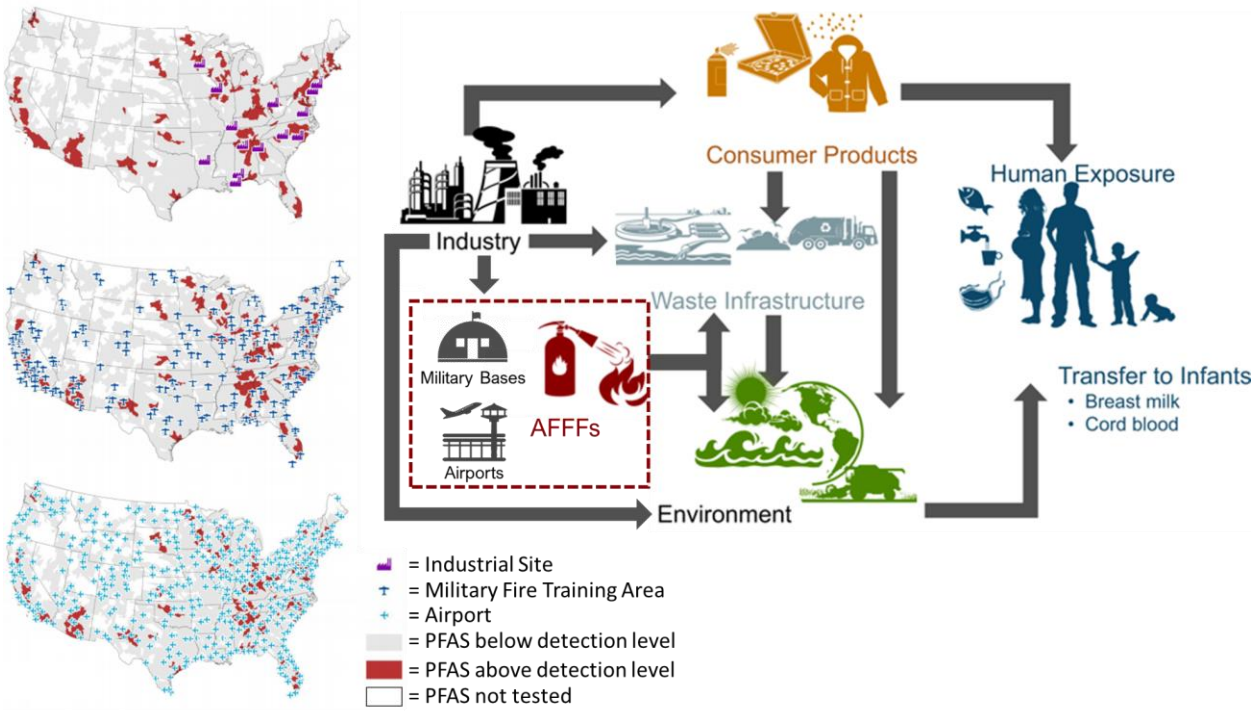

Figure 1-3. Major sources of human exposure to per- and polyfluoroalkyl substances. Humans are directly exposed to PFAS through the ambient environment (e.g. air), consumer products, house dust, drinking water, and diet. For developing humans, exposure can occur transplacentally *in utero* and through breastmilk. Environmental PFAS contamination is caused by waste and pollution generated by industrial complexes in the manufacturing or use of PFAS, including in the manufacturing of downstream products containing PFAS, such as aqueous film-forming foams (AFFFs). Environmental PFAS contamination is also caused by run-off of PFAS-containing AFFFs at military training bases and airports. Figure adapted from Sunderland et al. (2019) and Hu et al. (2016).

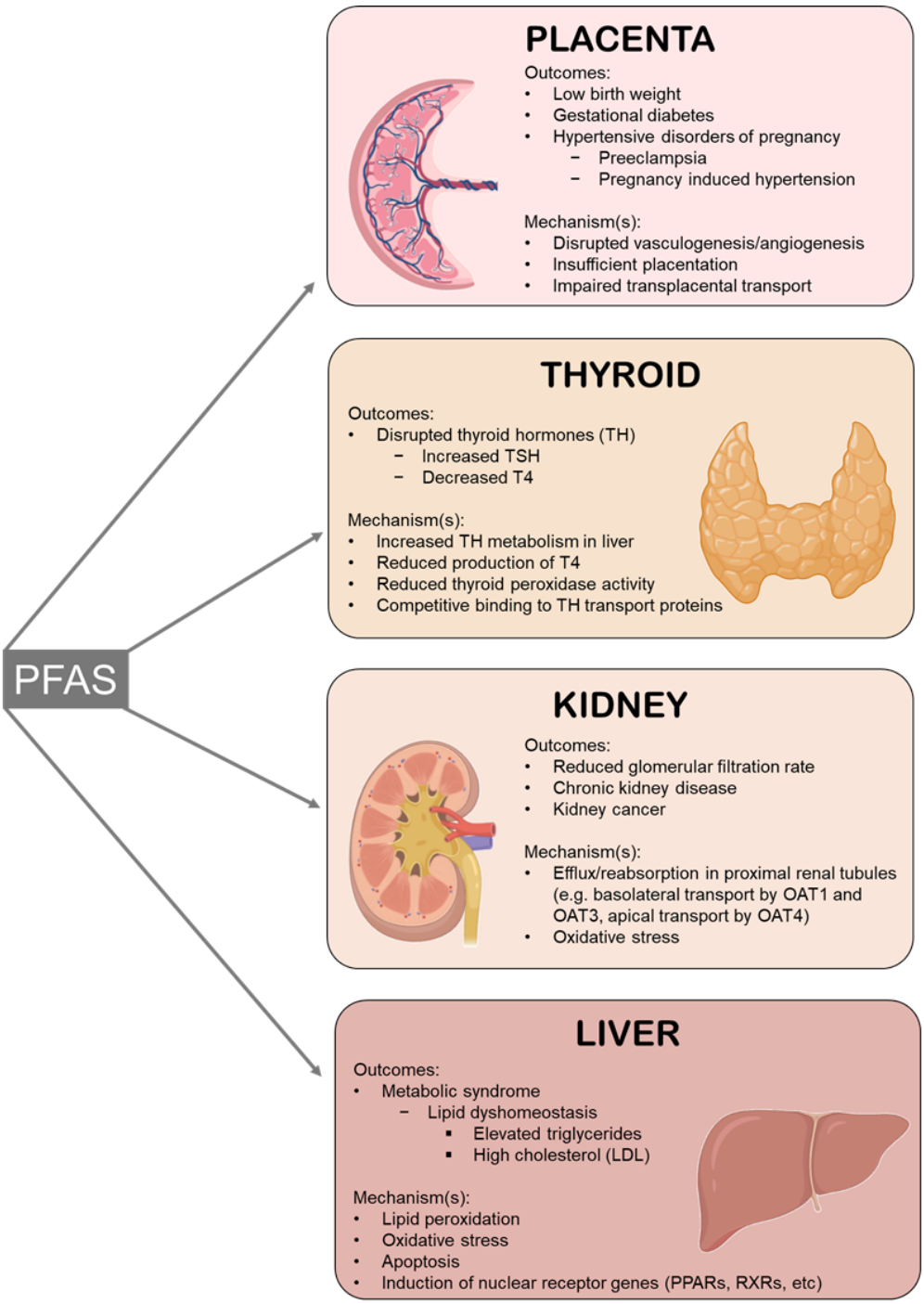

Figure 1-4. Summary of adverse health outcomes associated with PFAS exposure, the target tissue implicated by the outcomes, and hypothesized mechanism(s) of PFAS toxicity.

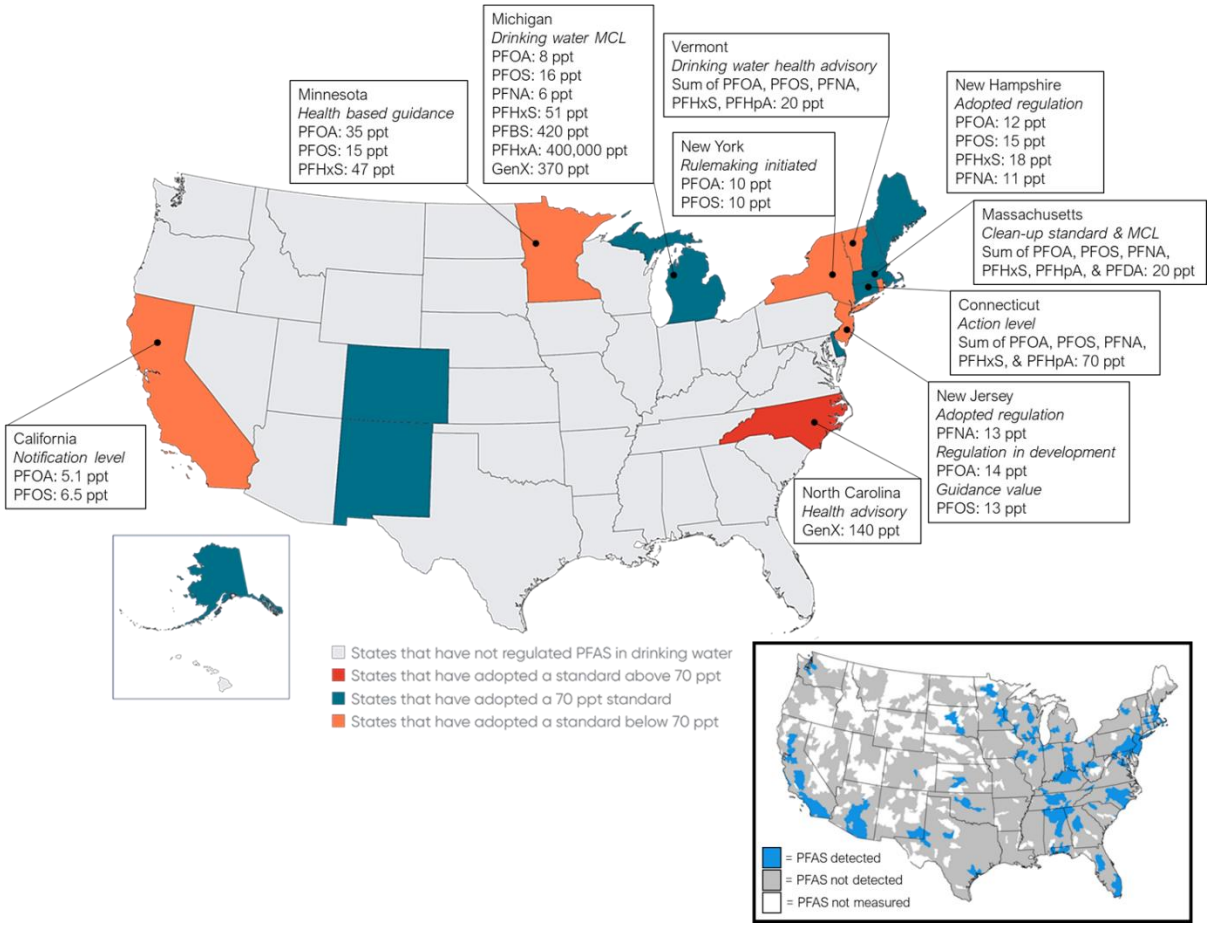

Figure 1-5. Responses of US states to PFAS contamination compared to nationwide PFAS levels (inset). Most state actions are non-enforceable and include notification levels, maximum contamination limits (MCLs), health advisories or guidance, and action levels. Several states have adopted enforceable regulation, such as New Hampshire and New Jersey, while other states are actively in pursuit of enforceable legislation, such as New York. There are some states with considerable PFAS contamination but no statewide action, including Alabama, New Mexico, and Kentucky. Figure adapted from Hu et al. (2018), Bryan Cave Leighton Paisner, LLP (used with permission), and http://www.saferstates.com/toxic-chemicals/pfas/.

CHAPTER 2: ASSOCIATIONS BETWEEN LONGITUDINAL SERUM PERFLUOROALKYL SUBSTANCE (PFAS) LEVELS AND MEASURES OF THYROID HORMONE, KIDNEY FUNCTION, AND BODY MASS INDEX IN THE FERNALD COMMUNITY COHORT [1]

2.1 Introduction

Per- and polyfluoroalkyl substances (PFAS) are a diverse class of manufactured compounds used in a wide range of industrial processes and consumer products, and infer unique properties including resistance to stains, thermal stability, and repellency to oil and water (ATSDR 2015). In addition to their widespread use, PFAS are highly resistant to degradation due to their strong carbon-fluorine bonds and can persist in the body and the environment for years (Fu et al. 2016; Olsen et al. 2007). Due to their ubiquitous presence in aquatic environments, exposure to PFAS through drinking water is an ongoing community-based concern, although exposure is known to occur via other routes including diet. PFAS contamination of drinking water is associated with spatial proximity to industrial point source pollution, military fire training run-off, and wastewater treatment plants, and is common in the U.S. (Hu et al. 2016). A recent biomonitoring effort determined that drinking water sources for as many as six million Americans exceed the US Environmental Protection Agency's (US EPA) lifetime health advisory level (70 ng/L) for the combined concentration of perfluorooctanoic acid (PFOA) and perfluorooctanesulfonic acid (PFOS) (Hu et al. 2016). There are also occurrences of extremely

[1] This chapter was adapted from a previously published manuscript in Environmental Pollution. The original citation is as follows: Blake, B.E., Pinney, S.M., Hines, E.P., Fenton, S.E., & Ferguson, K.K. (2018). Associations between longitudinal serum perfluoroalkyl substance (PFAS) levels and measures of thyroid hormone, kidney function, and body mass index in the Fernald Community Cohort. Environmental Pollution, 242, 894-904.

high exposure in association with accidental drinking water contamination. For example, in 2005 a class action lawsuit regarding the release of PFOA (C8) since the 1950s by the Washington Works (DuPont) plant in Parkersburg, WV resulted in a settlement and subsequent establishment of the C8 Science Panel. The C8 Science Panel carried out exposure and health studies in the affected Mid-Ohio Valley communities and has reported probable links between PFOA exposure and high cholesterol, kidney cancer, and thyroid disease, among other human diseases (C8 Science Panel). A recent report describes elevated serum PFOA concentrations in a different Mid-Ohio River Valley population, as early as 1991, exposed to contaminated drinking water from the Ohio River and Ohio River Aquifer, known to be contaminated by industrial waste (Herrick et al. 2017).

As a chemical class, PFAS are fluorinated organic compounds containing at least one fully fluorinated carbon atom (for a thorough explanation of classification, see Buck et al. 2011). In general, PFAS consist of a carbon backbone with multiple fluorine atoms, but vary in carbon chain length, functional groups, and branching patterns. For example, PFOA and PFOS have an eight-carbon chain (C8), but the functional group of PFOA is carboxylic acid while the functional group of PFOS is sulfonic acid. Perfluorononanoic acid (PFNA) and PFOA share the same functional group, but PFNA has a nine-carbon backbone (C9). Differing functional groups, carbon chain lengths, and branching patterns impart varying degrees of environmental and biological persistence (Conder et al. 2008; Lindstrom et al. 2011). For example, it has been theorized that the longer the carbon chain, the greater the extent of bioaccumulation, and PFAS with a sulfonic acid group (e.g. PFOS) tend to bioaccumulate more than carboxylated PFAS (e.g. PFOA) (Conder et al. 2008). Importantly, depending on the compound, the half-lives of the ≥ C6

PFAS are estimated to range from two to nine years (Fu et al. 2016; Olsen et al. 2007) and may vary between women and men (Fu et al. 2016; Wong et al. 2014).

PFAS exposure has been associated with multiple adverse health effects in humans, including perturbations in thyroid (Melzer et al. 2010; Olsen et al. 2001; Wen et al. 2013), kidney (Shankar et al. 2011; Watkins et al. 2013), and metabolic function (Fisher et al. 2013; Lin et al. 2009; Olsen et al. 1998). Major US PFAS manufacturers have committed to voluntarily eliminate the use of certain PFAS in product content and to decrease emissions through their participation in the EPA Stewardship Program (3M Company 2000; US EPA 2000). However, concerns regarding exposure still exist due to the persistence of these contaminants in the environment and in the human body. For example, it has been reported that PFOA cannot be fully eliminated from municipal water systems, and other recent reports confirm this problem for other PFAS (Higgins and Luthy 2006; Sun et al. 2016). Although the manufacturing of certain PFAS has been phased out, there remain concerns regarding the production of their congeners, and numerous new PFAS are being introduced to the marketplace (Sun et al. 2016).

Previous human studies of PFAS exposure and health consequences have primarily focused on occupationally exposed groups or nationally representative populations. Studies of occupationally exposed populations provide important insight into human health consequences associated with chronic, high levels of PFAS exposure, but are limited in scope as workers are often exposed to complex mixtures, are typically exposed as adults, and the historical exposure levels for workers are often unknown (Lindstrom et al. 2011). Few studies have examined highly exposed non-occupational populations and even fewer have collected longitudinal data spanning multiple years (Emmett et al. 2006; Lindstrom et al. 2011; Steenland et al. 2010; Stubleski et al. 2017). Because PFAS are known to persist in the body and environment for years, biomonitoring

efforts focused on highly exposed populations with long-term periods of follow up would provide invaluable information on the health risks imposed by this chemical class. The data presented herein uniquely offer the ability to examine temporal trends in PFAS levels as well as their relationship to chronic disease indicators within and between individuals over nearly two decades.

Serum samples collected as early as 1991 in the Fernald Community Cohort (FCC) were recently analyzed for PFAS levels (Herrick et al. 2017), and were used in the present analysis to examine PFAS measurements in relation to repeated measures of thyroid hormones (Total T4 and thyroid stimulating hormone, TSH), estimated glomerular filtration rate (eGFR), and body mass index (BMI). Each of the health outcomes used in the present analysis can be used as potential indicators of chronic health outcomes in routine medical examinations.

2.2 Methods

2.2.1 Study Population

The FCC was an eighteen-year medical surveillance program for residents living in proximity to a former U.S. Department of Energy uranium processing site in Fernald, Ohio, that may have been exposed to uranium dust due to the activities of the Feed Materials Production Center (FMPC). The FCC recruited on a volunteer basis by local media advertisements describing the program eligibility beginning in 1990. Eligible participants in the FCC lived or worked within a 5-mile radius of the FMPC for a minimum of 2 continuous years between January 1, 1952 and December 18, 1984, a time span representing the period during which FMPC uranium emissions occurred prior to becoming public knowledge.

Initial medical examinations and testing were administered to adult participants between December 1990 and December 1991. At the initial examination, a physician performed a comprehensive physical examination and conducted several diagnostic tests, which have been

described in detail elsewhere (FCC website; Wones et al. 2009). All participants completed a questionnaire at the initial examination as well, which included information on demographic characteristics, including age, gender, marital status, education level, income, and race/ethnicity (for more detail, see FCC website; Wones et al. 2009). Reexaminations were offered to participants every 2-3 years; questionnaires were administered yearly. At each reexamination, a complete physical examination, including height and weight measurement, was conducted along with laboratory testing of blood and urine for routine clinical chemistry (Pinney et al. 2003). Upon enrollment into the program, and at each examination, all participants signed a consent form for use of biospecimens and data in future research studies (Pinney et al. 2003). Additional information on eligibility, design, and participant characteristics has been described previously (FCC website; Wones et al. 2009).

Although the medical monitoring program was initially established to assess the impact of exposure to radiation and uranium released by the FMPC, a majority of the FCC (~60%) were not exposed to uranium above background levels (FCC website; Killough et al. 1996). Drinking water contamination by PFAS became a concern after several studies of residents living along the Ohio River in Ohio and West Virginia reported serum PFOA concentrations exceeding background U.S. population medians (Braun et al. 2016; Emmett et al. 2006; Kato et al. 2011; Pinney et al. 2003). A total of 210 participants were selected from the FCC after being identified as at high risk for exposure to PFAS based on living in zip codes bordering the Ohio River sometime after 1980. Members of the cohort selected for the PFAS study likely were not exposed to uranium above background levels (Killough et al. 1996), as they were selected based on low exposure according to an algorithm developed by the exposure assessment study. The number of persons on whom serum PFAS were measured was limited by available funds.

Selected participants preferentially had ≥3 serum samples collected in different calendar years. To reach 517 samples, some persons with only 2 samples were randomly selected from a much larger pool.

2.2.2 Exposure Measurements

Serum from the initial enrollment exam and from subsequent follow-up examinations between the years of 1991 to 2008 was analyzed for 8 PFAS congeners. PFAS were measured in serum samples by the CDC using a solid phase extraction high performance liquid chromatography (HPLC) tandem mass spectrometry (MS) method (Kato et al. 2011; Kuklenyik et al. 2005). Values below the LOD (< 0.1 μg/L or <0.2 μg/L [PFOS]) were imputed using LOD/√2 (Hornung and Reed 1990). All PFAS measurements were log-normally distributed and natural log-transformed for statistical analyses.

To compare serum concentrations with levels from a nationally representative US population, we drew data from the CDC Fourth Annual Report on Human Exposure to Environmental Chemicals (CDC 2013). We used geometric means and 95% confidence intervals for adult serum PFOA and PFOS levels from the available National Health and Nutrition Examination Survey (NHANES) cycles: 1999-2000, 2003-2004, 2005-2006, 2007-2008, and 2009-2010.

2.2.3 Outcome Measurements

Measurements related to thyroid disruption, kidney function, and body composition were selected based on the list of available measures in the FCC database. Thyroid stimulating hormone (TSH) and total thyroxine (Total T4) were selected as outcome measurements of thyroid disruption. TSH and Total T4 were measured in serum during medical examinations as part of the clinical chemistry panel. Additional information regarding thyroid hormone measurement methods and reference ranges are shown in Table A1-1. It should be noted that

Total T4 was only measured at exams that took place from 1991 to 1996 and that TSH was measured at exams from 1996 to 2008 due to changes in medical protocols. Because of this shift in practice, repeated measurements of Total T4 were available on a small number of study participants. However, all other outcomes were measured in at least one participant for each year between 1991-2008. Distributions of both thyroid hormones were log-normally distributed and natural log transformed for statistical models. Of the 210 participants, 20 reported taking thyroid-specific medications during the period of observation and were removed from all analyses with TSH or Total T4 as the outcome measurement.

Kidney function was evaluated using estimated glomerular filtration rate (eGFR), which was calculated using the Chronic Kidney Disease Epidemiology Collaboration (CDK-EPI) equation for estimating GFR on the natural scale, which includes variables for serum creatinine as well as age, sex, and race (Levey et al. 2009), as described in Table A1-2.

Body composition was evaluated using BMI. Weight and height were recorded at each medical examination, and BMI was calculated by dividing weight in kilograms by height in meters squared. For visits where height was missing, an average of height measurements for that participant was imputed to calculate BMI.

2.2.4 Statistical Analysis

Statistical analyses were conducted in R, Version 3.3.3 (R Core Team, 2017). Demographic characteristics of the study population and distributions of exposure and outcome variables at enrollment were examined. Then, to assess variability in serum PFAS and outcome measurements over time, intra-class correlation coefficients (ICC) and 95% confidence intervals were calculated using the ICC package (Wolak et al. 2012). The ICC value is the ratio of inter-individual variability to intra- plus inter-individual variability and indicates the consistency of repeated measures. The ICC falls within a range from zero to one, with a value of one indicating

no intra-individual variability (i.e., perfect reliability) (Rosner and Warzecha 2011). ICC values were calculated for PFAS measurements taken over a 1-5 year and 10-18 year period in order to examine shorter term versus longer term stability. PFAS trends over time were assessed by calculating geometric means and standard deviations by year of sample collection. Trends in serum PFAS concentrations over time were assessed using a linear mixed effect (LME) model in the lme4 package (Bates et al. 2015). Spearman correlation coefficients were calculated using non-log transformed values of PFAS at first measurement.

To assess the association between serum PFAS levels and outcomes, LME models were used to evaluate repeated measures of each serum PFAS in relation to each outcome, also using the lme4 package (Bates et al. 2015). Final sample sizes differed for each model because not all outcomes were assessed at each of the time points when PFAS were measured. A linear model was fit to the data for Total T4 measurements, as there was an insufficient number of participants with repeated measures (144 observations on 142 individuals) to fit an LME model to the data. Age at enrollment, year of measurement, and sex were included *a priori* in all models, and additional covariates were examined for inclusion in final models using a forward stepwise procedure. Additional covariates examined included: household income (<$20k/yr, $20k-50k/yr, >$50k/yr); highest attained education level (<college, some college or graduate, >college); marital status (married, not married); and BMI (continuous, in kg/m^2, except models where BMI was the outcome). Fully adjusted models included covariates that resulted in at least a 10% change in the corresponding beta estimate for any of the PFAS when added to the model. Covariates were kept the same for models of individual PFAS but were allowed to differ by outcome.

The relationship between serum PFAS levels and outcome measures was modeled in two ways. First, a repeated measures LME model was used to model the relationship between repeated serum PFAS levels and repeated outcome measures observed at the same time point. Second, to model latent effects of PFAS exposure, a LME model was used to model the relationship between the first serum PFAS measurement and all available outcome measurements (regardless of whether the outcome measurement occurred prior to the first PFAS measurement). Because PFAS tend to persist for years in human serum, we can reasonably assume that outcomes measured 1-8 years before the first serum PFAS measurement could still be associated with exposure. However, in a sensitivity analysis we created a LME model where we included the first serum PFAS measurement and only outcome measurements that were subsequent to that measurement. Finally, because PFAS are known endocrine disrupting compounds that may have sex-specific effects, we performed sensitivity analyses to examine the sex-stratified relationships between repeated measures of PFAS and each outcome measure using our primary repeated measures models. Adjusted sex-stratified models included the same covariates as the full parent models. The interaction of PFAS and sex was tested in the parent model by including an interaction term between PFAS and sex, as well as an interaction term between sex and each covariate (Buckley et al. 2017).

Effect estimates are expressed in tables as the percent change in outcome measure in association with an interquartile range (IQR) increase in PFAS. Because eGFR was not log-transformed, IQR estimates for eGFR are expressed as the percent change in eGFR relative to the median eGFR concentration in association with an IQR increase in PFAS.

2.3 Results

The population studied was primarily White and married, with a median age of 38 years at the time of enrollment, although some individuals (N = 8) were younger than 20 years at

enrollment (Table 2-1). Sixty percent of the participants were women and about 7% had achieved a college education. Approximately half of participants were considered overweight or obese at enrollment (BMI > 25 kg/m^2). Median chronic health indicator measurements at enrollment were similar to what has been reported for the general US population in this age range for TSH (median = 1.53 µIU/mL), Total T4 (median = 7.65 µg/dL), and eGFR (median = 103.8 mL/min per 1.73 m^2, Table A1-3). Similar to the general US population, BMI at enrollment was in the range of normal weight for approximately half of the participants and overweight or obese for the remaining half. BMI and eGFR were measured most often during the study period, whereas TSH and Total T4 varied over time based on changes in standard medical practices (Table A1-4). The median number of repeated measures for chronic health indicators was: BMI= 7, eGFR= 7, TSH= 5, and Total T4= 1 (Table A1-5).

At the time of the first serum measurement for each participant (N = 210), all compounds were detected in 100% of samples except for PFOSA (22% < LOD), PFDeA (28% < LOD), and Et-PFOSA (2% < LOD) (Table 2-2). Median concentrations of serum PFOS were highest, followed by PFOA. Most serum PFAS measurements were collected from 1991-1995 and 2007-2008, and participants had a median of 3 repeated measures of serum PFAS (Supplemental Tables 2-4 & 2-5). Spearman correlations between PFAS at first measurement were strongest between PFNA and PFDeA, and both PFOA and PFOS were positively correlated with all other measured PFAS; only positive correlations between PFAS were detected (Figure 2-1, Table A1-6). Intraclass correlation coefficients (ICCs) were more stable for every PFAS over a period of 1-5 years compared to a period of 10-18 years (Table 2-3). Compounds with the highest degree of stability over a 1-5 year period were PFHxS>PFOA>PFNA>Et-PFOA>PFOS. Only two

compounds maintained some stability when measured over 10-18 years, PFHxS (ICC= 0.71) and PFOA (ICC= 0.58). ICCs over the same time periods did not differ between men and women.

Geometric mean (95% confidence intervals) serum PFAS concentrations are shown by year of sample collection in Figure 2-2, with corresponding NHANES geometric means (95% confidence intervals) from available study years. Concentrations of serum PFAS by year of measurement for FCC participants are shown in Table A1-7. Median serum concentrations and geometric means of all PFAS measurements combined have been previously reported for the FCC in Herrick et al. (2017); here we report serum PFAS levels by year of measurement in the FCC. Serum PFAS concentrations tended to decrease over time except for PFNA and PFDeA, which increased. PFOSA and Et-PFOSA were relatively low from 1991 to 1998 and then fell below the limit of detection (Figure 2-2F & G). The change in serum PFAS concentrations between samples has been previously reported for the FCC in Herrick et al. (2017), which was greatest for PFOS (a mean decrease of 6.4 μg/L between samples) and PFOA (a mean decrease of 2.6 μg/L between samples).

Serum levels of PFOS were comparable between FCC and NHANES participants between 2000 and 2008 (Figure 2-2B), as both decreased by ~45% over an eight-year period. On the other hand, serum concentrations of PFOA differed markedly between the two groups (Figure 2-2A). Geometric mean serum PFOA levels were approximately three times greater in the FCC samples measured in 1999 than in samples from NHANES from 2000-2001. Although PFOA serum levels decreased in both populations over time, PFOA levels in the FCC participants remained significantly higher than levels reported in NHANES. Serum PFHxS concentrations were approximately 1.4 times greater in the FCC compared to NHANES and remained relatively stable over time (Figure 2-2D).

2.3.1 Associations with Thyroid Hormone Levels

In crude repeated measures models, we observed significant positive associations between PFOS and TSH (Table A1-8). The adjusted repeated measures model included covariates for age, year of measurement, sex, education, income, marital status, and BMI. In the adjusted repeated measures model, an IQR increase in serum PFOS was associated with a 9.75% (95% CI= 1.72, 18.4) increase in TSH (Table 2-4). No other significant associations were detected in in our primary models. In our crude models of latent effects, i.e., all outcome measures modeled in association with the first serum PFAS measurement, we did not detect associations between PFAS and Total T4 or TSH (Table A1-9). Associations observed in crude latent models were similar in our sensitivity analysis, which included thyroid hormone measures subsequent to the first PFAS measurement (Table A1-10).

In the adjusted latent model, we observed a positive association between serum PFNA and Total T4. The adjusted latent model included covariates for age, year of measurement, sex, education, income, marital status, and BMI. An IQR increase in serum PFNA was associated with a 3.02% (95% CI= 0.05, 6.07) increase in Total T4 (Table 2-5). This association was similar, but less precise, when we only included Total T4 measurements that were subsequent to the first PFNA measurement (Table A1-11). We did not detect any latent effects for TSH.

Sex-stratified models and models with an interaction term for sex were adjusted for the same covariates as the repeated measures models. In models with interaction terms for sex, we detected a significant sex difference in the association between serum PFNA and Total T4 ($p<0.05$; Table A1-12). For women, an IQR increase in PFNA was associated with a 6.41% (95% CI= 0.55, 12.6) increase in Total T4, whereas in men an IQR increase in PFNA was associated with a -2.23% (95% CI= -7.70, 3.60) change in Total T4. A similar sex-specific pattern was observed with respect to serum PFHxS and TSH levels; in women an IQR increase

in PFHxS was associated with a -7.46% (95% CI= -19.9, 6.98) change in serum TSH whereas in men an IQR increase in PFHxS was associated with a 20.7% (95% CI= -1.60, 43.4) increase in TSH ($p<0.05$ for the interaction term, Table A1-13). However, the associations between PFAS and thyroid hormone were not consistent between the main effect of sex and in the models containing an interaction term for sex.

2.3.2 Associations with Kidney Function

In crude models, we observed significant associations between all PFAS and eGFR except for PFOA (PFOA, p=0.06; Table A1-8). The adjusted repeated measures model included covariates for age, year of measurement, sex, education, income, marital status, and BMI. In fully adjusted models, PFNA, PFHxS, and PFDeA were inversely associated with eGFR, while Me-PFOSA and Et-PFOSA were positively associated with eGFR (Table 2-4). An IQR increase in serum PFNA, PFHxS, and PFDeA was associated with a -1.61% (95% CI=-3.00, -0.22), -2.06% (95% CI=-3.53, -0.59), and -2.20% (95% CI= -4.25, -0.14) change in eGFR, respectively. An IQR increase in serum Me-PFOSA was associated with a 1.53% (95% CI= 0.34, 2.73) increase in eGFR. In adjusted models of latent effects, an IQR increase in serum PFOS was associated with a -1.72% (95% CI= -3.29, -0.15) change in eGFR (Table 2-5). In the sensitivity analysis examining outcome measures occurring after the first serum PFAS measurement only, this association was consistent (Table A1-11). Additionally, in that analysis, we observed that PFOSA was associated with a -1.87% (95% CI= -3.72, -0.02) change in eGFR. No interactions were detected by sex for the relationships between PFAS and eGFR (Table A1-14).

2.3.3 Associations with Body Mass Index

In crude repeated measures models of serum PFAS and BMI, we observed significant negative associations with PFOA, PFOS, PFOSA, Me-PFOSA, and Et-PFOSA, and significant positive associations with PFNA and PFDeA and BMI (Table A1-8). However, these

associations were attenuated and non-significant in the adjusted models (Table 2-4). Adjusted models included covariates for age, year of measurement, sex, education, income, and marital status. We did not detect any associations between PFAS and BMI in latent models, and there were no significant interactions by sex (Table 2-5 and Table A1-15).

2.4 Discussion

In participants from an 18-year biomonitoring cohort, we examined serum levels of eight PFAS over time and investigated the associations with measures of thyroid function, kidney function, and body mass index. Temporal trends in adult serum PFAS concentrations observed in this population with above-average exposure reflect patterns similar to those observed in the general US population and in other industrialized nations around the world (Axmon et al. 2014; Gomis et al. 2017; Haug et al. 2009; Kato et al. 2011; Nøst et al. 2014; Olsen et al. 2012; Stubleski et al. 2017; Yeung et al. 2013). Serum concentrations of PFOS, PFOSA, PFNA, PFDeA, and Me-PFOSA were similar in our study population compared to those observed in the NHANES during the same time period. However, serum concentrations of PFOA in our study population were approximately three times higher than those reported for adults in the NHANES—a pattern that persisted across the study period of 1991 to 2008. Serum PFHxS was approximately 1.4 times greater in the FCC than NHANES for similar years of study.

Similar to trends observed in the FCC, adult serum PFOS and PFOA levels worldwide generally began to decline after the year 2000, but serum PFNA and PFHxS levels tended to remain the same or in some cases increase over time (Axmon et al. 2014; Gomis et al. 2017; Haug et al. 2009; Kato et al. 2011; Nøst et al. 2014; Olsen et al. 2012; Stubleski et al. 2017; Yeung et al. 2013). The global decline in serum PFOS and PFOA levels aligns with the voluntary efforts to phase out PFOS by its major US manufacturer 3M in 2001 (3M Company 2000a; 3M Company 2000b; USEPA 2000). It should be noted that while 3M began to phase out

PFOS in 2001, EPA-facilitated PFOA phase out efforts did not begin until 2006 (USEPA 2006). In this study, we report serum PFAS levels between 1991 and 2008, providing insight into the shift in PFAS burden during the time period over which PFAS phase outs were initiated in the US. In the population described here, serum PFOS measurements from 2006-2008 were approximately 45% lower than measurements obtained from 1991-1998.

It is possible that compound half-lives may play a role in their temporal stability. The half-lives of PFOA and PFOS are estimated to be 2-4 years and 4-6 years, respectively, whereas PFHxS has an estimated half-life of 8-10 years (Olsen et al. 2007). Although serum levels of PFHxS were low in our study, the high degree of stability in levels measured over a period of 1-5 years (ICC= 0.91) as well as a period of 10-18 years (ICC= 0.71) corresponds to what would be expected from a compound with a long half-life. PFOA similarly exhibited stability over the 1-5 year period (ICC = 0.80), though not to the same extent as PFHxS, which could be due in part to its shorter half-life. Additionally, the greater decrease in ICC for PFOA when comparing across the 1-5 (ICC= 0.80) and 10-18 year periods (ICC= 0.58) may be indicative of its shorter half-life. Although PFOS has an intermediate half-life compared with PFOA and PFHxS, PFOS exhibited the most dramatic decrease in ICC when comparing the 1-5 year period (ICC= 0.66) and 10-18 year period (ICC= 0.16). This is likely due to the voluntary US phase-out of PFOS that began in 2001 and was further propagated by additional EPA regulation. Other PFAS exhibited dramatic shifts in ICC values between the two time periods, including PFOSA, PFDeA, Me-PFOSA, and Et-PFOSA, which is due in part to serum levels falling below the limit of detection at later time points during the study period.

PFAS are suspected to be endocrine disruptors that target the thyroid and alter thyroid hormones. The thyroid is considered a target of PFAS by way of influencing multiple biological

mechanisms involved in thyroid homeostasis, including thyroid hormone biosynthesis, transport, metabolism, and interfering with thyroid receptors in target tissues (Boas et al. 2009). A proposed mechanism of action of PFAS hypothesizes that circulating T4 levels are reduced by competitive binding of PFAS to thyroid hormone transport proteins (Weiss et al. 2009), increased T4 metabolism in the thyroid and liver, and reduced thyroid production of T4 (Webster et al. 2014). Experimental work in animals supports this hypothesis by demonstrating that PFAS induce hypothyroidism (Yu et al. 2009).

Previous studies have examined the association between exposure to PFAS and thyroid hormones, and the findings have varied greatly across studies. Several studies conducted using the NHANES database have shown positive associations between PFOA and total T3 (Jain 2013; Webster et al. 2016; Wen et al. 2013), TSH (Jain 2013; Lewis et al. 2015), and self-reports of current thyroid disease (Melzer et al. 2010). PFHxS has been associated with increases in total T4 across the general US population (Jain 2013) as well as with sex-specific positive associations in women (Wen et al. 2013). Further evaluation of thyroid transport proteins in blood samples from these individuals would be needed to address the potential mechanism of competitive binding by PFAS.

Here we report a positive association between serum PFOS and TSH, which is consistent with the association between PFOA and TSH in the general US population reported by Jain et al. (2013). Additionally, in an occupationally exposed population, a positive association was observed between serum PFOA and TSH (Olsen and Zobel 2007). Our result differs from these studies as we observed a positive association between serum PFOS and TSH, but not serum PFOA and TSH. In rats, a single oral dose of PFOS has been shown to induce a reduction in T4 without a concomitant change in TSH (Chang et al. 2008), which may suggest that multiple

exposures are needed for the TSH effect. Species differences may account for these disparate responses, or it is more likely that compensatory mechanisms stemming from feedback loops as a response to chronic, low levels of exposure differ from physiological changes in response to a single exposure.

We also observed a positive association between the first serum measurement of PFNA and subsequent levels of Total T4. This positive association has been observed with other PFAS (PFHxS) and Total T4 in the general population (Jain 2013). In sex-stratified analyses, we found this association was significant only among women. The female-specific trend is consistent with findings from Wen et al. (2013), who reported a positive association between PFHxS and Total T4 in women, as well as with studies from neonatal populations, where prenatal PFAS exposure was associated with T4 levels in female neonates (de Cock et al. 2014; Shah-Kulkarni et al. 2016). Additionally, we report a significant inverse association between serum PFOS and Total T4 that was stronger in men, although the interaction by sex was not statistically significant. Inverse associations have previously been noted between prenatal PFAS exposure and T4 levels in male neonates (de Cock et al. 2014; Preston et al. 2018). Parallel sex-specific associations between PFAS and TSH were not observed, possibly due to non-overlapping years of Total T4 and TSH measurement (see Table A1-1). Due to shifts in medical practice during the course of participant exams, Total T4 measurements were performed from 1991 to 1996, whereas TSH was measured at exams occurring after 1996. Because serum levels of some PFAS shifted substantially between the period of 1991-1996 and 1997-2008, associations with TSH and Total T4 may be less comparable. Thyroid hormones play critical roles in human health and development, and disruptions at any life stage warrant further study to understand potential underlying mechanisms.

The kidney is another target of PFAS as it is involved in their excretion and it is hypothesized that PFAS may damage the kidneys via reabsorption of PFAS across the renal tubules (Han et al. 2011). This reabsorption is hypothesized to occur due to renal tubule efflux transporters which actively transport PFAS back into systemic circulation, contributing to their long half lives in the human body (Han et al. 2011). In rats, PFOA and PFOS have been shown to induce renal hypertrophy, injury, and cellular proliferation (Cui et al. 2009). Additionally, previous cross-sectional human studies have reported associations between PFAS and reduced kidney function in adults and adolescents. Shankar et al. (2011) reported an association between increased serum PFOA and PFOS and reduced glomerular filtration rate, described as chronic kidney disease, in adults from the NHANES study. Kataria et al. (2015) reported a similar trend of reduced glomerular filtration in adolescents with PFOA and PFOS exposures in the highest quartile using the NHANES data. Reduced glomerular filtration was also associated with serum PFOA, PFOS, PFNA, and PFHxS in a highly exposed population of adolescents (Watkins et al. 2013). Here we similarly report a reduction in estimated glomerular filtration rate associated with serum levels of PFNA, PFDeA, and PFHxS. We also observed a negative association between serum PFOA and PFOS levels and eGFR in adjusted models, although the association was not statistically significant. In addition to concerns over reduced eGFR, increases in eGFR are similarly associated with a higher risk for cardiovascular morbidity and mortality and can reflect hyperfiltration, which is observed in pre-diabetes and pre-hypertension (Shastri and Sarnak 2011). We also report an increase in eGFR with increasing exposure to Me-PFOSA.

Although the mechanisms of toxicity are not well understood for each individual PFAS, it is possible that individual compounds impact target tissues via different modes of action. For example, peroxisome proliferator alpha (PPARα) is a suspected nuclear receptor target of PFAS

and is expressed in the liver and kidney. However, the extent to which PFAS activate PPARα is thought to vary by carbon chain length and functional group, with some PFAS exhibiting high levels of PPARα activation (e.g. PFOA) and others exhibiting none (e.g. PFDeA) (Wolf et al. 2008). It is possible that some PFAS alter kidney function via activation of nuclear receptor PPARα and others may exert their effects through other toxicological mechanisms such as mitochondrial dysfunction (Hagenaars et al. 2013). With respect to interpretation of the findings reported here on kidney function, reverse causation is a potential limitation of the association between serum PFAS and eGFR (Dhingra et al. 2017) but is less likely in this study due to its longitudinal study design. Rather than elevated serum PFAS causing reduced glomerular filtration, it is possible that an unidentified factor caused reduced glomerular filtration which in turn resulted in greater accumulation of serum PFAS in the body. However, given the breadth of studies demonstrating similar associations, we assume the PFAS are causing the lowered eGFR and this likely extends the half-life of PFAS.

PFAS are suspected obesogens, and obesogenic potential of PFAS has been evidenced by *in vitro* and *in vivo* experiments. PFAS have been shown to induce adipocyte differentiation and lipid metabolism in cell culture (Watkins et al. 2015). In mice, PFOA has been shown to disrupt insulin and leptin and increase body weight following prenatal exposure (Hines et al. 2009). Here we did not observe any statistically significant associations between PFAS and BMI in repeated measures models, latent models, or sex-stratified models. Other studies in adults have also produced inconsistent findings of associations between PFAS and measures of body composition or metabolic function (Lin et al. 2009; Nelson et al. 2010). In fact, in this study, more than 50% of the participants were overweight or obese at the first PFAS measure, limiting our ability to detect effects. The FCC participants may have been exposed to PFAS many years prior to the

first collection used to measure their PFAS serum levels, and this may have influenced their BMI; more data from the cohort are needed to address this question.

Associations between PFAS and health outcomes across the epidemiological literature are not entirely consistent, which may be due in part to varying degrees of toxicity both by congener and in terms of target tissue. For example, in regard to thyroid toxicity via competitive binding to thyroid hormone transport proteins, PFAS congeners exhibit markedly different binding potencies with PFHxS, PFOA, and PFOS having higher binding potencies than other PFAS (Weiss et al., 2009). Differences in congener action may be influenced by chemical functionalities such as the degree of fluorination, carbon chain length, and the functional end group. This same concept may apply to congener-specific effects on kidney function, where differences in congener functionalities may also influence the renal elimination rate and serum half-life of individual PFAS congeners (Han et al. 2011).

There are several potential limitations in our report. First, despite the longitudinal nature and large number of samples analyzed in this study, we had a modest number of study participants. However, the statistical power is improved through including repeated measures for both exposure and outcome measures. The age range of the population is wide, and some at younger ages may not yet be old enough to exhibit clinical health effects of PFAS exposure such as decreased GFR. In addition, the population described here is ethnically homogenous and predominantly female (61%), which may limit the degree to which our findings can be extrapolated to other populations. As mentioned above, it is possible that reverse causation may bias our results, particularly with associations examined between serum PFAS and eGFR, but evaluation of repeated measures in this study makes this less likely. Finally, it is possible that the relationship between thyroid hormone and GFR may contribute to the associations with serum

PFAS. Reduced GFR is a consequence of hypothyroidism whereas increased GFR is a consequence of hyperthyroidism (Basu and Mohapatra 2012). It is possible that PFAS indirectly affect GFR through disrupting the thyroid, or that PFAS affect the thyroid and kidney independently, or that reverse causation stemming from thyroid disease-related alterations in GFR accounts for the associations reported herein. A combination of reverse causality with respect to GFR and true adverse effect on the thyroid could be responsible for the associations reported herein, and the relative magnitude of the two inputs has yet to be explored.

There is potential for important mixtures effects between PFAS or between PFAS and other co-pollutant exposures. The extent to which PFAS interact in mixtures has been explored minimally, and the critical question of which PFAS congener within mixtures is the most toxic for a given outcome also has yet to be explored. We found a pattern of correlation between PFAS similar to that reported in a study of young girls, living in the same area (Pinney, 2014). Due to limitations in sample size we were unable to estimate mixtures effects, however the potential for combined effects of PFAS warrants further investigation. Additionally, since drinking water was the main environmental source of PFAS exposure in this study, it is possible that there is residual confounding from other contaminants that end up in drinking water, such as common industrial and agricultural byproducts like nitrates and mercury. We did not estimate exposure to these other compounds in our study, so were unable to investigate this potential co-pollutant confounding.

The primary strength of this study is the combination of repeated measures for serum PFAS levels and health outcomes over a long period of observation. This allowed for the calculation of ICC values for eight different PFAS, which to our knowledge has only been done previously in a pregnancy cohort (Papadopoulou et al. 2015). Additionally, measurements were

obtained for certain PFAS that are currently underrepresented in the literature (PFDeA, PFOSA, Et-PFOSA, and Me-PFOSA) either due to being below the limit of detection in most populations or because they were not included in serum analyses. Because we had detectable levels of these compounds in the FCC, we were able to examine for the first time the associations between these compounds and chronic health outcomes in a human population. Additionally, though the sample size is relatively small, the repeated measures design for both PFAS serum measurements and health outcomes instills a high degree of confidence in associations described by LME models. Our report is more powerful than studies with a single serum PFAS and outcome measurement, as we describe the association between serum PFAS and kidney function over time with repeated measures for each participant, providing a critical perspective on this relationship, which may be heavily influenced by the long half-lives of PFAS. Although some of the effects on clinical measures of chronic disease would not be clinically significant for most members of the population, they do represent a population shift with exposure, and may result in clinical disease for those with already borderline function.

2.5 Conclusions

In repeated measures models examining the association between a panel of eight PFAS and outcomes relating to thyroid function, kidney function, and body mass index, we found significant associations between PFAS and thyroid stimulating hormone, Total T4, and estimated glomerular filtration rate. We did not observe any significant associations between PFAS and BMI. Associations between PFAS and thyroid hormones were generally positive whereas associations between PFAS and kidney function were generally negative, although there were

differences observed by PFAS congener. Future work further describing temporal trends in PFAS exposure and measures of chronic diseases would provide critical insight to the human health risks associated with this chemical class.

Table 2-1. Demographic characteristics at enrollment (1991-1994) of 210 Fernald Community Cohort participants with PFAS measurements.

Characteristic		N (%) or median (25^{th}, 75^{th} percentile)
Age (years)		38.0 (29.3, 48.7)
Sex	Female	129 (61)
	Male	81 (39)
Race/Ethnicity	White	209 (99)
	Native American	1 (<1)
Education	< College	85 (40)
	Some college or graduate	100 (48)
	> College	18 (7)
	missing	7 (3)
Marital status	Married	141 (67)
	Not married	56 (27)
	missing	4 (2)
Annual income	< $20,000	39 (19)
	$20,000 -$50,000	105 (50)
	> $50,000	50 (24)
	missing	16 (8)
Body mass index	< 25 kg/m^2	99 (47)
	25 to <30 kg/m^2	77 (37)
	> 30 kg/m^2	33 (16)
	missing	1 (<1)

Abbr: PFAS = perfluoroalkyl substance

Table 2-2. Serum levels of perfluoroalkyl substances (PFAS) (µg/L), at first measurement for PFAS (N = 210).

PFAS Name	Abbr	# Carbons	N (%) < LOD*	Min	25th	Median	75th	Max
Perfluorooctanoic acid	PFOA	C8	0 (0)	1.8	7.83	12.7	19.5	91.1
Perfluorooctanesulfonic acid	PFOS	C8	0 (0)	4.8	21.6	28.4	35.7	77.3
Perfluorooctane sulfonamide	PFOSA	C8	47 (22)	< LOD	0.10	0.20	0.30	1.60
Perfluorononanoic acid	PFNA	C9	0 (0)	0.10	0.40	0.50	0.70	3.50
Perfluorohexane sulfonic acid	PFHxS	C6	0 (0)	0.50	1.70	2.65	4.10	34.3
Perfluorodecanoic acid	PFDeA	C10	58 (28)	< LOD	0.07	0.10	0.20	0.90
2-(*N*-methyl perfluorooctane sulfonamide) acetic acid	Me-PFOSA	C8	0 (0)	0.20	0.50	0.85	1.20	9.10
2-(*N*-ethyl perfluorooctane sulfonamide) acetic acid	Et-PFOSA	C8	4 (2)	< LOD	1.33	2.05	3.38	41.5

Abbr: LOD=Limit of detection, CI=confidence interval

*LOD = 0.1 µg/L for all PFAS, except PFOS (LOD = 0.2 µg/L)

Table 2-3. Intraclass correlation coefficients (95% confidence intervals) for PFAS measured over a period of 1-5 years[a] and 10-18 years[b].

PFAS	1-5 years N = 63	10-18 years N = 147
PFOA	0.80 (0.68, 0.88)	0.58 (0.49, 0.67)
PFOS	0.66 (0.48, 0.78)	0.16 (0.05, 0.27)
PFOSA	0.48 (0.24, 0.65)	-0.01 (-0.11, 0.10)
PFNA	0.77 (0.64, 0.86)	0.14 (0.03, 0.26)
PFHxS	0.91 (0.85, 0.94)	0.71 (0.64, 0.77)
PFDeA	0.49 (0.26, 0.67)	0.15 (0.04, 0.27)
Me-PFOSA	0.35 (0.09, 0.56)	-0.11 (-0.20, -0.01)
Et-PFOSA	0.69 (0.53, 0.81)	-0.44 (-0.47, -0.40)

[a] Median first and last year of measurement for individuals observed for 1-5 years = 1992, 1995

[b] Median first and last year of measurement for individuals observed for 10 -18 years = 1991, 2008

Table 2-4. Adjusted[a] percent change (95% confidence interval)[b] in chronic disease indicators in association with an interquartile range difference in serum PFAS concentrations from repeated measures models[c].

	TSH N = 154, 122		Total T4 N = 144, 144		eGFR N = 476, 192		BMI N = 477, 192	
PFAS	**% Δ (95% CI)**	**p**	**% Δ (95% CI)**	**p**	**% Δ (95% CI)**	**p**	**% Δ (95% CI)**	**p**
PFOA	-0.48 (-9.68, 9.65)	0.92	-1.18 (-5.12, 2.92)	0.57	-0.83 (-2.44, 0.77)	0.31	-0.96 (-2.67, 0.79)	0.28
PFOS	9.75 (1.72, 18.4)	**0.02**	-0.51 (-4.00, 3.1)	0.78	-0.68 (-1.90, 0.54)	0.27	0.21 (-0.96, 1.39)	0.73
PFOSA	-0.14 (-15.4, 17.8)	0.99	-1.29 (-5.80, 3.44)	0.59	0.04 (-1.71, 1.80)	0.96	-0.31 (-1.95, 1.36)	0.72
PFNA	3.41 (-6.42, 14.3)	0.52	3.06 (-0.85, 7.13)	0.13	-1.61 (-3.00, -0.22)	**0.02**	0.65 (-0.73, 2.04)	0.36
PFHxS	1.97 (-7.73, 12.7)	0.71	1.74 (-1.73, 5.33)	0.33	-2.06 (-3.53, -0.59)	**0.01**	0.45 (-1.29, 2.23)	0.61
PFDeA	11.0 (-4.45, 28.8)	0.18	2.51 (-2.94, 8.25)	0.38	-2.20 (-4.25, -0.14)	**0.04**	0.67 (-1.33, 2.71)	0.51
Me-PFOSA	-5.38 (-13.8, 3.82)	0.25	0.12 (-4.27, 4.71)	0.96	1.53 (0.34, 2.73)	**0.01**	-0.52 (-1.64, 0.61)	0.36
Et-PFOSA	3.06 (-7.17, 14.4)	0.58	1.29 (-2.35, 5.05)	0.49	1.23 (-0.07, 2.53)	0.06	-0.15 (-1.23, 0.95)	0.79

N= Observations, subjects

[a] Covariates for adjusted models included age, year of measurement, sex, education, income, and marital status. Models of TSH, Total T4, and eGFR additionally include BMI as a covariate

[b] IQR values of eGFR are interpreted as percent change in eGFR relative to the population median in association with an interquartile range difference in serum PFAS concentrations (median eGFR = 102.8 mL/min per 1.73 m^2)

[c] Total T4 beta estimates were determined using a linear model without repeated measures

Table 2-5. Adjusted[a] percent change (95% confidence interval)[b] in chronic disease indicators in association with an interquartile range difference in serum PFAS concentrations from latent models[c].

	TSH N = 730, 161		Total T4 N = 224, 224		eGFR N = 1223, 192		BMI N = 1227, 192	
PFAS	**% Δ (95% CI)**	**p**	**% Δ (95% CI)**	**p**	**% Δ (95% CI)**	**p**	**% Δ (95% CI)**	**p**
PFOA	-2.29 (-11.5, 7.87)	0.65	0.12 (-2.82, 3.14)	0.94	-0.74 (-2.45, 0.96)	0.39	0.74 (-2.69, 4.29)	0.28
PFOS	1.83 (-6.87, 11.3)	0.69	0.33 (-2.35, 3.08)	0.81	-1.72 (-3.29, -0.15)	**0.03**	1.67 (-1.49, 4.93)	0.73
PFOSA	-1.45 (-12.0, 10.4)	0.80	-0.81 (-4.24, 2.74)	0.65	-1.67 (-3.51, 0.18)	0.08	-3.06 (-6.71, 0.73)	0.72
PFNA	-5.37 (-13.9, 4.05)	0.26	3.02 (0.05, 6.07)	**0.05**	-1.17 (-2.75, 0.41)	0.15	1.55 (-1.73, 4.93)	0.36
PFHxS	0.75 (-8.1, 10.45)	0.87	1.21 (-1.51, 4.01)	0.39	-1.16 (-2.66, 0.35)	0.13	2.04 (-1.06, 5.23)	0.61
PFDeA	-4.53 (-17.1, 9.90)	0.52	1.19 (-3.08, 5.65)	0.59	-0.8 (-3.15, 1.54)	0.50	-0.61 (-5.33, 4.35)	0.51
Me-PFOSA	-5.40 (-14.4, 4.54)	0.28	1.15 (-1.89, 4.29)	0.46	-0.39 (-2.01, 1.24)	0.64	-0.26 (-3.79, 3.40)	0.36
Et-PFOSA	0.14 (-8.41, 9.50)	0.97	1.52 (-1.13, 4.23)	0.27	-0.67 (-2.19, 0.86)	0.39	0.59 (-2.27, 3.54)	0.79

N= Observations, subjects

[a] Covariates for adjusted models included age, year of measurement, sex, education, income, and marital status. Models of TSH, Total T4, and eGFR additionally include BMI as a covariate

[b] IQR values of eGFR are interpreted as percent change in eGFR relative to the population median in association with an interquartile range difference in serum PFAS concentrations (median eGFR = 102.8 mL/min per 1.73 m^2).

[c] Total T4 beta estimates were determined using a linear model without repeated measures

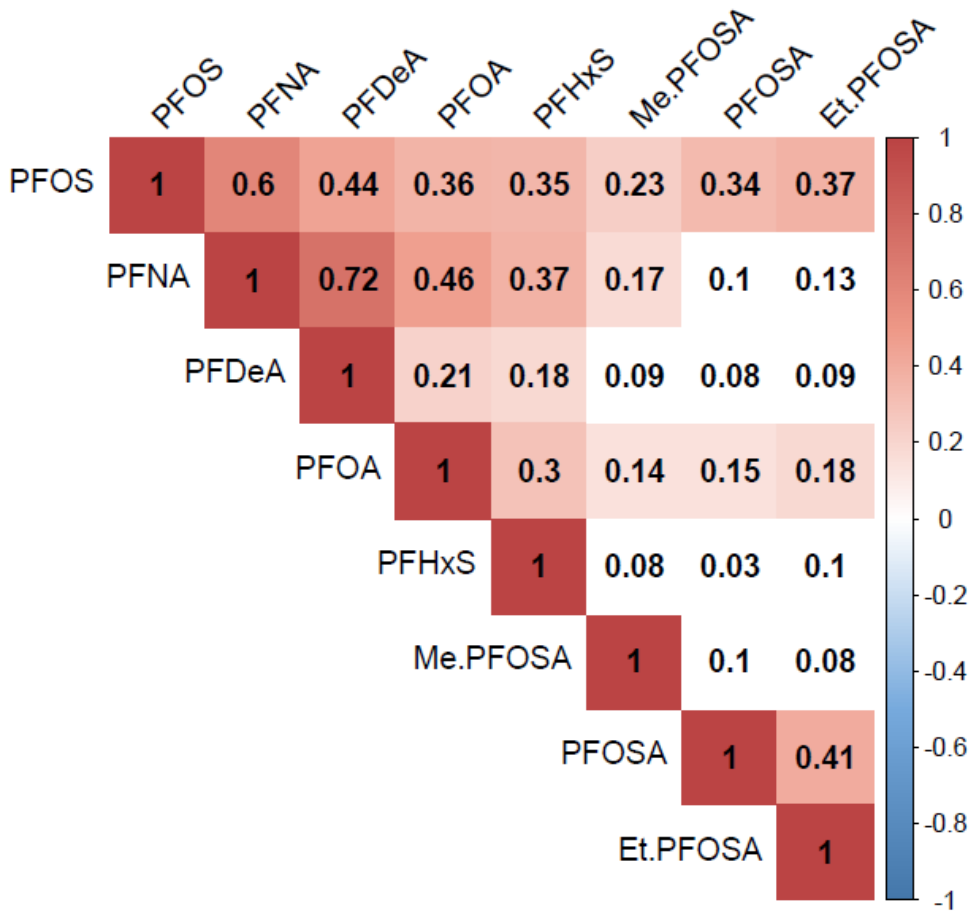

Figure 2-1. Heatmap illustrating the Spearman correlation coefficients of PFAS at first measurement. Correlations with significance are colored (P<0.05) and only positive correlations were detected. Statistically non-significant correlations are uncolored.

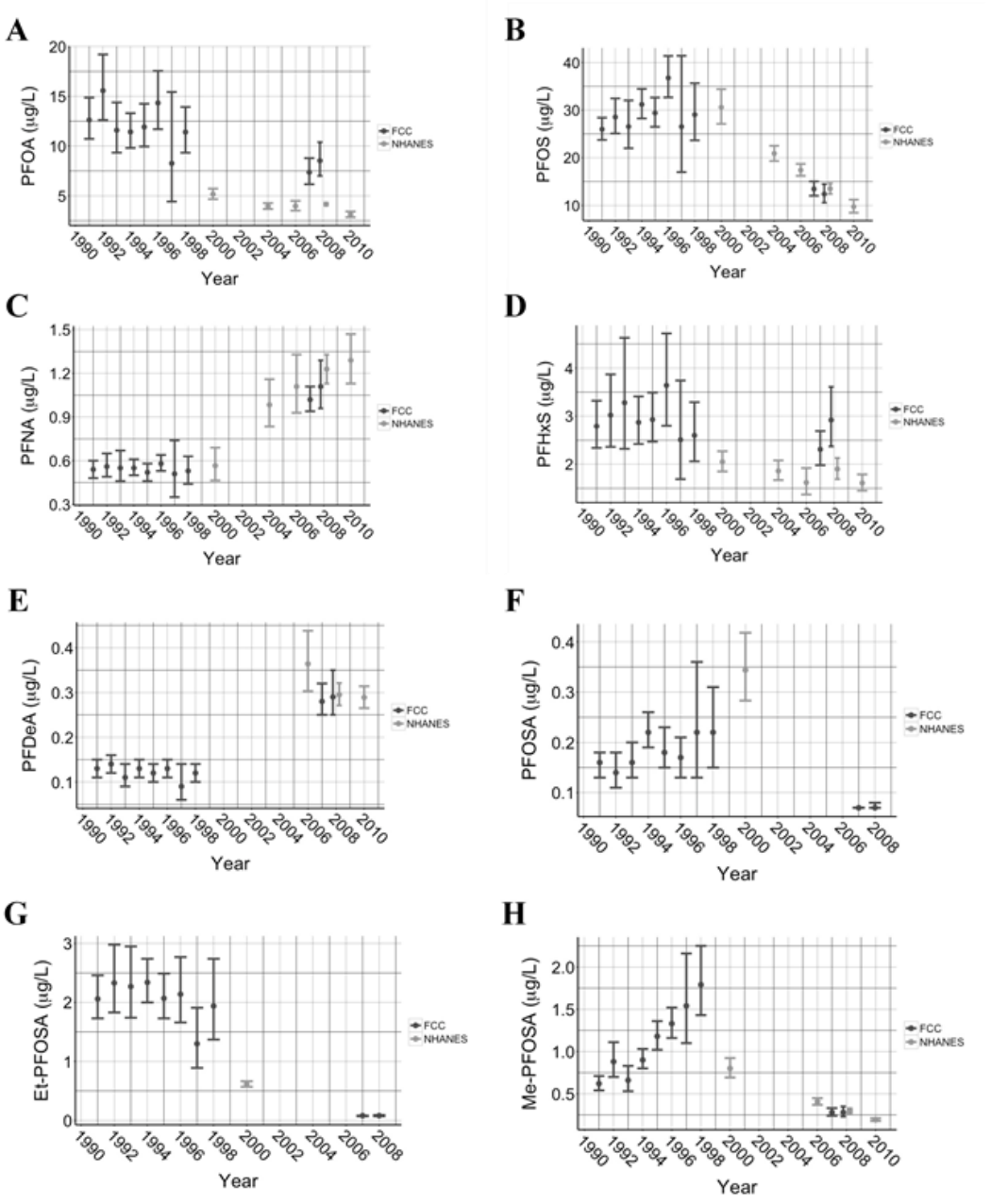

Figure 2-2. Geometric means (GM) for serum concentrations of perfluoroalkyl substances measured in the Fernald Community Cohort compared to national averages obtained from the National Health and Nutrition Examination Survey (NHANES). NHANES data were available for the 1999-2000 (N= 1019), 2003-2004 (N= 1454), 2005-2006 (N= 1480), 2007-2008 (N=1743), and 2009-2010 (N= 1869) cycles for **(A)** PFOA, **(B)** PFOS, **(C)** PFNA, **(D)** PFHxS, **(F)** PFOSA, **(G)** Et-PFOSA, and **(H)** Me-PFOSA. NHANES data were available for **(E)** PFDeA for all cycles except 1999-2000. Note: NHANES did not report GM for years when too great a proportion of measurements fell below the limit of detection (2003-2004: PFOSA, PFDeA, Et-PFOA, and Me-PFOSA; 2005-06, 2007-08, & 2009-10: PFOSA, Et-PFOSA). Error bars represent GM ± 95% confidence intervals for FCC (*N* = 9-86) and NHANES (*N* = 1019-1869).

CHAPTER 3: EVALUATION OF MATERNAL, EMBRYO, AND PLACENTAL EFFECTS IN CD-1 MICE FOLLOWING GESTATIONAL EXPOSURE TO PERFLUOROOCTANOIC ACID (PFOA) OR HEXAFLUOROPROPYLENE OXIDE DIMER ACID (HFPO-DA OR GENX) [1]

3.1 Introduction

Perfluorooctanoic acid (PFOA) is a fully fluorinated, eight-carbon synthetic chemical belonging to the class of compounds known as poly- and perfluoroalkyl substances (PFAS). PFAS are used in a wide range of industrial processes and consumer products and are globally ubiquitous, persistent, and detectable in nearly all humans living in industrialized nations (ATSDR 2019; Kato et al. 2011). Although humans are exposed to PFAS through multiple routes, drinking water is one of the most well understood sources of exposure (Hu et al. 2016).

Within the general U.S. population, serum levels of PFOA have declined from a geometric mean of 5.2 ng/mL in 1999-2000 (Centers for Disease and Prevention 2009) to 1.56 ng/mL in 2015-2016 (CDC 2019). This shift is likely the result of efforts by the U.S. Environmental Protection Agency to reduce environmental emissions and to phase out U.S. production and use of PFOA by 2015 (Agency 2006). Similarly, in 2017 the European Union placed restrictions on the production and use of PFOA (EU 2017). Despite such efforts, exposure to PFOA remains a concern due to its long human half-life (~3.5 years; (Olsen et al. 2007)), environmental persistence (Lindstrom et al. 2011), and the fact that longer chain/precursor PFAS

[1] This chapter was adapted from a previously published manuscript in Environmental Pollution. The original citation is as follows: Blake, B.E., Cope H.A., Hall S.M., Keys R.D., Mahler B.W., McCord J.M., Scott B., Stapleton H.M., Strynar M.J., Elmore S.A., Fenton S.E. (2020). Evaluation of maternal, embryo, and placental effects in CD-1 mice following gestational exposure to perfluorooctanoic acid (PFOA) or hexafluoropropylene oxide dimer acid (HFPO-DA or GenX), 13:128.

chemicals can degrade and form PFOA. In response to restrictions on PFOA, manufacturers have increased production on replacement compounds with alternative chemistries aimed at making the compounds less bioaccumulative and with shorter serum half-lives, however toxicity data for these alternative PFAS are limited (Bao et al. 2018).

Hexafluoropropylene oxide dimer acid (HFPO-DA), referred to herein as GenX, is a PFOA replacement compound. GenX, or HFPO-DA, has received intense public scrutiny in North Carolina (U.S.A.) since its discovery in and contamination of the Cape Fear River basin following release from a manufacturing facility (Strynar et al. 2015; Sun et al. 2016a). GenX (or HFPO-DA) has also been measured in the environment in other regions of the U.S. including the Ohio River (Hopkins et al. 2018), as well as in other countries including the Xiaoquing River in China (Brandsma et al. 2018), and the Rhine River in Europe (Heydebreck et al. 2015).

PFAS are detectable in the serum of pregnant women and in cord blood, and the ratio of the concentration of PFOA in maternal serum to cord serum is typically ~1:1 (Kim et al. 2011; Monroy et al. 2008). Maternal exposure to PFOA has been associated with multiple adverse health outcomes, including increased gestational weight gain (Ashley-Martin et al. 2016), pregnancy-induced hypertension (Darrow et al. 2013), preeclampsia (Savitz et al. 2012; Stein et al. 2009), and reduced birth weight (Apelberg et al. 2007; Fei et al. 2007; Johnson et al. 2014; Kobayashi et al. 2017; J. Lam et al. 2014; Rijs and Bogers 2017). Based on a systematic review of the literature and meta-analysis, the shift in birth weight associated with PFOA exposure has been estimated to be -18.9 g birthweight per 1 ng/mL increase in serum PFOA (95% CI: -29.8, -7.9; Johnson et al. 2014).

In mice, the reproductive and developmental effects of gestational exposure to PFOA are well documented. Previous studies have shown gestational exposure to PFOA in mice results in

maternal liver damage (Lau et al. 2006), maternal hypolipidemia (Yahia et al. 2010), and reduced embryo weight (Koustas et al. 2014). It has been estimated from a meta-analysis of data from 8 mouse studies that the shift in mice is -0.023 g pup birthweight per 1 mg/kg body weight/day increase in PFOA dose to pregnant dams (95% CI: -0.29, -0.016; Koustas et al. 2014). In contrast, there is a paucity of data regarding the reproductive and developmental effects of GenX. A previous reproductive and developmental toxicity study of GenX in CD-1 mice determined the no observed adverse effect level (NOAEL) for reproductive toxicity and maternal systemic toxicity (microscopic changes in maternal liver) was 5 mg/kg/day HFPO-DA (GenX; DuPont-18405-1037). A recent study in rats showed limited gestational exposure to HFPO-DA (GenX) resulted in a lowest observed adverse effect level (LOAEL) for disrupted maternal thyroid hormone (LOAEL: 30 mg/kg/day) and lipids (LOAEL: 125 mg/kg/day), upregulated gene expression in PPAR signaling pathways in both maternal and embryo liver (LOAEL: 1 mg/kg/day), and lower body weights in gestationally exposed female offspring (LOAEL: 125 mg/kg/day; Conley et al. 2019). Additional studies examining the reproductive and developmental effects of GenX are needed.

The biological mechanism through which PFOA exerts adverse effects on embryo growth is not known, but the placenta is a suspected target tissue. The placenta is critical for embryo growth and development, and disruptions in placental development or function can lead to adverse outcomes for both maternal and embryo health. Previous animal studies have examined the effect of gestational exposure to PFOA on maternal mammary gland development and embryo growth (Macon et al. 2011; White et al. 2007), but effects on the placenta have yet to be evaluated. The aims of this study were to compare the effects of gestational exposure to PFOA

and a replacement, GenX, on gestational weight gain, embryo growth, liver pathology, and placental development/morphology.

3.2 Methods

3.2.1 Animals

Naïve female CD-1 mice between 7.5 – 15.5 weeks of age from the NIEHS colony were bred in-house on a single night and copulatory plug positive females were identified on embryonic day (E) 0.5. Pregnant dams were singly housed in ventilated polypropylene cages and received nesting materials, NIH-31 diet (Zeigler Bros., Inc., Gardners, PA, USA), and reverse-osmosis deionized water *ad libitum*. Animals were housed in humidity-and-temperature controlled rooms, 25°C and 45–60% average humidity, with standard 12 h light cycles. All animal procedures were approved by the NIEHS Animal Care and Use Committee (ASP #2017-0022).

3.2.2 Dosing Solutions

PFOA (Perfluorooctanoic acid ammonium salt, CAS# 3825-26-1) was purchased from Millipore Sigma (Darmstadt, Germany) and GenX (HFPO-DA; Ammonium 2,3,3,3-tetrafluoro-2-(heptafluoropropoxy)propanoate, CAS# 62037-80-3) was purchased from SynQuest Laboratories (Alachua, FL, USA). PFOA and GenX dosing solutions were prepared in RODI water and administered to mice once daily via oral gavage. Daily doses were administered between 0700 and 0800 and adjusted to the body weight of the mouse based on the previous day's weight at a volume of 0.01 mL per gram body weight (bw). PFOA doses of 5 mg/kg bw/day (high dose) and 1 mg/kg bw/day (low dose) were selected based on previous work that demonstrated a reduction in neonatal weight gain (Lau et al. 2006; White et al. 2007). The dose of 1 mg/kg bw/day PFOA, used in the mouse developmental toxicity study of Lau et al. 2006, provided a lowest effect dose which was used to set the reference dose within the EPA's drinking

water lifetime health advisory level (HAL) of 70 ppt PFOA (822-R-16-005 2016). Given that the state of North Carolina has a provisional health goal of 140 ppt GenX (double the PFOA HAL), we selected doses of GenX (10 mg/kg bw/day, high dose; 2 mg/kg bw/day, low dose) to mirror doses of PFOA previously used in HAL decision making.

3.2.3 Study Design

This experiment was conducted over two blocks (Block 1 and Block 2) to achieve a total of N = 11-13 litters per treatment group and euthanasia timepoint (E11.5 and E17.5). The experimental design of the second block was identical to the first block of the study and experimental methods were similar but expanded upon to include more rigorous and detailed measurements. Copulatory plug positive mice (E0.5) were weighed to obtain a baseline bodyweight and placed into one of five groups. Once all mice were assigned to groups, mean body weights were calculated and a few animals were reassigned so that mean body weights in each group were similar. This was done to avoid confounding effects of baseline bodyweight. Treatment groups were then randomly assigned a color by using a random sequence generator. Experimenters and dosing technicians were blinded to the treatment group to which the color groups corresponded throughout the duration of the study, including at necropsy. Randomly assigned treatment groups included in each block: vehicle control (deionized water only), 1 mg/kg bw/day PFOA, 5 mg/kg bw/day PFOA, 2 mg/kg bw/day GenX, and 10 mg/kg bw/day GenX. Pregnant dams were dosed via oral gavage from E1.5 to E11.5 or from E1.5 to E17.5. The euthanasia timepoints were selected *a priori* to examine effects of gestational PFOA or GenX exposure on embryo and placental growth prior to placental maturation (E11.5) as well as after full placental maturation (E17.5; (Watson and Cross 2005)). The E11.5 early gestation timepoint was selected as it overlaps a critical period of placental development in the mouse where the placenta undergoes vascularization with the uterine wall and chorioallantoic branching of vessels

begins (Watson and Cross 2005). The E17.5 late gestation timepoint was selected so that embryo weight changes that may be related to treatment would be evident.

3.2.4 Necropsy

On the day of necropsy, dams received daily oral gavage between 0700 and 0800, were weighed, and then euthanized humanely by swift decapitation and serum was collected. In Block 1, necropsies were completed from 0800 to 1600 and in Block 2 necropsies were completed from 0800 to 1200. Sera from dams euthanized in Block 1 were snap frozen for internal dosimetry analyses. Sera from Block 2 dams were reserved for clinical chemistry analyses. In both blocks, the uterus was removed, and total implantation sites were counted based on gross observation of an implantation nodule along the uterine horn. Viable embryos, nonviable embryos, and sites of resorption were counted based on gross observation. Embryos were considered viable if they were properly formed, were not pale in color, and were of similar size to neighboring embryos. Embryos that were poorly formed and pale in color (without heartbeat) were considered nonviable. Sites of resorption were defined as a dark red-appearing clot-like nodule apparent on gross observation.

From each uterus, first viable embryos and their matched placentas were collected in succession within a horn and immediately snap frozen (N = 2-5 per litter) and subsequent embryos were collected for growth measurements (N = 2-11 per litter). Additional placentas were collected and placed in 4% paraformaldehyde (PFA) for histological analysis (Block 2 only). Amniotic fluid was collected by needle aspiration from litters euthanized at E11.5 and snap frozen in liquid nitrogen. Embryo livers were collected from litters euthanized at E17.5 and snap frozen in liquid nitrogen. Dam livers were weighed and a portion of the left lateral lobe was placed in 4% PFA for histology and another portion of the same lobe was snap frozen in liquid nitrogen. A third liver section was obtained from Block 2 dams and fixed in McDowell and

Trump's fixative for electron microscopy (EM; McDowell and Trump 1976). Gross lesions were collected when observed and placed in 4% PFA for histology. Dam kidneys were removed, and a cross section was prepared from the right kidney and a longitudinal section was prepared from the left kidney, and both sections were fixed in 4% PFA for histological analysis.

3.2.5 Tissue Preparation/histology/clinical Measures

Dam livers, kidneys, and placentas were trimmed and embedded by the NIEHS Mouse Embryo Phenotyping Core. Tissues collected at necropsy were fixed in 4% PFA for 72 hours, paraffin embedded, and 5 µm sections were prepared and stained with hematoxylin and eosin (H&E). Pathology was evaluated and a pathology review conducted by Susan A. Elmore (DACVP). Pathology reviews were conducted as an informed approach analysis (e.g. "non-blinded" analysis; see Sills et al. 2019). Select tissue slides were scanned using the Aperio AT2 Scanner. Images were then captured for publication using the Aperio ImageScope software. Serum and urine obtained from dams in Block 2 were analyzed using the AU480 clinical chemistry analyzer (Beckman Coulter Inc., Brea, CA, USA). Reagents and calibration standards used to measure alkaline phosphatase (ALP), alanine aminotransferase (ALT), aspartate aminotransferase (AST), blood urea nitrogen (BUN), serum creatinine (Cre), urine creatinine (Ucrea), glucose (Glu), total protein (TP), triglyceride (Trig), high density lipoprotein (HDL), cholesterol (Chol), and albumin (ALB) were purchased from Beckman Coulter Inc. (Melville, NY, USA). Reagents for sorbitol dehydrogenase (SDH), total bile acid (TBA), and micro total protein were purchased from Sekisui Diagnostics (Framingham, MA, USA). The reagent used to measure low density lipoprotein (LDL) was purchased form Diazyme Laboratories (Poway, CA, USA).

3.2.6 Transmission Electron Microscopy

Block 2 dam liver portions stored in McDowell and Trump's fixative (McDowell and Trump 1976) were processed using a Leica EM TP processor. Briefly, samples were rinsed with buffer, post-fixed in 1% osmium tetroxide in 0.1M phosphate buffer, rinsed in distilled water, dehydrated, and embedded in Ply/Bed 812 epoxide resin. Blocks were trimmed and semithin sections (~0.5 um) were stained with 1% toluidine blue O in 1% sodium borate to ascertain areas of interest. Ultrathin sections (90-110 nM) were cut from areas of interest and placed on 200 mesh copper grids, stained with uranyl acetate and lead citrate, and digital images were captured using a Gatan Orius SC 1000 side mount camera attached to a FEI Company Techani T12 transmission electron microscope (TEM). In general, peroxisomes were smaller than mitochondria, round with a dark, electron-dense, granular matrix and surrounded by a single membrane. Mitochondria were round to elongated, had a matrix that was less electron-dense than peroxisomes and contained crista, and were surrounded by an inner and outer membrane. Samples were analyzed by Robert D. Keys, PhD.

3.2.7 Placental Thyroid Hormone Quantification

Thyroid hormones (TH; triiodothyronine, T3; thyroxine, T4; reverse triiodothyronine, rT3) in placenta were analyzed according to the methods described in (Leonetti et al. 2016). Briefly, ~300 mg (207-526 mg) of 2-3 pooled placental tissues of same-sex embryos was homogenized and digested 16h overnight in Pronase Protease, (*Streptomyces griseus*) solution (EMD Millipore Corp, Billerica, MA, USA). Each pooled sample of 2-3 placentas was considered as one biological replicate and included placentas from the same litter, when possible. Three biological replicates were used for each treatment group and each sex. Samples were spiked with an antioxidant solution (containing 37.5 mg/mL each of citric acid, ascorbic acid, and dithiothreitol) and ^{13}C isotopically labeled internal standards (T4, T3 and rT3), and cold

acetone was added to stop the digestion reaction. Samples were vortex mixed and centrifuged three times for 2 min at 10,000 rcf, and the supernatants were collected and combined. Sample pH was adjusted with 6 M hydrochloric acid to pH<2. A liquid-liquid extraction with cyclopentane was performed, and the cyclopentane layer discarded. Briefly, 1 mL of cyclopentane was added to the supernatant and vortexed before the sample was centrifuged for 3 min at 3,000 rcf and the cyclopentane layer discarded, and this was repeated three times. A liquid-liquid extraction with ethyl acetate was performed. Briefly, 3 mL of ethyl acetate was added to the extract and vortexed before being shaken on a plate shaker for 30 minutes, centrifuged for 3 min at 3,000 rcf, and the ethyl acetate layer collected, and this was repeated three times. Ethyl acetate extracts were dried down to 50 µL under a gentle nitrogen stream and resuspended in 1 mL of 0.01 M hydrochloric acid in 10% methanol. Samples were purified by solid phase extraction using SampliQ OPT cartridges (3 mL, 50 mg; Agilent Technologies, Santa Clara, CA, USA). Final extracts in 400 µL of 1:1 methanol:water were filtered using Whatman Mini-UniPrep Syringeless Filters (PTFE, 0.2 µm; GE Healthcare, Piscataway, NJ, USA). Extracts were analyzed on an Agilent HPLC Model 1260 with a Phenomenex (Torrance, CA, USA) Synergi 50 mm x 2 mm Polar-RP column (2.5 µm) coupled to an Agilent Model 6460 tandem mass spectrometer with electrospray ionization (HPLC-MS/MS-ESI). Mobile phases consisted of 10 mM formic acid in methanol and 10 mM formic acid in water. Laboratory processing blanks were extracted alongside the placental tissues to monitor background levels. No THs were detected in the blank ssamples. Method detection limits (MDLs) were calculated using a signal to noise value of three for each analyte (T3, T4, and rT3). Values were normalized to the wet weight of placenta extracted for a final value of ng hormone / g placenta. Values below the MDL (T4: 0.84 ng/g, T3: 0.42 ng/g, rT3: 0.67 ng/g) were imputed using the

calculation MDL*0.5, and values lacking a quantifiable peak on mass spectrometry were excluded from the analysis.

3.2.8 Internal Dosimetry

Maternal serum, maternal liver, amniotic fluid, and whole embryos were analyzed for PFOA and GenX concentrations using methods similar to those previously reported (Conley et al. 2019; McCord et al. 2018; Reiner et al. 2009; Rushing et al. 2017). Solid tissues were homogenized in RODI water at a ratio of approximately 1:3 tissue mass (mg) to liquid volume (µL). Maternal serum, amniotic fluid, and tissue homogenates (25 µL) were spiked with internal standard suspended in 0.1 M formic acid in a denaturation step, followed by a subsequent protein crash using ice cold acetonitrile. Samples were vortex mixed after addition of formic acid and acetonitrile then centrifuged at 10,000xg for 5 min. Extract supernatants were separated using a Waters ACQUITY UPLC (Waters Corporation) fitted with a Waters ACQUITY UPLC BEH C18 Column (130Å; 1.7 µm; 2.1 mm X 50 mm). Detection was performed using a Waters Quattro Premier XE tandem quadrupole mass spectrometer in negative ionization mode. Stable isotopes of PFOA ($^{13}C_3$, MPFOA, Wellington Laboratories) or GenX ($^{13}C_3$, M3HFPO-DA, Wellington Laboratories) were used as internal standards for quantification of vehicle control samples (run against a nine-point calibration curve of 0 – 100 ng/mL) and experimental samples (run against a nine-point calibration curve of 200 – 20,000 ng/mL). Vehicle control and dosed animal samples were quantified for both PFOA and GenX using respective isotope labeled chemicals and calibration curves.

3.2.9 Embryo/placental Growth Metrics

Gross observations were recorded at necropsy. Embryo sex was determined by PCR amplification of the Sry gene (F: 5’ GCTTCAGTAATCTCAGCACCTAGAA 3’, R: 3’ CACATTGGCATGATAGCTCCAAATT 5’) using a snipped portion of tissue (TransnetYX, Inc).

Embryos and their placentas were weighed separately as wet tissue. Images of embryos were obtained on a Leica Z16 APO imaging scope and embryo length was measured as snout-to-rump distance using FIJI (Schindelin et al. 2012) and Zen 2 Blue (Zeiss, Germany).

3.2.10 Statistical Analysis

Data were analyzed in R (version 1.1.456). Sample sizes for each endpoint are reported in the accompanying figure legends or tables. A threshold of $P < 0.05$ was used for determining statistical significance unless otherwise noted. Analyses combining data from both experimental blocks were performed after verifying the absence of experimental block effects. Single observation dam outcomes (e.g. liver weight, relative liver weight, implantation sites, resorptions, viable embryos, and internal dose metrics) were analyzed by analysis of variance using the *lme4* (Bates et al. 2014) and *lmerTest* packages (Kuznetsova et al. 2017). Simultaneous tests for general linear hypotheses were corrected for multiple comparisons of means using Tukey contrasts in the package *multcomp* (Hothorn et al. 2009).

For all statistical tests adjusting for litter size as a fixed effect in the model, litter size was defined as the number of viable embryos. Gestational weight gain on the day of sacrifice was adjusted for litter size using a general linear model. To compare gestational weight gain growth curves, gestational weight gain was measured as the percent change in body weight compared to E0.5 and analyzed using mixed effects models controlling for litter size and accounting for repeated measures of dams over time.

Embryo and placental metrics were analyzed using mixed effect models and included *a priori* fixed effects of treatment group and litter size and a random effects term for the dam using the lme4 package. Embryo and placental metrics included: embryo weight, embryo length, placental weight, and embryo:placenta weight ratios, a meaningful predictor of fetal birth outcomes in humans (Hayward et al. 2016). To account for potential introduction of random

effects, the study block (Block 1 or Block 2) and experimenter handling of embryo/placental tissues (Experimenter A or Experimenter B) were included as additional random effects. Models were fit in a stepwise procedure for random effects and final models included treatment group and litter size as fixed effects using the *lmerTest* package (Kuznetsova et al. 2017). All final models included dam as a random effect but were allowed to vary in inclusion of experimenter and experimental block random effects based on likelihood ratio test results. Point estimates and 95% confidence intervals were determined from the final model using the Wald method. The number of individual observations for each outcome (embryo weight, placenta weight, embryo:placental weight ratio) and the number of litters evaluated in the mixed effect models is shown in Table A2-1.

To document the effects of PFOA and GenX on the placenta, placentas were assessed for histopathological lesions in 5-6 litters per treatment group for both timepoints, with an average of 7 individual placentas evaluated per litter. Analyses of histopathological data included placentas collected from viable embryos and excluded fused placentas and placentas collected from sites of resorption, which did not occur more frequently than at expected background levels in this strain. Histopathological lesions of evaluated placenta were evaluated using two statistical approaches. The first approach assumed the absence of litter effects and considered each placenta evaluated within a treatment group to be a totally independent observation, regardless of its litter of origin. These data were analyzed as counts using a generalized linear model with a Poisson regression using the package *lme4* (Bates et al. 2014). The second approach considered the litter as the biological unit and compared the relative incidence of placental lesions (e.g. % within normal limits) to adjust for differences in the total number of observations across litters within and between treatment groups. These data were analyzed using a linear model. Both approaches

were subjected to simultaneous tests for general linear hypotheses to correct for multiple comparisons using Tukey contrasts in the package *multcomp* (Hothorn et al. 2009).

Thyroid hormone concentrations in the placenta were quantified and the ratios of T3:T4 and rT3:T4 in E17.5 placentas were assessed to evaluate potential disruption of peripheral thyroid hormone control (e.g. impacts on thyroid deiodinase activity). Each endpoint was analyzed for sex*treatment interaction or for an overall effect of sex. Placenta thyroid hormones were analyzed by analysis of variance using *lme4* (Bates et al. 2014). Simultaneous tests for general linear hypotheses were corrected for multiple comparisons of means using Tukey contrasts in the package *multcomp* (Hothorn et al. 2009). Placental thyroid hormones and their ratios were initially analyzed with embryo sex as an interaction term in the model, with dose group as the predictor variable. Inclusion of a sex interaction or sex covariate in the final model was examined in a stepwise fashion. Internal dosimetry data were analyzed by analysis of variance. Simultaneous tests for general linear hypotheses were corrected for multiple comparisons of means using Tukey contrasts in the package *multcomp* (Hothorn et al. 2009).

3.3 Results

3.3.1 Internal Dosimetry

Maternal serum, maternal liver, amniotic fluid (E11.5 only), and whole embryo dosimetry varied based on compound, dose, and timepoint. Urine collection was attempted at necropsy of pregnant dams exposed to GenX but was unable to be consistently collected in sufficient volume for dosimetry analysis. Concentrations of GenX in the serum of dams exposed daily to 10 mg/kg of GenX was equivalent to the concentration of PFOA in serum of dams exposed to 5 mg/kg/day of PFOA at E11.5 (118.1 ± 10.4 µg GenX/mL serum and 117.3 ± 20.6 µg PFOA/mL serum, respectively; Figure 3-1A & B, Table A2-2). In contrast, GenX accumulation in the serum of dams exposed to 2 mg/kg/day GenX was 32% higher than the

accumulation of PFOA in serum of dams exposed to 1 mg/kg/day PFOA (33.5 ± 15.7 µg GenX/mL serum and 25.4 ± 3.7 µg PFOA/mL serum, respectively; Figure 3-1A & B, Table A2-2). Serum levels of either dose of PFOA or GenX measured at E17.5 were lower from those measured at E11.5 (Figure 3-1A & B, Tables A2-2 & A2-3). This could be explained by a dilution effect caused by blood volume expansion over the course of gestation or may be due to increased transfer to embryos over time.

Accumulation of PFOA in the maternal liver was greater than accumulation of GenX, regardless of dose level or collection timepoint (Figure 3-1C & D, Tables A2-2 & A2-3). While maternal serum levels of PFOA or GenX were surprisingly roughly equivalent at E11.5 in dams exposed to PFOA or GenX, respectively, the accumulation of PFOA in the maternal liver was markedly higher in mice exposed to PFOA than the accumulation of GenX in liver of mice exposed to GenX (Figure 3-1C & D, Tables A2-2 & A2-3). It appeared that bioaccumulation of PFOA in the liver had reached a maximum of approximately 160 - 180 µg PFOA/g liver by E17.5 regardless of PFOA dose group (Figure 3-1C & Table A2-3). When comparing across low (1 mg/kg/day PFOA vs 2 mg/kg/day/GenX) and high (5 mg/kg/day PFOA vs 10 mg/kg/day GenX) dose groups at each time point, the fold-change comparing GenX accumulation in the liver to the PFOA accumulation in the liver was: 7.6-fold lower (2 mg/kg GenX vs 1 mg/kg PFOA, E11.5), 8.9-fold lower (10 mg/kg GenX vs 5 mg/kg PFOA, E17.5), 11.2-fold lower (10 mg/kg GenX vs 5 mg/kg PFOA, E17.5), and 39.7-fold lower (2 mg/kg GenX vs 1 mg/kg PFOA, E17.5; Figure 3-1C & D, Tables A2-2 & A2-3). Unlike PFOA, GenX did not significantly bioaccumulate further in dam livers between E11.5 and E17.5 (Figure 3-1D, Tables A2-2 & A2-3).

Amniotic fluid concentrations of PFOA and GenX were roughly equivalent when comparing the accumulation in dams exposed at the high (5 mg/kg/day PFOA vs 10 mg/kg/day GenX) and low doses (1 mg/kg/day PFOA vs 2 mg/kg/day GenX; Figure 3-2A & C, Table A2-2). Comparing across PFOA and GenX dose groups, embryo accumulation at E11.5 was greatest in mice exposed to 10 mg/kg/day GenX (3.21 ± 0.5 µg/g), followed by mice exposed to 5 mg/kg/day PFOA (2.34 ± 0.3 µg/g), 2 mg/kg/day GenX (0.91 ± 0.2 µg/g), and 1 mg/kg/day PFOA (0.80 ± 0.10 µg/g; Figure 3-2B & 3-2D, Table A2-2). At E17.5, embryo accumulation was not different between sexes for either compound at the doses tested (Figure 3-2B & 3-2D, Table A2-3). Concentrations of PFOA or GenX in embryos was greater when measured at E17.5 than at E11.5, suggesting accumulation of both compounds over time in the embryo regardless of the shorter half-life of GenX (Figure 3-2B & 3-2D, Tables A2-2 & A2-3).

3.3.2 Maternal Outcomes

Gross anomalies were visually evident in some dams upon necropsy; excess abdominal fluid, edematous tissues, clotted placentas, and two fetuses attached to a single placenta were noted. However, these findings were unexpected *a priori*, thus were not looked for in each animal, were not reported by dose group, and require further investigation in future studies.

Mean dam body weights at E0.5 were similar across all treatment groups, including PFOA and GenX, for either sacrifice timepoint and did not differ from vehicle controls (Table 3-1). The relative change in dam body weight from E0.5 to the time of collection (% change in weight; gestational weight gain [GWG]) was significantly greater after exposure to 10 mg/kg/day GenX at E11.5 (7.4% greater body weight gain at E11.5 relative to vehicle controls, $P < 0.05$; Table 3-1). The number of implantation sites, viable embryos, nonviable embryos, and resorptions did not significantly differ among treatment groups, including PFOA and GenX, at either timepoint relative to the vehicle controls, although 10 mg/kg/day GenX treated dams had

fewer implantation sites and viable embryos at E17.5 (Table A2-4). When controlling for litter size, relative GWG was significantly greater than controls in 10 mg/kg/day GenX treated mice (E11.5: 7.1% greater compared to controls; E17.5: 19.1% greater compared to controls) and 5 mg/kg/day PFOA treated mice (E17.5: 14.5% greater compared to controls; Table A2-5). Effect estimates from mixed effect models adjusting for repeated measures of relative GWG (dataset shown in Figure 3-3C), litter size, and gestational/embryonic day showed significantly higher relative GWG in mice exposed to 10 mg/kg/day GenX (E11.5 and E17.5, Figure 3-3A & B), 2 mg/kg/day GenX (E17.5, Figure 3-3B), and 5 mg/kg/day PFOA (E17.5, Figure 3-3B).

Dam liver weights were significantly higher in all treated groups compared to vehicle controls at E11.5 (Table 3-1). At E17.5, absolute liver weights of dams were significantly higher in the 5 mg/kg/day PFOA, 2 mg/kg/day GenX, and 10 mg/kg/day GenX treatment groups compared to vehicle controls (Table 3-1). Dam relative liver weight (as a percent of body weight) was significantly higher in both PFOA and GenX treatment groups relative to vehicle controls at E11.5 and E17.5 (Table 3-1). At E11.5, vehicle control livers exhibited either normal hepatocellular features with uniform hepatocellular size and cytoplasmic glycogen or minimal centrilobular hepatocellular hypertrophy with decreased glycogen, consistent with pregnancy at this stage of gestation. At E17.5, vehicle control livers exhibited hepatocellular changes consistent with pregnancy at this stage of gestation (minimal to mild centrilobular hepatocellular hypertrophy with karyomegaly, increased mitotic figures, decreased glycogen, and increased basophilic granular cytoplasm (Figure 3-4A & 3-5A). Compared with their respective controls, all livers (100% incidence) from both PFOA and GenX treated dams at E11.5 and E17.5 showed a variety of adverse outcomes (Figure A2-1), including some degree of cytoplasmic alteration, characterized by varying degrees of hepatocellular hypertrophy with decreased glycogen and

intensely eosinophilic granular cytoplasm (Figures 3-4C & 3-4E, 3-5C & 3-5E; Table A2-6 & A2-7). As the severity increased, there was extension of the cytoplasmic alteration into the midzonal and periportal regions. As the cytoplasmic alteration increased in severity, there was an observed decrease in mitoses and increase in apoptotic cell death (Figures 3-4E & 3-5E). A few livers from exposed animals contained focal regions of classic necrosis. Incidence of liver lesions and vacuolation are reported in Tables A2-6 & A2-7.

Histopathological liver findings from a subset of E17.5 dams, including all dose groups for PFOA, GenX, and vehicle controls for comparison, were further evaluated using transmission electron microscopy (TEM). All vehicle control livers exhibited normal ultrastructure for this stage of gestation. In the centrilobular regions with hepatocellular hypertrophy there was abundant glycogen, prominent rough endoplasmic reticulum (RER) with abundant ribosomes, numerous lysosomes, and minimal vacuolation with vacuoles often containing remnant membrane material as myelin figures (Figures 3-4B and 3-5B). Livers from mice exposed to 1 mg/kg/day PFOA exhibited enlarged hepatocytes with increased cytoplasmic organelles consistent with mitochondria and peroxisomes, evenly dispersed glycogen and small vacuoles in the centrilobular regions (Figure 3-4D) compared to vehicle controls. Livers from mice exposed to 5 mg/kg/day PFOA exhibited abnormal ultrastructure with abundant organelles consistent with mitochondria and peroxisomes, highly prevalent cytoplasmic vacuolation, reduced RER with fewer ribosomes, and less abundant glycogen (Figure 3-4F). Livers from mice exposed to 2 mg/kg/day GenX exhibited abnormal ultrastructure with enlarged hepatocytes containing more abundant cytoplasmic organelles consistent with mitochondria and peroxisomes, and vacuolation (Figure 3-5D). Livers from mice exposed to 10 mg/kg/day GenX exhibited abnormal ultrastructure with enlarged hepatocytes containing abundant organelles consistent with

mitochondria and peroxisomes, and prevalent vacuolation often with remnant membrane material as myelin figures, abundant RER with few ribosomes present, and unevenly dispersed glycogen appearing as clustered clumps (Figure 3-5F). At the level of TEM, PFOA and GenX generally caused a variety of cellular alterations: increased vacuolation, increased numbers of cytoplasmic organelles consistent with mitochondria and peroxisomes, reduced glycogen stores and reduction of RER ribosomes (Figure A2-2). Marked clumping of glycogen was a unique observation in livers of mice exposed to 10 mg/kg/day GenX, likely a secondary effect due to abundant mitochondria, peroxisomes, and RER.

Kidney weights and relative kidney weights of dams exposed to either dose of PFOA or GenX did not differ from vehicle controls at E11.5 (Table 3-1). At E17.5, 10 mg/kg/day GenX exposed mice exhibited higher kidney weight relative to vehicle controls (both absolute kidney weight and relative kidney weight; Table 3-1). Kidney cross sections and longitudinal sections were histopathologically evaluated at E11.5 and E17.5 timepoints, and diagnoses were made with no threshold: cortical glomeruli; cortical and medullary tubules; papillary collecting ducts; parenchyma; and vascular tree including renal artery, interlobar artery, interlobular artery, arcuate artery, and renal veins. Kidneys from vehicle control and treated animals were histologically within normal limits.

3.3.3 Clinical Chemistry

Dam serum triglyceride levels were significantly lowered at E11.5 across all treatment groups compared to controls in a dose-response manner (5 mg/kg/day PFOA and 10 mg/kg/day GenX lowered triglycerides by 58% and 61%, respectively; 1 mg/kg/day PFOA and 2 mg/kg/day GenX lowered triglycerides by 37% and 43%, respectively; Table 3-2). At E17.5, dam serum triglycerides were significantly lower in 5 mg/kg/day PFOA and 10 mg/kg/day GenX treated mice (66% lower and 74% lower, respectively; Table 3-3).

At E11.5, serum glucose levels in dams exposed to 5 mg/kg/day PFOA and 10 mg/kg/day GenX were lower relative to controls (20% and 18% lower, respectively), but this shift did not reach statistical significance (Table 3-2; $P = 0.06$ and $P = 0.20$, respectively). By E17.5, serum glucose remained lower in 5 mg/kg/day PFOA and 10 mg/kg/day GenX exposed mice, but this shift was also not statistically significant (Table 3-3; $P = 0.41$ and $P = 0.42$, respectively).

At E11.5, dams exposed to 2 mg/kg/day GenX exhibited higher cholesterol and high density lipoprotein (HDL) compared with controls (66% and 56% higher, respectively; Table 3-2). E11.5 dams exposed to 5 mg/kg/day PFOA and 10 mg/kg/day GenX similarly exhibited higher cholesterol and HDL levels relative to controls, but this shift did not reach statistical significance ($P = 0.42$ and $P = 0.42$, respectively; Table 3-3). By E17.5, treatment related effects on cholesterol and HDL appeared to be generally attenuated (Table 3-3). At E17.5, mice exposed to 5 mg/kg/day PFOA and 10 mg/kg/day GenX exhibited lower LDL (50% lower and 31% lower, respectively), but only the shift in PFOA-exposed mice was significant (Table 3-3).

Dams exposed to 5 mg/kg/day PFOA and 10 mg/kg/day GenX exhibited higher alanine aminotransferase (ALT) relative to controls (a 172% increase and a 200% increase, respectively), but these shifts were not statistically significant with *post hoc* corrections (Table 3-2). By E17.5, treatment group related effects on ALT were attenuated. At E17.5, dams exposed to 5 mg/kg/day PFOA exhibited lower serum albumin, increased aspartate aminotransferase (AST), increased sorbitol dehydrogenase (SDH), and lower total serum protein relative to controls (Table 3-3). Similar shifts occurred in mice exposed to 10 mg/kg/day GenX with respect to AST, SDH, and total protein, but were not statistically significant (Table 3-3). Overall, GenX and PFOA liver pathology was consistent across dose groups and time points (100% incidence of cytoplasmic

alteration, Table A2-6 & S7) while changes in ALT, AST, and SDH measurements were not statistically significant across all GenX or PFOA dose groups or time points.

3.3.4 Embryo and Placenta Outcomes

Although the number of implantation sites, viable embryos, nonviable embryos, or resorptions did not significantly differ across treatment groups at E11.5 or E17.5 (Table A2-4), we evaluated embryos and their placentas for differences in weight. At E11.5, there were no significant differences in viable embryo weight, placental weight, or embryo:placental weight ratios across treatment groups relative to vehicle controls (Table A2-8). At E17.5, significantly lower viable embryo weight was observed in 5 mg/kg/day PFOA treated mice (5 mg/kg/day PFOA embryos were 129 mg lower in body weight than vehicle control embryos based on mixed effect model estimates; Figure 3-6A & Table A2-8). At E17.5, placental weight was significantly higher in 5 mg/kg/day PFOA and 10 mg/kg/day GenX treated mice relative to vehicle controls (an estimated 21 mg and 15.5 mg increase in placental weight relative to controls, respectively; Figure 3-6B & Table A2-8). Embryo:placental weight ratios (mg:mg) were significantly reduced relative to controls in 5 mg/kg/day PFOA and 10 mg/kg/day GenX treated mice at E17.5 (Figure 3-6C & Table A2-8).

At E11.5, placental lesions were relatively sparse and mostly included labyrinth atrophy, labyrinth necrosis, or early fibrin clot formation. At E11.5, there were no differences in the incidence of placentas within normal limits (WNL) across treatment groups (Table A2-9). At E17.5, placental abnormalities were observed in all treatment groups and tended to occur as litter-specific effects (e.g. most or all placenta within one litter were affected), and the most common lesions included labyrinth congestion (Figure 3-7B), labyrinth atrophy (Figure 3-7C), early fibrin clots (Figure A2-3A), labyrinth necrosis (Figure 3-7D), and placental nodules (Figure A2-3B). Placental nodules were most likely resorption of an adjacent twin. Placentas of mice

exposed to 5 mg/kg/day PFOA exhibited labyrinth congestion as the most common lesion whereas placentas of mice exposed to either 2 mg/kg/day or 10 mg/kg/day GenX primarily exhibited atrophy of the labyrinth (Figure 3-8 & Table A2-10). Early fibrin clots were most common in placentas of mice exposed to 10 mg/kg/day GenX (Figure 3-8 & Table A2-10). At E17.5, placentas WNL were significantly lower in mice exposed to 5 mg/kg/day PFOA or 10 mg/kg/day GenX when all evaluated placentas were considered as independent observations (regardless of litter of origin; Table A2-10). Placental lesions were also evaluated to account for litter effects by using the proportion of placenta within a litter that were WNL (% WNL). Comparing placenta using this method showed a reduction in placenta WNL in mice exposed to 5 mg/kg/day PFOA, 2 mg/kg/day GenX, and 10 mg/kg/day GenX (Table A2-10).

3.3.5 Placental Thyroid Hormones

For all placental thyroid hormone endpoints, sex*treatment interaction and sex as a covariate did not significantly influence model fit and were not incorporated in the final linear model (Table A2-11). Placentas exposed to 10 mg/kg/day GenX had significantly higher T4 relative to controls (60% increase; Table 3-4). This effect occurred in both male and female placentas, but statistical significance was attenuated *post hoc* in sex-stratified models likely due to low sample sizes. There was a trend towards a significant effect of higher T4 in placentas exposed to 2 mg/kg/day GenX (38% increase, Table 3-4), but this effect was attenuated after applying *post hoc* corrections for multiple tests. Similarly, a trend towards lower T3:T4 ratio was observed in placentas exposed to 10 mg/kg/day GenX, but this effect was attenuated after applying *post hoc* corrections. There were no other significant effects of sex or treatment on placental rT3, T3, T3:T4 ratio, or rT3:T4 ratio.

3.4 Discussion

Our prior work in mice has consistently shown reduced birthweight resulting from gestational exposure to PFOA (Macon et al. 2011; White et al. 2007), but we did not examine effects on the placenta, a critical organ that facilitates embryo growth, nor did we examine the effects of replacement PFAS congeners. Here we present evidence consistent with previous reports of PFOA-reduced embryo growth and provide novel evidence indicating that the pregnant dam liver and placenta are sensitive targets of both PFOA and a replacement PFAS, GenX. Adverse placental and maternal effects were most prominent in late gestation (E17.5) in mice gestationally exposed to 5 mg/kg/day PFOA and 10 mg/kg/day GenX, but 2 mg/kg/day GenX also exhibited significant effects on maternal liver and placenta. Future studies should investigate adverse effects at doses lower than 2 mg/kg/day GenX to determine more precise percent responses at different lower dose levels using a benchmark dose approach.

It is well documented in humans and animal models that PFAS readily pass from maternal serum to the developing embryo via the placenta (Chen et al. 2017b; Yang et al. 2016a; Yang et al. 2016b) and that PFOA transplacentally transfers to the mouse offspring (Fenton et al. 2009). Here we report transplacental transfer of both PFOA and GenX, higher placenta weight, higher incidence of placental lesions, and lower embryo-placenta weight ratios in mice exposed to 5 mg/kg/day PFOA or 10 mg/kg/day GenX.

In humans, placental weight and placental-to-fetal (also reported as feto-placental) weight ratios are clinically relevant endpoints that have been associated with adverse pregnancy outcomes (Hutcheon et al. 2012; Risnes et al. 2009; Thornburg et al. 2010). The placenta is a critical organ that mediates the transport of nutrients, oxygen, waste, and xenobiotics between mother and embryo, and it is rarely evaluated in reproductive toxicity studies. We chose the placenta as a focal endpoint due to its importance in studies of human pregnancy outcomes

(Hutcheon et al. 2012; Risnes et al. 2009), its role as a programming agent of latent health outcomes in both the mother and child (Thornburg et al. 2010), and our own hypothesis that it is a key target tissue of PFAS.

Placental insufficiency (PI) occurs when functional capacity of the placenta is limited or deteriorates, resulting in reduced transplacental transfer of oxygen and nutrients to the fetus (Gagnon 2003). Reduction or impairment of placental blood flow (Chaddha et al. 2004), aberrant fibrin depositions or other thrombo-occlusive damage in the placenta (Chaddha et al. 2004), and disruption of maternal-placental thyroid hormones (Belet et al. 2003) are all believed to contribute to PI pathogenesis in women. We provide evidence illustrating pathological and physiological features that are concordant with PI in our experimental mouse model. Here we show maternal exposure to PFOA or GenX induced atrophy, necrosis, and congestion of the murine placental labyrinth (suggestive of impaired transplacental transfer of nutrients and/or oxygen), aberrant formation of early fibrin clots, and disruption of placental thyroid hormones (GenX only). These data are suggestive of a PI phenotype induced by maternal exposure to PFAS in mice that deserves further investigation.

In epidemiological studies, disproportionately large placentas increase risk for adverse health outcomes in neonates (Hutcheon et al. 2012) and adult offspring (Risnes et al. 2009). The placenta influences cardiovascular disease (CVD) risk in the offspring (Risnes et al. 2009), and the functional capacity of the placenta is likely the driver of fetal heart fitness (Thornburg et al. 2010). Placentas that are disproportionately large relative to fetal size tend to exhibit reduced functional capacity with respect to optimal blood flow and vascular resistance (Risnes et al. 2009; Salafia et al. 2006), which could lead to both adverse perinatal (Hutcheon et al. 2012) and adult CVD outcomes (Thornburg et al. 2010). Here we show higher placenta weights that were

disproportionate to embryo weights in mice exposed to PFOA and GenX. Whether the increased placental weight is due to pathological changes or is a compensatory mechanism to protect the developing fetus is not known. The extent to which gestational exposure to these environmental contaminants could adversely impact perinatal and adult offspring health outcomes, especially cardiovascular outcomes, should be the focus of future studies.

A previous report has shown dose-dependent necrotic changes in placenta of mice exposed to 10 mg/kg/day and 25 mg/kg/day PFOA, and pup mortality and gestational weight loss were evident (Suh et al. 2011). Here, placental lesions in mice exposed to 2 mg/kg/day GenX, 10 mg/kg/day GenX, and 5 mg/kg/day PFOA at E17.5 occurred at a significantly higher incidence compared to controls, and the labyrinth was the specific target. This is significant because maternal-embryo exchange of oxygen, nutrients, and waste occurs in the placental labyrinth. Adverse placental effects of 5 mg/kg/day PFOA and 10 mg/kg/day GenX occurred at both the litter level as well as across all placenta evaluated, regardless of litter, and adverse placental effects of 2 mg/kg/day GenX were significant when considered at the level of the litter as a unit. The lowest doses tested in this study resulting in adverse placental pathology were 2 mg/kg/day GenX and 5 mg/kg/day PFOA. Given that maternal serum accumulation and embryo deposition of PFOA and GenX were similar at the high (5 mg/kg PFOA vs 10 mg/kg GenX) and low doses (1 mg/kg PFOA vs 2 mg/kg GenX), and that the placenta is at the interface between these two compartments, the disparate patterns in adverse placenta histopathology suggest that the placenta may be more sensitive to the effects of GenX vs. PFOA. The mechanisms of toxicity towards the placenta may also differ between the two PFAS and will be pursued in on-going studies.

Thyroid hormones (TH) play a critical role in neurodevelopment (de Escobar et al 2004; Porterfield et al 1993). PFAS are hypothesized thyroid disrupters in humans (Coperchini et al. 2017; Webster et al. 2016), including in pregnant women (Ballesteros et al. 2017; Berg et al. 2015; Wang et al. 2014; GM Webster et al. 2014). Generally, maternal PFAS levels during pregnancy are associated with shifts in TH levels consistent with hypothyroidism (e.g. elevated TSH), which is associated with increased risk for low birth weight (Alexander et al. 2017). It is possible that PFAS chemicals exert some adverse effects on embryo growth via TH disruption across the maternal-placental-embryo unit. Indeed, Conley et al. (2019) reported maternal serum total triiodothyronine (T3) and thyroxine (T4) were reduced in rats exposed to 125 – 500 mg/kg/day HFPO-DA (GenX) during gestational days 14-18. Maternal serum THs could not be measured due to volume constraints in our study. As the placenta regulates the degree to which maternal THs pass to the developing fetus, and it maintains the optimal balance of the thyroid hormones throughout embryo development (Chan et al. 2009), the relationship between PFAS-induced maternal TH changes and placental function requires additional study, especially given the role of TH in fetal neurodevelopment.

In a systematic review and meta-analysis of nonhuman evidence for effects of PFOA on birthweight, it was estimated that a 1-unit (1 mg/kg body weight/day) increase in PFOA is associated with a -0.023 g (95% CI: -0.029, -0.016) shift in pup birth weight (Koustas et al. 2014). Here we report a -0.028 g (95% CI: -0.114, 0.586) shift in embryo weight on E17.5 in mice exposed to 1 mg/kg/day PFOA and a -0.129 g (95% CI: -0.215, -0.043) shift in mice exposed to 5 mg/kg/day PFOA. Effects on embryo weight at E17.5 in this study can be summarized as most severe to least severe: 5 mg/kg/day PFOA (-0.129 g), 10 mg/kg/day GenX (-0.042 g), 1 mg/kg/day PFOA (-0.023 g), and 2 mg/kg/day GenX (-0.009 g). An industry study

of CD-1 mice exposed to 5 mg/kg/day HFPO-DA (GenX) from preconception through weaning showed reduced pup weight at PND 1 that persisted through PND 21 with effects more severe in male offspring (DuPont-18405-1037). In rats, mean embryo weights were decreased in rats exposed to 100 mg/kg/day HFPO-DA (GenX) for 15 days of gestation (Edwards 2010a) and in a different study female birth weights were reduced after 5 days of gestational exposure at 125 mg/kg (Justin M Conley et al. 2019). To our knowledge, there are no human data showing associations between maternal GenX exposure and birth weight outcomes.

Several human cohort studies have shown that higher levels of prenatal or early life PFOA exposure is associated with increased adiposity in childhood (Braun et al. 2016; Fleisch Abby et al. 2017) and metabolic disruption in young adulthood (Domazet et al. 2016). Additionally, it is known that low birth weight is associated with adult diseases, including metabolic syndrome in both humans and animals (Barker 2004). Due to the environmental ubiquity of a mixture of PFAS chemicals, it is difficult to unravel the relative contributions of prenatal and postnatal (e.g. chronic, lifelong) exposure and adverse health outcomes. Animal studies allow for discrete measurement of health outcomes associated with specific critical periods of exposure, and future work should investigate metabolic disruption in offspring exposed *in utero*, to provide key insights on the metabolic programming capacity of PFAS.

In the present study, PFOA (5 mg/kg/day) and GenX (2 mg/kg/day or 10 mg/kg/day) exposures resulted in significantly higher gestational weight gain (GWG) in mice, with significant effects emerging at an earlier point in gestation in mice exposed to GenX and occurring at a lower dose than PFOA (2 mg/kg/day GenX vs 5 mg/kg/day PFOA). In contrast, a decrease in mean maternal weight gain was reported in a recent study of gestational exposure to HFPO-DA (GenX) in rats exposed to 250 or 500 mg/kg/day (Conley et al. 2019). Although these

findings are not consistent with the higher gestational weight gain reported here, it is possible that statistical methods (absolute change in maternal weight vs relative change in weight analyzed using repeated measures models), differing windows of exposure (five days during mid to late gestation vs exposure throughout gestation), and interspecies differences in preliminary PFAS elimination rates (GenX elimination half-life in rats ~5h vs ~20h in mice, (Gannon et al. 2016)) could explain these disparate results. Additionally, different elimination rates of the compound make comparison of equivalent or similar external doses a challenge. In fact, dam serum concentrations of rats exposed to 500 mg/kg/day from GD 14-18 reported in Conley et al. (2019) were of similar magnitude to those observed in mice exposed to 10 mg/kg/day throughout gestation in the present study (~100 µg/mL). Similarly, serum concentrations from pregnant mice in the current study exposed to 2 mg/kg/day GenX (HFPO-DA) were roughly equivalent (~33 µg/mL) to serum concentrations obtained from rat dams exposed to 62.5 mg/kg/day HFPO-DA (GenX) in the study by Conley et al. (2019).

Higher GWG observed in our PFOA-exposed mice is consistent with findings reported in humans; interquartile increases in GWG were associated with elevated cord blood levels of PFOA (OR = 1.33; 95% CI: 1.13 – 1.56; (Ashley-Martin et al. 2016)). Similarly, other legacy PFAS compounds such as perfluorooctane sulfonate (PFOS) are positively associated with GWG (Jaacks et al. 2016). However, our data describing the relationship between maternal exposure to GenX and increased GWG in a mouse model are novel. Importantly, higher GWG is associated with adverse outcomes for both mother and infant in humans, including increased risk for pregnancy-associated hypertension (with or without smaller birth weights), gestational diabetes (GD), postpartum weight retention, increased risk for unsuccessful breastfeeding, and increased risk for stillbirth, infant mortality, and preterm birth (Council 2010). These disorders share many

risk factors, but it is not fully understood to what extent their etiologies are interrelated and/or interdependent (Villar et al. 2006), or what mechanisms may be driving them. Our data suggest a need for additional study of the adverse maternal and offspring health outcomes associated with GenX exposure.

Liver toxicity is a consistent finding in animal studies of PFOA (Li et al. 2017) and other PFAS, but studies examining GenX are limited. Here we report similar histopathological findings in livers of exposed pregnant dams to those previously described by our group (and others) in offspring prenatally exposed to PFOA, including increased extent of hepatocellular hypertrophy, cytoplasmic alteration, and increased mitochondria (Filgo et al. 2015; Lau et al. 2006). We hypothesize that the consistent and persistent hepatic cytoplasmic alterations seen following PFAS exposures leads to increased incidence and/or distribution of cell death, which is consistent with the decrease in mitotic figures compared to control liver sections. This constellation of lesions is considered adverse and is incompatible with long-term normal liver function. The maternal liver responds to estrogen produced by the placenta and produces thyroid binding globulin, which in turn regulates the level of maternal circulating thyroid hormones (Nader et al. 2009). Altered maternal liver function due to PFOA or GenX exposure could play an important role in mediating placental and embryo outcomes.

In addition to consistently observed histopathological changes in the liver induced by either PFOA or GenX, maternal clinical chemistry indicated shifts in liver enzymes, including higher ALT (10 mg/kg/day GenX, E11.5), higher ALP (10 mg/kg/day GenX, E17.5), higher AST (5 mg/kg/day PFOA, E17.5), and higher SDH (5 mg/kg/day PFOA, E17.5). Our TEM findings build upon a growing body of evidence demonstrating potential mechanisms of PFAS-

induced hepatic toxicity other than peroxisome proliferating receptor (PPAR) and demonstrate this for the first time with GenX.

In a previous reproductive and developmental toxicity study of HFPO-DA (GenX) in CD-1 mice, 5 mg/kg/day was determined to be the NOAEL for reproductive toxicity and maternal systemic toxicity (based on microscopic changes in maternal liver; DuPont-18405-1037; (Edwards 2010b)). Here we are not able to report a NOAEL as significant adverse effects occurred in the lowest GenX dose group evaluated in this study (2 mg/kg/day). We demonstrate adverse systemic toxicity of dams exposed to 2 mg/kg/day GenX including microscopic alterations in the liver, higher GWG, and higher incidence of placental lesions. Dam serum GenX concentrations obtained at E17.5 in the present study were comparable to dam plasma concentrations reported by DuPont-18405-1037: 22.9 µg/mL (present study, 2 mg/kg/day on E17.5), 36.4 µg /mL (DuPont-18405-1037, 5 mg/kg/day on lactation day 21), and 58.5 µg/mL (present study, 10 mg/kg/day on E17.5; compared in Figure A2-4). However, it should be noted that in the present study at all tested doses of both PFOA and GenX, maternal serum concentrations were higher at E11.5 than E17.5. This could be explained by maternal off-loading of body burden to developing embryos and other maternal tissues (i.e. liver) and rapid expansion of maternal blood volume throughout the course of pregnancy.

There are several limitations to this study regarding experimental design, sample sizes, and interspecies differences. Due to performing the experiment over two experimental blocks, some endpoints were only evaluated from one of the two blocks, limiting statistical power. Some effects may have reached statistical significance with a larger number of observations. The two-block design did not impair the strength of the effect when significant effects were present in endpoints evaluated at both time points, which was verified by statistical analysis. It is possible

that variance in half-life, amount of exposure to these chemicals, and other interspecies differences may limit the human relevance of the findings reported here. Although the mouse and human both have discoid hemochorial placenta, the maternal-placental-embryo unit in mice differs from that in humans in other ways, including the labyrinthine vs villous structure, the number of offspring carried during each pregnancy (~14 vs ~1), and gestation length (~20 days vs ~280 days). Although there are distinct interspecies differences between humans and mice, the outbred CD-1 mouse was selected in the current study due to its genetic diversity. While the CD-1 mouse is sensitive to PFOA, compared to other inbred mouse strains (Tucker et al. 2015), significant treatment-related effects were still detectable despite its greater biologic variability in response. It is not known whether there are strain differences in sensitivity to GenX, which should be investigated in future studies.

3.5 Conclusion

In a comparative reproductive and developmental study in mice of PFOA and a replacement, GenX, we report adverse effects of both compounds against the maternal-embryo-placental unit. Both PFOA and GenX induced elevated GWG, higher maternal liver weights, adverse microscopic pathological changes in the maternal liver, and abnormal histopathological lesions in mature placenta. Importantly, we provide evidence that illustrates GenX (as low as 2 mg/kg/day) significantly affects the maternal-embryo-placental unit differently than its predecessor PFOA, and that this alternative compound may have a unique mechanism(s) of reproductive toxicity in this model system. Lastly, we build a case for the importance of evaluating the placenta as a critical tissue in studies of developmental and reproductive toxicity through utilizing clinically relevant, translational endpoints to illustrate the unique susceptibility of this organ to the adverse effects of GenX

Table 3-1. Maternal indices at embryonic day 11.5 and 17.5 (Mean ± SD, N = 11-13).

Embryonic day	Maternal index	Vehicle Control	1 mg/kg bw/day PFOA	5 mg/kg bw/day PFOA	2 mg/kg bw/day GenX (HFPO-DA)	10 mg/kg bw/day GenX (HFPO-DA)
11.5	E0.5 weight (g)	30.6 ± 5.5	31.2 ± 3	31.1 ± 3.2	29.7 ± 2.2	30.7 ± 2.5
11.5	Weight at necropsy (g)	37.9 ± 4.3	38.8 ± 2.4	40.2 ± 3.5	38.3 ± 3.2	40.0 ± 2.5
11.5	Weight at necropsy (% change from E0.5)	24.9 ± 9.2	24.7 ± 6.3	29.6 ± 6.3	28.9 ± 5.4	32.3 ± 9.6*
11.5	Liver weight (g)	2.2 ± 0.3	2.9 ± 0.2*	4.5 ± 0.5*	3.1 ± 0.2*	4.2 ± 0.5*
11.5	Relative liver weight (% body weight)	5.9 ± 0.7	7.4 ± 0.5*	11.0 ± 0.9*	8.1 ± 0.5*	10.2 ± 0.7*
11.5	Kidney weight (g)	0.20 ± 0.01	0.20 ± 0.02	0.21 ± 0.03	0.22 ± 0.02	0.23 ± 0.06
11.5	Relative kidney weight (% body weight)	0.53 ± 0.01	0.51 ± 0.04	0.51 ± 0.05	0.54 ± 0.04	0.52 ± 0.11
17.5	E0.5 weight (g)	30.5 ± 3.3	28.5 ± 3.8	29.1 ± 3.4	28.2 ± 3.5	28.7 ± 3.6
17.5	Weight at necropsy (g)	56.3 ± 5.6	54.6 ± 5.3	57.4 ± 6.0	55.4 ± 6.5	56.7 ± 5.5
17.5	Weight at necropsy (% change from E0.5)	86.0 ± 22.8	92.6 ± 17.1	98.7 ± 20.2	97.3 ± 15.2	98.5 ± 15.7
17.5	Liver weight (g)	2.7 ± 0.3	3.1 ± 0.4	5.3 ± 0.5*	3.5 ± 0.5*	4.6 ± 0.4*
17.5	Relative liver weight (% body weight)	4.8 ± 0.3	5.6 ± 0.5*	9.3 ± 0.7*	6.3 ± 1.0*	8.1 ± 0.5*
17.5	Kidney weight (g)	0.21 ± 0.02	0.22 ± 0.04	0.24 ± 0.03	0.21 ± 0.02	0.25 ± 0.02*
17.5	Relative kidney weight (% body weight)	0.37 ± 0.04	0.40 ± 0.04	0.40 ± 0.03	0.37 ± 0.02	0.43 ± 0.03*

Note: N = 6-8 for kidney weight and relative kidney weight

* $P < 0.05$ relative to vehicle control (ANOVA with *post hoc* multiple comparison correction using Tukey contrasts)

Table 3-2. Clinical chemistry panel of dam serum at embryonic day 11.5.

Measurement	Vehicle control Mean ± SD, N	1 mg/kg/day PFOA Mean ± SD, N	5 mg/kg/day PFOA Mean ± SD, N	2 mg/kg/day GenX Mean ± SD, N	10 mg/kg/day GenX Mean ± SD, N
ALB (g/dl)	2.48 ± 0.18, 5	2.42 ± 0.22, 5	2.36 ± 0.21, 5	2.75 ± 0.33, 4	2.8 ± 0.17, 3
ALP (U/L)	68.8 ± 13.0, 5	54.6 ± 4.4, 5	56.6 ± 35.6, 5	58.4 ± 9.0, 5	83.0 ± 25.8, 5
ALT (U/L)	26.0 ± 5.6, 5	28.8 ± 11.5, 5	70.8 ± 16.2, 5	24.2 ± 13.7, 5	78.2 ± 62.0, 5
AST (U/L)	63.6 ± 9.9, 5	144.6 ± 167.6, 5	92.6 ± 20.3, 5	69.0 ± 22.0, 5	136.8 ± 138.9, 4
BUN (mg/dl)	16.0 ± 2.1, 5	15.0 ± 2.7, 5	15.8 ± 1.3, 5	18.3 ± 4.6, 4	13.7 ± 1.5, 3
Chol (mg/dl)	56.4 ± 4.6, 5	68.8 ± 18.0, 5	69.4 ± 9.9, 5	93.4 ± 27.8*, 5	77.0 ± 16.4, 4
Cre (mg/dl)	0.21 ± 0.02, 5	0.2 ± 0.05, 5	0.18 ± 0.03, 5	0.2 ± 0.04, 4	0.18 ± 0.02, 3
Glu (mg/dl)	275.2 ± 39.5, 5	278.4 ± 27.8, 5	220.4 ± 22.1, 5	249.3 ± 25.8, 4	226.7 ± 28.9, 3
HDL (mg/dl)	32.2 ± 1.5, 5	34.8 ± 10.9, 5	42.6 ± 4.0, 5	50.2 ± 15.7*, 5	43.3 ± 6.1, 4
LDL (mg/dl)	10.8 ± 1.3, 5	12.2 ± 1.9, 5	10.6 ± 1.5, 5	15 ± 4.8, 4	12.5 ± 1.9, 4
SDH (U/L)	9.4 ± 7.5, 5	8.4 ± 7.8, 5	12.4 ± 8.3, 5	7.0 ± 6.5, 4	8.0 ± 3.65, 4
TBA (µM/L)	2.0 ± 0.71, 5	1.5 ± 0.58, 4	2.0 ± 0.0, 5	1.4 ± 0.55, 5	35.3 ± 67.8, 4
TP (g/dl)	4.22 ± 0.18, 5	4.04 ± 0.3, 5	3.78 ± 0.22, 5	4.5 ± 0.48, 4	4.37 ± 0.29, 3
Trig (mg/dl)	205.6 ± 56.0, 5	130.4 ± 16.2*, 5	86.4 ± 15.8*, 5	117.6 ± 33.9*, 5	80.3 ± 14.4*, 4
Ucrea (mg/dl)	54.4 ± NA, 1	92.0 ± 13.1, 4	50.1 ± 33.8, 4	53.2 ± 14.0, 3	82.9 ± 33.2, 5

Abbr: ALB = Albumin; ALP = Alkaline phosphatase; ALT = Alanine aminotransferase; AST = aspartate aminotransferase; BUN = Blood urea nitrogen; Chol = Cholesterol; Cre = Creatinine; Glu = Glucose; HDL = High density lipoprotein; LDL = Low density lipoprotein; SDH = Sorbitol dehydrogenase; TBA = Total bile acids; TP = Total protein; Trig = Triglycerides; Ucrea = Urinary creatinine

* $P < 0.05$ relative to vehicle control (ANOVA with post hoc multiple comparison correction using Tukey contrasts)

Table 3-3. Clinical chemistry panel of dam serum at embryonic day 17.5.

Measurement	Vehicle control Mean ± SD, N	1 mg/kg/day PFOA Mean ± SD, N	5 mg/kg/day PFOA Mean ± SD, N	2 mg/kg/day GenX Mean ± SD, N	10 mg/kg/day GenX Mean ± SD, N
ALB (g/dl)	2.23 ± 0.21, 4	2.04 ± 0.09, 5	1.53 ± 0.27*, 6	2.32 ± 0.26, 5	2.26 ± 0.3, 5
ALP (U/L)	58.0 ± 7.8, 4	50.2 ± 4.2, 5	74.8 ± 23.8, 6	55.4 ± 11.8, 5	88.8 ± 13.0*, 5
ALT (U/L)	13.0 ± 7.5, 4	7.0 ± 4.3, 5	16.8 ± 7.7, 6	4.4 ± 3.9, 5	9.6 ± 2.1, 5
AST (U/L)	81.0 ± 6.5, 4	73.0 ± 14.0, 5	172.2 ± 63.1*, 6	65.6 ± 12.1, 5	113.2 ± 36.6, 5
BUN (mg/dl)	16.0 ± 2.9, 4	16.4 ± 1.7, 5	18.7 ± 5.3, 6	13.6 ± 1.1, 5	15.2 ± 1.8, 5
Chol (mg/dl)	75.5 ± 11.6, 4	83.8 ± 20.0, 5	68.5 ± 16.4, 6	86.6 ± 17.1, 5	97.4 ± 8.4, 5
Cre (mg/dl)	0.18 ± 0.04, 4	0.2 ± 0.01, 5	0.16 ± 0.06, 6	0.17 ± 0.03, 5	0.15 ± 0.06, 5
Glu (mg/dl)	129.3 ± 11.7, 4	121.0 ± 17.3, 5	112.0 ± 15.8, 6	123.2 ± 13.1, 5	111.6 ± 15.5, 5
HDL (mg/dl)	34.0 ± 10.2, 4	37.2 ± 6.2, 5	38.8 ± 11.2, 6	39.4 ± 8.5, 5	50.0 ± 8.9, 5
LDL (mg/dl)	22.0 ± 0.8, 4	24.0 ± 10.7, 5	11.0 ± 3.0, 5	20.0 ± 3.9, 5	15.2 ± 2.9, 5
SDH (U/L)	5.5 ± 7.9, 4	3.4 ± 6.1, 5	24.3 ± 11.2*, 6	1.2 ± 2.2, 5	11.4 ± 6.8, 5
TBA (µM/L)	3.8 ± 0.96, 4	3.0 ± 1.2, 5	8.0 ± 7.9, 6	4.8 ± 3.0, 5	6.2 ± 4.2, 5
TP (g/dl)	4.2 ± 0.37, 4	3.9 ± 0.11, 5	2.8 ± 0.39*, 6	4.1 ± 0.36, 5	3.9 ± 0.52, 5
Trig (mg/dl)	472.5 ± 78.9, 4	364.0 ± 272.9, 5	159.0 ± 65.5*, 6	257.0 ± 120.3, 5	120.6 ± 31.7*, 5
Ucrea (mg/dl)	25.8 ± 15.8, 2	24.7 ± 23.1, 2	11.5 ± 5.9, 3	18.6 ± 5.1, 4	20.2 ± 15.7, 4

Abbr: ALB = Albumin; ALP = Alkaline phosphatase; ALT = Alanine aminotransferase; AST = aspartate aminotransferase; BUN = Blood urea nitrogen; Chol = Cholesterol; Cre = Creatinine; Glu = Glucose; HDL = High density lipoprotein; LDL = Low density lipoprotein; SDH = Sorbitol dehydrogenase; TBA = Total bile acids; TP = Total protein; Trig = Triglycerides; Ucrea = Urinary creatinine

* $P < 0.05$ relative to vehicle control (ANOVA with post hoc multiple comparison correction using Tukey contrasts)

Table 3-4. Placental thyroid hormone measurements at embryonic day 17.5.

Hormone	Vehicle control Mean ± SD, N (a,b)	1 mg/kg/day PFOA Mean ± SD, N (a,b)	5 mg/kg/day PFOA Mean ± SD, N (a,b)	2 mg/kg/day GenX Mean ± SD, N (a,b)	10 mg/kg/day GenX Mean ± SD, N (a,b)
rT3 (ng/g)	1.2 ± 0.7, 5 (4, 1)	0.7 ± 0.4, 6 (3, 3)	1.4 ± 0.7, 5 (5, 0)	1.7 ± 0.8, 6 (6, 0)	1.6 ± 0.3, 6 (6, 0)
T3 (ng/g)	0.3 ± 0.2, 6 (1, 5)	0.2 ± 0, 6 (0, 6)	0.2 ± 0, 4 (0, 4)	0.3 ± 0.2, 5 (0, 5)	0.2 ± 0, 6 (0, 6)
T4 (ng/g)	3.8 ± 0.6, 6 (6, 0)	2.5 ± 1.0, 6 (6, 0)	2.8 ± 1.3, 6 (6, 0)	5.3 ± 1.7, 6 (6, 0)	6.1 ± 1.1*, 6 (6, 0)
T3:T4 ratio	0.07 ± 0.04, 6	0.09 ± 0.03, 6	0.07 ± 0.02, 4	0.05 ± 0.01, 5	0.03 ± 0.01, 6
rT3:T4 ratio	0.33 ± 0.19, 5	0.30 ± 0.21, 6	0.45 ± 0.05, 5	0.32 ± 0.12, 6	0.27 ± 0.08, 6

Abbr: rT3 = reverse triiodothyronine, T3 = triiodothyronine, T4 = thyroxine, MDL = method detection limit

* $P < 0.05$ relative to vehicle control (ANOVA with post hoc multiple comparison correction using Tukey contrasts)

Note: Sample sizes are expressed as the total number of samples (N) as well as the number of samples above the MDL (a) and below the MDL (b). Non-quantifiable samples below the MDL were imputed using the calculation MDL*0.5. MDL values were: T4: 0.84 ng/g, T3: 0.42 ng/g, rT3: 0.67 ng/g.

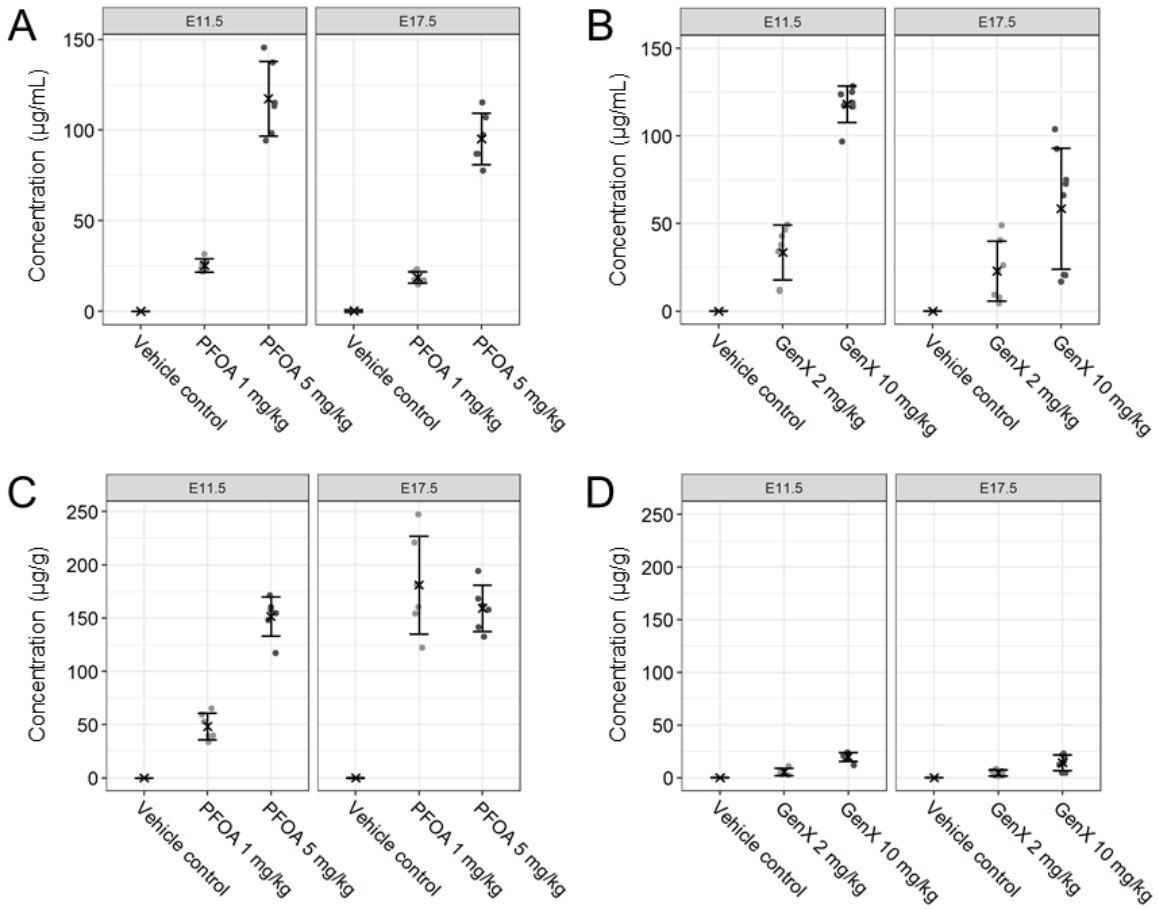

Figure 3-1. Internal dosimetry of PFOA and GenX (also HFPO-DA) in maternal serum and liver at embryonic day (E) 11.5 and E17.5. (A) Maternal serum concentration (µg PFOA/ mL serum) at E11.5 and E17.5, (B) maternal serum concentration (µg GenX/ mL serum) at E11.5 and E17.5, (C) maternal liver concentration (µg PFOA/ g liver) at E11.5 and E17.5, and (D) maternal liver concentration (µg GenX/ g liver) at E11.5 and E17.5 were determined by high performance liquid chromatography tandem mass spectrometry. Treatment group mean values are denoted with an "X" flanked above and below by error bars showing standard deviation and individual data points are shown as grey circles (N = 6-8). Vehicle control (VC) samples were quantified for PFOA and GenX; all VC means were below the LOD of 10 ng/mL for both PFOA and GenX except for maternal serum (0.211 ± 0.55 µg/mL). Statistical comparisons of internal dosimetry across all treatment groups are shown in Tables A2-2 and A2-3.

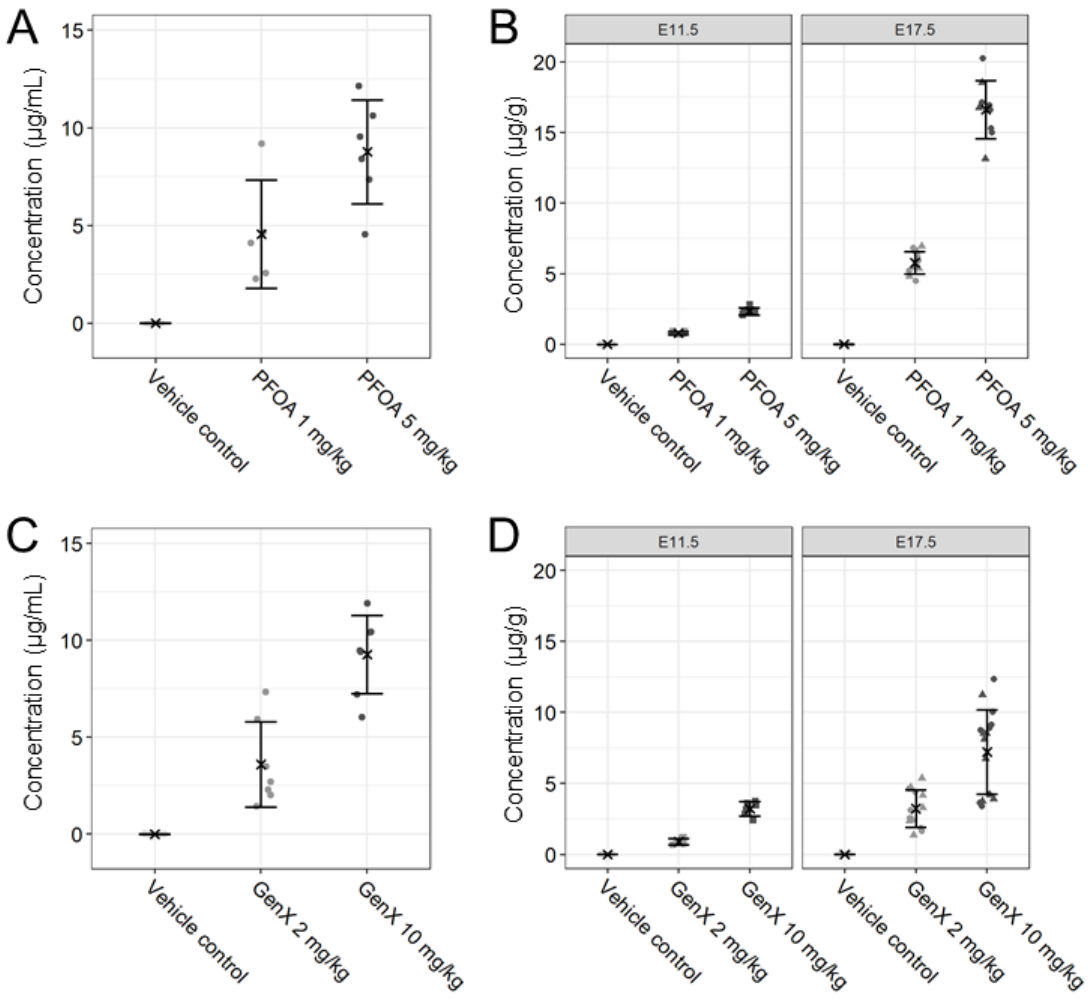

Figure 3-2. Internal dosimetry of PFOA and GenX (also HFPO-DA) in amniotic fluid and whole embryos. (A) Amniotic fluid concentration (µg PFOA/ mL amniotic fluid) at embryonic day (E) 11.5, (B) whole embryo concentration (µg PFOA/ g embryo) at E11.5 and E17.5, (C) amniotic fluid concentration (µg GenX/ mL amniotic fluid) at E11.5, and (D) whole embryo concentration (µg GenX/ g embryo) at E11.5 and E17.5 were determined by high performance liquid chromatography tandem mass spectrometry. Treatment group mean values are denoted with an "X" flanked above and below by error bars showing standard deviation, and individual data points are shown as grey squares, circles, or triangles (N = 6-8). Triangles = E17.5 male embryos, circles = E17.5 female embryos, and squares = pooled E11.5 embryos (B and D). Vehicle control (VC) samples were quantified for PFOA and GenX; all VC means were below the LOD of 10 ng/mL for both PFOA and GenX. Statistical comparisons of internal dosimetry across all treatment groups are shown in Tables A2-2 and A2-3.

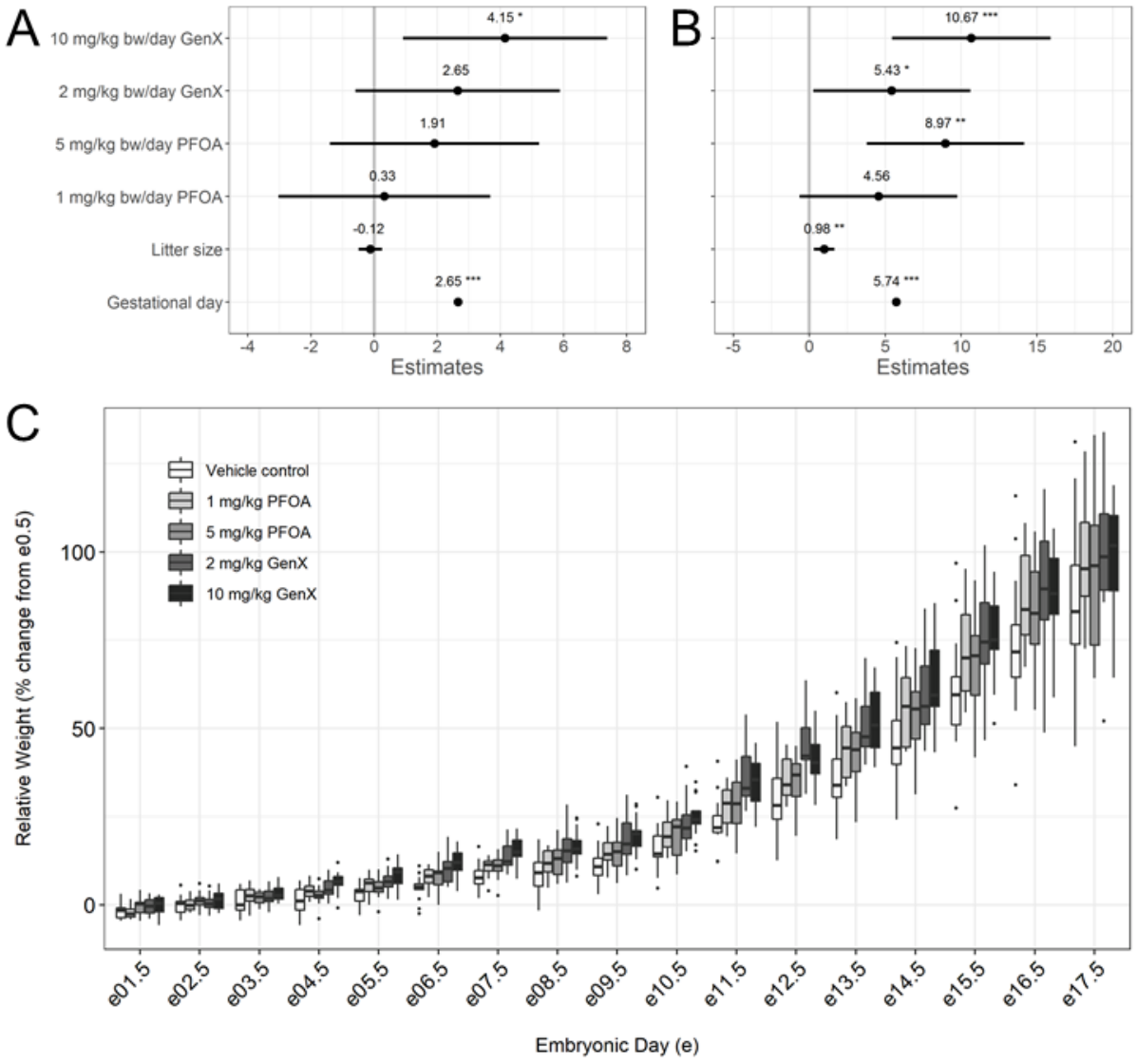

Figure 3-3. Gestational weight gain (GWG) repeated measure mixed effect model estimates for pregnant dams exposed to PFOA or GenX (also HFPO-DA). Effect estimates for pregnant dams exposed through embryonic day 11.5 (A) or 17.5 (B) are centered around the vehicle control group (y = 0) and show the point estimate of the relative change in dam weight (% change from E0.5) with 95% confidence intervals (CI). (C) Boxplots of relative weight gain over time, with the upper and lower hinges corresponding to the first and third quartiles (25^{th} and 75^{th} percentiles), the middle hinge corresponding to the median, and the upper whisker extending to the highest value that is within 1.5 times the distance between the first and third quartiles (inter-quartile range, IQR) of the hinge and the lower whisker extending to the lowest value within 1.5 times the IQR of the hinge. N = 11-13 dams per treatment group. *P < 0.05, **P < 0.01, ***P <0.001; Beta estimate 95% confidence intervals do not overlap zero (Repeated measures mixed effect model adjusting *a priori* for litter size and gestational (embryonic) day as fixed effects and the dam as a random effect, vehicle control as reference group).

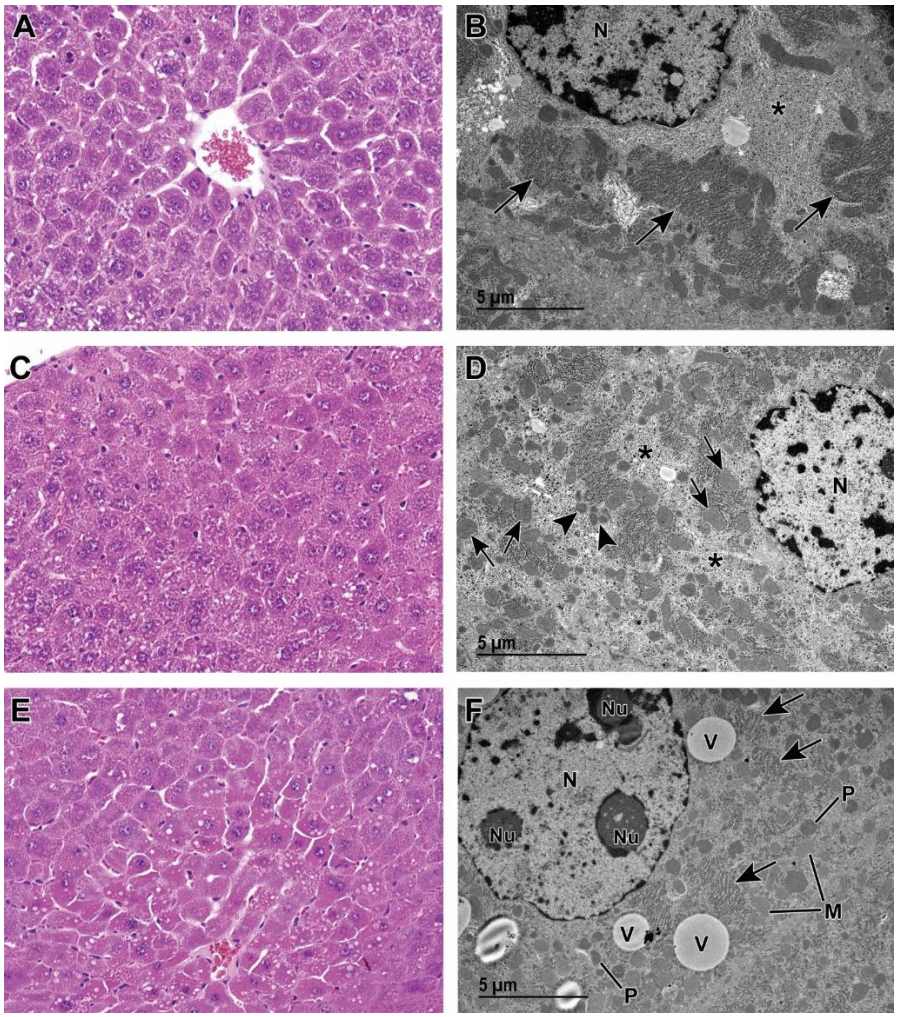

Figure 3-4. Light and transmission electron microscopy (TEM) of liver from vehicle control (VC) and PFOA-exposed pregnant dams at embryonic day (E) 17.5. Light microscopic image (A) at 40X magnification of liver from a VC pregnant dam (control) showing centrilobular hepatocellular hypertrophy with karyomegaly, increased basophilic granular cytoplasm and decreased glycogen. Corresponding (B) TEM magnification shows prominent rough endoplasmic reticulum (arrows) with abundant ribosomes and evenly dispersed, abundant glycogen (asterisk) (see Figure A2-3A). Light microscopic image (C) at 40X magnification of liver from a pregnant dam at E17.5 and treated with 1 mg/kg/day PFOA. Although this liver appears to be within normal limits when viewed with light microscopy, TEM (D) reveals an increase in scattered vacuoles (see Figure A2-3B), decreased, evenly dispersed glycogen (asterisks), as well as abundant mitochondria (arrows) and peroxisomes (arrowheads). Light microscopic image (E) at 40X magnification of liver from a pregnant dam at E17.5 and treated with 5 mg/kg/day PFOA. Increased cytoplasmic vacuoles are evident at this light microscopic level. TEM (F) reveals abundant cytoplasmic organelles consistent with mitochondria (M) and peroxisomes (P), extensive vacuoles (V), less prominent rough endoplasmic reticulum (arrows) with fewer ribosomes and less abundant glycogen (see A2-3C and A2-3D) TEM = transmission electron microscopy, NU = nucleolus, N = nucleus.

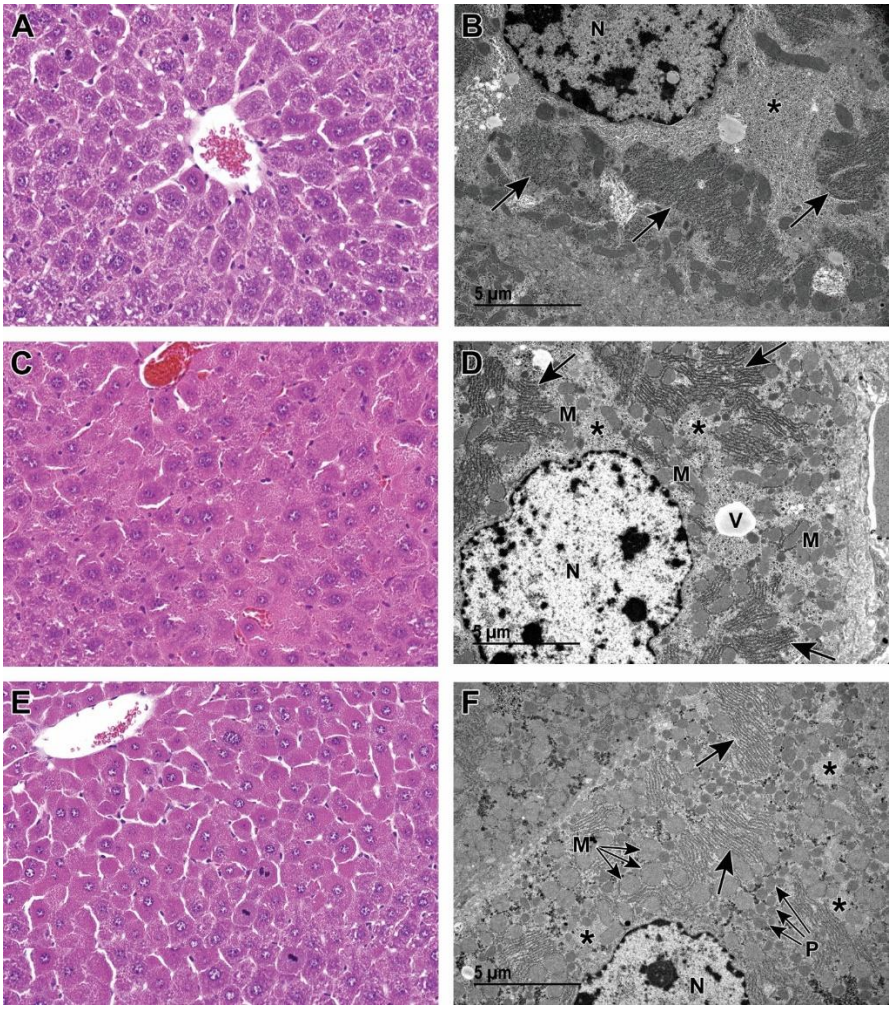

Figure 3-5. Light and transmission electron microscopy (TEM) of liver from vehicle control (VC) and GenX-exposed pregnant dams at embryonic day (E) 17.5. Light microscopic image (A) at 40X magnification of liver from a VC pregnant dam showing centrilobular hepatocellular hypertrophy with karyomegaly, increased basophilic granular cytoplasm and decreased glycogen. Corresponding medium (B) TEM magnification shows prominent rough endoplasmic reticulum (arrows) with abundant ribosomes and evenly dispersed, abundant glycogen (asterisk) (see Figure A2-3A). Light microscopy at 40X magnification (C) and transmission electron microscopy (D) of liver from a pregnant dam at E17.5 treated with 2 mg/kg/day GenX (also HFPO-DA) or 10 mg/kg/day GenX (E and F). Marked cytoplasmic alteration is evident in (C) and (E). TEM (D and F, see Figures A2-3E and A2-3F, respectively) reveals an abundance of cytoplasmic organelles, consistent with mitochondria (M) and peroxisomes (P), that increase with increasing dose (D compared to F). Note also the decreased glycogen (asterisks) as well as the vacuole (V) and rough endoplasmic reticulum (arrows) and N = nucleus.

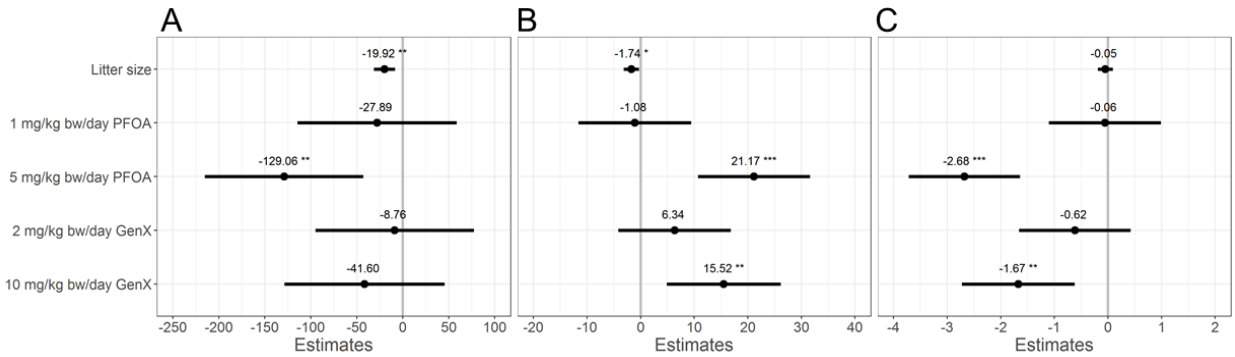

Figure 3-6. Mixed effect model estimates for (A) embryo weight (mg), (B) placental weight (mg), and (C) embryo:placental weight ratios (mg:mg) after exposure *in utero* to PFOA or GenX (also HFPO-DA) at embryonic day (E) 17.5. Effect estimates are centered around the vehicle control group (y = 0) and show the point estimate of the relative change in weight (mg; A & B) or weight ratio (mg:mg; C) with 95% confidence intervals (CI). *$P < 0.05$, **$P < 0.01$, ***$P < 0.001$; Beta estimate 95% confidence intervals do not overlap zero (Mixed effect model adjusting *a priori* for litter size as a fixed effect and the dam as a random effect, vehicle control as reference group). Adjusted estimates and 95% CI are shown in Table A2-8.

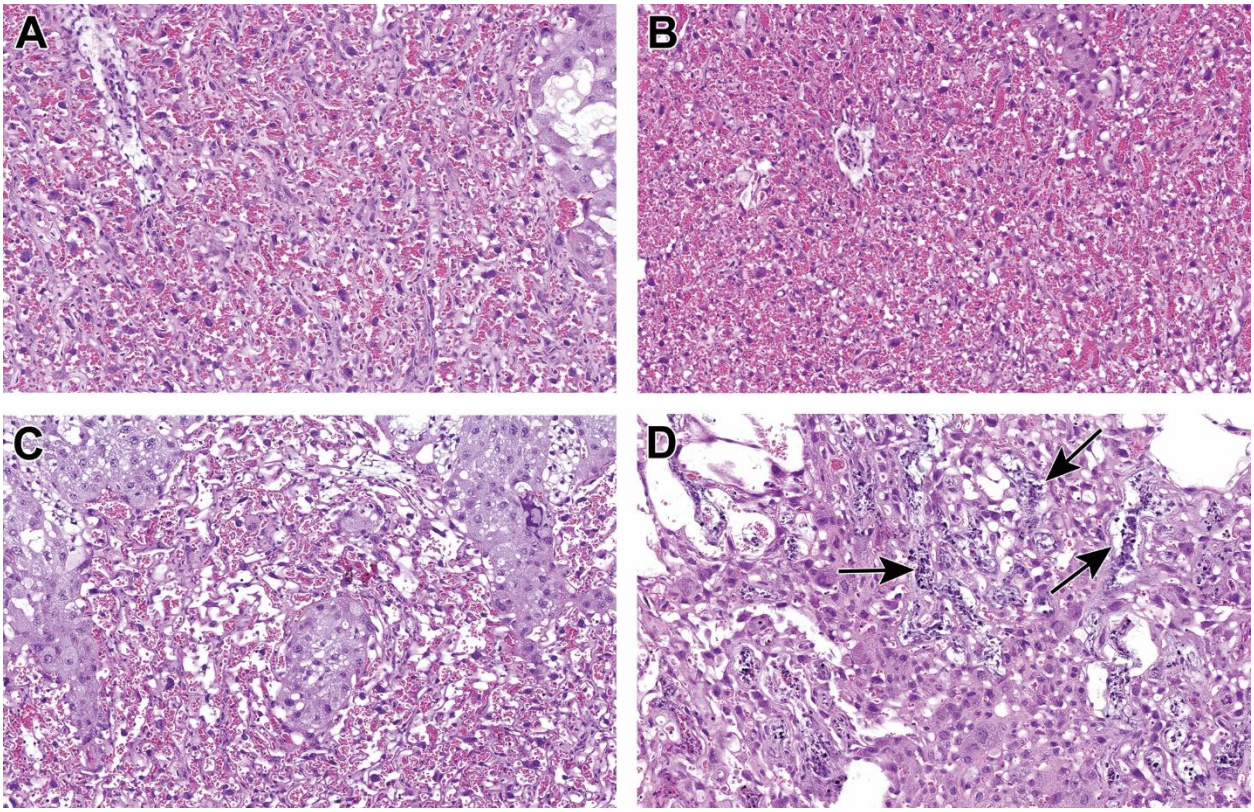

Figure 3-7. Representative examples of histopathological placenta findings observed in dams at embryonic day (E) 11.5 and E17.5, treated with PFOA or GenX (also HFPO-DA). (A) Normal labyrinth from a vehicle control dam at E17.5. (B) Labyrinth congestion in a dam at E17.5 that was treated with 10 mg/kg/day GenX (C) Moderate labyrinth atrophy of the trilaminar trophoblast layer at E17.5 in a dam treated with 10 mg/kg/day GenX. (D) Labryrinth necrosis (arrows) in a E17.5 dam that was treated with 10 mg/kg/day GenX. All images at 20X magnification.

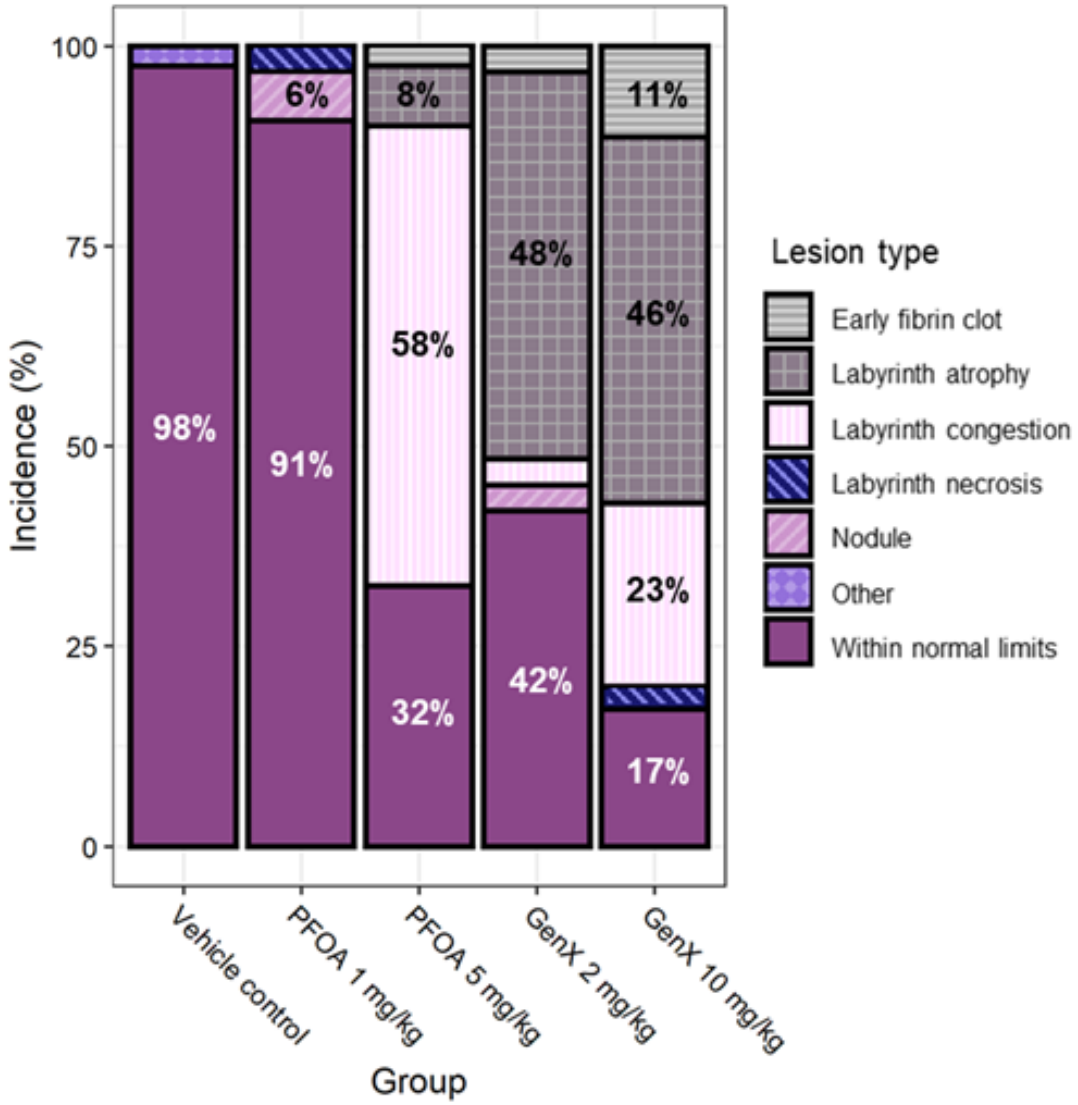

Figure 3-8. Incidence of placenta lesions across treatment groups at embryonic day 17.5. N = 5-6 litters with 31-41 placentas evaluated per treatment group (an average of 6-8 placentas per litter). Incidence values <4% are not numerically indicated, but all values and statistical comparisons of placenta lesion incidences across treatment groups at E17.5 are shown in Table A2-10.

CHAPTER 4: IN VITRO CHARACTERIZATION OF PLACENTAL TOXICITY FOR 42 PERFLUOROALKYL SUBSTANCES

4.1 Introduction

Per- and polyfluoroalkyl substances (PFAS) comprise a class of over 5,000 unique chemicals that have become ubiquitous in the environment (Kaboré et al. 2018; Pan et al. 2018), detectable in biological matrices across humans and wildlife around the globe (Houde et al. 2006), and problematic contaminants in air, food, and drinking water (Sunderland et al. 2019). Pregnant women and their developing offspring are thought to be particularly vulnerable to the PFAS due to associations between maternal PFAS exposure and adverse pregnancy outcomes, such as low birth weight (Chen et al. 2012; Fei et al. 2007; Johnson et al. 2014), increased gestational weight gain (Ashley-Martin et al. 2016), preeclampsia (Huang et al. 2019; Wikström et al. 2019b), gestational hypertension (Holtcamp 2012; Huang et al. 2019), and gestational diabetes (Matilla-Santander et al. 2017; Wang et al. 2018). The placenta is involved in the etiology of these pregnancy conditions (Pijnenborg et al. 1991) and PFAS pass from the maternal to fetal compartments through the placenta (Chen et al. 2017a; Wang et al. 2019; Zhao et al. 2017). While it is not well understood how maternal exposure to PFAS may contribute to adverse pregnancy outcomes, the effect of PFAS on the placental function is likely critical.

The placenta is essential for the establishment and maintenance of pregnancy and disruptions in its development or function, such as placental insufficiency, are detrimental to maternal-fetal health (Chaddha et al. 2004). Placental insufficiency broadly describes pregnancy complications of placental origin that occur when the placenta is unable to deliver an adequate

supply of nutrients and oxygen to the fetus (Chaddha et al. 2004). Environmental pollutants have been previously shown to increase risk for placenta-mediated pregnancy complications (NTP 2016; Laine et al. 2015), including maternal exposure to certain PFAS, such as perfluorooctanoic acid (PFOA) (Stein et al. 2009) and perfluorooctane sulfonate (PFOS) (Wikström et al. 2019b). However, the placental toxicity of even well-studied PFAS like PFOA and PFOS is not understood. Additionally, there is an immense knowledge gap regarding the placental toxicity of the other ~5,000 PFAS compounds in use worldwide. Furthermore, there is an urgent need for data on emerging and alternative chemistry PFAS, such as GenX, which have recently impacted highly-exposed communities (Sun et al. 2016b). Blake et al. (2020) demonstrated the toxicity of GenX and its predecessor towards the placenta in mice at administered doses relevant to risk assessment and reported different histopathological phenotypes, suggesting unique mechanisms of action for the two compounds. However, the rapidly expanding universe of PFAS compounds as well as the critical need for data on emerging contaminants precludes the feasibility of animal studies as the exclusive source of data to be used in risk assessment.

In vitro experimental systems are an affordable and efficient way to approach complicated multi-compound toxicity screening efforts. Human-derived JEG-3 placental trophoblasts have been previously implemented in toxicity studies of environmental exposures representing a model system of the placenta. The JEG-3 cell line is particularly relevant as it is composed of multinucleated syncytiotrophoblasts, which facilitate the exchange of nutrients, waste, and gases between the maternal and fetal compartments in human placenta. The mechanism(s) through which PFAS alter fetal growth via disruption of placental function is not well understood but may occur due to alterations in placental gene expression pathways involved in nutrient or xenobiotic transport, oxidative stress, endocrine function, and metabolism. There

are limited data on the ability of PFAS to induce gene expression changes in the placenta, but previous work has shown JEG-3 exposure to PFOA or PFOS inhibits aromatase activity *in vitro* (Gorrochategui et al. 2014) and PFOA exposure during gestation *in vivo* decreases expression of placental prolactin-family genes in mice (Suh et al. 2011).

This study leveraged JEG-3 placental trophoblast cells in the linear proliferation phase to execute a multiplexed high-throughput toxicity screen to evaluate a panel of 42 PFAS. The aim was to generate robust dose-response data corresponding to cell viability, cellular proliferation, and mitochondrial membrane potential, and extract relevant model parameters (e.g. EC50 values) to further characterize and categorize PFAS compounds by bioactivity and chemical features. Two compounds of high public health interest were selected for gene expression analysis in JEG-3 cells to investigate effects on expression of 46 genes involved in placental function.

4.2 Methods

4.2.1 Cell Culture

JEG-3 human choriocarcinoma trophoblastic cells (American Type Culture Collection, VA, USA) were maintained in sterile-filtered Minimum Essential Media (MEM) supplemented with L-glutamine and phenol red (Thermo Fisher Scientific, MA, USA), 10% (v/v) heat-inactivated BenchMark Fetal Bovine Serum (Gemini Bio, CA, USA), 1% (v/v) sodium pyruvate (Thermo Fisher Scientific, MA, USA), and 1% (v/v) penicillin streptomycin (Sigma Aldrich, MO, USA). Cells were maintained in a humidified incubator at 37°C with 5% CO_2. JEG-3 cells were cultured in 10 cm tissue culture plates and cell passage numbers were recorded.

4.2.2 Experimental Design

A total of 42 perfluoroalkyl substances (PFAS) were evaluated (Table A3-1). PFAS stock solutions were maintained in 100% methanol as previous work has shown certain PFAS degrade when stored in dimethyl sulfoxide (DMSO; Gaballah et al. 2020). Each PFAS was tested across

a 10-point linear concentration curve ranging from 50 – 500 µM (50 µM steps), except for perfluoroheptanesulfonic acid (CAS# 375-92-8; concentration curve of 23.25 – 232.5 µM [23.25 µM steps]) and 6:2 fluorotelomer phosphate diester (CAS# 57677-95-9; concentration curve of 37.5 – 375 µM [37.5 µM steps]). The vehicle control condition consisted of 97.5% media + 2.5% methanol to match the concentration of methanol in the media at the highest PFAS concentration tested (500 µM). Menadione (50 – 500 µM) was used as a positive control for cell viability. PFAS were de-identified and assigned random numbers to eliminate bias. Chemical exposure plate maps were designed so that all experimental conditions were tested in at least technical duplicates per plate. The outer edges of each plate received media alone and were excluded from all analyses to avoid edge effects. Each plate map included 14 technical replicates of the vehicle control condition and 14 technical replicates of media only. Biological replicates were defined as 384 well plates tested on separate days using different cell passages. The experimental workflow is depicted in Figure 4-1.

JEG-3 cells were counted using a Z2 Coulter Particle Counter (Beckman Coulter, CA, USA) and seeded at a density of 2,500 cells per well in black-walled, clear bottom 384 well plates and allowed to adhere overnight. Approximately 24 hours later, 384 well plates (Sigma Aldrich, MO, USA) were imaged using an IncuCyte Zoom live cell imager (Essen BioScience Inc, MI, USA) to obtain cellular confluence measurements prior to chemical dosing (0 hours). Media was then removed from wells and replaced with fresh media containing chemical treatments (exposure media) using a Viaflo liquid handling device (Integra Biosciences, NH, USA). Within 30 minutes of exposure media application, plates were again imaged for cellular confluence using the IncuCyte Zoom. Plates were incubated with exposure media for 24 hours and then imaged again using the IncuCyte Zoom (24 hours).

4.2.3 Proliferation

Plate well bottom images obtained with the IncuCyte Zoom were evaluated using automated cell masking. The automated cell masking program was developed by B.E.B. following the manufacturer's instructions and using IncuCyte Zoom base software. Cell masking parameters were defined using a training set of JEG-3 cell images with low, medium, and high confluence. Cell proliferation was calculated as the difference in cellular confluence at 24 hours and 0 hours.

4.2.4 Mitochondrial Membrane Potential (MMP)

The JC-10 assay was used to evaluate mitochondrial membrane potential (Enzo Life Sciences, NY, USA). In cells with polarized mitochondrial membranes, the JC-10 dye localizes to the mitochondrial matrix and forms red fluorescent aggregates (540/590 nm). In cells with depolarized mitochondrial membranes, the JC-10 dye localizes in the cytoplasm and converts to a green fluorescent monomer (490/525 nm). In healthy cells, the JC-10 dye concentrates in the mitochondrial matrix and fluoresces red and in apoptotic or necrotic cells, the JC-10 dye diffuses out of mitochondria and fluoresces green. Mitochondrial membrane potential is calculated as the ratio of the green and red fluorescence intensities within a well.

At the end of the 24 hour exposure period, exposure media was removed from the plate. The plate wells were washed with 1x phosphate buffered saline (1xPBS). After washing, the JC-10 reagent was suspended in fresh 1xPBS and 20 µL was added to each well at a final concentration of 20 µM (Enzo Life Sciences, NY, USA). The plate was then incubated for 1 hour at 37°C. After 1 hour, the fluorescence intensities at excitation/emission wavelengths of 490/525 nm and 540/590 nm, respectively, were measured using a Clariostar (BMG Labtech, Offenburg, Germany) plate reader.

4.2.5 Viability

After the plate was evaluated using the JC-10 assay, cell viability was measured using the CellTiter-Glo (CTG) Luminescent Cell Viability Assay (Promega, WI, USA). CTG reagent was added to each well at a volume of 20 µL. The plate was left at room temperature to incubate for 5 minutes and then 20 µL from each well was transferred to a low-volume, round-bottom, white 384 well plate (Sigma Aldrich, MO, USA). The CTG reagent lyses cellular and mitochondrial membranes and binds to adenosine triphosphate (ATP) released by cells, which produces a luminescence signal that can be monitored via an appropriate plate reader. The intensity of the luminescence was considered a proxy measure for the number of live cells in a well. The luminescence intensities were measured using a Clariostar plate reader.

4.2.6 Cell Morphology

Images obtained using the IncuCyte were visually examined at the highest exposure levels (450-500 µM) and compared to baseline, pre-exposure images as well as media only and vehicle control images. Overt cell death, irregular cell borders, atypical cell shape, atypical appearing nuclei (e.g. enlarged or diminished in size), and unusual extracellular artifacts were noted.

4.2.7 Gene Expression

JEG-3 cells were seeded at a density of 80,000 cells per well in 6 well plates and allowed to adhere overnight (24 hours). The following day, JEG-3 media was removed and replaced with exposure media, then returned to the incubator for 24 hours. The test compounds included PFOA (CAS# 335-67-1; 0, 1, and 100 µM) and perfluoro-2-methyl-3-oxahexanoic acid (CAS# 13252-13-6, also referred to as GenX; 0, 3, 300 µM). These test compounds were selected *a priori* due to their high public health relevance. Each 6 well plate contained the three doses for either PFOA or GenX, with each condition in technical duplicate. Replicates containing PFOA or GenX

exposure were completed with three separate plates (N = 3). After 24h, exposure media was aspirated and cells were washed in ice cold 1xPBS, which was then aspirated. Each well received 500 µL of TRIzol reagent (Thermo Fisher Scientific, MA, USA) and cells were harvested into the TRIzol using a cell scraper. Technical duplicate wells within a plate were combined to generate a single sample of ~1000 µL. RNA was isolated from the resulting samples using RNeasy Mini Kits (Qiagen, Hilden, Germany). Isolated RNA was validated for purity using a NanoDrop 2000 (Thermo Fisher Scientific, MA, USA). 100 ng of mRNA from each sample was then analyzed using a custom gene expression code set (NanoString, Seattle, WA, USA). The custom code set included 46 genes selected for their downstream involvement in placental development (e.g. *WNT4*), endocrine signaling (e.g. *CYP19A1*), fetal growth/nutrient sensing (e.g. *IGF2*), inflammation (e.g. *IL6*), oxidative stress (e.g. *SOD1, GPX1*), and xenobiotic transport/metabolism (e.g. *ABCG2, MRP3*; see Table A3-4 for full gene list). Gene expression of the custom code set was examined using the NanoString platform (www.nanostring.com). Samples were analyzed per NanoString specifications. Briefly, 100 ng of each prepared RNA samples was used. RNA expression was quantified on the nCounter Digital Analyzer and raw and adjusted counts were generated with nSolver (v4.0) software.

4.2.8 Data Processing and Statistical Analysis

Proliferation, MMP, and cell viability data were analyzed using a custom data analysis script in R v 1.2.5019 (R Core Team 2019). Briefly, raw data points corresponding to the confluence measurements at 0 hours and 24 hours (proliferation), the fluorescence intensities corresponding to MMP, and the relative luminescence units (RLU) corresponding to cell viability were imported directly from Microsoft Excel into the R programming environment, RStudio. Separate plates run on separate days using different JEG-3 passages were considered as biologic replicates. Technical replicates within a plate for proliferation, MMP, and cell viability

endpoints were first evaluated as pseudoreplicates, but this precluded robust dose-response model fits thus technical replicates of experimental values within a plate were considered as independent data points. After excluding plate edges, all remaining data points were preprocessed by eliminating wells with confluence values <20% and >80% at 0h. Cellular proliferation was calculated by subtracting the cellular confluence at 0h from the cellular confluence at 24h to yield Δ confluence. MMP was calculated as the ratio of red:green fluorescence intensities.

Prior to evaluating experimental data, data obtained from control wells (wells exposed to media only and wells exposed to 2.5% (v/v) methanol) were evaluated for quality control. Control wells were examined for variability in response within and between plates. Average confluence at 0h was compared across control conditions and plates. Plates that passed quality control were included in subsequent data analyses and plates that failed to pass quality control were rejected.

Preprocessed raw data points were then transformed to relative values based on the mean of control wells within in a plate using the following formula: [experimental value / average(all control values)]*100. These relative values were then used to perform dose-response modeling using the *bmd* package (Ritz 2010). All endpoints were fit to four parameter dose-response curves without constraints. Models were fit to each endpoint (proliferation, MMP, and viability) for each PFAS tested. Model estimates were reviewed manually and model fits were accepted if the following criteria were met: (1) estimated EC50 was within the range of the tested dose-response curve (50 – 500 µM), (2) standard deviations no larger than a doubling of the EC50 estimate itself, and (3) the dose-response model did not fail to converge (e.g. no "NaN" or "NA" values in R output). EC50 values that met these criteria were extracted and used in subsequent

data categorizations and visualizations. Raw model output values including those that did not meet inclusion criteria are shown in Table A3-2.

Data were also analyzed using predetermined statistical cutoffs (e.g. rough binning) in order to further categorize individual compounds by activity. For all endpoints, vehicle control normalized values corresponding to each dose tested for each congener were averaged within and between biological replicates to produce a single value for each dose tested per individual compound (e.g. 10 experimental doses resulted in a total of 10 data points per congener per endpoint). The values were then categorized based on deviance from the range of normalized vehicle control values (e.g. normalized test value > normalized vehicle control mean + 2*normalized vehicle control standard deviation or normalized test value < normalized vehicle control mean - 2*normalized vehicle control standard deviation). This method allowed for the identification of compounds that may perturb endpoints above or below the expected range of normal depending on dose, allowing for identification of potential nonmonotonic dose-response relationships precluded by 4-parameter dose-response modeling.

Gene expression data were processed using the nCounter Digital Analyzer (NanoString, Seattle, WA, USA). Raw and adjusted counts were generated with nSolver (v4.0) software (NanoString, Seattle, WA, USA). Data were adjusted utilizing the manufacturer's positive and negative experimental control probes, as well as housekeeping genes (*ACTA2*, *ACTB*, *B2M*, *LDHA*, *RNA18S5*, and *ROLYR2L*). All samples passed nSolver's initial QA/QC controls and replicates were very well correlated with R^2 values greater than 0.99. Adjusted data were then imported into Partek v7.0 (St. Louis, MO, USA), log2 transformed and quantile normalized for further QA/QC and statistical analyses. To identify significant differences in gene expression, genes with mRNA counts below the threshold of detection of 20 were removed (N = 2 genes for

GenX; *GH2* and *IGFBP5*). Fold change values were analyzed by ANOVA with *post hoc* false discovery rate adjustment (FDR) of $p < 0.1$. Normalized gene expression values were visualized using *pheatmap* with Euclidean clustering of genes and dose groups (Kolde and Kolde 2015).

4.3 Results

Overall, dose-response modeling of PFAS effects against JEG-3 cell viability, proliferation, and MMP resulted in quantification of an EC50 value that met inclusion criteria for at least one of the three evaluated endpoints for 33 of 42 compounds (79%; Table 4-1). EC50 values were obtained for all three endpoints for 13 PFAS (31%), for two of three endpoints for 15 PFAS (36%), for one of three endpoints for 3 PFAS (7%), and zero of three endpoints for 9 PFAS (21%; Table 4-1). Cells exposed to vehicle control (methanol 2.5% v/v in media) did not differ from cells exposed to media only in either cellular morphology or viability after 24h (Figure A3-1). The positive control for cell death, menadione, reliably induced cell death which was apparent upon visual inspection of the plate wells (Figure A3-2) at an EC50 of 205.5 ± 47.1 µM (Table 4-1).

4.3.1 Viability

Dose-response curve modeling provided viability EC50 estimates for 27 of 42 PFAS (66%) that met EC50 criteria (Table 4-1 & Figure 4-2). Cell viability EC50 values ranged from 35.7 µM (CAS# 678-39-7) to 486.7 µM (CAS# 375-85-9; Table 4-1). Among PFAS from which a viability EC50 estimate was calculated, the five compounds with the lowest EC50 ± SE were: 8:2 Fluorotelomer alcohol (CAS# 678-39-7; 36 ± 37 µM), 8:2 Fluorotelomer sulfonic acid (CAS# 39108-34-4; 160 ± 46 µM), perfluorooctane sulfonamide (CAS# 754-91-6; 176 ± 5 µM), perfluorodecanoic acid (CAS# 335-76-2; 181 ± 26 µM), 6:2 Fluorotelomer phosphate monoester (CAS# 57678-01-0; 183 ± 22 µM; Table 4-1 & Figure A3-3). Examples of structures and live cell images are shown in Figure 4-3.

Rough binning of test compounds resulted in 10 PFAS (24%) that reduced cell viability relative to vehicle control treatment after 24h in at least one dose: Perfluoro-3,6-dioxadecanoic acid (CAS# 137780-69-9), perfluorooctane sulfonic acid (CAS# 1763-23-1), perfluoro-3,6,9-trioxatridecanoic acid (CAS# 151772-59-7), perfluoroundecanoic acid (CAS# 2058-94-8), perfluorodecanoic acid (CAS# 335-76-2), perfluorononanoic acid, 2-(N-ethylperflurooctanesulfonamido) acetic acid (CAS# 2991-50-6), 8:2 fluorotelomer phosphate diester (CAS# 678-41-1), ammonium perfluoro-2-methyl-3-oxahexanoate (CAS# 62037-80-3), and sodium perfluoropentanesulfonate (CAS# 630402-22-1; Table A3-3). Menadione also reduced cell viability relative to vehicle control treatment using rough binning.

A total of 13 PFAS (31%) increased cell viability in at least one dose relative to vehicle control: Perfluoro-3,6-dioxaheptanoic acid (CAS# 151772-58-6), perfluorododecanoic acid (CAS# 307-55-1), perfluorohexanoic acid (CAS# 307-24-4), perfluoropentanoic acid (CAS# 2706-90-3), 1H,1H-nonafluoropentyl p-toluenesulfonate (CAS# 883499-79-4), 7H-perfluoroheptanoic acid (CAS# 1546-95-8), perfluorobutanesulfonic acid (CAS# 375-73-5), perfluorobutanoic acid (CAS# 375-22-4), perfluorodecanoic acid (CAS# 335-76-2), perfluorohexanesulfonic acid (CAS# 355-46-4), 6:2 fluorotelomer phosphate diester (CAS# 678-41-1), perfluorotridecanoic acid (CAS# 72629-94-8), and 2H,2H,3H,3H-perfluorooctanoic acid (CAS# 883499-79-4; Table A3-3).

4.3.2 Proliferation

Dose-response curve modeling provided proliferation EC50 estimates for 28 of 42 PFAS (68%) that met EC50 criteria (Table 4-1 & Figure 4-2). Cell proliferation EC50 values ranged from 114.0 µM (perfluorooctanamide, CAS# 423-54-1) to 441.3 µM (8-H-perfluorooctanoic acid, CAS# 13973-14-3; Table 4-1). Of PFAS from which a proliferation EC50 estimate was calculated, the five compounds with the lowest EC50 ± SE were: Perfluorooctanamide (CAS#

423-54-1; 114.0 ± 35.6 µM), 6:2 fluorotelomer phosphate diester (CAS# 57677-95-9; 141.6 ± 39.4 µM), perfluorooctane sulfonamide (CAS# 754-91-6; 159.8 ± 90.0 µM), 6:2 Fluorotelomer phosphate monoester (CAS# 57678-01-0; 193 ± 4 µM), and 2-(N-Ethylperfluorooctanesulfonamido)acetic acid (CAS# 2991-50-6; 204 ± 18 µM; Table 4-1 & Figure A3-4). Examples of structures and live cell images are shown in Figure 4-4.

Rough binning of test compounds resulted in 19 PFAS (45%) that reduced cellular proliferation relative to vehicle control treatment in at least one dose: Perfluoro-3,6-dioxadecanoic acid (CAS# 137780-69-9), perfluoro-3,6-dioxaheptanoic acid (CAS# 151772-58-6), perfluoro-3,6,9-trioxadecanoic acid (CAS# 151772-59-7), perfluorooctanesulfonic acid (CAS# 1763-23-1), perfluoro-3,6,9-trioxatridecanoic acid (CAS# 330562-41-9), perfluorohexanoic acid (CAS# 307-24-4), perfluoroundecanoic acid (CAS# 2058-94-8), 1H,1H-nonafluoropentyl p-toluenesulfonate (CAS# 883499-79-4), 7H-perfluoroheptanoic acid (CAS# 1546-95-8), perfluorodecanoic acid (CAS# 335-76-2), perfluorooctanoic acid (CAS# 335-67-1), perfluoroheptanoic acid (CAS# 375-85-9), perfluorohexanesulfonic acid (CAS# 355-46-4), perfluorononanoic acid, 2-(N-ethylperfluorooctanesulfonamido) acetic acid (CAS# 2991-50-6), 6:2 fluorotelomer phosphate diester (CAS# 678-41-1), 8:2 fluorotelomer phosphate diester (CAS# 678-41-1), perfluoroheptanesulfonic acid (CAS# 375-92-8), and perfluorotridecanoic acid (CAS# 72629-94-8; Table A3-3). Menadione also reduced proliferation relative to vehicle control treatment using rough binning.

Rough binning of test compounds resulted in 10 PFAS (24%) that increased cellular proliferation relative to vehicle control treatment in at least one dose: Perfluoro-2-methyl-3-oxahexanoic acid (CAS# 13252-13-6), 2-(N-ethylperfluorooctanesulfonamido) acetic acid (CAS# 13252-13-6), 2,2-difluoro-2-(trifluoromethoxy)acetate sodium salt (CAS# 21837-98-9),

2H,2H,3H,3H-perfluorooctanoic acid (CAS# 914637-49-3), 6:2 fluorotelomer phosphate diester (CAS# 678-41-1), 6:2 fluorotelomer sulfonic acid (CAS# 27619-97-2), ammonium perfluoro-2-methyl-3-oxahexanoate (CAS# 62037-80-3), perfluoroheptanesulfonic acid (CAS# 375-92-8), perfluorotridecanoic acid (CAS# 72629-94-8), and sodium perfluoropentanesulfonate (CAS# 630402-22-1; Table A3-3).

4.3.3 Mitochondrial Membrane Potential

Dose-response curve modeling provided MMP EC50 estimates for 19 of 42 PFAS (45%) that met EC50 criteria (Table 4-1). MMP EC50 values ranged from 86.2 µM (perfluorohexanesulfonic acid; CAS# 355-46-4) to 368.0 µM (perfluoro-3,6-dioxaheptanoic acid; CAS# 151772-58-6). Of PFAS from which a MMP EC50 estimate was calculated, the five compounds with the lowest EC50 ± SE were: Perfluorohexanesulfonic acid (CAS# 355-46-4; 86.2 ± 72.3 µM), 6:2 fluorotelomer alcohol (CAS# 678-39-7; 95.1 ± 15.3 µM), perfluorohexanoic acid (CAS# 307-24-4; 140.9 ± 11.1 µM), 8-H-perfluorooctanoic acid (CAS# 13973-14-3; 147.3 ± 27.1 µM), and 2H,2H,3H,3H-perfluorooctanoic acid (CAS# 883499-79-4; 158.6 ± 17.7 µM; Table 4-1 & Figure A3-5). Examples of structures and live cell images are shown in Figure 4-5.

Rough binning of compounds by reduced MMP relative to vehicle control treatment after 24h in at least one dose resulted in 15 PFAS (35%): Perfluoro-2-methyl-3-oxahexanoic acid (CAS# 13252-13-6), perfluoro-3,6-dioxadecanoic acid (CAS# 137780-69-9), perfluoro-3,6-dioxaheptanoic acid (CAS# 151772-58-6), perfluoro-3,6,9-trioxadecanoic acid (CAS# 151772-59-7), perfluorooctanesulfonic acid (CAS# 1762-23-1), perfluro-3,6,9-trioxatridecanoic acid (CAS# 330562-41-9), perfluorohexanoic acid (CAS# 307-24-4), perfluoroundecanoic acid (CAS# 2058-94-8), perfluorobutanesulfonic acid (CAS# 375-73-5), perfluorobutanoic acid (CAS# 375-22-4), perfluorooctanoic acid (CAS# 335-67-1), perfluorodecanoic acid (CAS# 335-

76-2), perfluorononanoic acid (CAS# 375-95-1), 2-(N-ethylperfluorooctanesulfonamido) acetic acid (CAS# 2991-50-6), and 8:2 fluorotelomer phosphate diester (CAS# 678-41-1; Table A3-3). Menadione also reduced MMP relative to vehicle control treatment after 24h using rough binning. Rough binning of compounds by increased MMP relative to vehicle control treatment after 24h in at least one dose resulted in 0 PFAS (0%).

4.3.4 Differential Gene Expression Analysis

After 24 hours of exposure to PFOA at 1 or 100 µM or GenX at 3 or 300 µM, 21 genes with significantly altered gene expression were identified (FDR $p < 0.1$; Figure 4-3 & Table A3-4). Gene expression was most affected after exposure to 300 µM GenX (N = 15 genes; Figure 4-3 & Table A3-4). Gene expression was significantly altered after exposure to 1 µM PFOA (*AHRR* & *CYP2E1*), 100 µM PFOA (*17BHSD1, ABCG2, IGFR2,* & *WNT4*), or 3 µM GenX (*ABCG2* & *GPX1*; Figure 4-6 & Table A3-4).

4.4 Discussion

We evaluated the effect of 42 unique PFAS on cell viability, proliferation, and mitochondrial membrane potential after a 24 hour exposure in human-derived placental JEG-3 trophoblasts. Implementation of this multiplexed high throughput toxicity screen resulted in a robust dataset from which dose-response model estimates could be extracted for at least one endpoint in roughly 80% of evaluated PFAS. This experimental platform provides a rapid method for simultaneous evaluation of multiple PFAS compounds across three biologically relevant endpoints. To our knowledge, 34 of the 42 PFAS evaluated here have never been investigated for effects on JEG-3 cell viability, proliferation, or mitochondrial membrane potential. Thus, this work provides novel and critical toxicity data for multiple PFAS. Furthermore, we investigated the effect of sub-cytotoxic exposure to two PFAS of high public

health relevance, PFOA and GenX, on expression of 46 genes in JEG-3 cells and report shifts in gene expression consistent with those reported in preeclampsia.

Unlike previously reported data in other cell lines (Buhrke et al. 2013), we did not observe a consistent relationship between carbon chain length and cell viability. Additionally, EC50 estimates for cell viability reported in our study for PFOA, PFOS, PFNA, and PFDoA were not consistent with those reported by Gorrochategui et al (2014). However, these differences could be explained in part by differences in experimental methods, such as the utilization of different cell viability assays and different dose-response curves (linear vs logarithmic) (Gorrochategui et al. 2014).

During placental development, careful coordination between trophoblast proliferation and apoptosis is critical for a healthy and fully functioning placenta (Huppertz and Herrler 2005a; Pollheimer and Knöfler 2005). Disruption of the balance between trophoblast proliferation and apoptosis has been shown in preeclampsia and intrauterine growth restriction (Huppertz and Herrler 2005). Our data demonstrate the potential for a variety of PFAS to disrupt the normal proliferative behavior of placental trophoblasts. Further studies are required to determine the extent to which the observed reductions in cell viability were due to mechanisms specific to cytotoxicity and/or disruptions in apoptotic pathways.

Placental mitochondria play a critical role in maintaining a healthy pregnancy, and placental mitochondrial dysfunction occurs in pregnancy conditions such as preeclampsia and gestational diabetes (Fisher et al. 2020). It has been hypothesized that mitochondrial-based signaling (via reactive oxygen species generation) may be the driver of placental adaptations to mitigate damage, thus causing adverse placental outcomes when mitochondria are no longer able to maintain the appropriate reactive oxygen species/anti-oxidant balance (Fisher et al. 2020).

Here we provide evidence suggesting PFAS have the potential to harm the placenta via disruption of trophoblast mitochondrial function. Future investigations should further interrogate the effects of PFAS on trophoblast mitochondrial respiration and reactive oxygen species generation.

Optimal placental and fetal growth is carefully balance between complex and overlapping systems across the maternal-placental-fetal interface, including the management of inflammation, oxidative stress, endocrine signaling, and the metabolism and transport of nutrients and xenobiotics. After exposure to PFOA or GenX, JEG-3 cells exhibited shifts in gene expression suggesting potential dysregulation of key genes involved in maintaining these processes. ATP Binding Cassette subfamily G Member 2, ABCG2 (also known as breast cancer resistance protein, or BCRP), is localized to the apical membrane of placental syncytiotrophoblasts and functions as an efflux transporter (Mao 2008). ABCG2 protects the fetus by limiting the transplacental transfer of xenobiotics through transport back into maternal circulation (Mao 2008). Here we show upregulation of *ABCG2* expression in JEG-3 cells after exposure to GenX (3 or 300 μM) or PFOA (100 μM) for 24 hours. Previous work has shown *ABCG2* expression is regulated in placental cells *in vitro* by progesterone and 17β-estradiol (Wang et al. 2006). It is possible that PFOA and GenX influence *ABCG2* expression via noncanonical progesterone receptor signaling pathways (Wang et al. 2006), or that *ABCG2* upregulation is a compensatory response to increase placental efflux of PFOA and GenX, thereby limiting fetal exposure.

17β-Hydroxysteroid dehydrogenase 1 (17β-HSD1) serves a dual function in estrogen activation and androgen inactivation and plays a critical role in establishing estradiol (E2) concentration. 17β-HSD1 primarily catalyzes the reduction of estrone (E1) into E2, which is

more active. E2-mediated signaling in trophoblasts is hypothesized to play a role in *ABCG2* expression and function (Ellinger et al. 2018). Previous work has implicated dysregulation of *17β-HSD1* expression in preeclampsia (Ishibashi et al. 2012). However, Ishibashi et al. (2012) showed decreased expression of *17β-HSD1*. Here we show a significant increase in *17β-HSD1* expression after 24 hours of exposure to 100 µM PFOA or 300 µM GenX. These divergent findings may be explained by the post-translational targeting of *17β-HSD1* transcripts by miRNAs upregulated in preeclamptic placentas. It is possible that the post-translational miRNAs involved in regulation of *17β-HSD1* transcripts and downstream protein expression are not fully conserved in JEG-3 cells. Indeed, miRNA expression profiles differ between JEG-3 cells and primary human placental trophoblasts (Morales-Prieto et al. 2012).

Placental oxidative stress is strongly associated with the pathogenesis of preeclampsia (Bilodeau 2014; Burton and Jauniaux 2004). Glutathione peroxidase 1 (GPX1) protects cells against oxidative damage through catalyzing the reduction of organic hydroperoxides and hydrogen peroxide by glutathione. Furthermore, decreased expression of *GPX1* has been reported in preeclamptic placentas (Mistry et al. 2010; Roland-Zejly et al. 2011; Vanderlelie et al. 2005). Here we show a significant reduction in *GPX1* expression in JEG-3 cells after 24 hours of exposure to 3 µM or 300 µM GenX, with a similar non-significant trend of decreased expression after exposure to 100 µM PFOA. In JEG-3 cells exposed to 300 µM GenX, expression of G Protein-Coupled Estrogen Receptor 1 (*GPER1*) and superoxide dismutase 1 (*SOD1*) was disrupted. Previous work has implicated a role for GPER1 in the modulation of oxidative damage in the placenta via inhibition of aldehyde oxidase 1 (*AOX1*), resulting in oxidative damage and impaired function (Maiti et al. 2017). In rats, increased *SOD1* expression has been shown to indicate placental response to oxidative stress, suggesting the increase in

SOD1 expression observed in this study may indicate a compensatory mechanism towards the effects of GenX exposure. Taken together, these data suggest PFAS such as GenX may induce gene expression patterns consistent with excess oxidative stress, which is associated with adverse pregnancy outcomes like preeclampsia.

Despite the changes in JEG-3 gene expression induced after exposure to low concentrations of GenX, high concentrations of GenX tested in the screen did not induce consistent effects that could be modeled using dose-response analyses. This is important and may be due to low internal accumulation of GenX in JEG-3 cells in culture, recently shown by Bangma et al. (2020, *in review*). These findings also contradict those reported by Blake et al. (2020), which showed GenX exposure during pregnancy in an *in vivo* model resulted in lesions in the placental labyrinth at a lower administered dose than PFOA. These disparate findings may be due to limitations of the biological translatability of the *in vitro* JEG-3 monolayer system used in the present study and/or interspecies differences between human and mouse placental sensitivity towards PFAS.

There are several important caveats to this study. Primarily, the dose-response modeling estimates should not be overinterpreted. This efficient, high-throughput toxicity screen was designed to provide dose-response model estimates that could then be used as a general guide to help inform dose selection in future experiments and potentially prioritize the most toxic PFAS for future studies. The tradeoff between robustness and efficiency (in terms of both time and cost) is applicable to these data and should be taken into consideration. One caveat to implementing a multiplexed screen is that dose-response model estimates for endpoints could potentially occur as an artifact of cytotoxicity. We examined this relationship and found proliferation and cell viability were significantly but inconsistently correlated ($R^2 = 0.18$,

$p<0.05$). Thus, careful attention should be paid to interpreting proliferation and MMP estimates generated in this study, as there is a possibility these parameters were driven by overt cytotoxicity for certain PFAS. While the quality control and data processing implemented in this study attempted to avoid cytotoxicity-driven artifacts, the current experimental workflow precludes the ability to completely prevent such artifacts. Additionally, while the JEG-3 cell line is a useful model of human placental trophoblasts, it is likely that toxicity profiles and gene expression changes may not translate to human biology specifically because *in vivo* the placenta is a dynamic tissue that develops over time, as opposed to relatively static cell culture conditions. These findings would be significantly strengthened by follow up studies utilizing primary trophoblasts or *ex vivo* tissue to confirm the findings reported here.

Lastly, external dose (e.g. the concentration of PFAS in the cell culture media) might not correspond to the bioavailable dose or the internal dose in JEG-3 cells or other *in vitro* systems. Previous work has shown that PFAS have varying binding affinity towards serum proteins (Beesoon et al. 2015; Jones et al. 2003). Given that serum proteins are a necessary and common component of cell culture media, it is possible that the bioavailability of PFAS to the JEG-3 cells is lower than the initial concentration in the media. Therefore, the EC50 estimates reported here may underestimate the effects of PFAS towards cell viability, proliferation, and MMP. A recent report showed the intracellular concentration (e.g. internal dose) of PFOA and PFOS was higher after exposure in serum-free media compared to serum-containing media in JEG-3 cells (Bangma et al. 2020, *in review*). Interestingly, Bangma et al. (2020) similarly report shifts in placental trophoblast gene expression in JEG-3 cells with very low levels of intracellular GenX accumulation, suggesting placental trophoblast sensitivity towards PFAS like GenX is nuanced and may require different readouts than the endpoints included in the present study.

In this study we set out to develop a high-throughput toxicity screen to evaluate the effect of 42 unique PFAS on placental trophoblast viability and function as well as examine gene expression changes elicited by exposure to two PFAS selected due to their high public health relevance. Our data provide critical and novel basic PFAS toxicity data in JEG-3 placental trophoblasts and highlight the potential of these compounds to disrupt critical aspects of trophoblast biology, such as cellular proliferation and mitochondrial function. We also demonstrate the ability of PFOA and GenX to induce significant shifts in gene expression after 24 hours of exposure at concentrations as low as 1 µM and 3 µM, respectively. Taken together, these data suggest the placental trophoblasts as a target of PFAS and further study to determine mechanisms of toxicity are needed.

Table 4-1. Dose-response curve EC50 estimates for JEG03 cell viability, proliferation, and mitochondrial membrane potential (MMP) after exposure to PFAS.

NAME	CASRN	Viability EC50 ± SD (µM)	Proliferation EC50 ± SD (µM)	MMP EC50 ± SD (µM)
Perfluoro-2-methyl-3-oxahexanoic acid	13252-13-6	*nc*	*nc*	*nc*
Perfluoro-3,6-dioxadecanoic acid	137780-69-9	*nc*	282.8 ± 25.7	350.1 ± 16.1
8-H-Perfluorooctanoic acid	13973-14-3	317.5 ± 182.9	441.3 ± 18.1	147.3 ± 27.1
Perfluoro-3,6-dioxaheptanoic acid	151772-58-6	326.5 ± 85.7	351.3 ± 11.8	368.1 ± 22.6
Perfluoro-3,6,9-trioxadecanoic acid	151772-59-7	267.2 ± 26.8	302.9 ± 30.1	*nc*
7H-Perfluoroheptanoic acid	1546-95-8	222.8 ± 60.2	294.4 ± 48.2	*nc*
Perfluorooctanesulfonic acid	1763-23-1	291.2 ± 9.1	294.2 ± 5.8	352.9 ± 6.7
Perfluoroundecanoic acid	2058-94-8	266.1 ± 12.4	229.5 ± 13.3	200.1 ± 4.0
2,2-Difluoro-2-(trifluoromethoxy)acetate sodium salt	21837-98-9	*nc*	*nc*	*nc*
Perfluoropentanoic acid	2706-90-3	*nc*	*nc*	174.7 ± 68.4
6:2 Fluorotelomer sulfonic acid	27619-97-2	*nc*	*nc*	*nc*
2-(N-Ethylperfluorooctanesulfonamido) acetic acid	2991-50-6	202.7 ± 44.7	203.6 ± 17.7	*nc*
Perfluorobutylsulfonamide	30334-69-1	*nc*	*nc*	*nc*
Perfluorohexanoic acid	307-24-4	*nc*	*nc*	142.4 ± 12.6
Perfluorododecanoic acid	307-55-1	361.1 ± 30.8	317.8 ± 24.5	*nc*
Perfluoro-3,6,9-trioxatridecanoic acid	330562-41-9	194.9 ± 54.6	332.4 ± 34.1	*nc*
Perfluorooctanoic acid	335-67-1	357.7 ± 16.9	344.1 ± 12.2	360.2 ± 18.0
Perfluorodecanoic acid	335-76-2	180.7 ± 25.6	234.0 ± 22.8	235.8 ± 159.6
Perfluorohexane sulfonic acid	355-46-4	288.7 ± 29.6	251.6 ± 21.7	86.6 ± 71.5
Perfluorobutanoic acid	375-22-4	226.0 ± 115.7	209.2 ± 359.8	*nc*
Perfluorobutane sulfonic acid	375-73-5	330.4 ± 35.0	223.2 ± 76.7	*nc*
Perfluoroheptanoic acid	375-85-9	486.7 ± 408.6	277.4 ± 81.6	*nc*
Perfluoroheptane sulfonic acid	375-92-8	*nc*	296.2 ± 201.3	*nc*
Perfluorononanoic acid	375-95-1	332.6 ± 10.3	326.1 ± 5.5	304.6 ± 13.6
5H-Octafluoropentanoic acid	376-72-7	353.7 ± 28.6	333.7 ± 56.5	*nc*
Perfluoro-3-methoxypropanoic acid	377-73-1	303.7 ± 28.2	204.1 ± 110.9	93.1 ± 131.6
8:2 Fluorotelomer sulfonic acid	39108-34-4	159.5 ± 45.7	321.3 ± 171.2	331.1 ± 5.7
Perfluorooctanamide	423-54-1	*nc*	114.0 ± 35.6	294.6 ± 66.1
6:2 Fluorotelomer phosphate diester	57677-95-9	*nc*	141.8 ± 39.2	*nc*
6:2 Fluorotelomer phosphate monoester	57678-01-0	182.7 ± 21.7	193.3 ± 3.8	248.0 ± 62.1
8:2 Fluorotelomer phosphate monoester	57678-03-2	359.8 ± 30.3	250.7 ± 37.6	312.5 ± 29.8

Menadione	58-27-5	205.5 ± 47.1	157 ± 21.4	*nc*
Ammonium perfluoro-2-methyl-3-oxahexanoate	62037-80-3	*nc*	*nc*	*nc*
Sodium perfluoropentane sulfonate	630402-22-1	*nc*	*nc*	*nc*
6:2 Fluorotelomer alcohol	647-42-7	415.4 ± 70.6	*nc*	332.4 ± 44.1
8:2 Fluorotelomer alcohol	678-39-7	35.7 ± 36.5	*nc*	95.1 ± 15.3
8:2 Fluorotelomer phosphate diester	678-41-1	*nc*	*nc*	*nc*
Perfluorotridecanoic acid	72629-94-8	*nc*	388.1 ± 124.9	*nc*
Perfluorooctane sulfonamide	754-91-6	175.9 ± 4.9	160.0 ± 87.8	227.4 ± 369.9
9-H-Perfluorononanoic acid	76-21-1	349.9 ± 43.1	*nc*	186.9 ± 27.6
Perfluoro(4-methoxybutanoic) acid	863090-89-5	*nc*	*nc*	*nc*
2H,2H,3H,3H-Perfluorooctanoic acid	883499-79-4	*nc*	306.1 ± 47.9	158.6 ± 17.7
1H,1H-Nonafluoropentyl p-toluene sulfonate	914637-49-3	*nc*	*nc*	*nc*

Abbr: nc = an EC50 was not calculable based on poor dose-response model fit

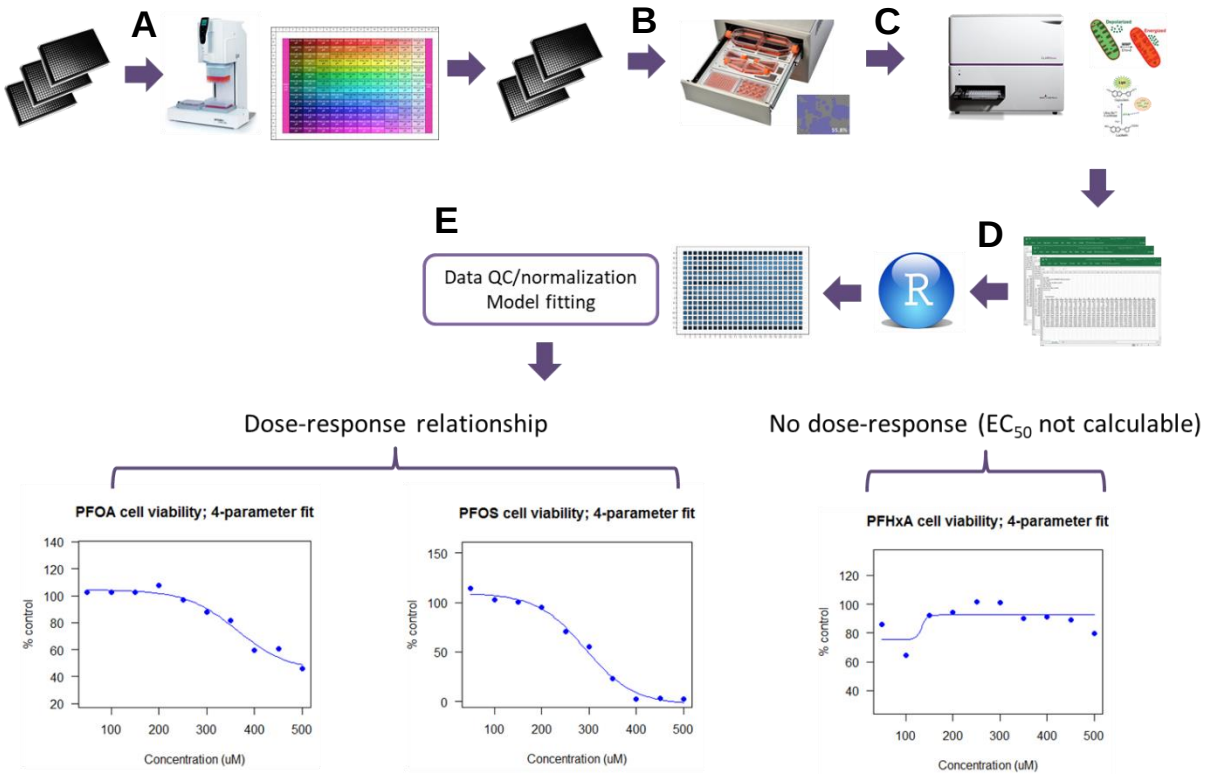

Figure 4-1. Experimental workflow to conduct efficient high-throughput toxicity screening of PFAS using JEG-3 cells. (A) JEG-3 cells were seeded in 384 well plates and exposed to test chemicals using a liquid handling device. Test chemicals were randomized and experimenters were blinded to their identity during the exposure period. (B) Cell growth was monitored over the 24 hour exposure period using a live cell imager. (C) Mitochondrial membrane potential and cell viability assays were multiplexed and read by fluorescence and luminescence intensities, respectively. (D) Raw data were imported into R and run through a custom script. (E) Four parameter dose-response curves were fit to the data and model estimates were extracted.

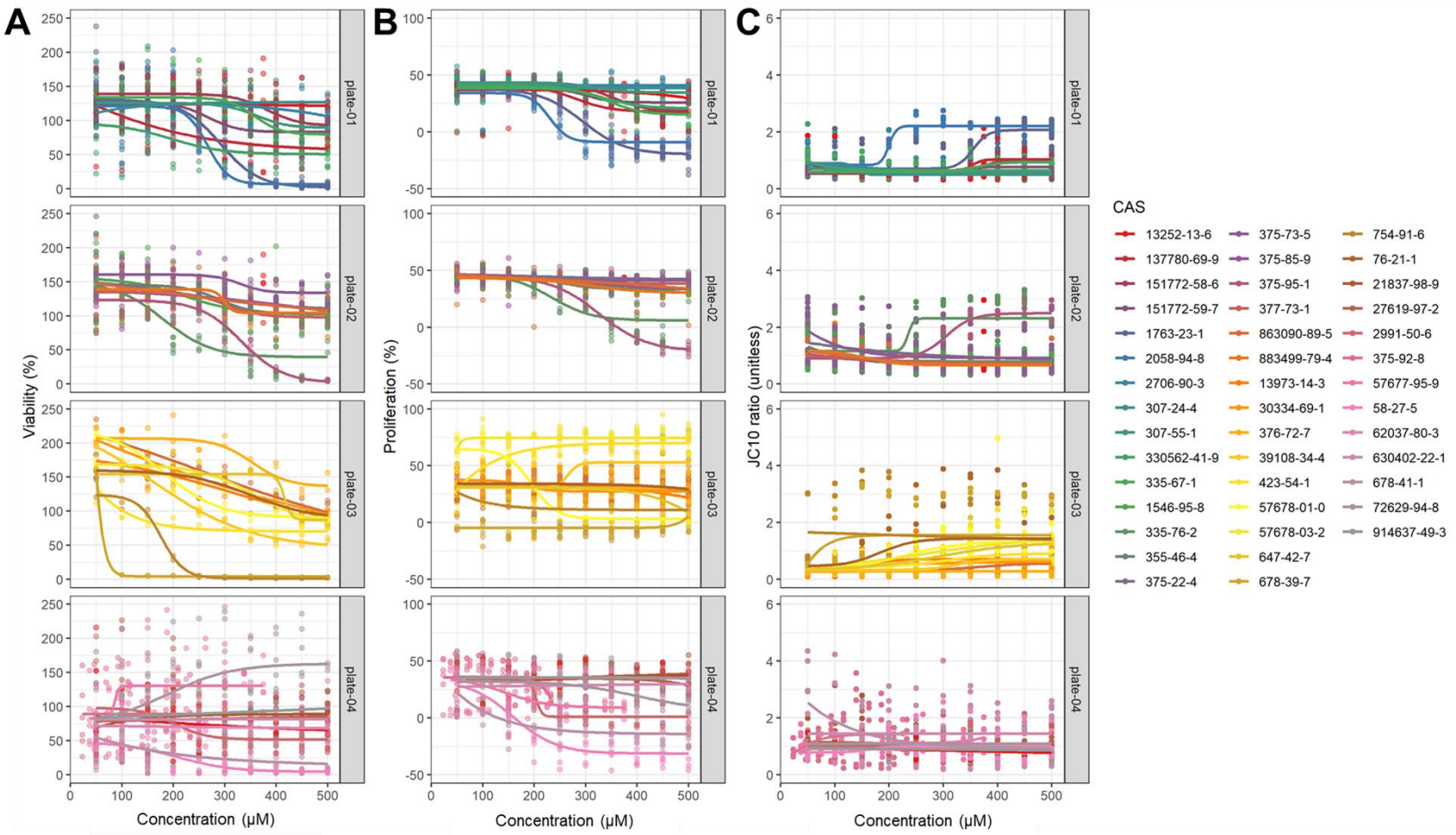

Figure 4-2. Dose-response modeling results obtained from JEG-3 cells exposed to 42 different PFAS congeners for 24 hours corresponding to (A) viability, (B) proliferation, and (C) mitochondrial membrane potential (MMP). Data were fit to a four-parameter dose-response model with no constraints and EC50 estimates were extracted. N = 3 biological replicates.

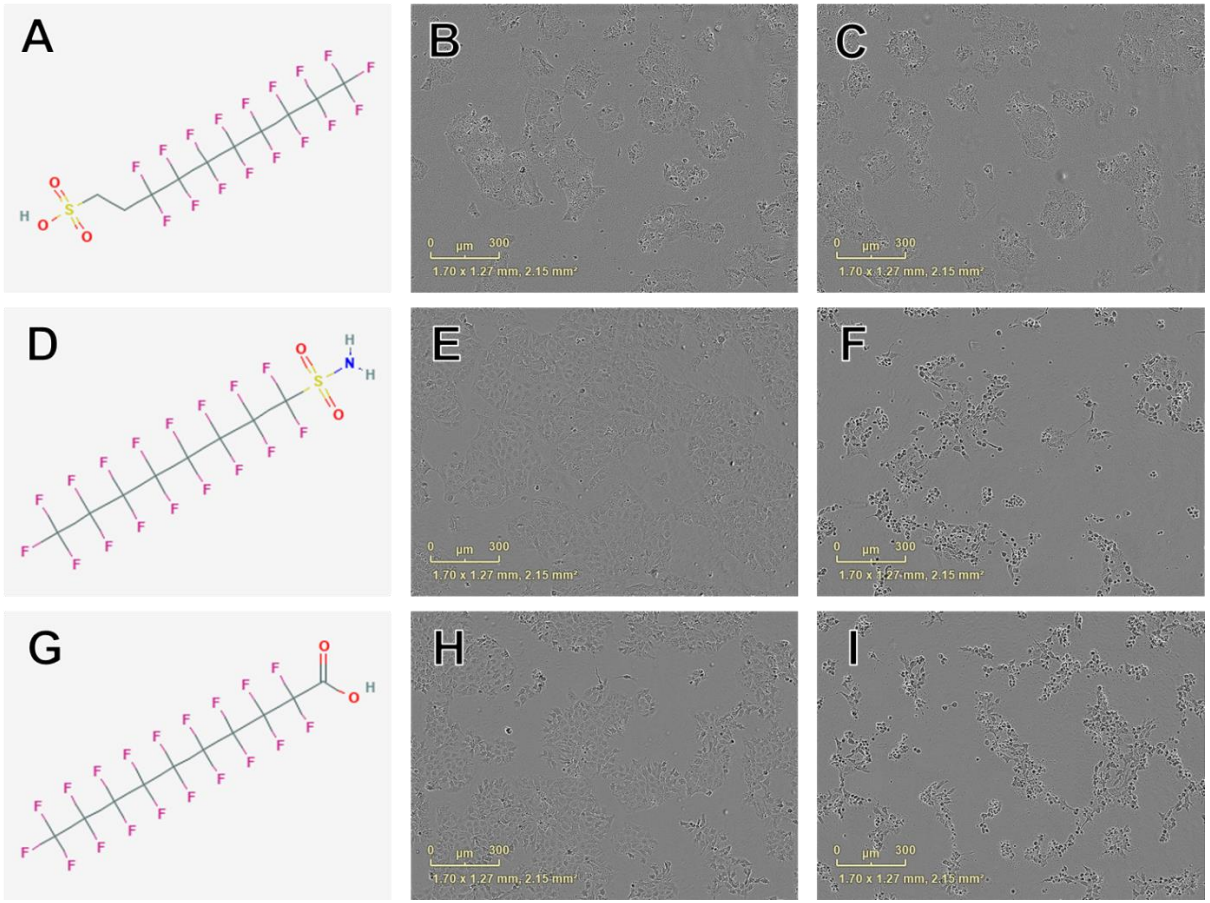

Figure 4-3. Examples of chemical structures and corresponding live cell images obtained from JEG-3 cells after 24 hours exposure to PFAS with most pronounced effects on cellular viability. A) Structure of 8:2 fluorotelomer sulfonic acid (CAS# 39108-34-4; viability EC50 ± SE: 160 ± 46 µM); B) Image of cells exposed to 300 µM CAS# 39108-34-4; C) Image of dead cells exposed to 500 µM CAS# 39108-34-4; D) Structure of perfluorooctane sulfonamide (CAS# 754-91-6; EC50 ±SE: 176 ± 5 µM); E) Image of cells exposed to 150 µM CAS# 754-91-6; F) Image of cells exposed to 300 µM CAS# 754-91-6; G)Structure of perfluorodecanoic acid (CAS# 335-76-2; EC50 ± SE: 181 ± 26 µM); H) Image of cells exposed to 250 µM CAS# 335-76-2; I) Image of cells exposed to 350 µM 335-76-2. Mild to moderate cell stress is apparent in B, E, and H marked by darkened, condensed nuclei and increased fibroblastic projections. Moderate to severe cell stress and death is apparent in C, F, and I.

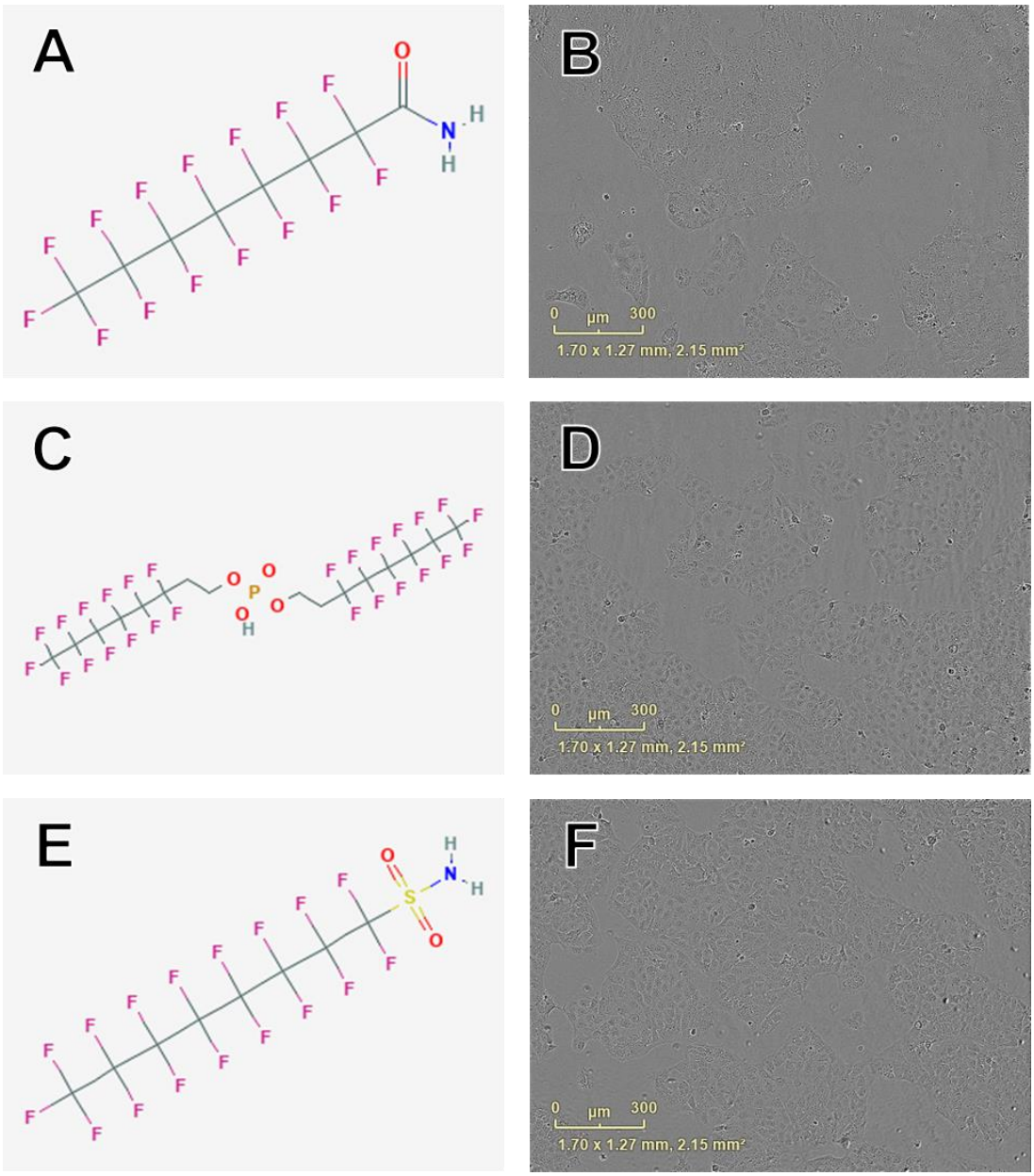

Figure 4-4. Examples of chemical structures and corresponding live cell images obtained from JEG-3 cells after 24 hours exposure to PFAS with most pronounced effects on cellular proliferation. A) Structure of perfluorooctanamide (CAS# 423-54-1; EC50 ± SE: 114.0 ± 35.6 µM); B) Live cell image of cells exposed to 150 µM CAS# 423-54-1; C) Structure of 6:2 fluorotelomer phosphate diester (CAS# 57677-95-9; EC50 ± SE: 141.6 ± 39.4 µM); D) Image of cells exposed to 150 µM CAS# 57677-95-9; E) Structure of perfluorooctane sulfonamide (CAS# 754-91-6; EC50 ± SE: 159.8 ± 90.0 µM); F) Image of cells exposed to 150 µM CAS# 754-91-6. No overt cell death is apparent in B, D, or F.

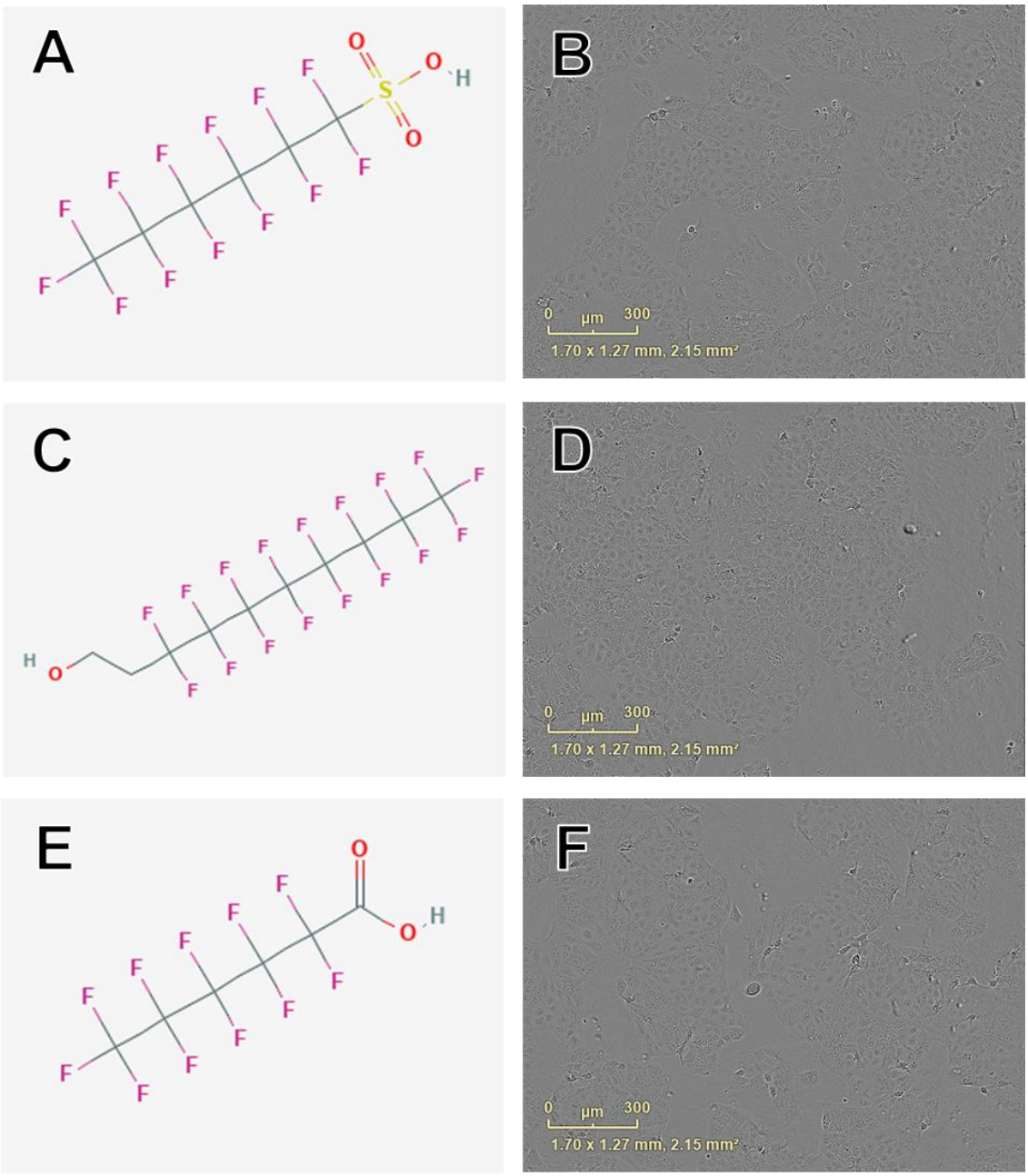

Figure 4-5. Examples of chemical structures and corresponding live cell images obtained from JEG-3 cells after 24 hours exposure to PFAS with most pronounced effects on mitochondrial membrane potential. A) Structure of perfluorohexanesulfonic acid (CAS# 355-46-4; EC50 ± SE: 86.2 ± 72.3 µM); B) Live cell image of cells exposed to 150 µM CAS# 355-46-4; C) Structure of 6:2 fluorotelomer alcohol (CAS# 678-39-7 EC50 ± SE: 95.4 ± 17.1 µM); D) Image of cells exposed to 50 µM CAS# 678-39-7; E) Structure of perfluorohexanoic acid (CAS# 307-24-4; EC50 ± SE: 140.9 ± 11.10 µM); F) Image of cells exposed to 150 µM CAS# 307-24-4. No overt cell death is apparent in B, D, or F.

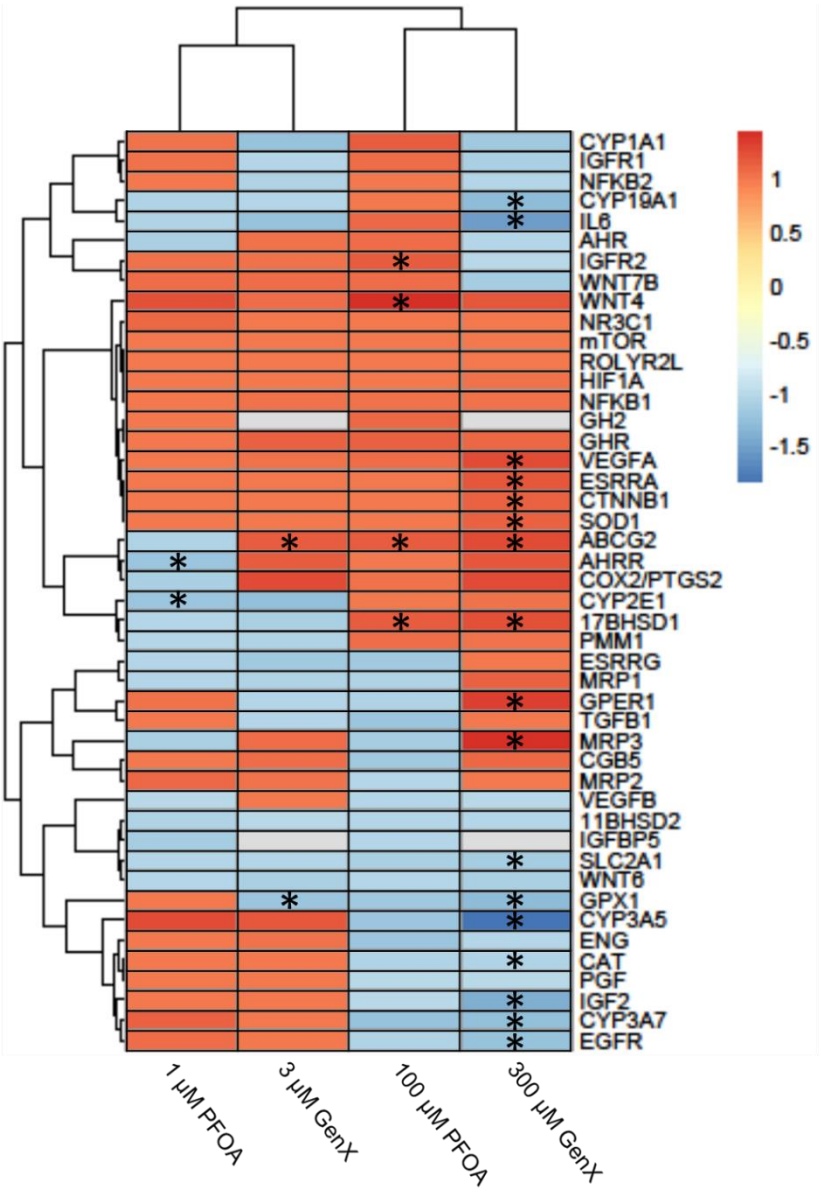

Figure 4-6. Heatmap illustrating gene expression changes in a set of 46 genes evaluated in JEG-3 cells after exposure to PFOA or GenX for 24 hours. Fold-change is indicated by the scale bar and colors on the heatmap. Experimental group fold-change values were compared to corresponding vehicle controls by ANOVA. Asterisks indicate significant shifts in gene expression at a false discovery rate of $p<0.1$ (N = 3). *GH2* and *IGFBP5* gene expression counts were below the threshold of detectivity in cells exposed to 3 or 300 µM GenX and are shown in grey.

CHAPTER 5: CONCLUSIONS AND FUTURE PERSPECTIVES

5.1 Summary

This dissertation summarizes a transdisciplinary scientific approach to evaluate the adverse health effects of per- and polyfluoroalkyl substances, with a special focus on the placenta as a critical target tissue. Human epidemiologic, animal model, and cell culture methodologies used in this body of work have provided critical insight on the human health consequences of PFAS exposure. Through examining an 18-year longitudinal, repeated measures dataset derived from a human biomonitoring study, the association between serum PFAS levels and two key adverse health outcomes, thyroid disruption and reduced kidney function, were demonstrated (Blake et al. 2018). A comparative developmental and reproductive toxicity study in CD-1 mice demonstrated that a replacement compound for PFOA, GenX, may pose a greater threat to the maternal-placental-embryo unit than previously estimated, and that both PFOA and GenX disrupt placental physiology and function (Blake et al. 2020). Transcriptome-wide gene expression analysis of CD-1 mouse placentas exposed developmentally to PFOA or GenX revealed disruptions in cholesterol and fatty acid transport, metabolism, and biosynthesis pathways. A high-throughput toxicity screen using human-derived placental trophoblasts determined toxicity profiles for 42 unique PFAS and found significant shifts in trophoblast gene expression following sub-cytotoxic exposures to GenX or PFOA that were consistent with those observed in preeclampsia. Taken together, these data collectively illustrate several key overarching findings: 1) the extent to which any one PFAS can induce a particular health outcome is congener-specific, 2) replacement or alternative chemistry PFAS may not be as safe

as initially advertised, and 3) the developing maternal-placental-embryo unit is uniquely sensitive and the placenta itself is a target of PFAS.

5.2 Impact of Findings

In Chapter 2, longitudinal human biomonitoring data spanning 18 years were leveraged to retrospectively examine the association between serum PFAS levels and biomarkers of chronic health conditions, including thyroid and kidney disease. Most human epidemiologic studies of PFAS-related health effects have utilized cross-sectional data, such as the NHANES dataset. Here, the use of robust statistical models to evaluate repeated measures of both serum PFAS levels and biomarkers of chronic disease over time significantly strengthens the ability to draw causal inferences from epidemiologic data. The variability of within- and between-individual serum PFAS repeated measurements was also determined as intraclass correlation coefficients (ICCs), which had only been reported in one other study (Papadopoulou et al. 2015) at the time of publication and provide critical insight to the temporal trends in PFAS exposure in this study population. This study significantly strengthened the existing body of literature by providing longitudinal evidence to support previous cross-sectional reports of kidney and thyroid disruption by PFAS exposure.

The most impactful findings from Chapter 2 were that serum levels of three different PFAS (PFNA, PFHxS, and PFDeA) were significantly negatively associated with kidney function and serum levels of PFOS were significantly positively associated with TSH levels (e.g. hypothyroidism). Notably, serum levels of PFOS measured in this study population were similar to those measured in the general US population, which suggests that many US citizens could be at increased risk for thyroid disruption by exposure to PFAS like PFOS.

Although the biomarkers measured in Chapter 2 were collected from adults, it is possible, and in fact very likely, that this population had been exposed to PFAS through drinking water for

their entire lifetime. The point sources of PFAS pollution are the DuPont facilities several hundred miles upstream of the Ohio River, in Parkersburg, West Virginia, which began using PFAS at the industrial scale (roughly >900 tons per year) by 1948 (Funderburg 2010). The study population was an average age of 38 years at enrollment into the biomonitoring program, which began in 1990. This means the average study participant was *in utero* between 1951-1952, several years after DuPont had initiated pollution of PFAS into tributaries feeding into the Ohio River aquifer. If we assume that study participants were lifelong residents of this small rural region of the Mid-Ohio valley, we can similarly assume these individuals were exposed to PFAS throughout *in utero* development, early childhood, adolescence, and into adulthood. Thus, some of the chronic health conditions identified in this adult population could have been significantly influenced by early life exposures.

In Chapter 3, a known developmental and reproductive toxicant, PFOA, was compared to an alternative chemistry PFAS congener brought to market to replace it, commonly known as GenX. This study was designed using CD-1 mice to directly compare PFOA and GenX doses relevant to regulatory decision making and included endpoints relating to maternal, embryo, and placental health. Here it was demonstrated that while externally administered doses of GenX were double those of PFOA, internal dosimetry for PFOA and GenX were similar in maternal serum, amniotic fluid, and whole embryos. This observation was unexpected as the elimination rate of GenX by CD-1 mice was previously estimated to be much more rapid than PFOA [GenX half-life: ~20 hours (Gannon et al. 2016); PFOA half-life: 17-19 days (Lau 2012; Lou et al. 2009)]. Given these substantially different elimination rates, greater internal accumulation of PFOA was expected in this study design (one dose every 24 hours). It is possible that these unexpected internal dosimetry results could be due to fluid retention caused by hypertension in

the pregnant mice. This study was not designed to collect the data needed to confirm this hypothesis, but gross observations during necropsy procedures (such as excess abdominal fluid in the pregnant dams and restricted urination at the time of euthanasia) suggest this could have been occurring. The serendipitous observation of this hypertension-like phenotype has resulted in the genesis of a new area of research within our group, which is focused on developing the scientific tools and methods needed to study hypertensive disorders of pregnancy in mice.

Interestingly, maternal liver accumulation of GenX was ~20-fold lower in mice exposed to GenX relative to PFOA accumulation in mice exposed to PFOA. Despite this, 2 mg/kg and 10 mg/kg GenX induced adverse liver pathology to a similar extent as 1 mg/kg PFOA and 5 mg/kg PFOA, respectively. Given the 20-fold lower liver accumulation of GenX, the implication is that GenX is a more potent liver toxicant than PFOA. This is in direct contradiction to previously reported toxicokinetic data provided by industry-funded studies.

The lowest observed adverse effect level (LOAEL) for GenX in this study was 2 mg/kg GenX, which induced placental lesions and cytoplasmic alterations in maternal liver, and significantly increased gestational weight gain. If the same risk assessment calculations applied to developmental and reproductive studies of 1 mg/kg PFOA to determine the US EPA lifetime health advisory level of 70 ppt (822-R-16-005 2016) were applied to this study, the resulting lifetime health advisory level for GenX would be 37 ppt. This is substantially lower than the current North Carolina state health goal of 140 ppt GenX in drinking water. It is critical to note that the US EPA risk assessment method uses maternal internal serum dosimetry rather than the orally administered dose. In my opinion, using administered oral doses in rodent toxicity studies of PFAS ultimately results in proposed regulatory levels that are not adequately protective. Due to the well reported interspecies differences in elimination rates, with rodents much more

efficiently excreting PFAS than humans, it is counterproductive to ignore results from studies based on “biologically irrelevant” oral doses. This is unique from other classes of environmental contaminants where human and rodent metabolism and excretion is similar.

In Chapter 3, a novel adverse PFAS-related phenotype in mouse placenta is described. *In utero* exposure to either PFOA or GenX resulted in elevated placental weights, reduced placental efficiency, and lesions affecting trophoblasts in the placental labyrinth. Importantly, lesions were apparent after exposure to 2 mg/kg GenX (but not 1 mg/kg PFOA) without alterations in placental weight or fetal:placental weight ratios. The different patterns in lesion subtype incidence between PFOA and GenX, with labyrinth congestion more common after exposure to PFOA and labyrinth atrophy more common after exposure to GenX, led me to hypothesize that PFOA and GenX were affecting the placenta through unique molecular mechanisms of action. However, results presented in Appendix 4 from transcriptome-wide gene expression analyses suggest the opposite. Evaluation of canonical pathways with significantly altered gene expression patterns in placentas showed that liver X receptor/retinoid X receptor (LXR/RXR) activation was significantly altered across all treatment groups and timepoints, relative to respective controls. Notably, significant shifts in gene expression and pathways occurred in E11.5 placentas, which did not exhibit shifts in tissue weight or adverse histopathology. Similarly, significant alterations in gene expression pathways were detected in E11.5 placentas exposed to 1 mg/kg PFOA, which also did not exhibit significant shifts in tissue weight or histopathology. Such alterations in placental gene expression likely influence function, and may contribute to developmental programming of latent cardiometabolic health conditions. This work would be significantly strengthened by transcriptome-wide gene expression analysis of maternal livers. It is possible that disruptions in placental sterol transport pathways are not due to a direct

effect of PFAS exposure but rather indirect sequelae of effects on maternal liver cholesterol and bile acid biosynthesis.

This work builds a case for the importance of evaluating the placenta as a critical tissue in studies of developmental and reproductive toxicity through utilizing clinically relevant, translational endpoints to illustrate the unique susceptibility of this organ to the adverse effects of two PFAS: PFOA and its replacement GenX. We hypothesized the placenta as a target tissue for PFAS and our data are the first to demonstrate congener-specific effects of PFAS on placental physiology. Given the similarities in enriched pathways when comparing gene expression profiles across GenX and PFOA treatment groups, it is possible that congener-specific effects on placenta lesion incidence could be an artifact of sample size. Placenta lesions tended to affect all placenta in a litter or none. Given the relatively small sample size at the level of the litter (N = 5-6 per group), it is possible that a more robust sample size would provide a more consistent incidence of labyrinth atrophy, congestion, and necrosis across PFOA and GenX dose groups. However, placental sensitivity and compensatory mechanisms in response to environmental insults are likely nuanced, so it is possible that the reported differences in lesion profiles are honest signals of subtle differences in gene expression patterns when comparing PFOA and GenX. This may require a different gene expression platform with greater read depth, such as RNA-seq, to identify candidate genes.

The novel hypertensive-like maternal phenotype and novel adverse placental phenotypes described in Chapter 3 have led to a robust follow-up study in CD-1 mice. The aims of this follow-up study are to further evaluate the cardiometabolic programming effects of *in utero* exposure to PFOA (0, 0.1, or 1 mg/kg/day) or GenX (0, 0.2, 1, or 2 mg/kg/day) through using lower doses during gestational exposure. Males and females will both be evaluated for latent

cardiometabolic effects, such as disruptions in serum lipids, altered body mass composition, and body weight gain over time. Based on the findings in Chapter 3, I would expect offspring exposed to 2 mg/kg GenX during development to be most likely to exhibit disrupted cardiometabolic homeostasis in adulthood.

In Chapter 4, a panel of 42 different PFAS were evaluated using human-derived placental trophoblasts (JEG-3 cells) in an *in vitro* high-throughput toxicity screen (HTTS). The goal of this chapter was to develop an *in vitro* screening tool to help categorize PFAS by their placental bioactivity in order to prioritize compounds for further study. While HTTS provides potential for rapid data generation, it is unclear how well this model system translates to whole organism biology. For example, in Chapter 3 both GenX and PFOA induced adverse pathology in mouse placenta at equivalent internal doses, but GenX did not induce an equivalent or more toxic response than PFOA in JEG-3 cells. In fact, GenX was not cytotoxic at any of the doses tested in the JEG-3 HTTS. However, these conclusions are drawn based on the external doses of PFOA and GenX in the HTTS (e.g. the concentration of the chemical in the cell culture media) and binding of PFAS to serum proteins in the cell culture medium may affect bioavailability. This experimental design would be significantly strengthened by using *ex vivo* human placental explants, primary placental cell lines, or placental cell spheroids. While these approaches may offer greater biologic relevance, they come at the cost of reduced efficiency and increased cost. Interestingly, exposure to sub-cytotoxic concentrations of PFOA or GenX induced gene expression changes in JEG-3 cells, including genes involved with nutrient transport, endocrine signaling, oxidative stress, and inflammation. Several genes identified in this experiment are common with genes altered in preeclamptic placentas, such as decreased expression of *GPX1*. However, these data are derived from a small pilot gene expression experiment and would be

significantly strengthened by follow up experiments, including validation by qPCR and protein expression quantitation by Western blot.

Collectively, this dissertation has substantially contributed to the existing knowledge on PFAS toxicity, specifically in the area of developmental and reproductive toxicity. This dissertation has served to both bolster existing associations between exposure to PFAS and adverse health outcomes, as well as provide greatly needed data to fill critical knowledge gaps. Novel findings have led to multiple new projects that will continue to explore how exposure to PFAS affects our health. Additionally, data presented in Chapter 3 will likely influence regulatory decisions on GenX drinking water standards at the federal level by the US EPA and the state level by the North Carolina Department of Environmental Quality.

5.3 Future Studies

There are several critical gaps in knowledge that have yet to be addressed. **First, the novel hypertensive-like phenotype in pregnant mice exposed to PFOA or GenX discovered in Chapter 3 should be further studied and characterized.** This would be accomplished through repeating the experimental design described in Chapter 3 regarding the dosing schedule but including lower doses for both chemicals. Pregnant CD-1 mice exposed daily to PFOA or GenX would be evaluated for clinically relevant endpoints pertinent to human hypertensive disorders of pregnancy, including high blood pressure (BP), uterine and placental blood flow, proteinuria, hematologic changes, and elevated liver enzymes. Elevated BP, proteinuria, elevated liver enzymes, and hematologic changes are all clinically relevant diagnostic criteria for pregnant women with hypertension (Mammaro et al. 2009). This study would provide the opportunity to include toxicokinetic measurements of compound elimination rates in pregnant mice, an important and unanswered question in the literature. Previous work has demonstrated the half-life of both PFOA and GenX in CD-1 mice, however it remains unclear whether the elimination

kinetics are altered by pregnancy, especially given the evidence that these compounds may in fact disrupt fluid retention via the novel hypertensive-like phenotype described in Chapter 3. Therefore, it is possible that the half-life of either PFOA or GenX is significantly altered by exposure-related changes in kidney function and fluid retention. This may be especially relevant for GenX, as maternal internal dosimetry data shown in Chapter 3 highlight the unexpected extent to which GenX accumulated in maternal serum, amniotic fluid, and whole embryos.

Separate cohorts of pregnant mice would be evaluated for elimination toxicokinetics and hypertension measurements. Mice assigned to the elimination toxicokinetics group would be orally gavaged on E0.5 with their respective treatment and serum, urine, and feces would be collected at 2, 4, 8, 12, 24 hours post-exposure (24hr collection immediately prior the subsequent dose). Urine, feces, and serum collection at the 2 to 24 hours post-exposure timepoints would occur daily post-exposure from E0.5 to E17.5. Treatment groups would include 0, 0.1, 1, and 5 mg/kg/day PFOA and 0, 0.1, 1, 2, and 10 mg/kg GenX. Each treatment group would consist of pregnant and nonpregnant female mice (N = 3 pregnant and N = 3 non-pregnant mice per group). Urine, serum, and feces samples would be measured for PFOA or GenX to determine elimination kinetics over the course of daily exposure during pregnancy. Serum and urine samples would be analyzed using high performance liquid chromatography tandem mass spectrometry (HPLC MS-MS). This could then be directly compared to the data collected at the same timepoints from non-pregnant females exposed to the same dose levels to evaluate whether elimination kinetics of PFOA or GenX are altered in pregnant mice.

Pregnant mice assigned to the hypertension measurements cohort would include the same dose groups as in the toxicokinetics group (N = 3 per group) and would be housed in metabolic

cages. Mice allocated to this group would be housed in the metabolic caging for two weeks prior to breeding in order to desensitize the mice to this type of housing.

BP could be monitored in mice using radiotelemetry methods described by Butz and Davisson (2001). This method would require telemetry probe implantation surgery prior to mouse breeding but would allow for continual BP monitoring. If this approach were not feasible due to cost or technical limitations, the CODA noninvasive tail-cuff BP system (Kent Scientific Corporation, CT, USA) could be used for obtaining BP measurements.

BP monitoring and placental blood flow would be evaluated at three points during gestation: prior to full vascularization of the uterine wall (E9.5), after full vascularization of the uterine wall (E12.5), and once the placenta has fully matured (E15.5). Ultrasound of placental blood flow would be evaluated using a transcutaneous micro-ultrasound (Model 770 with a 30-MHz transducer; VisualSonics, Toronto, Canada) of the uterine arteries to quantify uterine artery hemodynamics (e.g. blood velocity, following methods described by Qu et al. 2014) as well as placental oxygenation (following methods described by Kulandavelu et al. 2012). Serum would be collected via the tail vein and assessed for hematologic changes (e.g. thrombocytopenia indicated by low platelet count and hemolysis indicated by elevated hemoglobin) and elevated liver enzymes (e.g. aspartate aminotransferase, AST; alanine aminotransferase, ALT; alkaline phosphatase, ALP; lactate dehydrogenase, LDH), which would be determined through clinical chemistry analyses, as described in Chapter 3.

Urine would be collected daily throughout pregnancy from the collection reservoir in the metabolic caging. Total urinary volume would be measured at the end of each daily collection period, as it is possible that fluid retention would occur in PFOA or GenX-exposed pregnant mice. Reduced total urinary volume in treated mice would suggest increased fluid retention,

while increased levels of protein in the urine would suggest hypertension. It is possible that urine collection may not be possible due to restricted/limited urination or that pregnant mice may not tolerate long-term housing in metabolic caging despite pre-pregnancy desensitization training. If this were the case, body composition could be evaluated using a Bruker Minispec Whole Body Composition Analyzer (MA, USA). This method would allow for noninvasive determination of body mass of pregnant mice, including the proportion of lean tissue, fat, and fluid.

This set of experiments would provide critical insight into the novel hypertensive-like phenotype discovered in mice exposed to PFOA or GenX during gestation through (1) determining the elimination kinetics of PFOA and GenX in pregnant mice compared to nonpregnant females to evaluate whether pregnancy (or treatment-related hypertensive effects during pregnancy) influences elimination rate and (2) evaluating clinically relevant endpoints related to human hypertensive disorders of pregnancy, such as elevated blood pressure, proteinuria, elevated liver enzymes, and low platelets.

Given the results reported in Chapter 3, I would expect elimination kinetics of GenX and PFOA to be altered in pregnant mice. I would expect a slower urinary elimination rate for both compounds, which would be slower in a dose-responsive manner (e.g. slower elimination with increasing doses). This would be caused by increased fluid retention possibly via an increased severity of hypertension across the dose-response curve. Because the half-life of PFOA in mice is ~14 days, altered elimination in pregnant mice might be difficult to quantitate given the daily dosing schedule. However, I would predict altered elimination kinetics for GenX to be more easily quantified given its ~20 hour half-life in mice.

I would also anticipate increased blood pressure, proteinuria, and elevated liver enzymes in mice exposed to PFOA or GenX during pregnancy, with greater increases across the dose-

response curve. Additionally, I would expect impaired uterine blood flow (e.g. disrupted blood velocity) and reduced placental oxygenation in pregnant mice exposed to PFOA or GenX.

Second, predictive frameworks should be constructed for identifying thyroid disrupting potential of unstudied PFAS. Disruptions in thyroid hormones may be a critical driver of other PFAS-related adverse health outcomes. Although disruptions in thyroid hormones are not consistently reported across the human epidemiologic literature, this could be due to the compensatory nature of endocrine feedback loops, different levels of PFAS exposure across human populations, and inconsistent methods for evaluating disrupted thyroid hormones (e.g. measuring TSH only or T4 only). Multiple studies of pregnant women have implicated thyroid disruption as a consequence of maternal PFAS exposure (Berg et al. 2015; Webster et al. 2014; Yang et al. 2016, and others). Predicting the potential for unstudied PFAS to disrupt thyroid hormones is necessary in order to develop regulatory frameworks designed to be protective of this highly sensitive subpopulation.

Thyroid hormones maintain metabolic homeostasis in liver, kidney, and placenta. Specifically, thyroid hormones regulate lipogenesis gene expression, including indirect regulation of hepatic lipogenesis transcription via effects on expression and activity of required transcription factors, such as liver X receptors. Given the role of thyroid hormones in hepatic fatty acid and cholesterol synthesis/metabolism, the alterations in maternal hepatocytes (e.g. increased mitochondria and peroxisomes) in mice exposed to PFOA and GenX, the gene expression pathway data implicating cholesterol and lipid transport disruption in PFOA and GenX-exposed placentas, and disrupted thyroid hormone (T4) in GenX-exposed placenta described in Chapter 3, it is possible that disruptions in maternal thyroid hormones initiate a

cascade of adverse effects that impact the function of multiple organ systems, including liver and placenta.

PFAS exposure is generally associated with hypothyroidism. Many of the adverse outcomes associated with PFAS exposure can also occur as a consequence of hypothyroidism. Hypothyroidism is associated with increased serum triglycerides and cholesterol as well as non-alcoholic fatty liver disease (Sinha et al. 2018), increased systemic vascular resistance, decreased cardiac output, decreased renal blood flow, and reduced glomerular filtration rate (van Hoek and Daminet, 2009).

One hypothesized mechanism through which PFAS disrupt thyroid hormones is via competitive binding to thyroid hormone transport proteins (Weiss et al 2009). Given the observation in Chapter 3 that GenX disrupted placental thyroid hormone levels in mice and that multiple human studies have shown associations between maternal PFAS exposure and disrupted thyroid hormones during pregnancy, determining the thyroid disrupting potential of emerging alternative PFAS is a critical step to identify compounds posing the greatest risk to the health of pregnant women and their developing offspring. Although machine learning has recently been leveraged to classify the bioactivity of ~3,000 PFAS, this effort was unable to include thyroid hormone binding protein bioactivity due to insufficient data in the existing body of literature (Cheng and Ng, 2019). However, Cheng and Ng (2019) identified the importance of characterizing binding affinities of PFAS to thyroid hormone transport proteins in the context of human health. In this same vein, a recent review by Hall and Peng (2020) identified protein-chemical interactions as both the current bottleneck as well as the critical knowledge gap in adverse outcome pathway (AOP), HTTS, and computational toxicology methodologies.

Thus, characterizing the binding affinities of replacement PFAS to thyroid hormone transport proteins is sorely needed. GenX is just one of many "alternative chemistry" PFAS, several of which have also contaminated the Cape Fear River (CFR) in North Carolina. Characterizing the transthyretin, thyroid binding globulin, and albumin binding affinities of these replacement/alternative PFAS would provide important, human health relevant data. McCord and Strynar (2019) identified non-legacy PFAS in the CFR, 22 of which have associated CASRNs and could be curated for thyroid hormone transport protein binding affinity assays.

A combination of traditional and computational toxicology methods would be employed to evaluate the thyroid hormone transport protein-PFAS interactions. First, competitive binding assays would be conducted for the 22 novel PFAS identified as pollutants in the CFR. Competitive binding affinities for transthyretin, thyroid binding globulin, and albumin against thyroxine (T4) would be determined via direct fluorescent binding assays and radioligand binding assays using methods described by Ren et al. (2016) and Weiss et al. (2009). Data obtained from these experiments would be used in a combination of classification-based and regression-based quantitative structure-activity relationship (QSAR) models (based on methods described by Kar et al. 2017). These results would be compared to molecular docking simulations of the PFAS in the binding pockets of transthyretin, thyroid binding globulin, and albumin using methods described by Ng and Hungerbuehler (2015). If QSAR and molecular docking data were consistent with experimental data, these computational models may provide a framework for predicting thyroid disruption by PFAS.

Third, the challenges posed by interspecies extrapolation of PFAS toxicity data could be ameliorated by a transgenic mouse model expressing human OAT4 in kidney and placenta. One of the major limitations of mouse-to-human toxicity data extrapolation for PFAS

is the massive difference in elimination rate. This is likely due to the lack of a rodent homolog for the OAT4 gene. In humans, OAT4 is expressed in kidney tubular cells and placenta trophoblasts. In human kidney, OAT4 is situated on the apical membrane and is thought to contribute to renal reabsorption of PFAS, thus causing localized damage to the renal tubules, ultimately damaging the kidney and reducing glomerular filtration rate. In human placental trophoblasts, OAT4 is located on the basolateral side facing the fetal blood supply and is thought to play a role in transporting PFAS out of fetal circulation, through the placenta, and back into the maternal blood supply for subsequent elimination.

Reduced kidney function is well reported in human studies in association with PFAS exposure but altered kidney function and/or kidney pathology are not observed in rodent models. In Chapter 3, no adverse histopathological changes were observed in mice exposed to PFOA or GenX throughout gestation; only a slight yet statistically significant increase in relative kidney weight was noted. The lack of a rodent OAT4 homolog may explain the lack of kidney effects in rodent studies of PFAS exposure and the much faster elimination rate. This rapid elimination rate requires exposing mice and rats to high oral doses that are not human-relevant in order to recapitulate other human-relevant PFAS-related endpoints. Therefore, a mouse line humanized for the OAT4 gene should be generated. This novel transgenic mouse model would require validation prior to PFAS exposure studies, assuming knocking in OAT4 would not result in embryonic lethality. OAT4 gene and protein expression would need to be validated by qPCR and Western blot, respectively.

Once validated, toxicokinetic studies on the humanized OAT4 mice would be performed in adult mice to first determine whether elimination rates are indeed slower. Then the next step would be to conduct a chronic 90-day low-dose exposure study and determine whether the dose-

response curve is left-shifted as would be expected if elimination rates were slower. Kidney function could be specifically evaluated following methods described by Stevens & Oltean (2018) alongside parameters previously evaluated to determine whether effects on other tissues are modulated by the presence of humanized OAT4 in the kidneys (for example, cytoplastic alteration of hepatocytes, increased liver weight, immune function).

If the data obtained from this transgenic mouse model demonstrated the predicted slower elimination kinetics, reduced kidney function, and kidney damage, it would be prudent to repeat the gestational exposure experiments with PFOA and GenX at human relevant exposure levels. Using the humanized OAT4 mice in a gestational exposure experiment would enhance the mouse-to-human extrapolation of adverse PFAS-induced maternal, placental, and embryo outcomes as the human placenta also expresses OAT4.

Fourth, the potential for epigenetic mechanisms of placental effects due to PFAS exposure. There is increasing evidence for the role of placental epigenetics in hypertensive disorders of pregnancy like preeclampsia (Choudhury and Friedman, 2012). In a study by von Straten et al. (2010), a specific pattern of CpG nucleotide hypermethylation in fetal liver LXRα gene promoter was observed at E19.5 in offspring of protein-restricted dams. It has yet to be determined whether the gene expression pathway enrichment patterns described in Appendix 4 (such as LXR/RXR activation) are influenced by altered methylation in associated gene promoters. This question could be explored using mouse placentas from the study described in Chapter 3. Placenta DNA methylation would be assessed using a CpG island microarray following manufacturer's protocols (Agilent, CA, USA). Based on the similarities between differential methylation of the LXRα gene promoter in fetal livers exposed to protein-restriction identified in von Straten et al. (2010) and the enrichment of the gene expression in the

LXR/RXR activation pathway in rat placentas exposed to protein-restriction identified by (Daniel et al. 2016) to the data presented here in Appendix 4, I would expect the LXRα gene promoter to similarly exhibit hypermethylation in placentas exposed to PFOA or GenX *in utero*.

5.4 Final Thoughts

The relationship between PFAS exposure and adverse health effects in humans is complex and an exceptionally difficult area of study. As such, the ability to synthesize translational and transdisciplinary scientific research methods will be required if the field is to continue moving forward.

APPENDIX 1: SUPPLEMENTARY INFORMATION FOR CHAPTER 2

Table A1-1. Thyroid hormone reference ranges and methods of measurement.

Endpoint	Years	Reference range	Laboratory	Method
T4, total	1990-1996	4.5-11.5 µg/dL	UCMC	Reference method: Immunoassay Definitive Method: Isotope dilution mass spectrometry Primary Standard: L-Thyroxine Sodium Salt Secondary Standard: T4 in human serum matrix
TSH	1990-1996	0.40-5.00 uIU/mL	UCMC	Reference method: Isometric assay Definitive Method: Cytochemical bioassay Primary Standards: WHO second IRB International Reference Preparation Second Standard: TSH in human serum matrix
	1990-1996	0.47-6.90 uIU/mL	AL	
	1997-2000	0.36-5.80 uIU/mL	CCHMC	
	2001-2002	0.49-4.67 uIU/mL	CCHMC	
	2003-2004	0.34-4.82 uIU/mL	CCHMC	

Abbr: TSH= thyroid stimulating hormone; WHO= World Health Organization: IRB= International Review Board; UCMC= University of Cincinnati Medical Center, Dept. of Pathology and Laboratory Medicine; AL= Health Alliance Laboratory, Cincinnati OH; CCHMC= Cincinnati Children's Hospital Medical Center

Table A1-2. The CKD-EPI equation for estimating GFR on the natural scale*.

Sex	Ethnicity	Serum Creatinine (mg/dL)	Equation for eGFR
Female	White	≤ 0.7	$144 \times (S_{cr}/0.7)^{-0.329} \times 0.993^{Age}$
	Other	> 0.7	$144 \times (S_{cr}/0.7)^{-1.209} \times 0.993^{Age}$
Male	White	≤ 0.9	$141 \times (S_{cr}/0.7)^{-0.411} \times 0.993^{Age}$
	Other	> 0.9	$141 \times (S_{cr}/0.7)^{-1.209} \times 0.993^{Age}$

Abbr: eGFR= estimated glomerular filtration rate; Scr= serum creatinine
*adapted from Levey et al., 2009

Table A1-3. Chronic disease indicators at first measurement.

Indicator	N	Min	25th	Median	75th	Max
TSH (µIU/mL)	177	0.25	1.08	1.53	2.21	6.4
Total T4 (µg/dL)	184	3.80	6.80	7.65	7.78	13.5
eGFR (mL/min per 1.73 m^2)	209	49.0	86.9	103.8	118.7	143.3
BMI (kg/m^2)	210	17.6	22.7	25.3	28.0	47.1

Abrr: TSH=thyroid stimulating hormone, eGFR=estimated glomerular filtration rate, BMI=Body mass index

Table A1-4. Number of chronic disease indicators and PFAS measurements among FCC participants for by year.

Year	BMI	TSH	Total T4	eGFR	PFAS
1991	90	3	79	90	70
1992	62	1	56	63	38
1993	31	0	29	31	31
1994	88	5	12	86	85
1995	66	2	5	65	63
1996	45	3	3	45	41
1997	71	8	55	72	9
1998	67	60	0	68	26
1999	93	81	0	94	4
2000	76	66	0	74	0
2001	89	79	0	89	1
2002	74	63	0	74	0
2003	85	75	0	85	0
2004	79	71	0	79	0
2005	78	69	0	78	0
2006	88	79	0	88	3
2007	89	82	0	89	86
2008	61	55	0	61	60
Total	**1332**	**802**	**239**	**1331**	**517**

Table A1-5. Frequency of repeated measures among participants for chronic disease indicators and PFAS measurements.

	Distribution of repeated measures among participants									Participants with ≥1 measurement	Total measurements
	0	**1**	**2**	**3**	**4**	**5**	**6**	**7**	**8**		
BMI	0	3	10	16	11	13	29	46	82	210	1332
TSH	13	14	12	11	27	64	43	3	3	177	802
Total T4	6	129	55	0	0	0	0	0	0	184	239
eGFR	1	2	10	15	12	12	30	48	80	209	1331
PFAS	0	10	93	107	0	0	0	0	0	210	517

Table A1-6. Spearman correlation coefficients and corresponding p-values for PFAS at first measurement.

	PFOS	**PFOA**	**PFOSA**	**PFNA**	**PFHxS**	**PFDeA**	**Me-PFOSA**	**Et-PFOSA**
PFOS	1.00 (NA)	**0.36 (<0.05)**	**0.34 (<0.05)**	**0.60 (<0.05)**	**0.35 (<0.05)**	**0.44 (<0.05)**	**0.23 (<0.05)**	**0.37 (<0.05)**
PFOA	**0.36 (<0.05)**	1.00 (NA)	**0.15 (<0.05)**	**0.46 (<0.05)**	**0.30 (<0.05)**	**0.21 (<0.05)**	**0.14 (<0.05)**	**0.18 (<0.05)**
PFOSA	**0.34 (<0.05)**	**0.15 (<0.05)**	1.00 (NA)	0.10 (0.16)	0.03 (0.65)	0.08 (0.24)	0.10 (0.16)	**0.41 (<0.05)**
PFNA	**0.60 (<0.05)**	**0.46 (<0.05)**	0.10 (0.17)	1.00 (NA)	**0.37 (<0.05)**	**0.72 (<0.05)**	**0.17 (<0.05)**	0.13 (0.06)
PFHxS	**0.35 (<0.05)**	**0.30 (<0.05)**	0.03 (0.65)	**0.37 (<0.05)**	1.00 (NA)	**0.18 (<0.05)**	0.08 (0.27)	0.10 (0.16)
PFDeA	**0.44 (<0.05)**	**0.21 (<0.05)**	0.08 (0.24)	**0.72 (<0.05)**	0.18 (0.03)	1.00 (NA)	0.09 (0.21)	0.09 (0.18)
Me-PFOSA	**0.23 (<0.05)**	**0.14 (<0.05)**	0.10 (0.16)	**0.17 (<0.05)**	0.08 (0.23)	0.09 (0.21)	1.00 (NA)	0.08 (0.27)
Et-PFOSA	**0.37 (<0.05)**	**0.18 (<0.05)**	**0.41 (<0.05)**	0.13 (0.06)	0.10 (0.48)	0.09 (0.60)	0.08 (0.27)	1.00 (NA)

Table A1-7. Geometric mean concentrations[1] of PFAS by year of serum collection.

Year	N	PFOA		PFOS		PFOSA		PFNA	
		% <LOD	GM ± GSD	% <LOD	GM ± GSD	% <LOD	GM ± GSD	% <LOD	GM ± GSD
1991	70	0	12.6 ± 1.98	0	26.0 ± 1.46	25.7	0.16 ± 2.03	0	0.54 ± 1.58
1992	38	0	15.6 ± 1.89	0	28.5 ± 1.48	23.7	0.14 ± 2.00	0	0.56 ± 1.51
1993	31	0	11.6 ± 1.80	0	26.5 ± 1.67	16.1	0.16 ± 1.76	0	0.55 ± 1.67
1994	85	0	11.4 ± 2.03	0	31.2 ± 1.58	18.8	0.22 ± 2.15	1.2	0.55 ± 1.61
1995	63	0	11.9 ± 2.04	0	29.4 ± 1.51	25.4	0.18 ± 2.37	0	0.52 ± 1.58
1996	41	0	14.3 ± 1.90	0	36.8 ± 1.45	19.5	0.17 ± 2.05	0	0.58 ± 1.34
1997	9	0	8.26 ± 2.26	0	26.5 ± 1.79	11.1	0.22 ± 1.95	0	0.51 ± 1.62
1998	26	0	11.4 ± 1.64	0	29.0 ± 1.66	19.2	0.22 ± 2.43	0	0.53 ± 1.60
1999	4	0	15.5 ± 2.81	0	34.0 ± 1.54	50.0	0.22 ± 4.28	0	0.49 ± 1.18
2006	3	0	9.30 ± NA	0	44.3 ± NA	0	0.20 ± NA	0	0.60 ± NA
2007	86	0	11.9 ± 2.64	0	16.1 ± 1.97	100	0.07 ± 1.00	0	0.64 ± 1.66
2008	60	0	7.36 ± 2.28	0	13.4 ± 1.68	100	0.07 ± 1.00	0	1.02 ± 1.48
p		**<0.01**		**<0.01**		**<0.01**		**<0.01**	

Year	N	PFDeA		PFHxS		Me-PFOSA		Et-PFOSA	
		% <LOD	GM ± GSD	% <LOD	GM ± GSD	% <LOD	GM ± GSD	% <LOD	GM ± GSD
1991	70	30.0	0.13 ± 1.84	0	2.79 ± 2.08	0	0.62 ± 1.79	0	2.06 ± 2.08
1992	38	18.4	0.14 ± 1.63	0	3.02 ± 2.13	0	0.88 ± 2.03	0	2.33 ± 2.09
1993	31	29.0	0.11 ± 1.66	0	3.28 ± 2.57	0	0.66 ± 1.86	0	2.27 ± 2.05
1994	85	25.9	0.13 ± 1.84	0	2.87 ± 2.22	0	0.90 ± 1.80	0	2.34 ± 2.07
1995	63	33.3	0.12 ± 1.75	0	2.93 ± 1.98	0	1.18 ± 1.75	0	2.07 ± 2.06
1996	41	24.4	0.13 ± 1.76	0	3.64 ± 2.29	0	1.33 ± 1.53	0	2.14 ± 2.26
1997	9	66.7	0.09 ± 1.76	0	2.51 ± 1.68	0	1.54 ± 1.54	0	1.30 ± 1.64
1998	26	42.3	0.12 ± 1.67	0	2.60 ± 1.79	0	1.79 ± 1.75	0	1.94 ± 2.36
1999	4	50.0	0.08 ± 1.22	0	1.80 ± 1.69	0	1.57 ± 1.24	0	1.83 ± 2.86
2006	3	0	0.20 ± NA	0	2.60 ± NA	0	1.10 ± NA	0	5.00 ± NA
2007	86	33.3	0.16 ± 2.10	0	2.98 ± 1.63	0	0.73 ± 2.19	100	0.07 ± 1.00

2008	60	1.2	0.28 ± 1.70		0	2.31 ± 2.04		8.1	0.28 ± 2.16		88.4	0.08 ± 1.20
p			**<0.01**			**<0.01**			**<0.01**			**<0.01**

[1] Geometric mean concentrations calculated from linear model beta estimates for lognormal PFAS

Abbr: LOD (limit of detection) = 0.01 μg/L for all compounds, except PFOS (LOD = 0.02 μg/L); PFOA, perfluorooctanoic acid; PFOS, perfluorooctanesulfonic acid; PFOSA, perfluorooctanesulfonamide; PFNA, perfluorononanoic acid; PFDeA, perfluorodecanoic acid; PFHxS, perfluorohexane sulfonate; Me-PFOSA, 2-(N-methyl-perfluorooctane sulfonamido) acetic acid; Et-PFOSA, 2-(N-ethyl-perfluorooctane sulfonamido) acetic acid; SE, standard error

Table A1-8. Crude[a] percent change (95% confidence interval)[b] in chronic disease indicators in association with an interquartile range difference in serum PFAS concentrations from repeated measures models[c].

	TSH N = 172, 136		Total T4 N = 150, 150		eGFR N = 514, 209		BMI N = 516, 210	
PFAS	**% Δ (95% CI)**	**p**	**% Δ (95% CI)**	**p**	**% Δ (95% CI)**	**p**	**% Δ (95% CI)**	**p**
PFOA	3.00 (-5.48, 12.2)	0.50	-1.60 (-5.53, 2.49)	0.44	1.89 (-0.08, 3.85)	0.06	-4.79 (-6.37, -3.17)	**<0.01**
PFOS	10.4 (4.92, 16.1)	**<0.01**	-1.42 (-4.74, 2.01)	0.41	2.41 (1.38, 3.45)	**<0.01**	-3.43 (-4.23, -2.63)	**<0.01**
PFOSA	7.69 (-2.64, 19.1)	0.16	-1.30 (-5.71, 3.31)	0.58	4.82 (3.24, 6.39)	**<0.01**	-5.25 (-6.54, -3.95)	**<0.01**
PFNA	-1.25 (-8.14, 6.16)	0.74	2.07 (-1.65, 5.93)	0.28	-5.15 (-6.38, -3.92)	**<0.01**	4.75 (3.65, 5.87)	**<0.01**
PFHxS	2.10 (-6.62, 11.6)	0.65	0.85 (-2.59, 4.41)	0.63	-2.62 (-4.65, -0.58)	**0.01**	-1.02 (-2.88, 0.88)	0.29
PFDeA	-0.24 (-10.6, 11.3)	0.97	1.84 (-3.47, 7.44)	0.51	-7.12 (-8.98, -5.27)	**<0.01**	6.54 (4.85, 8.26)	**<0.01**
Me-PFOSA	3.34 (-2.51, 9.54)	0.28	1.11 (-3.14, 5.54)	0.62	3.98 (2.95, 5.01)	**<0.01**	-3.84 (-4.75, -2.92)	**<0.01**
Et-PFOSA	3.70 (0.08, 7.45)	**0.05**	2.45 (-1.22, 6.26)	0.20	2.47 (1.94, 3.01)	**<0.01**	-2.37 (-2.76, -1.98)	**<0.01**

N= Observations, subjects

[a] Covariates for adjusted models included age, year of measurement, sex, education, income, and marital status. Models of TSH, Total T4, and eGFR additionally include BMI as a covariate

[b] IQR values of eGFR are interpreted as percent change in eGFR relative to the population median in association with an interquartile range difference in serum PFAS concentrations (median eGFR = 102.8 mL/min per 1.73 m^2)

[c] Total T4 beta estimates were determined using a linear model without repeated measures

Table A1-9. Crude[a] percent change (95% confidence interval)[b] in chronic disease indicators in association with an interquartile range difference in serum PFAS concentrations from latent models[c].

	TSH N = 802, 177		Total T4 N = 239, 239		eGFR N = 1331, 209		BMI N = 1332, 210	
PFAS	**% Δ (95% CI)**	**p**	**% Δ (95% CI)**	**p**	**% Δ (95% CI)**	**p**	**% Δ (95% CI)**	**p**
PFOA	-2.43 (-11.3, 7.32)	0.61	-0.10 (-3.10, 2.99)	0.95	-3.66 (-6.85, -0.46)	**0.03**	1.84 (-1.59, 5.38)	0.30
PFOS	5.80 (-2.53, 14.84)	0.18	-0.75 (-3.34, 1.91)	0.58	-6.66 (-9.42, -3.90)	**<0.01**	2.1 (-0.96, 5.25)	0.18
PFOSA	-3.45 (-13.4, 7.59)	0.53	-0.41 (-3.89, 3.19)	0.82	-1.38 (-4.93, 2.16)	0.44	-2.93 (-6.59, 0.87)	0.13
PFNA	0.28 (-8.02, 9.33)	0.95	1.88 (-0.87, 4.70)	0.18	-7.19 (-9.94, -4.44)	**<0.01**	3.28 (0.09, 6.58)	**0.05**
PFHxS	2.88 (-5.3,0 11.8)	0.50	0.38 (-2.26, 3.09)	0.78	-4.11 (-6.81, -1.41)	**<0.01**	1.94 (-1.05, 5.03)	0.21
PFDeA	0.97 (-11.1, 14.7)	0.88	0.60 (-3.50, 4.88)	0.78	-7.49 (-11.7, -3.30)	**<0.01**	0.78 (-3.82, 5.61)	0.74
Me-PFOSA	-7.50 (-16.0, 1.89)	0.12	2.15 (-1.01, 5.42)	0.19	3.12 (0.03, 6.21)	**0.05**	-1.85 (-5.3, 1.73)	0.31
Et-PFOSA	0.15 (-7.96, 8.99)	0.97	2.76 (0.05, 5.53)	**0.05**	0.90 (-2.00, 3.79)	0.54	-0.18 (-3, 2.73)	0.90

N= Observations, subjects

[a] Covariates for adjusted models included age, year of measurement, sex, education, income, and marital status. Models of TSH, Total T4, and eGFR additionally include BMI as a covariate

[b] IQR values of eGFR are interpreted as percent change in eGFR relative to the population median in association with an interquartile range difference in serum PFAS concentrations (median eGFR = 102.8 mL/min per 1.73 m^2).

[c] Total T4 beta estimates were determined using a linear model without repeated measures

Table A1-10. Crude[a] percent change (95% confidence interval)[b] in chronic disease indicators in association with an interquartile range difference in serum PFAS concentrations from sensitivity analysis of latent models[c].

	TSH N = 796, 177		Total T4 N = 199, 199		eGFR N = 1278, 209		BMI N = 1280, 210	
PFAS	**% Δ (95% CI)**	**p**	**% Δ (95% CI)**	**p**	**% Δ (95% CI)**	**p**	**% Δ (95% CI)**	**p**
PFOA	-2.92 (-11.8, 6.85)	0.55	-1.28 (-4.50, 2.05)	0.45	-3.69 (-6.89, -0.50)	**0.02**	1.67 (-1.76, 5.22)	0.35
PFOS	5.28 (-3.07, 14.4)	0.22	-0.68 (-3.51, 2.22)	0.64	-6.82 (-9.57, -4.07)	**<0.01**	1.98 (-1.08, 5.13)	0.21
PFOSA	-3.89 (-13.8, 7.17)	0.48	1.21 (-2.74, 5.32)	0.56	-1.59 (-5.12, 1.95)	0.38	-2.94 (-6.61, 0.86)	0.13
PFNA	0.37 (-7.98, 9.48)	0.93	2.24 (-0.72, 5.29)	0.14	-7.16 (-9.91, -4.41)	**<0.01**	3.18 (-0.02, 6.48)	**0.05**
PFHxS	3.04 (-5.19, 12.0)	0.48	0.47 (-2.27, 3.29)	0.74	-4.03 (-6.73, -1.33)	**<0.01**	1.83 (-1.17, 4.91)	0.24
PFDeA	0.82 (-11.3, 14.6)	0.90	1.89 (-2.58, 6.55)	0.41	-7.61 (-11.8, -3.44)	**<0.01**	0.68 (-3.93, 5.51)	0.78
Me-PFOSA	-8.21 (-16.7, 1.18)	0.09	1.83 (-1.75, 5.54)	0.32	2.97 (-0.13, 6.06)	0.06	-1.73 (-5.2, 1.87)	0.34
Et-PFOSA	-1.22 (-9.38, 7.68)	0.78	3.55 (0.56, 6.63)	**0.02**	0.67 (-2.25, 3.59)	0.65	-0.43 (-3.27, 2.49)	0.77

N= Observations, subjects

[a] Covariates for adjusted models included age, year of measurement, sex, education, income, and marital status. Models of TSH, Total T4, and eGFR additionally include BMI as a covariate

[b] IQR values of eGFR are interpreted as percent change in eGFR relative to the population median in association with an interquartile range difference in serum PFAS concentrations (median eGFR = 102.8 mL/min per 1.73 m^2).

[c] Total T4 beta estimates were determined using a linear model without repeated measures

Table A1-11. Adjusted[a] percent change (95% confidence interval)[b] in chronic disease indicators in association with an interquartile range difference in serum PFAS concentrations from sensitivity analysis of latent models[c].

	TSH N = 724, 161		Total T4 N = 188, 188		eGFR N = 1174, 192		BMI N = 1179, 192	
PFAS	**% Δ (95% CI)**	**p**	**% Δ (95% CI)**	**p**	**% Δ (95% CI)**	**p**	**% Δ (95% CI)**	**p**
PFOA	-2.87 (-12.1, 7.31)	0.57	-1.03 (-4.22, 2.27)	0.54	-0.87 (-2.59, 0.84)	0.32	0.63 (-2.79, 4.18)	0.72
PFOS	1.10 (-7.61, 10.6)	0.81	0.15 (-2.83, 3.23)	0.92	-2.00 (-3.57, -0.42)	**0.01**	1.65 (-1.52, 4.91)	0.31
PFOSA	-2.10 (-12.7, 9.79)	0.72	0.44 (-3.61, 4.66)	0.83	-1.87 (-3.72, -0.02)	**0.05**	-3.06 (-6.72, 0.74)	0.11
PFNA	-5.25 (-13.9, 4.25)	0.27	3.06 (-0.21, 6.43)	0.07	-1.21 (-2.79, 0.37)	0.14	1.49 (-1.79, 4.88)	0.38
PFHxS	1.05 (-7.88, 10.9)	0.82	1.03 (-1.81, 3.95)	0.48	-1.16 (-2.67, 0.34)	0.13	2.01 (-1.09, 5.21)	0.21
PFDeA	-4.71 (-17.3, 9.80)	0.51	2.28 (-2.33, 7.11)	0.34	-0.95 (-3.30, 1.39)	0.43	-0.6 (-5.32, 4.36)	0.81
Me-PFOSA	-6.21 (-15.2, 3.74)	0.21	0.33 (-3.19, 3.97)	0.86	-0.41 (-2.05, 1.24)	0.63	-0.31 (-3.85, 3.35)	0.87
Et-PFOSA	-1.63 (-10.3, 7.80)	0.72	1.89 (-1.14, 5.02)	0.23	-1.06 (-2.64, 0.51)	0.19	0.48 (-2.4, 3.44)	0.75

N= Observations, subjects

[a] Covariates for adjusted models included age, year of measurement, sex, education, income, and marital status. Models of TSH, Total T4, and eGFR additionally include BMI as a covariate

[b] IQR values of eGFR are interpreted as percent change in eGFR relative to the population median in association with an interquartile range difference in serum PFAS concentrations (median eGFR = 102.8 mL/min per 1.73 m^2).

[c] Total T4 beta estimates were determined using a linear model without repeated measures

Table A1-12. Adjusted percent change in Total T4* in association with an interquartile range difference in serum PFAS concentrations in sex-stratified and interaction models relative to the median.

	Total T4				
	Female		**Male**		**Sex*Total T4**
	N = 81, 81		**N = 63, 63**		**N = 144, 144**
PFAS	**% change (95% CI)**	**p**	**% change (95% CI)**	**p**	**p**
PFOA	-1.62 (-6.88, 3.94)	0.56	-2.71 (-9.05, 4.08)	0.43	0.81
PFOS	1.69 (-3.28, 6.91)	0.52	-5.29 (-10.1, -0.26)	**0.04**	0.06
PFOSA	-4.41 (-10.3, 1.86)	0.17	4.42 (-2.86, 12.3)	0.25	0.08
PFNA	6.41 (0.55, 12.6)	**0.03**	-2.23 (-7.70, 3.60)	0.45	**0.05**
PFHxS	2.42 (-2.04, 7.09)	0.30	-0.01 (-5.80, 6.13)	1.00	0.82
PFDeA	6.54 (-1.66, 15.4)	0.13	-3.17 (-10.2, 4.43)	0.41	0.09
Me-PFOSA	1.19 (-5.37, 8.20)	0.73	-1.16 (-6.93, 4.97)	0.71	0.62
Et-PFOSA	2.53 (-2.91, 8.28)	0.37	-0.60 (-5.70, 4.76)	0.82	0.43

*Individuals taking thyroid-specific medications were excluded from thyroid hormone analyses. Covariates included in the sex-stratified and interaction models were the same as the covariates used in the parent model (Table 2-4).

Table A1-13. Adjusted percent change in thyroid stimulating hormone[a] in association with an interquartile range difference in serum PFAS concentrations in sex-stratified and interaction models[b].

	TSH				
	Female		**Male**		**Sex*TSH**
	N = 92, 75		**N = 62, 47**		**N = 154, 122**
PFAS	**% change (95% CI)**	**p**	**% change (95% CI)**	**p**	**p**
PFOA	-6.64 (-17.8, 5.97)	0.31	9.38 (-7.47, 29.3)	0.47	0.19
PFOS	5.13 (-5.29, 16.7)	0.36	21.4 (6.55, 38.3)	**0.01**	0.12
PFOSA	-9.29 (-25.9, 11.1)	0.36	21.1 (-11.6, 65.9)	0.44	0.14
PFNA	0.06 (-12.9, 14.9)	0.99	9.74 (-6.39, 28.6)	0.31	0.42
PFHxS	-7.46 (-19.9, 6.98)	0.31	20.7 (-1.60, 43.4)	0.35	**0.03**
PFDeA	11.3 (-9.08, 36.2)	0.32	15.9 (-8.74, 47.2)	0.43	0.86
Me-PFOSA	-6.47 (-17.5, 6.00)	0.31	-4.71 (-17.7, 10.3)	0.76	0.78
Et-PFOSA	-2.12 (-14.1, 11.5)	0.75	8.76 (-9.68, 31.0)	0.44	0.37

[a] Individuals taking thyroid-specific medications were excluded from thyroid hormone analyses.
[b] Covariates included in the sex-stratified and interaction models were age, education, income, marital status, and BMI.

Table A1-14. Adjusted percent change in eGFR relative to the population median* in association with an interquartile range difference in serum PFAS concentrations in sex-stratified and interaction models.

	eGFR				
	Female		**Male**		**Sex*eGFR**
	N = 289, 115		**N = 187, 77**		**N = 476, 192**
PFAS	**% change (95% CI)**	**p**	**% change (95% CI)**	**p**	**p**
PFOA	-1.38 (-3.41, 0.65)	0.18	0.95 (-3.08, 4.98)	0.64	0.38
PFOS	-1.32 (-3.37, 0.73)	0.21	0.71 (-2.75, 4.16)	0.69	0.46
PFOSA	-0.17 (-2.07, 1.74)	0.86	0.35 (-3.01, 3.70)	0.84	0.86
PFNA	-1.98 (-4.25, 0.29)	0.09	-2.15 (-5.32, 1.02)	0.19	0.74
PFHxS	-1.98 (-3.77, -0.18)	**0.03**	-2.03 (-4.54, 0.48)	0.12	0.74
PFDeA	-2.99 (-5.48, -0.49)	**0.02**	-0.14 (-4.41, 4.13)	0.95	0.26
Me-PFOSA	0.83 (-1.08, 2.74)	0.40	3.78 (1.25, 6.32)	**<0.01**	0.12
Et-PFOSA	5.66 (-0.22, 11.5)	0.06	2.84 (-4.54, 10.2)	0.45	0.57

*Female median eGFR = 109.7 mL/min per 1.73 m^2, male median eGFR = 87.9 mL/min per 1.73 m^2, overall median eGFR = 102.1 mL/min per 1.73 m^2. Covariates included in the sex-stratified and interaction models were the same as the covariates used in the parent model (Table 2-4).

Table A1-15. Adjusted percent change in body mass index in association with an interquartile range difference in serum PFAS concentrations in sex-stratified and interaction models*.

	BMI				
	Female		Male		Sex*BMI
	N = 321, 129		N = 187, 77		N = 477, 192
PFAS	% change (95% CI)	p	% change (95% CI)	p	p
PFOA	-0.72 (-3.01, 1.62)	0.54	-0.71 (-3.10, 1.74)	0.57	0.79
PFOS	0.48 (-1.13, 2.11)	0.56	-0.19 (-1.69, 1.33)	0.80	0.53
PFOSA	-0.13 (-2.46, 2.25)	0.91	-0.48 (-2.37, 1.44)	0.62	0.78
PFNA	0.82 (-1.09, 2.77)	0.40	-0.26 (-1.99, 1.50)	0.77	0.42
PFHxS	0.32 (-2.04, 2.73)	0.79	2.23 (-0.10, 4.61)	0.06	0.91
PFDeA	0.48 (-2.36, 3.40)	0.74	0.31 (-2.01, 2.69)	0.80	0.41
Me-PFOSA	-0.12 (-1.87, 1.66)	0.89	-1.10 (-2.20, 0.00)	0.05	0.89
Et-PFOSA	0.06 (-1.54, 1.68)	0.95	-0.2 0(-1.39, 1.00)	0.57	0.42

*Covariates included in the sex-stratified and interaction models were age, education, income, and marital status

APPENDIX 2: SUPPLEMENTARY INFORMATION FOR CHAPTER 3

Table A2-1. Number of total observations and litters represented in mixed effect models (observations, litters).

Embryonic day	Dose group	Embryo Weight	Embryo length	Placenta weight	Embryo:Placental weight ratio
11.5	Vehicle Control	68, 13	24, 8	68, 13	68, 13
11.5	1 mg/kg bw/day PFOA	64, 11	18, 6	62, 11	62, 11
11.5	5 mg/kg bw/day PFOA	66, 11	18, 6	65, 11	65, 11
11.5	2 mg/kg bw/day GenX (HFPO-DA)	71, 12	21, 7	70, 12	70, 12
11.5	10 mg/kg bw/day GenX (HFPO-DA)	62, 12	21, 7	62, 12	62, 12
17.5	Vehicle Control	80, 13	24, 8	80, 13	80, 13
17.5	1 mg/kg bw/day PFOA	66, 12	21, 7	66, 12	66, 12
17.5	5 mg/kg bw/day PFOA	73, 12	18, 6	73, 12	73, 12
17.5	2 mg/kg bw/day GenX (HFPO-DA)	68, 12	21, 7	68, 12	68, 12
17.5	10 mg/kg bw/day GenX (HFPO-DA)	66, 13	24, 8	66, 13	66, 13

Table A2-2. Internal dosimetry of tissues at embryonic day 11.5 including maternal serum, maternal liver, amniotic fluid, and whole embryo (Mean ± SD, N = 6-8).

Biological matrix	1 mg/kg bw/day PFOA	5 mg/kg bw/day PFOA	2 mg/kg bw/day GenX (HFPO-DA)	10 mg/kg bw/day GenX (HFPO-DA)
Maternal serum (µg/mL)	25.4 ± 3.7‡	117.3 ± 20.6	33.5 ± 15.7**	118.1 ± 10.4
Amniotic fluid (µg/mL)	4.6 ± 2.8*,‡	8.8 ± 2.7	3.6 ± 2.2**,§	9.3 ± 2.0
Maternal liver (µg/g)	48.3 ± 12.5*,†,‡	151.5 ± 18.5	5.45 ± 3.43§	19.9 ± 4.2††
Whole embryo (µg/g)	0.80 ± 0.10*,‡	2.34 ± 0.27	0.91 ± 0.22**,§	3.21 ± 0.51††

ANOVA with *post hoc* multiple comparison correction using Tukey contrasts:
* $P < 0.05$ 1 mg/kg/day PFOA vs 5 mg/kg/day PFOA
† $P < 0.05$ 1 mg/kg/day PFOA vs 2 mg/kg/day GenX
‡ $P < 0.05$ 1 mg/kg/day PFOA vs 10 mg/kg/day GenX
§ $P < 0.05$ 2 mg/kg/day GenX vs 5 mg/kg/day PFOA
** $P < 0.05$ 2 mg/kg/day GenX vs 10 mg/kg/day GenX
†† $P < 0.05$ 10 mg/kg/day GenX vs 5 mg/kg/day PFOA
Note: Vehicle control (VC) samples were quantified for PFOA and GenX (HFPO-DA); all VC means were below the limit of detection (LOD) of 10 ng/mL for both PFOA and GenX (HFPO-DA)

Table A2-3. Internal dosimetry of tissues at embryonic day 17.5 including maternal serum, maternal liver, male whole embryo and female whole embryo (Mean ± SD, N = 6-8).

Biological matrix	1 mg/kg bw/day PFOA	5 mg/kg bw/day PFOA	2 mg/kg bw/day GenX (HFPO-DA)	10 mg/kg bw/day GenX (HFPO-DA)
Maternal serum (µg/mL)	18.7 ± 3.2*,‡	95.1 ± 14.1	22.9 ± 17.1§,**	58.5 ± 34.5
Maternal liver (µg/g)	181.1 ± 46.0†,‡	159.2 ± 21.7	4.56 ± 2.80§	14.2 ± 7.6††
Whole embryo (µg/g)	5.78 ± 0.71*,†	16.4 ± 1.75	3.23 ± 1.28§,**	7.69 ± 2.92††
Male embryo (µg/g)	5.78 ± 0.82*	16.9 ± 1.88	3.04 ± 1.27§,**	7.55 ± 3.35††
Female embryo (µg/g)	5.78 ± 0.81*	16.1 ± 2.75	3.39 ± 1.44§,**	6.89 ± 2.72††

ANOVA with *post hoc* multiple comparison correction using Tukey contrasts:
* $P < 0.05$ 1 mg/kg/day PFOA vs 5 mg/kg/day PFOA
† $P < 0.05$ 1 mg/kg/day PFOA vs 2 mg/kg/day GenX
‡ $P < 0.05$ 1 mg/kg/day PFOA vs 10 mg/kg/day GenX
§ $P < 0.05$ 2 mg/kg/day GenX vs 5 mg/kg/day PFOA
** $P < 0.05$ 2 mg/kg/day GenX vs 10 mg/kg/day GenX
†† $P < 0.05$ 10 mg/kg/day GenX vs 5 mg/kg/day PFOA
Note: N = 3 for PFOA 5 mg/kg male embryo; Vehicle control (VC) samples were quantified for PFOA and GenX (HFPO-DA); all VC means were below the LOD of 10 ng/mL for both PFOA and GenX (HFPO-DA) except for maternal serum (0.211 ± 0.55 µg/mL)

Table A2-4. Litter parameters in mice gestationally exposed to PFOA or GenX from embryonic day 0.5 to 11.5 or 17.5 (Mean ± SD, N = 11-13).

Embryonic day	Litter parameter	Vehicle Control	1 mg/kg bw/day PFOA	5 mg/kg bw/day PFOA	2 mg/kg bw/day GenX (HFPO-DA)	10 mg/kg bw/day GenX (HFPO-DA)
11.5	No. implantation sites	13.7 ± 2.8	15.5 ± 2.7	14.5 ± 2.3	14.7 ± 2.7	14.8 ± 3.7
11.5	No. resorptions	0.6 ± 1.1	0.6 ± 0.5	0.5 ± 0.9	0.7 ± 0.8	0.9 ± 1.3
11.5	No. dead embryos	0.0 ± 0.0	0.0 ± 0.0	0.1 ± 0.3	0.0 ± 0.0	0.1 ± 0.3
11.5	No. viable embryos	13.1 ± 3.0	14.8 ± 2.5	13.9 ± 2.2	14.0 ± 2.9	13.8 ± 3.7
11.5	% resorbed[†]	4.6 ± 8.6	4.0 ± 3.3	3.6 ± 5.9	5.0 ± 6.2	5.6 ± 7.7
11.5	% nonviable[†]	0.0 ± 0.0	0.0 ± 0.0	0.6 ± 1.9	0.0 ± 0.0	2.1 ± 7.2
11.5	% viable[†]	95.4 ± 8.6	96.0 ± 3.3	95.9 ± 5.9	95.0 ± 6.2	92.4 ± 9.3
17.5	No. implantation sites	14.2 ± 2.9	13.5 ± 2.0	13.7 ± 2.1	13.8 ± 2.0	12.5 ± 3.1
17.5	No. resorptions	0.3 ± 0.5	0.3 ± 0.5	0.3 ± 0.5	0.2 ± 0.6	0.5 ± 0.7
17.5	No. dead embryos	0.1 ± 0.3	0.1 ± 0.3	0.0 ± 0.0	0.1 ± 0.3	0.0 ± 0.0
17.5	No. viable embryos	13.8 ± 3.2	13.1 ± 2.1	13.3 ± 1.9	13.5 ± 2.1	12.0 ± 3.0
17.5	% resorbed[†]	2.7 ± 4.6	2.6 ± 3.9	2.3 ± 3.4	1.2 ± 4.1	3.5 ± 5.3
17.5	% nonviable[†]	0.6 ± 2.3	0.6 ± 2.1	0.0 ± 0.0	0.7 ± 2.4	0.0 ± 0.0
17.5	% viable[†]	96.7 ± 4.8	96.8 ± 4.1	97.7 ± 3.4	98.1 ± 4.6	96.5 ± 5.3

[†]Calculated as percent of implantation sites

Note: $P > 0.05$ relative to vehicle control for all values (ANOVA with *post hoc* multiple comparison correction using Tukey contrasts)

Table A2-5. Relative gestational weight gain (% gain from embryonic day 0.5) at necropsy adjusting for litter size (adjusted model estimate and 95% confidence intervals; N = 11-13).

Dose group	E11.5 stimate (95% CI)	E11.5 Estimate (95% CI) relative to VC	E17.5 Estimate (95% CI)	E11.5 Estimate (95% CI) relative to VC
Vehicle control	17.3 (7.2, 27.4)	0 (0,0)	36.2 (10.8, 61.5)	0 (0,0)
1 mg/kg bw/day PFOA	16.2 (-0.2, 32.5)	-1.1 (-7.4, 5.1)	44.9 (6.5, 83.3)	8.7 (-4.3, 21.8)
5 mg/kg bw/day PFOA	21.6 (5.4, 37.9)	4.3 (-1.8, 10.5)	50.7 (12.2, 89.0)*	14.5 (1.4, 27.5)*
2 mg/kg bw/day GenX (HFPO-DA)	20.8 (4.7, 36.9)	3.5 (-2.5, 9.5)	48.7 (10.3, 87.1)	12.5 (-0.5, 25.6)
10 mg/kg bw/day GenX (HFPO-DA)	24.4 (8.1, 40.6)*	7.1 (0.9, 13.2)*	55.3 (16.7, 93.7)*	19.1 (5.9, 32.2)*

Abbr: E = embryonic day; VC = vehicle control

*$P < 0.05$; Beta estimate 95% confidence intervals relative to VC do not overlap zero (Generalized linear regression adjusted for litter size, with vehicle control as reference group)

Table A2-6. Incidence of liver histopathology in maternal livers at embryonic day 11.5.

Lesion type and severity	Vehicle Control N (%)	1 mg/kg/day PFOA N (%)	5 mg/kg/day PFOA N (%)	2 mg/kg/day GenX (HFPO-DA) N (%)	10 mg/kg/day GenX (HFPO-DA) N (%)
CA*, any severity	0 (0)	5 (100)	5 (100)	5 (100)	5 (100)
CA, minimal to mild	0 (0)	5 (100)	0 (0)	5 (100)	0 (0)
CA, moderate	0 (0)	0 (0)	0 (0)	0 (0)	2 (40)
CA, marked	0 (0)	0 (0)	5 (100)	0 (0)	3 (60)
Increase in mitotic figures	0 (0)	2 (40)	5 (100)	3 (60)	4 (80)
Increase in cell death†	0 (0)	1 (20)	3 (60)	4 (80)	3 (60)
Focal regions of classic necrosis	1 (20)	0 (0)	2 (40)	0 (0)	1 (20)
Vacuolation‡, any severity	0 (0)	0 (0)	5 (100)	0 (0)	5 (100)
Vacuolation, minimal	0 (0)	0 (0)	0 (0)	0 (0)	5 (100)
Vacuolation, mild	0 (0)	0 (0)	5 (100)	0 (0)	0 (0)
Vacuolation, moderate	0 (0)	0 (0)	0 (0)	0 (0)	0 (0)

Abbr: CA = cytoplasmic alteration

*CA was characterized as hepatocellular hypertrophy with decreased glycogen and intensely eosinophilic granular cytoplasm, with extension from periportal to midzonal regions with increasing severity

†Cell death included both apoptosis and single cell necrosis of individual hepatocytes

‡Vacuolation was graded by severity based on occurrence of clear, small, and round vacuoles in the cytoplasm of centrilobular hepatocytes in areas of cytoplasmic alteration as: minimal—rarely or occasionally seen as small clusters; mild—frequently seen as small clusters; moderate—seen in all centrilobular hepatocytes

Note: Histopathology was evaluated by a pathology working group and observations of increased mitotic figures and cell death were made relative to the vehicle control group; increase in mitotic figures and cell death was scored as minimal

Table A2-7. Incidence of liver histopathology in maternal livers at embryonic day 17.5.

Lesion type and severity	Vehicle Control N (%)	1 mg/kg/day PFOA N (%)	5 mg/kg/day PFOA N (%)	2 mg/kg/day GenX (HFPO-DA) N (%)	10 mg/kg/day GenX (HFPO-DA) N (%)
CA*, any severity	0 (0)	5 (100)	6 (100)	5 (100)	5 (100)
CA, minimal to mild	0 (0)	0 (0)	0 (0)	2 (40)	0 (0)
CA, moderate	0 (0)	5 (100)	0 (0)	3 (60)	0 (0)
CA, marked	0 (0)	0 (0)	6 (100)	0 (0)	5 (100)
Increase in mitotic figures	5 (100)	0 (0)	0 (0)	0 (0)	0 (0)
Increase in cell death[†]	0 (0)	5 (100)	6 (100)	0 (0)	5 (100)
Focal regions of classic necrosis	0 (0)	0 (0)	0 (0)	1 (20)	1 (20)
Vacuolation[‡], any severity	0 (0)	0 (0)	6 (100)	0 (0)	5 (100)
Vacuolation, minimal	0 (0)	0 (0)	0 (0)	0 (0)	2 (40)
Vacuolation, mild	0 (0)	0 (0)	0 (0)	0 (0)	3 (60)
Vacuolation, moderate	0 (0)	0 (0)	6 (100)	0 (0)	0 (0)

Abbr: CA = cytoplasmic alteration

*CA was characterized as hepatocellular hypertrophy with decreased glycogen and intensely eosinophilic granular cytoplasm, with extension from periportal to midzonal regions with increasing severity

[†]Cell death included both apoptosis and single cell necrosis of individual hepatocytes

[‡]Vacuolation was graded by severity based on occurrence of clear, small, and round vacuoles in the cytoplasm of centrilobular hepatocytes in areas of cytoplasmic alteration as: minimal—rarely or occasionally seen as small clusters; mild—frequently seen as small clusters; moderate—seen in all centrilobular hepatocytes

Note: Histopathology was evaluated by a pathology working group and observations of increased mitotic figures and cell death were made relative to the vehicle control group; increase in mitotic figures and cell death was scored as minimal

Table A2-8. Embryo and placental mixed effect model adjusted estimates and 95% confidence intervals (N = 11-13 dams with 62-80 observations per group).

Embryonic day	Dose group	Embryo weight (mg)	Embryo length (mm)	Placental weight (mg)	Embryo:Placental Weight Ratio
11.5	Vehicle Control	49.8 (29.2, 70.5)	18.4 (16.4, 20.3)	40.1 (19.0, 61.1)	1.08 (0.73, 1.43)
11.5	1 mg/kg bw/day PFOA	44.7 (11.1, 78.2)	17.5 (14.5, 20.4)	30.5 (-3.8, 64.7)	1.19 (0.62, 1.76)
11.5	5 mg/kg bw/day PFOA	45.3 (11.8, 78.7)	18.5 (15.6, 21.4)	31.2 (-2.9, 65.3)	1.21 (0.64, 1.77)
11.5	2 mg/kg bw/day GenX (HFPO-DA)	49.9 (16.7, 83.1)	17.6 (14.7, 20.5)	34.0 (0.1, 67.8)	1.22 (0.66, 1.78)
11.5	10 mg/kg bw/day GenX (HFPO-DA)	45.2 (12.0, 78.3)	17.4 (14.5, 20.3)	38.4 (4.5, 72.2)	1.08 (0.52, 1.64)
17.5	Vehicle Control	1378.6 (1206.3, 1550.8)	33.6 (31.1, 36.1)	130.8 (109.8, 151.8)	11.2 (9.2, 13.3)
17.5	1 mg/kg bw/day PFOA	1350.7 (1091.9, 1609.4)	33.6 (29.6, 37.6)	129.7 (98.2, 161.2)	11.1 (8.0, 14.3)
17.5	5 mg/kg bw/day PFOA	1249.5 (991.0, 1508.0)*	31.2 (27.2 35.3)*	151.9 (120.5, 183.4)*	8.5 (5.4, 11.6)*
17.5	2 mg/kg bw/day GenX (HFPO-DA)	1369.8 (1111.3, 1628.4)	32.7 (28.7, 36.6)	137.1 (105.6, 168.6)	10.6 (7.5, 13.7)
17.5	10 mg/kg bw/day GenX (HFPO-DA)	1337.0 (1077.5, 1596.4)	33.8 (29.8, 37.7)	146.3 (114.7, 177.9)*	9.5 (6.4, 12.7)*

Note: N = 6-8 dams with 18-24 observations per group for embryo length

*$P < 0.05$; Beta estimate 95% confidence intervals do not overlap zero (Mixed effect model adjusting *a priori* for litter size as a fixed effect and the dam as a random effect, vehicle control as reference group)

Table A2-9. Placental lesion index at embryonic day 11.5.

Placental outcome or sample size	Vehicle control	1 mg/kg bw/day PFOA	5 mg/kg bw/day PFOA	2 mg/kg bw/day GenX (HFPO-DA)	10 mg/kg bw/day GenX (HFPO-DA)
Total no. placenta evaluated	37	33	36	43	30
No. WNL (%)	35 (94.6)	32 (97.0)	32 (88.9)	41 (95.3)	30 (100)
No. abnormal (%)	2 (5.4)	4 (3.0)	4 (11.1)	2 (4.7)	0 (0.0)
No. labyrinth atrophy (%)	0 (0)	0 (0)	3 (8.3)	0 (0)	0 (0)
No. labyrinth congestion (%)	0 (0)	0 (0)	0 (0)	0 (0)	0 (0)
No. labyrinth necrosis (%)	0 (0)	0 (0)	1 (2.7)	0 (0)	0 (0)
No. early fibrin clot (%)	0 (0)	0 (0)	0 (0)	1 (2.8)	0 (0)
No. placental nodule (%)	0 (0)	0 (0)	0 (0)	0 (0)	0 (0)
No. other (%)[†]	2 (5.4)	1 (3.0)	0 (0)	1 (2.3)	0 (0)
No. litters evaluated	5	5	5	5	5
Mean no. placenta evaluated per litter (min, max)	7.4 (5, 10)	6.6 (4, 10)	7.4 (5, 10)	8.6 (4, 11)	6.2 (3, 11)
Mean WNL ± SD (%) per litter	6.4 ± 1.9 (95.0)	6.4 ± 1.9 (98.0)	6.4 ± 1.7 (88.3)	8.2 ± 2.8 (95.6)	6.0 ± 3.1 (97.1)
Mean abnormal ± SD (%) per litter	0.4 ± 0.9 (5.0)	0.2 ± 0.4 (2.0)	1.0 ± 1.4 (11.7)	0.4 ± 0.9 (4.4)	0 ± 0.0 (0)

Abbr: WNL = within normal limits

*$P < 0.05$ relative to vehicle control (general linear model using a Poisson distribution with *post hoc* multiple comparison correction using Tukey contrasts)

[†]Other lesions were considered spontaneous and not treatment related and included: Increased thickness of trilaminar trophoblast layers (vehicle control), decreased labyrinth area (vehicle control), absent labyrinth (PFOA 1 mg/kg), large focal labyrinth hemorrhage and thrombus (GenX 2 mg/kg)

Table A2-10. Placental lesion incidence at embryonic day 17.5.

Placental outcome or sample size	Vehicle control	1 mg/kg bw/day PFOA	5 mg/kg bw/day PFOA	2 mg/kg bw/day GenX (HFPO-DA)	10 mg/kg bw/day GenX (HFPO-DA)
Total no. placenta evaluated	41	32	40	31	35
No. WNL (%)	40 (97.6)	29 (90.6)	13 (32.5)*	13 (41.9)	6 (17.1)*
No. abnormal (%)	1 (2.4)	3 (9.4)	27 (67.5)*	18 (58.1)	29 (82.9)*
No. labyrinth atrophy (%)	0 (0)	0 (0)	3 (7.5)	15 (48.4)	16 (45.7)
No. labyrinth congestion (%)	0 (0)	0 (0)	23 (57.5)	1 (3.2)	8 (22.9)
No. labyrinth necrosis (%)	0 (0)	1 (3.1)	0 (0)	0 (0)	1 (2.9)
No. early fibrin clot (%)	0 (0)	0 (0)	1 (2.5)	1 (3.2)	4 (11.4)
No. placental nodule (%)	0 (0)	2 (6.3)	0 (0)	1 (3.2)	0 (0)
No. other (%)[†]	1 (2.4)	0 (0)	0 (0)	0 (0)	0 (0)
No. litters evaluated	5	5	6	5	5
Mean no. placenta evaluated per litter (min, max)	8.2 (7, 10)	6.4 (5, 8)	6.7 (5, 9)	6.2 (2, 8)	7.0 (3, 10)
Mean WNL ± SD (%) per litter	8.0 ± 0.7 (98.0)	5.8 ± 1.3 (91.4)	2.2 ± 2.7 (38.1)*	2.6 ± 2.8 (51.7)*	1.2 ± 2.7 (12.0)*
Mean abnormal ± SD (%) per litter	0.2 ± 0.4 (2.0)	0.6 ± 0.9 (8.6)	4.5 ± 3.8 (61.9)*	3.6 ± 3.6 (48.3)*	5.8 ± 3.0 (88.0)*

Abbr: WNL = within normal limits

*$P < 0.05$ relative to vehicle control (general linear regression using a Poisson distribution with *post hoc* multiple comparison correction using Tukey contrasts)

[†]Other lesions were considered spontaneous and not treatment related and included: Cortical necrosis with inflammatory cells (vehicle control)

Table A2-11. Sex stratified placental thyroid hormone measurements at embryonic day 17.5 (Mean ± SD, N = 1-3).

Hormone	Sex	Vehicle control	1 mg/kg/day PFOA	5 mg/kg/day PFOA	2 mg/kg/day GenX (HFPD-DA)	10 mg/kg/day GenX (HFPO-DA)
rT3 (ng/g)	Female	0.9 ± 0.8[†]	0.8 ± 0.4	1.6 ± 1.0	2.3 ± 0.6	1.9 ± 0.1
rT3 (ng/g)	Male	1.4 ± 0.6	0.5 ± 0.4	1.2 ± 0.1	1.0 ± 0.2	1.3 ± 0.3
T3 (ng/g)	Female	0.4 ± 0.3	0.2 ± 0	0.2 ± 0	0.3 ± 0.2	0.2 ± 0
T3 (ng/g)	Male	0.2 ± 0	0.2 ± 0	0.2 ± NA[†]	0.2 ± 0	0.2 ± 0
T4 (ng/g)	Female	3.6 ± 0.8	2.0 ± 0.4	3.5 ± 1.7	5.9 ± 2.3	6.5 ± 1.4
T4 (ng/g)	Male	4.0 ± 0.4	3.1 ± 1.2	2.2 ± 0.7	4.7 ± 1.1	5.8 ± 0.7
T3:T4 ratio	Female	0.095 ± 0.06	0.104 ± 0.02	0.065 ± 0.02	0.053 ± 0.02	0.032 ± 0.01
T3:T4 ratio	Male	0.05 ± 0.005	0.071 ± 0.02	0.083 ± NA[†]	0.044 ± 0.01	0.035 ± 0.004
rT3:T4 ratio	Female	0.291 ± 0.30	0.401 ± 0.22	0.441 ± 0.05	0.409 ± 0.08	0.302 ± 0.09
rT3:T4 ratio	Male	0.355 ± 0.17	0.196 ± 0.17	0.454 ± 0.07	0.225 ± 0.08	0.231 ± 0.04

Abbr: rT3 = reverse triiodothyronine, T3 = triiodothyronine, T4 = thyroxine, MDL = method detection limit
Note: $P > 0.05$ relative to vehicle control for all values including sex*treatment as an interaction term in the model (ANOVA with *post hoc* multiple comparison correction using Tukey contrasts); Sample sizes ranged from N = 1-3; Non-quantifiable samples below the MDL were imputed using the calculation MDL*0.5. MDL values were: T4: 0.84 ng/g, T3: 0.42 ng/g, rT3: 0.67 ng/g.

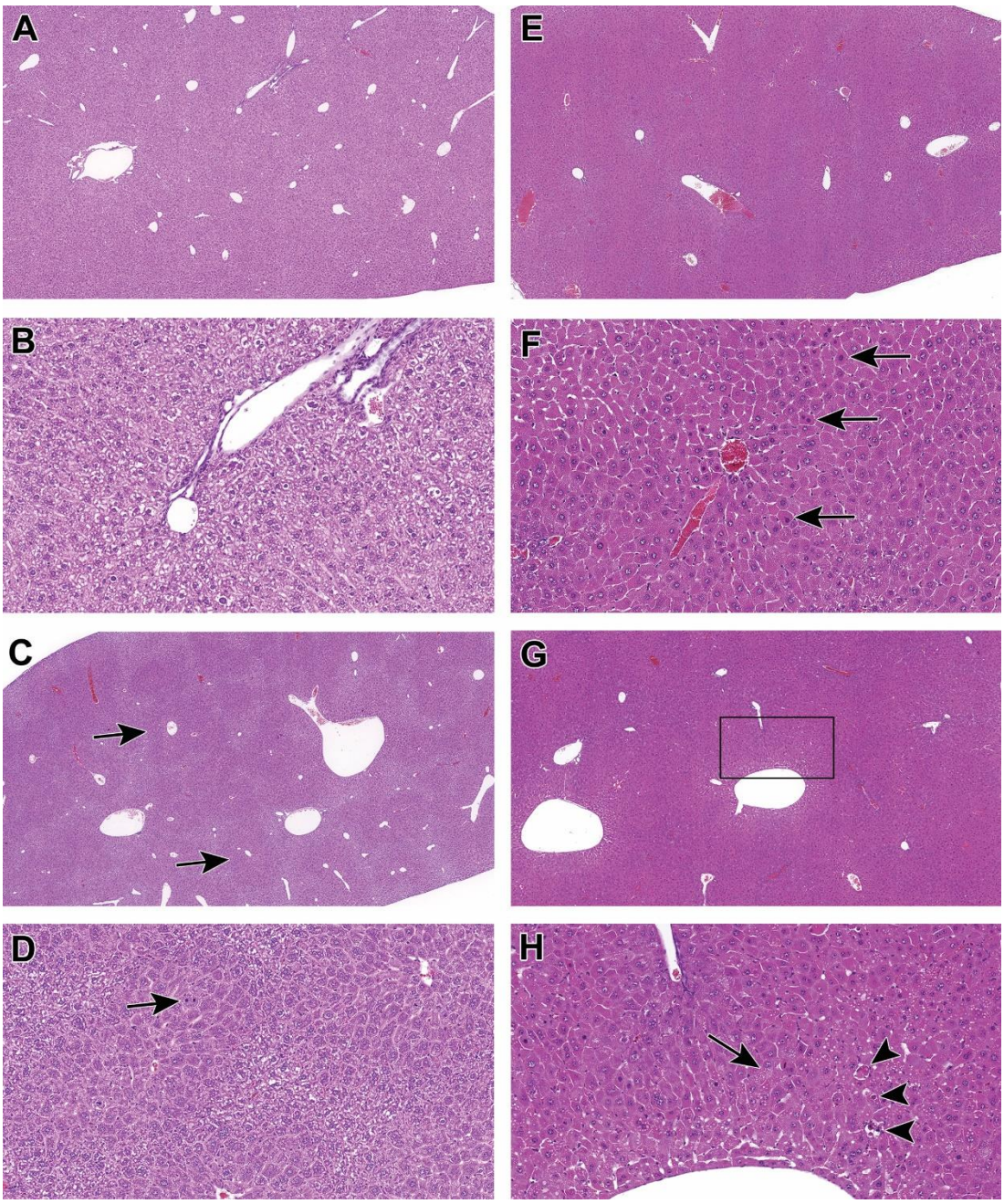

Figure A2-1. Representative examples of liver histology in pregnant dams at gestation days 11.5 and 17.5 exposed to either vehicle control (A, B, C, D) or treated with GenX (also HFPO-DA; E, F) or PFOA (G, H). (A) Liver from a pregnant dam at 11.5 days of gestation, exposed to vehicle control (4X). (B) Higher magnification of (A) illustrating the normal uniform hepatocellular size and cytoplasmic glycogen accumulation (20X). (C) Example of a liver from a pregnant dam at 17.5 days of gestation, exposed to vehicle control. The features of centrilobular hepatocellular hypertrophy (arrows), karyomegaly, increased mitotic figures, decreased glycogen, and increased basophilic granular cytoplasm are normal features for dam livers at this stage of pregnancy (4X). (D) Higher magnification of (C) illustrating the increased mitotic figures (arrow) decreased glycogen, and increased basophilic granular cytoplasm in the areas of centrilobular hepatocellular hypertrophy (20X). (E) Example of a liver from a pregnant dam at 11.5 days of gestation, exposed to 10 mg/kg/day of GenX. There is diffuse

moderate cytoplasmic alteration in this liver affecting the centrilobular, midzonal and periportal regions (4X). (F) Higher magnification of (E) illustrating the hepatocellular hypertrophy with decreased glycogen and eosinophilic granular cytoplasm. The arrows show examples of early hepatocellular apoptosis with condensed cytoplasm and condensed dark basophilic nuclear chromatin (20X). (G) Example of a liver from a pregnant dam at gestation day 17.5, exposed to 5 mg/kg/day PFOA with diffuse cytoplasmic alteration (4X). (H) Higher magnification of the boxed region in (G) showing cytoplasmic alteration with apoptosis (arrowheads) as well as accumulation of hepatocellular cytoplasmic small vacuoles with distinct borders (arrow; 20X).

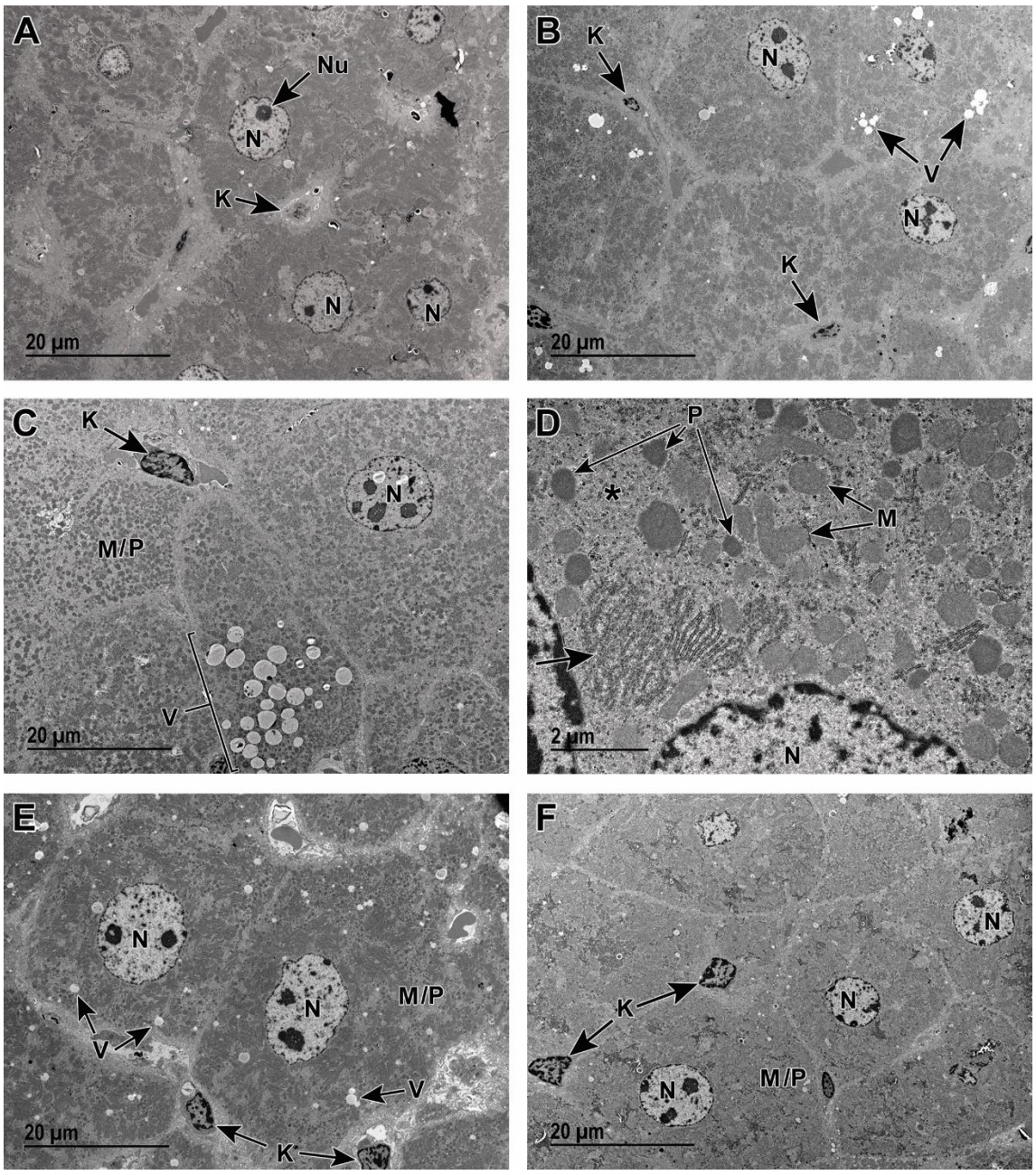

Figure A2-2. Transmission electron microscopy (TEM) of normal liver and livers exposed to PFOA or GenX (also HFPO-DA). (A) TEM of normal liver from a vehicle control pregnant dam at gestation day 17.5 showing prominent rough endoplasmic reticulum with abundant ribosomes and evenly dispersed, abundant glycogen (see Figures 4A or 5A H&E and 4B or 5B TEM). (B) TEM of liver from a pregnant dam at gestation day 17.5 and treated with 1 mg/kg/day PFOA. Although at 40X magnification light microscopy this liver appeared to be within normal limits (see Figures 4C H&E and D TEM), TEM reveals increased vacuolation (V), evenly dispersed glycogen, as well as abundant mitochondria and peroxisomes. (C and D) TEM of liver from a pregnant dam at gestation day 17.5 and treated with 5 mg/kg/day PFOA (see Figures 4E H&E and 4F TEM). Note the abundant cytoplasmic organelles consistent with mitochondria (M)

and peroxisomes (P), extensive vacuoles (V), less prominent rough endoplasmic reticulum (arrow) with fewer ribosomes and less abundant glycogen (asterisk). (E and F) Transmission electron microscopy of liver from a pregnant dam at gestation day 17.5 treated with 2 mg/kg/day GenX (E; see Figures 5C H&E and 5D TEM) or 10 mg/kg/day GenX (F; see Figures 5E H&E and 5F TEM). Note the abundance of cytoplasmic organelles consistent with mitochondria (M) and peroxisomes (P). K = Kupffer cell, N = nucleus, NU = nucleolus

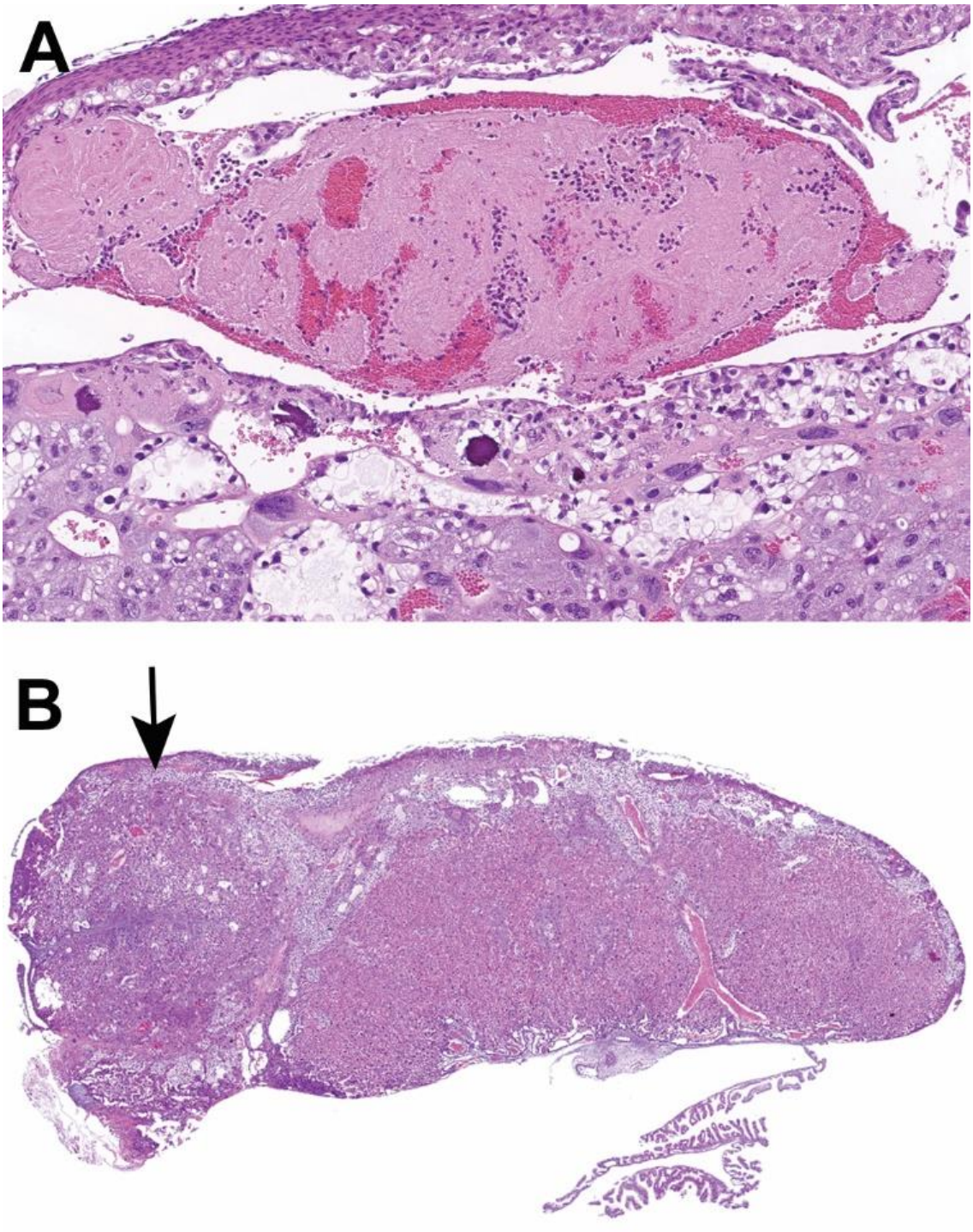

Figure A2-3. Representative examples of occasional histopathological placenta findings observed in dams at gestation day 17.5. (A) Early clot formation in a maternal artery in the decidua region of the placenta (20X). This dam was at gestation day 17.5 and treated with 10 mg/kg/day GenX (also HFPO-DA). Note the fibrin formation with trapped cells. (B) Nodule (arrow) of tissue from the junction zone of the placenta from a dam at gestational day 17.5 that was treated with 2 mg/kg/day GenX (2X).

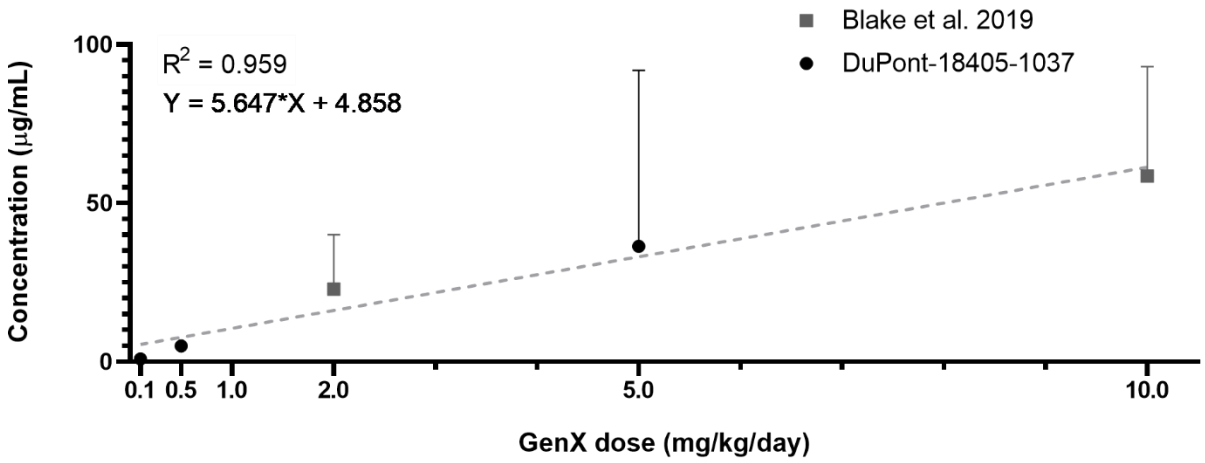

Figure A2-4. Comparison of maternal serum or plasma levels (mean ± SD) in CD-1 mice gestationally exposed to GenX (also HFPO-DA) at varying dose levels in a study conducted by DuPont-18405-1037 (Edwards 2010b; plasma measured on lactation day 21) and the present study (Blake et al. 2019; serum measured on E17.5).Maternal serum or plasma was collected less than 6 hours after oral gavage in both studies. Administered GenX dose and maternal serum or plasma concentration was linearly correlated across data from both studies ($R^2 = 0.959$, $P < 0.05$ for non-zero slope).

APPENDIX 3: SUPPLEMENTARY INFORMATION FOR CHAPTER 4

Table A3-1. List of perfluoroalkyl substances, identifiers, molecular formulas and weights.

Chemical name	CASRN	Molecular formula	Molecular weight	DTXSID	PubChem CID
Perfluoro-2-methyl-3-oxahexanoic acid	13252-13-6	C6HF11O3	330.053	DTXSID70880215	114481
Perfluoro-3,6-dioxadecanoic acid	137780-69-9	C8HF15O4	446.068	DTXSID50381073	2778677
8-H-Perfluorooctanoic acid	13973-14-3	C8H2F14O2	396.08	DTXSID70565479	14922999
Perfluoro-3,6-dioxaheptanoic acid	151772-58-6	C5HF9O4	296.045	DTXSID30382063	2782393
Perfluoro-3,6,9-trioxadecanoic acid	151772-59-7	C7HF13O5	412.059	DTXSID80380837	2778260
7H-Perfluoroheptanoic acid	1546-95-8	C7H2F12O2	346.072	DTXSID70165670	15243
Perfluorooctanesulfonic acid	1763-23-1	C8HF17O3S	500.13	DTXSID3031864	74483
Perfluoroundecanoic acid	2058-94-8	C11HF21O2	564.093	DTXSID8047553	77222
2,2-Difluoro-2-(trifluoromethoxy)acetate sodium salt	21837-98-9	C3F5NaO3	202.012	DTXSID50904660	88425486
Perfluoropentanoic acid	2706-90-3	C5HF9O2	264.047	DTXSID6062599	75921
6:2 Fluorotelomer sulfonic acid	27619-97-2	C8H5F13O3S	428.16	DTXSID6067331	119688
2-(N-Ethylperfluorooctanesulfonamido)acetic acid	2991-50-6	C12H8F17NO4S	585.23	DTXSID5062760	18134
Perfluorobutylsulfonamide	30334-69-1	C4H2F9NO2S	299.11	DTXSID30880251	10958205
Perfluorohexanoic acid	307-24-4	C6HF11O2	314.054	DTXSID3031862	67542
Perfluorododecanoic acid	307-55-1	C12HF23O2	614.101	DTXSID8031861	67545
Perfluoro-3,6,9-trioxatridecanoic acid	330562-41-9	C10HF19O5	562.083	DTXSID50375114	2760333
Perfluorooctanoic acid	335-67-1	C8HF15O2	414.07	DTXSID8031865	9554
Perfluorodecanoic acid	335-76-2	C10HF19O2	514.086	DTXSID3031860	9555
Perfluorohexanesulfonic acid	355-46-4	C6HF13O3S	400.11	DTXSID7040150	67734
Perfluorobutanoic acid	375-22-4	C4HF7O2	214.039	DTXSID4059916	9777
Perfluorobutanesulfonic acid	375-73-5	C4HF9O3S	300.09	DTXSID5030030	67815
Perfluoroheptanoic acid	375-85-9	C7HF13O2	364.062	DTXSID1037303	67818
Perfluoroheptanesulfonic acid	375-92-8	C7HF15O3S	450.12	DTXSID8059920	67820
Perfluorononanoic acid	375-95-1	C9HF17O2	464.078	DTXSID8031863	67821
5H-Octafluoropentanoic acid	376-72-7	C5H2F8O2	246.056	DTXSID50191038	120227
Perfluoro-3-methoxypropanoic acid	377-73-1	C4HF7O3	230.038	DTXSID70191136	120228
8:2 Fluorotelomer sulfonic acid	39108-34-4	C10H5F17O3S	528.18	DTXSID00192353	3016044
Perfluorooctanamide	423-54-1	C8H2F15NO	413.086	DTXSID60195123	67919
6:2 Fluorotelomer phosphate diester	57677-95-9	C16H9F26O4P	790.176	DTXSID50561590	14550408
6:2 Fluorotelomer phosphate monoester	57678-01-0	C8H6F13O4P	444.085	DTXSID90558000	14250578
8:2 Fluorotelomer phosphate monoester	57678-03-2	C10H6F17O4P	544.101	DTXSID60874027	57351110
Ammonium perfluoro-2-methyl-3-oxahexanoate	62037-80-3	C6H4F11NO3	347.084	DTXSID40108559	51342034
Sodium perfluoropentanesulfonate	630402-22-1	C5F11NaO3S	372.08	DTXSID50893449	87842193
6:2 Fluorotelomer alcohol	647-42-7	C8H5F13O	364.106	DTXSID5044572	69537
8:2 Fluorotelomer alcohol	678-39-7	C10H5F17O	464.122	DTXSID7029904	69619
8:2 Fluorotelomer phosphate diester	678-41-1	C20H9F34O4P	990.207	DTXSID90218051	3022253
Perfluorotridecanoic acid	72629-94-8	C13HF25O2	664.109	DTXSID90868151	3018355
Perfluorooctanesulfonamide	754-91-6	C8H2F17NO2S	499.14	DTXSID3038939	69785
9-H-Perfluorononanoic acid	76-21-1	C9H2F16O2	446.087	DTXSID50226894	6434
Perfluoro(4-methoxybutanoic) acid	863090-89-5	C5HF9O3	280.046	DTXSID60500450	12498036
2H,2H,3H,3H-Perfluorooctanoic acid	914637-49-3	C8H5F11O2	342.108	DTXSID20874028	14632790
1H,1H-Nonafluoropentyl p-toluenesulfonate	883499-79-4	C12H9F9O3S	404.25	DTXSID50382065	2782396

Note: DTXSID is the chemical ID for the Distributed Structure-Searchable Toxicity (DSSTox) Database

Table A3-2. Raw values for dose-response curve EC50 estimates for JEG03 cell viability, proliferation, and mitochondrial membrane potential (MMP) after exposure to PFAS.

Chemical name	CASRN	Viability EC50 ± SD (µM)	Proliferation EC50 ± SD (µM)	MMP EC50 ± SD (µM)
Perfluoro-2-methyl-3-oxahexanoic acid	13252-13-6	-7645.8 ± NaN	1109.9 ± 266.6	-441142.4 ± 10
Perfluoro-3,6-dioxadecanoic acid	137780-69-9	-35.1 ± 225.2	282.8 ± 25.7	350.1 ± 16.1
8-H-Perfluorooctanoic acid	13973-14-3	317.5 ± 182.9	441.3 ± 18.1	147.3 ± 27.1
Perfluoro-3,6-dioxaheptanoic acid	151772-58-6	326.5 ± 85.7	351.3 ± 11.8	368.1 ± 22.6
Perfluoro-3,6,9-trioxadecanoic acid	151772-59-7	267.2 ± 26.8	302.9 ± 30.1	310.1 ± NaN
7H-Perfluoroheptanoic acid	1546-95-8	222.8 ± 60.2	294.4 ± 48.2	-254.1 ± 10
Perfluorooctanesulfonic acid	1763-23-1	291.2 ± 9.1	294.2 ± 5.8	352.9 ± 6.7
Perfluoroundecanoic acid	2058-94-8	266.1 ± 12.4	229.5 ± 13.3	200.1 ± 4
2,2-Difluoro-2-(trifluoromethoxy)acetate sodium salt	21837-98-9	2432 ± NA	-38.4 ± NaN	144436.8 ± 10
Perfluoropentanoic acid	2706-90-3	882.2 ± NaN	831 ± NaN	174.7 ± 68.4
6:2 Fluorotelomer sulfonic acid	27619-97-2	-345.4 ± NaN	737.1 ± NaN	70608.3 ± 10
2-(N-Ethylperfluorooctanesulfonamido)acetic acid	2991-50-6	202.7 ± 44.7	203.6 ± 17.7	100201.9 ± 10
Perfluorobutylsulfonamide	30334-69-1	-533.2 ± 34.2	-722.6 ± 104.8	-495.8 ± 23.2
Perfluorohexanoic acid	307-24-4	-419.2 ± NaN	10418.5 ± 10	142.4 ± 12.6
Perfluorododecanoic acid	307-55-1	361.1 ± 30.8	317.8 ± 24.5	-158 ± NaN
Perfluoro-3,6,9-trioxatridecanoic acid	330562-41-9	194.9 ± 54.6	332.4 ± 34.1	29117.5 ± NA
Perfluorooctanoic acid	335-67-1	357.7 ± 16.9	344.1 ± 12.2	360.2 ± 18
Perfluorodecanoic acid	335-76-2	180.7 ± 25.6	234 ± 22.8	235.8 ± 159.6
Perfluorohexanesulfonic acid	355-46-4	288.7 ± 29.6	251.6 ± 21.7	86.6 ± 71.5
Perfluorobutanoic acid	375-22-4	226 ± 115.7	209.2 ± 359.8	52 ± 296.5
Perfluorobutanesulfonic acid	375-73-5	330.4 ± 35	223.2 ± 76.7	-181.7 ± NaN
Perfluoroheptanoic acid	375-85-9	486.7 ± 408.6	277.4 ± 81.6	-319.9 ± NaN
Perfluoroheptanesulfonic acid	375-92-8	1977 ± 2479.7	296.2 ± 201.3	874.5 ± 1752.1
Perfluorononanoic acid	375-95-1	332.6 ± 10.3	326.1 ± 5.5	304.6 ± 13.6
5H-Octafluoropentanoic acid	376-72-7	353.7 ± 28.6	333.7 ± 56.5	-680 ± 89.5
Perfluoro-3-methoxypropanoic acid	377-73-1	303.7 ± 28.2	204.1 ± 110.9	93.1 ± 131.6
8:2 Fluorotelomer sulfonic acid	39108-34-4	159.5 ± 45.7	321.3 ± 171.2	331.1 ± 5.7
Perfluorooctanamide	423-54-1	-261.2 ± NaN	114 ± 35.6	294.6 ± 66.1
6:2 Fluorotelomer phosphate diester	57677-95-9	-81.9 ± 638.9	141.8 ± 39.2	64401.7 ± 10
6:2 Fluorotelomer phosphate monoester	57678-01-0	182.7 ± 21.7	193.3 ± 3.8	248 ± 62.1
8:2 Fluorotelomer phosphate monoester	57678-03-2	359.8 ± 30.3	250.7 ± 37.6	312.5 ± 29.8
Menadione	58-27-5	205.5 ± 47.1	157 ± 21.4	195540.8 ± 10
Ammonium perfluoro-2-methyl-3-oxahexanoate	62037-80-3	-1440 ± 4280.5	996.9 ± 952.5	-120970.2 ± 10
Sodium perfluoropentanesulfonate	630402-22-1	1209.2 ± 11424.2	-1685.5 ± NA	543.3 ± NaN
6:2 Fluorotelomer alcohol	647-42-7	415.4 ± 70.6	537.2 ± NaN	332.4 ± 44.1
8:2 Fluorotelomer alcohol	678-39-7	35.7 ± 36.5	19.1 ± NaN	95.1 ± 15.3
8:2 Fluorotelomer phosphate diester	678-41-1	-723.2 ± 131.8	-167.5 ± NaN	-496.4 ± 816.2
Perfluorotridecanoic acid	72629-94-8	-111 ± NaN	388.1 ± 124.9	-1832.4 ± 10
Perfluorooctanesulfonamide	754-91-6	175.9 ± 4.9	160 ± 87.8	227.4 ± 369.9
9-H-Perfluorononanoic acid	76-21-1	349.9 ± 43.1	1227.3 ± 117.5	186.9 ± 27.6
Perfluoro(4-methoxybutanoic) acid	863090-89-5	17.7 ± NaN	696.4 ± NaN	-224.5 ± NaN
2H,2H,3H,3H-Perfluorooctanoic acid	883499-79-4	-493.8 ± 41.7	306.1 ± 47.9	158.6 ± 17.7
1H,1H-Nonafluoropentyl p-toluenesulfonate	914637-49-3	598.5 ± NaN	950.6 ± 670.8	71779.9 ± 10

Table A3-3. Rough binning of PFAS bioactivity in JEG-3 cells using lowest concentration (µM) at which the mean response value exceeded the mean control value ± 2*SD.

Chemical name	CASRN	Viability ↓	Viability ↑	Prolif ↓	Prolif ↑	MMP ↓
Perfluoro-2-methyl-3-oxahexanoic acid	13252-13-6	*na*	*na*	*na*	450	375
Perfluoro-3,6-dioxadecanoic acid	137780-69-9	400	*na*	300	*na*	400
8-H-Perfluorooctanoic acid	13973-14-3	*na*	*na*	*na*	*na*	*na*
Perfluoro-3,6-dioxaheptanoic acid	151772-58-6	*na*	200	400	*na*	400
Perfluoro-3,6,9-trioxadecanoic acid	151772-59-7	*na*	*na*	350	*na*	450
7H-Perfluoroheptanoic acid	1546-95-8	*na*	50	400	*na*	*na*
Perfluorooctanesulfonic acid	1763-23-1	300	*na*	250	*na*	350
Perfluoroundecanoic acid	2058-94-8	300	*na*	100	*na*	100
2,2-Difluoro-2-(trifluoromethoxy)acetate sodium	21837-98-9	*na*	*na*	*na*	50	*na*
Perfluoropentanoic acid	2706-90-3	*na*	200	*na*	*na*	*na*
6:2 Fluorotelomer sulfonic acid	27619-97-2	*na*	*na*	*na*	50	*na*
2-(N-Ethylperfluorooctanesulfonamido)acetic acid	2991-50-6	250	*na*	250	50	150
Perfluorobutylsulfonamide	30334-69-1	*na*	*na*	*na*	*na*	*na*
Perfluorohexanoic acid	307-24-4	*na*	300	100	*na*	100
Perfluorododecanoic acid	307-55-1	*na*	50	*na*	*na*	*na*
Perfluoro-3,6,9-trioxatridecanoic acid	330562-41-9	300	*na*	400	*na*	50
Perfluorooctanoic acid	335-67-1	*na*	200	350	*na*	450
Perfluorodecanoic acid	335-76-2	200	50	250	*na*	50
Perfluorohexanesulfonic acid	355-46-4	*na*	50	350	*na*	*na*
Perfluorobutanoic acid	375-22-4	*na*	50	*na*	*na*	50
Perfluorobutanesulfonic acid	375-73-5	*na*	50	*na*	*na*	50
Perfluoroheptanoic acid	375-85-9	*na*	*na*	450	*na*	*na*
Perfluoroheptanesulfonic acid	375-92-8	*na*	*na*	232.5	23.25	*na*
Perfluorononanoic acid	375-95-1	350	*na*	300	*na*	300
5H-Octafluoropentanoic acid	376-72-7	*na*	*na*	*na*	*na*	*na*
Perfluoro-3-methoxypropanoic acid	377-73-1	*na*	*na*	*na*	*na*	*na*
8:2 Fluorotelomer sulfonic acid	39108-34-4	*na*	*na*	*na*	*na*	*na*
Perfluorooctanamide	423-54-1	*na*	*na*	*na*	*na*	*na*
6:2 Fluorotelomer phosphate diester	57677-95-9	*na*	112.5	187.5	37.5	*na*
6:2 Fluorotelomer phosphate monoester	57678-01-0	*na*	*na*	*na*	*na*	*na*
8:2 Fluorotelomer phosphate monoester	57678-03-2	*na*	*na*	*na*	*na*	*na*
Menadione	58-27-5	50	*na*	150	*na*	300
Ammonium perfluoro-2-methyl-3-oxahexanoate	62037-80-3	350	*na*	*na*	50	*na*
Sodium perfluoropentanesulfonate	630402-22-1	350	*na*	*na*	200	*na*
6:2 Fluorotelomer alcohol	647-42-7	*na*	*na*	*na*	*na*	*na*
8:2 Fluorotelomer alcohol	678-39-7	*na*	*na*	*na*	*na*	*na*
8:2 Fluorotelomer phosphate diester	678-41-1	50	*na*	100	*na*	350
Perfluorotridecanoic acid	72629-94-8	*na*	150	450	50	*na*
Perfluorooctanesulfonamide	754-91-6	*na*	*na*	*na*	*na*	*na*
9-H-Perfluorononanoic acid	76-21-1	*na*	*na*	*na*	*na*	*na*
Perfluoro(4-methoxybutanoic) acid	863090-89-5	*na*	*na*	*na*	*na*	*na*
2H,2H,3H,3H-Perfluorooctanoic acid	883499-79-4	*na*	50	400	*na*	*na*
1H,1H-Nonafluoropentyl p-toluenesulfonate	914637-49-3	*na*	*na*	*na*	50	*na*

Abbr: *na* = not available

Table A3-4. Gene expression fold change data from JEG-3 cells after exposure to PFOA or GenX.

Gene	PFOA 1 µM		PFOA 100 µM		GenX 3 µM		GenX 300 µM	
	Fold change	P	Fold change	P	Fold change	P	Fold change	P
11BHSD2	-1.06	0.43	-1.03	0.70	-1.00	1.00	-1.01	0.95
17BHSD1	-1.02	0.59	1.17	0.01*	-1.11	0.12	1.23	0.01*
ABCG2	-1.07	0.39	1.18	0.07*	1.18	0.03*	1.26	0.01*
AHR	-1.09	0.31	1.08	0.36	1.04	0.42	-1.04	0.42
AHRR	-1.18	0.02*	1.00	1.00	1.18	0.50	1.19	0.46
CAT	1.02	0.81	-1.06	0.50	1.02	0.27	-1.05	0.05*
CGB5	1.00	1.00	-1.15	0.41	1.08	0.53	1.11	0.40
COX2	-1.11	0.74	1.03	0.92	1.27	0.20	1.27	0.20
CTNNB1	1.00	1.00	1.00	1.00	1.00	1.00	1.15	<0.01*
CYP19A1	-1.05	0.42	1.00	1.00	-1.03	0.78	-1.29	0.05*
CYP1A1	1.05	0.64	1.18	0.15	-1.22	0.14	-1.16	0.25
CYP2E1	-1.20	0.08	1.00	1.00	-1.26	0.36	1.04	0.86
CYP3A5	1.28	0.30	-1.18	0.46	1.19	0.60	-1.83	0.10*
CYP3A7	1.15	0.52	-1.22	0.36	1.01	0.93	-1.25	0.07*
EGFR	1.07	0.47	-1.07	0.46	1.00	1.00	-1.22	0.07*
ENG	1.02	0.81	-1.19	0.10*	1.04	0.42	-1.04	0.42
ESRRA	1.00	1.00	1.00	1.00	1.00	1.00	1.19	0.05*
ESRRG	-1.04	0.86	-1.16	0.47	-1.16	0.21	1.00	1.00
GH2	1.02	0.86	1.12	0.29	*na*	*na*	*na*	*na*
GHR	1.00	1.00	1.15	0.22	1.15	0.11	1.11	0.20
GPER1	1.02	0.76	-1.05	0.54	-1.02	0.86	1.34	0.06*
GPX1	1.00	1.00	-1.14	0.27	-1.18	0.07*	-1.29	0.01*
HIF1A	1.00	1.00	1.00	1.00	1.00	1.00	1.05	0.27
IGF2	1.00	1.00	-1.00	1.00	1.00	1.00	-1.38	0.01*
IGFBP5	-1.13	0.32	-1.02	0.85	*na*	*na*	*na*	*na*
IGFR1	1.03	0.75	1.08	0.38	-1.02	0.77	-1.10	0.24
IGFR2	1.05	0.46	1.16	0.04*	1.04	0.56	-1.00	0.95
IL6	-1.05	0.84	1.10	0.70	-1.23	0.34	-1.51	0.09*
MRP1	-1.03	0.60	-1.06	0.32	-1.05	0.57	1.14	0.20
MRP2	1.09	0.65	-1.03	0.87	1.05	0.82	1.00	1.00
MRP3	-1.08	0.66	-1.12	0.51	1.07	0.64	1.44	0.05*
mTOR	1.00	1.00	1.00	1.00	1.00	1.00	1.00	1.00
NFKB1	1.00	1.00	1.03	0.27	1.03	0.27	1.03	0.27
NFKB2	1.00	1.00	1.00	1.00	-1.07	0.13	-1.04	0.42
NR3C1	1.09	0.27	1.00	1.00	1.00	1.00	1.00	1.00
PGF	1.00	1.00	-1.00	1.00	1.00	1.00	-1.00	1.00
PMM1	-1.03	0.70	1.07	0.32	-1.05	0.41	1.05	0.43
ROLYR2L	1.00	1.00	1.00	1.00	1.00	1.00	1.00	1.00
SLC2A1	-1.02	0.88	-1.11	0.39	-1.04	0.48	-1.13	0.04*
SOD1	1.00	1.00	1.00	1.00	1.00	1.00	1.14	0.05*
TGFB1	1.00	1.00	-1.18	0.16	-1.04	0.51	1.00	1.00
VEGFA	1.00	1.00	1.08	0.11	1.04	0.37	1.27	<0.01*
VEGFB	-1.00	0.95	-1.04	0.36	1.00	1.00	-1.01	0.87
WNT4	1.25	0.26	1.45	0.09*	1.08	0.64	1.20	0.26
WNT6	-1.04	0.84	-1.02	0.91	-1.09	0.43	-1.09	0.43
WNT7B	1.06	0.39	1.06	0.39	1.07	0.55	-1.12	0.36

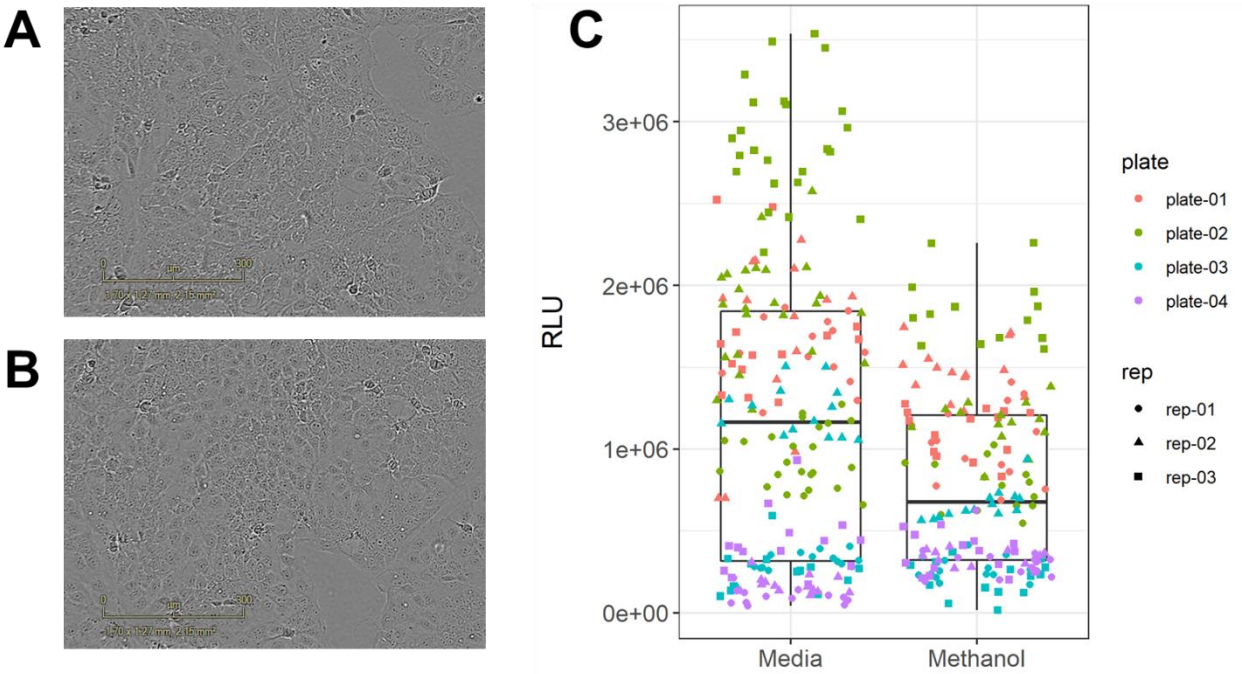

Figure A3-1. Representative live cell images and raw viability relative luminescence units (RLU) in JEG-3 cells after 24 hours exposure to media only or vehicle control (2% methanol, 98% media). (A) Representative image of JEG-3 cells exposed to media only. (B) Representative image of JEG-3 cells exposed to vehicle control. (C) Boxplots and raw cell viability RLU values for experimental replicates (N = 3, denoted by point shape) for experimental plates 1-4 (plate denoted by point color). The boxplot upper and lower hinges correspond to the first and third quartiles (25th and 75th percentiles), the middle hinge corresponds to the median, and the upper whisker extends to the highest value that is within 1.5 times the distance between the first and third quartiles (inter-quartile range, IQR) of the hinge and the lower whisker extends to the lowest value within 1.5 times the IQR of the hinge.

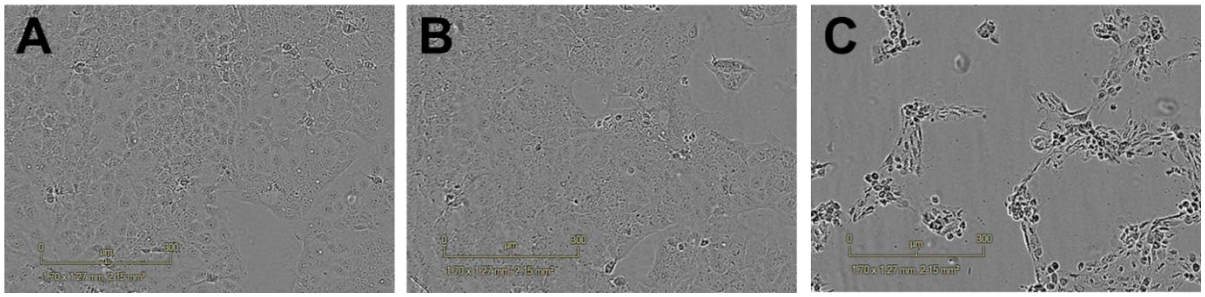

Figure A3-2. Representative images of JEG-3 cells after 24 hours exposure to (A) 0 µM, (B) 100 µM, and (C) 150 µM menadione (positive control for cell death). Complete cell death is apparent after exposure to 150 µM, while minimal cell death is visible at 100 µM.

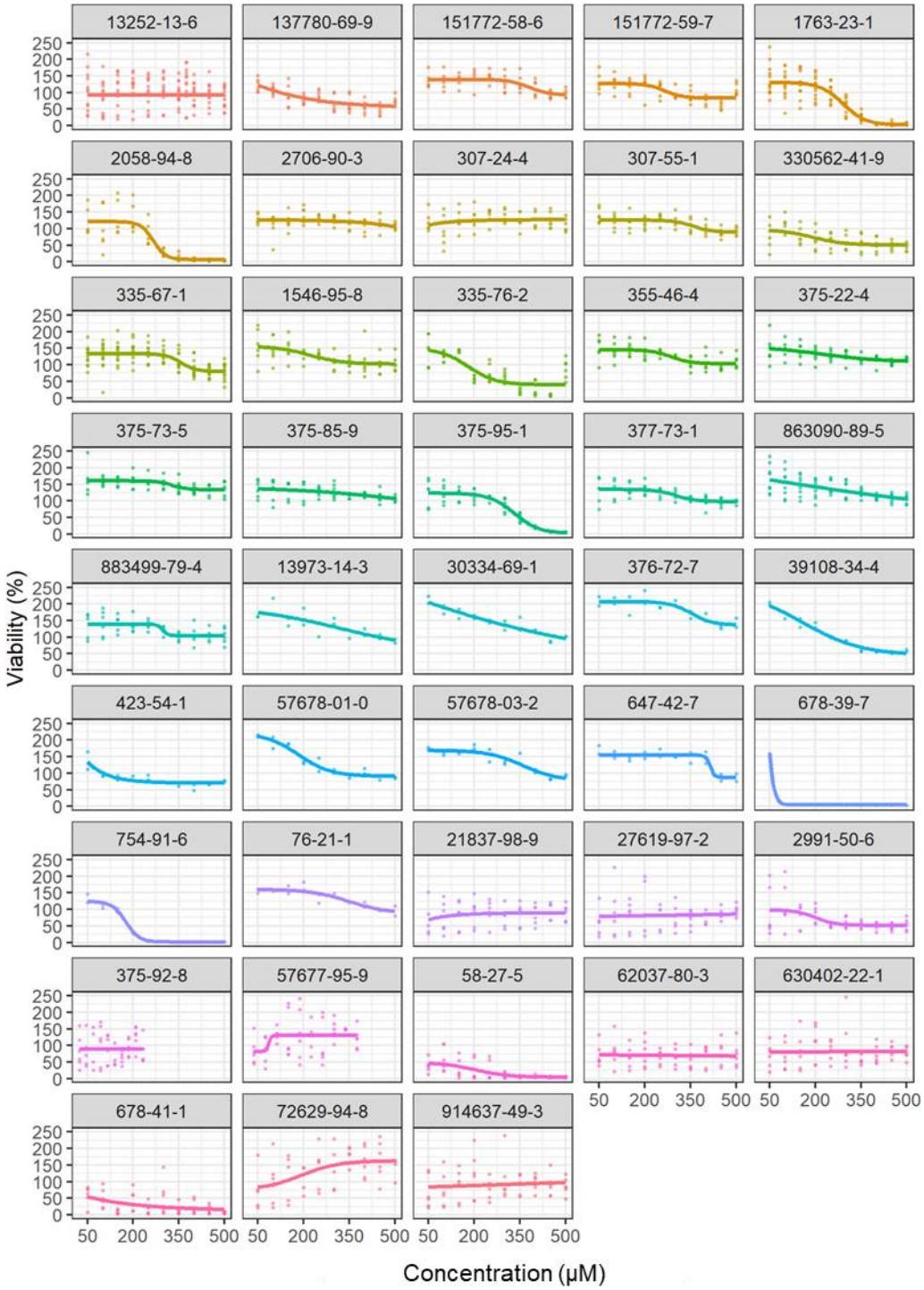

Figure A3-3. Dose-response model fits for cell viability after 24 hours exposure to PFAS. CAS numbers are shown in the grey header of individual plots.

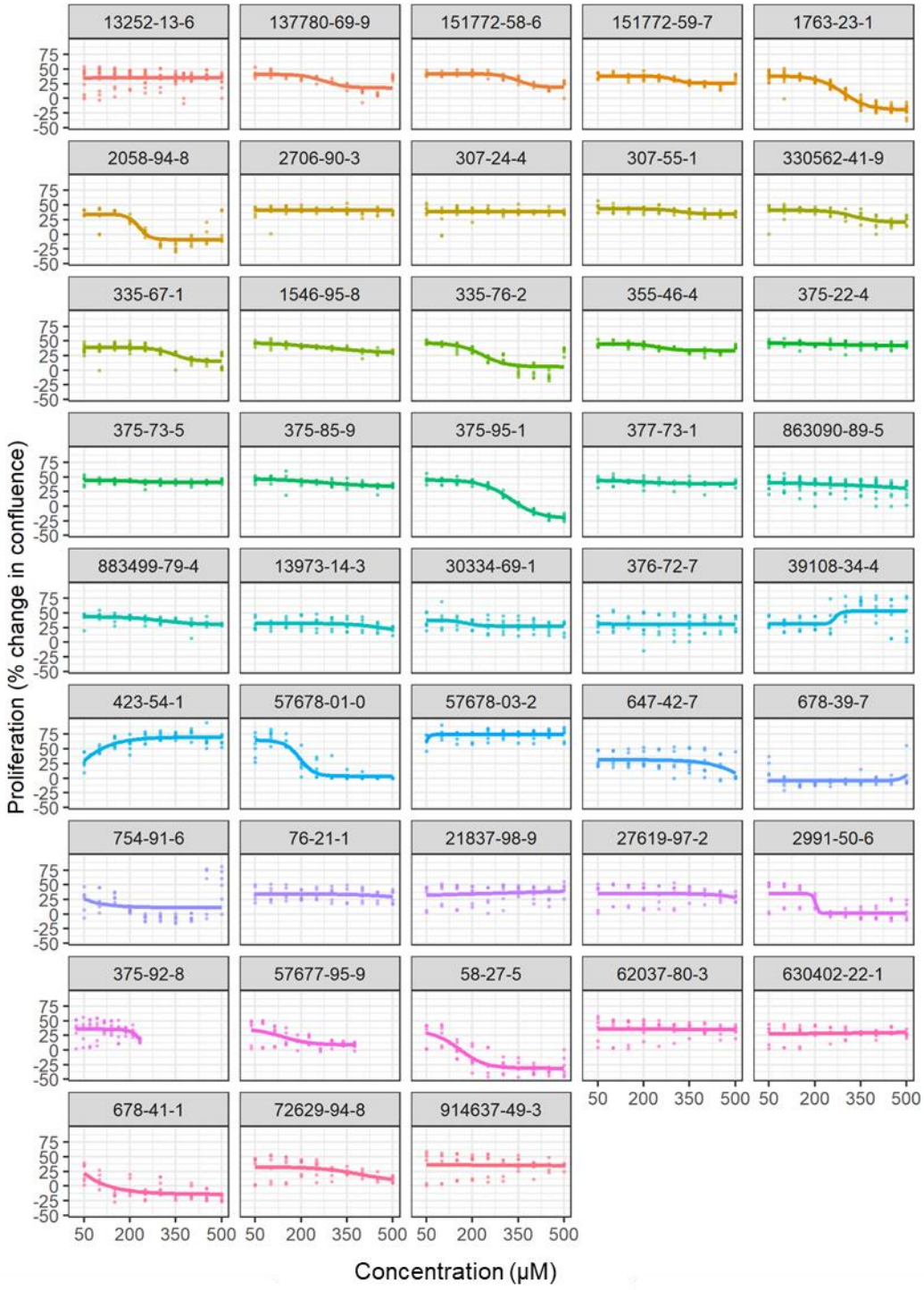

Figure A3-4. Dose-response model fits for cell proliferation after 24 hours exposure to PFAS. CAS numbers are shown in the grey header of individual plots.

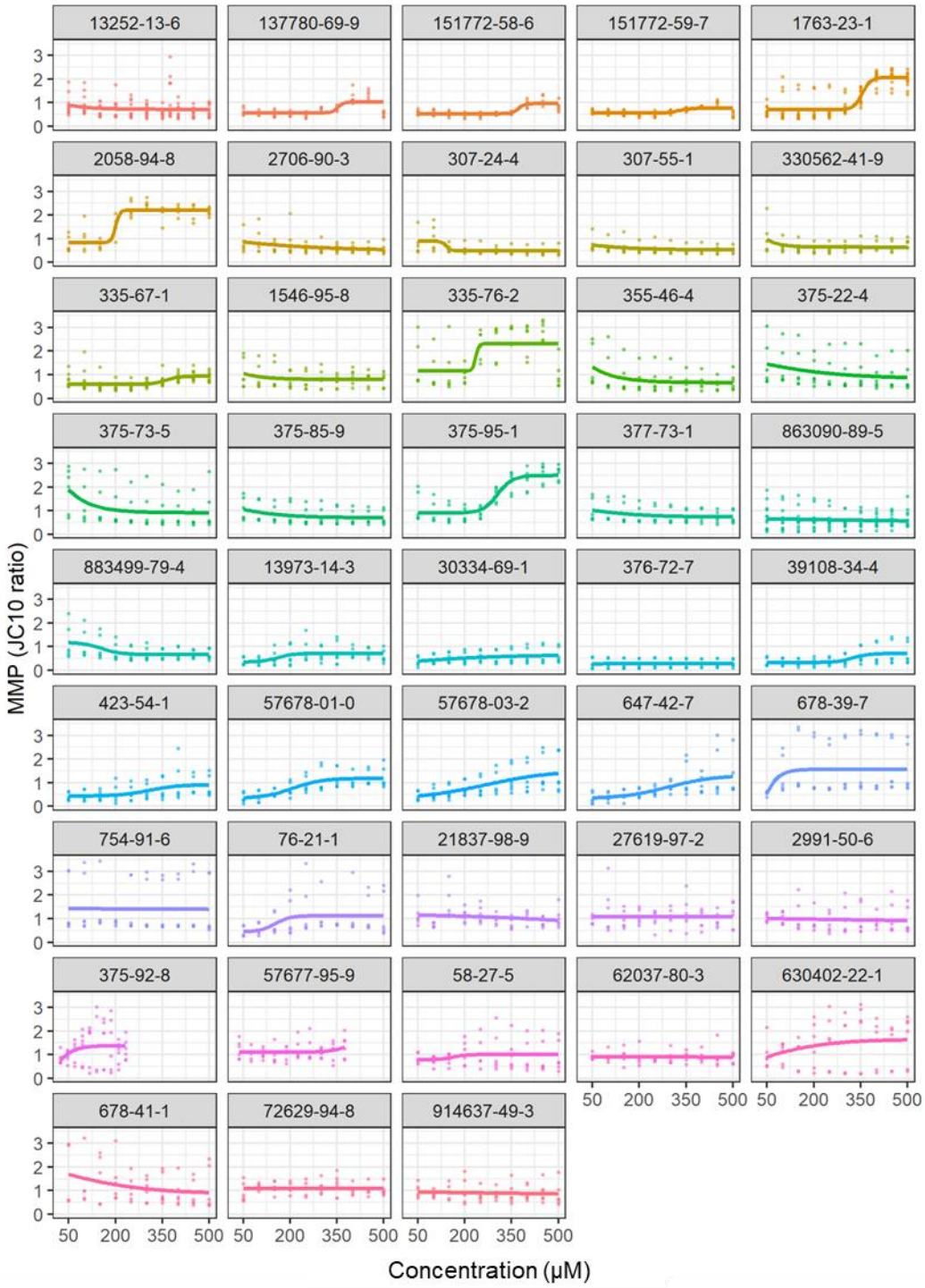

Figure A3-5. Dose-response model fits for cell mitochondrial membrane potential (MMP) after 24 hours exposure to PFAS. CAS numbers are shown in the grey header of individual plots. MMP was determined by the JC-10 ratio assay.

APPENDIX 4: TRANSCRIPTOME-WIDE PERTURBATIONS IN PLACENTAL GENE EXPRESSION INDUCED BYDEVELOPMENTAL EXPOSURE TO PERFLUOROOCTANOIC ACID (PFOA) OR HEXAFLUOROPROPYLENE OXIDE DIMER ACID (HFPO-DA OR GENX) IN CD-1 MICE

A4.1 Introduction

Perfluoroalkyl substances (PFAS) are a diverse class of chemicals used in industry and consumer products to make materials resistant to friction, water, and oil. Exposure is ubiquitous in industrialized populations (Hu et al. 2016; Kato et al. 2011), and previous studies suggest exposure to PFAS is associated with numerous adverse health effects in humans (Steenland et al. 2010). Perfluorooctanoic acid (PFOA) is one of the most well-studied and persistent PFAS (approximate half-life in humans is 2-4 years and 15-17 days in mice) and exposure to PFOA is associated with adverse health outcomes in women including gestational hypertension (Darrow et al. 2013), metabolic changes (Webster et al. 2014), and reduced fetal growth (Washino et al. 2009), among others. The association between maternal exposure to PFOA and reduced fetal growth has been substantiated by systematic reviews of both the human and animal literature (Johnson et al. 2014; Koustas et al. 2014; Lam et al. 2014), however the mechanism through which PFOA exerts its effects on fetal growth are not known.

Although PFOA has been phased out of production in the US, maternal exposure is still of concern due to its persistence in the environment and body. Replacement compounds, such as "GenX", are also of high concern as human exposure has been confirmed, but health risk is uncharacterized. The Cape Fear River in North Carolina is contaminated with GenX (Sun et al. 2016a) and serves as a drinking water source for approximately two million residents. GenX is reported to have a short half-life of hours to days in mice (unknown in humans). As multiple PFAS are suspected to target the placenta, a critical organ that modulates fetal growth, our hypothesis-driven study was designed to examine effects of PFOA (known to reduce birth

weight) and its replacement, GenX, on placental morphology, gene expression, and contribution to fetal weight gain in response to the GenX contamination in North Carolina drinking water systems. Additionally, Blake et al. (2020) found disruptions in placental physiology and function in mice after gestational exposure to GenX.

Therefore, we investigated the molecular mechanisms and pathways underpinning the relationship between prenatal exposure to PFOA or GenX and placental health. The aims of this study were to 1) identify and compare differentially expressed gene pathways in placenta after gestational exposure to PFOA or GenX and 2) determine whether exposure-modified gene pathways predict adverse apical endpoints observed *in vivo*. These data may be highly relevant to on-going health risk evaluations by the US EPA and many states, including North Carolina.

A4.2 Methods

Experimental methods to obtain tissues have been previously published by Blake et al. (2020). Briefly, CD-1 mice were randomly allocated into treatment groups on embryonic day (E) 0.5 and exposed daily via oral gavage to PFOA (0, 1, or 5 mg/kg) or GenX (0, 2, or 10 mg/kg) from embryonic day (E) 1.5 until the time of sacrifice (E11.5 or E17.5, N = 11-13 dams). We selected doses of PFOA known to induce effects on fetal growth based on previous work by our lab (Lau et al. 2006; White et al. 2007) and hypothesized that GenX exposure concentrations two-fold higher (i.e. “equivalent doses”) would similarly induce adverse effects. These doses would model the current two-fold difference in drinking water standards for PFOA/PFOS lifetime health advisory level set by the EPA (70 ppt) and the North Carolina state health goal for GenX (140 ppt). The sacrifice timepoints were selected a priori to examine effects of gestational PFOA/GenX exposure during early gestation and late gestation. The E11.5 early gestation timepoint was selected as it overlaps a critical period of placental development in the mouse where the placenta undergoes vascularization with the uterine wall and chorioallantoic branching

of vessels begins. The latter time was needed to measure effects on fetal growth (parturition is typically within 24 hours). These timepoints also allow for the comparison of immature/developing placenta (E11.5) and mature/developed placenta (E17.5). All experimenters were blinded to treatment groups throughout the study, including at necropsy. On the day of euthanasia, placentas were swiftly collected, weighed, and placed in 4% paraformaldehyde or immediately snap frozen in liquid nitrogen for later nucleic acid extraction. For samples collected at E17.5, a portion of fetal tissue corresponding to each snap frozen placenta was reserved and genotyped for the presence or absence of the sex determining region-Y (SRY) gene. Sex determination was not conducted for placentas collected at E11.5 as the embryo gametes are not yet fully developed and thus not producing sex-specific steroids, thereby mitigating potential sex-specific effects (Munger et al. 2013). By E17.5, fetal gametes are fully developed and previous reports have shown important sex-specific differences in placental gene expression and response to exogenous insults (Reynolds et al. 2015).

RNA was extracted from snap frozen placenta homogenates (N = 4-5 for each treatment group, timepoint, and sex [E17.5 only]) using RNeasy kits following manufacturer's protocols (Qiagen, Hilden, Germany). Briefly, snap frozen placentas were homogenized using a FastPrep-24™ 5G (MP Biomedicals, Valiant Co., Ltd, China) with Buffer RLT (Qiagen, Hilden, Germany) 2mL 2.4mm metal bead homogenization tubes (Thermo Fisher Scientific, Waltham, MA). Resulting purified RNA was subjected to quality control assessments using a NanoDrop™ 2000/2000c Spectrophotometer (Thermo Fisher Scientific, Waltham, MA) and Bioanalyzer High Sensitivity RNA Analysis (Agilent, Santa Clara, CA) to measure RNA quantity, quality, and purity. All RNA samples passed QC (260/280 > 2.0 and RIN > 5.0) and were diluted to a

standard concentration of 100 ng RNA/ 1 µL H_2O. Samples were then processed using the Clariom™ D Assay (Thermo Fisher Scientific, Waltham, MA).

Transcriptomic array data were normalized using the signal space transformation robust multiarray average (SST-RMA) method. Normalized data were analyzed with linear models for microarray data (LIMMA) Bioconductor package (v 3.38.3) implemented in R. Empirical Bayes moderated t-statistics were implemented for differential testing. SST-RMA normalized transcriptome data were imported into Ingenuity Pathway Analysis (IPA) software (Qiagen, Hilden, Germany). Gene expression pathway analysis was conducted using transcripts with a fold-change in expression of $\geq \pm 1.5$ and the Tox Analysis function in IPA. Analyses were repeated using a less stringent fold change cutoff of $\geq \pm 1.2$ to increase confidence in pathways identified using the more stringent cutoff of $\geq \pm 1.5$.

A4.3 Results

Canonical pathway analysis using differentially expressed genes demonstrated a high degree of similarity across chemicals, doses, timepoints, and sexes (Figure A4-1 & Table A4-1). The canonical pathway with significantly altered gene expression across all groups was the liver X receptor/retinoid X receptor (LXR/RXR) activation pathway (Figure A4-1 & Table A4-1). Acute phase response signaling was significantly altered for all groups except 10 mg/kg GenX E17.5 males, and the farnesoid X receptor/retinoid X receptor (FXR/RXR) activation and atherosclerosis signaling pathways were significantly altered for all groups except E11.5 2 mg/kg GenX and E11.5 5 mg/kg PFOA (Figure A4-1 & Table A4-1).

Toxicological pathway analysis was less consistent across dose groups, time points, and sexes (Figure A4-2). The most common significantly altered toxicological pathways were proximal tubule toxicity (all but E17.5 male 1 mg/kg PFOA) and liver damage (all but E17.5 male 10 mg/kg GenX). Other toxicological pathways with relatively consistent significant

alterations in gene expression included inflammation of liver (all but E17.5 male 10 mg/kg GenX and E11.5 5 mg/kg PFOA) and damage of kidney (all but E17.5 male 1 mg/kg PFOA and E11.5 5 mg/kg PFOA). Top canonical pathways share substantial overlap and can be grouped into three main clusters of pathways (Figure A4-3 & Table A4-2). These clusters included several important groups of pathways: inflammation and cholesterol/lipid transport pathways, mitochondrial fatty acid oxidation pathways, and steroid biosynthesis pathways. However, clustering of affected pathways was not as consistent across groups for mitochondrial fatty acid oxidation pathways, and steroid biosynthesis pathways.

A4.4 Discussion

Placental transcriptomic data were evaluated after gestational exposure to PFOA (1 or 5 mg/kg/day) or GenX (2 or 10 mg/kg/day) in order to determine molecular pathways underlying previously observed phenotypic changes. Based on differences in placental histopathology from this study, previously reported in Blake et al. (2020), we hypothesized that underlying gene expression in pathways involved in these pathologies would differ between placentas exposed to PFOA or GenX (Blake et al. 2020). We found a common group of molecular pathways universally altered by exposure, which play a critical role in placental cholesterol and lipid transport as well as inflammation and hemostasis in the placenta. This primarily included LXR/RXR activation, acute phase response signaling, FXR/RXR activation, and atherosclerosis signaling.

These findings are consistent with previous studies examining the effect of maternal undernutrition on the placental transcriptome in rodents. Protein restriction during rat gestation from conception to embryonic day 13 resulted in gene expression changes in pathways related to cholesterol and lipoprotein transport/metabolism and enriched pathways included LXR/RXR activation, FXR/RXR activation, atherosclerosis signaling, and clarthrin-mediated endocytosis

(Daniel et al. 2016). This study similarly identified pathway enrichment of LXR/RXR activation, FXR/RXR activation, and atherosclerosis signaling, suggesting maternal exposure to PFOA or GenX disrupted the placental transcriptome via nutrient sensing, signaling, and transport pathways.

Steroid hormones are required for the establishment and maintenance of pregnancy, and the placenta plays a critical role in their biosynthesis, metabolism, and transport between the maternal and fetal circulation (Woollett 2011). Cholesterol is an indispensable sterol in mammals as a precursor for steroid hormones and bile salts as well as an integral component of the plasma membrane and organelle membranes (Plösch et al. 2007). The developing embryo requires large quantities of cholesterol to accommodate rapid expansion of cellular mass, and disruptions in the appropriate delivery of cholesterol the embryo (whether too much or too little) can have detrimental effects (Plösch et al. 2007). The LXR has been proposed as a critical *in utero* regulator of cholesterol metabolism at the level of uptake and secretion, but not cholesterol synthesis (Plösch et al. 2007). LXR is part of the placental nutrient sensing system, and it serves to sense intracellular cholesterol concentrations (Plösch et al. 2007), and LXR/RXR activation has been identified as a putative mechanism of placental dysfunction (Larkin et al. 2014).

Furthermore, LXR is hypothesized to mediate adaptive responses to hypoxia and oxidative stress in cardiac tissue and the brain (Crisafulli et al. 2010; Sironi et al. 2008), but it is unclear whether the placenta adapts to such stressors via LXR. There is evidence suggesting LXR activation inhibits trophoblast differentiation and invasion (Fournier et al. 2008; Pavan et al. 2004), which is thought to lead to poor placentation and/or pregnancy disorders like preeclampsia (Larkin et al. 2014).

Preeclampsia is a complex pregnancy condition thought to represent a heterogenous syndrome resulting from a constellation of aberrations due to multiple pathogenic pathways (Lin et al. 2005). One hypothesized pathway is hypercoagulation leading to microthrombi in the placental circulation and decreased placental perfusion, resulting in maternal hypertension and proteinuria (Staff et al. 2010). The identification of disruptions in the innate immune response (e.g. IL-12 signaling and production in macrophages, acute phase response signaling) and blood coagulation systems (e.g. atherosclerosis signaling, coagulation system, intrinsic prothrombin activation pathway) are suggestive of immune maladaptation and hemostatic imbalance in response to PFOA or GenX exposure (Li and Huang 2009). Disruptions in the inflammatory response and hemostasis have been implicated in the etiology of adverse pregnancy outcomes including preeclampsia and intrauterine growth restriction (Li and Huang 2009).

Fatty acid uptake, metabolism, and oxidation in the placenta is critical to fuel the energetic demands of the placenta at all stages of development, and disruptions in mitochondrial fatty acid oxidation are associated with preeclampsia and HELLP syndrome (hemolysis, elevated liver enzymes, and low platelets; Shekhawat et al. 2003). Specifically, mitochondrial β-oxidation of fatty acids in the placenta comprises a significant metabolic energy source (Shekhawat et al. 2003). Although these pathways were not as consistently enriched across treatment groups and timepoints, the clustering of enriched pathways in E17.5 female placenta suggest that this may be an important response to GenX exposure at 10 mg/kg.

These data represent an explorative study of placental transcriptome-wide gene expression changes after gestational exposure to PFOA or GenX. Although validation studies are needed, the results suggest PFOA and GenX disrupt placental pathways involved in cholesterol and lipid nutrient transport, innate immune response (specifically inflammation), and hemostasis

(specifically blood coagulation systems). These pathways have translational relevance to human pregnancy conditions previously associated with maternal exposure to PFAS, including preeclampsia and other hypertensive disorders of pregnancy, and suggest a putative toxicological mechanism through which PFAS exert adverse effects on the maternal-placental-fetal unit.

Table A4-1. Summary of top canonical gene expression pathway p-values in placenta altered by exposure to PFOA or GenX.

	LXR/RXR Activation	Acute Phase Response Signaling	FXR/RXR Activation	Atherosclerosis Signaling	Coagulation System
E17.5 Female 10 mg/kg GenX	8.79E-05	0.005	4.41E-06	0.002	>0.05
E17.5 Female 2 mg/kg GenX	8.74E-25	5.69E-23	4.51E-21	3.84E-09	1.35E-10
E17.5 Female 5 mg/kg PFOA	2.98E-11	1.10E-04	2.06E-05	3.45E-04	>0.05
E17.5 Female 1 mg/kg PFOA	1.07E-16	4.68E-13	9.44E-15	5.96E-07	2.11E-08
E17.5 Male 10 mg/kg GenX	0.0033	>0.05	0.04	0.004	>0.05
E17.5 Male 2 mg/kg GenX	3.66E-12	4.90E-10	3.70E-09	1.44E-05	6.08E-07
E17.5 Male 5 mg/kg PFOA	1.86E-14	3.39E-13	2.51E-11	7.68E-09	2.76E-08
E17.5 Male 1 mg/kg PFOA	7.26E-07	1.35E-04	3.48E-04	3.03E-04	0.005
E11.5 10 mg/kg GenX	3.18E-08	5.77E-06	6.81E-04	0.01	>0.05
E11.5 2 mg/kg GenX	4.55E-05	1.22E-04	>0.05	>0.05	>0.05
E11.5 5 mg/kg PFOA	0.02	0.01	>0.05	>0.05	>0.05
E11.5 1 mg/kg PFOA	5.17E-17	6.09E-17	1.44E-16	1.17E-10	5.69E-11

Note: A fold-change cutoff of ≥±1.5 was used in these analyses

Table A4-2. Summary of top toxicological gene expression pathway p-values in placenta altered by exposure to PFOA or GenX.

	Proximal tubular toxicity	Liver Damage	Myocardial infarction	Hepatocellular carcinoma	Cirrhosis of liver
E17.5 Female 10 mg/kg GenX	7.8E-04	0.01	0.02	>0.05	0.01
E17.5 Female 2 mg/kg GenX	5.2E-05	1.6E-05	6.2E-05	1.2E-07	1.2E-05
E17.5 Female 5 mg/kg PFOA	0.002	0.005	>0.05	0.05	0.004
E17.5 Female 1 mg/kg PFOA	2.6E-09	3.9E-04	9.9E-06	5.0E-05	0.003
E17.5 Male 10 mg/kg GenX	1.1E-04	>0.05	>0.05	>0.05	>0.05
E17.5 Male 2 mg/kg GenX	9.8E-09	2.0E-04	1.2E-05	0.003	0.004
E17.5 Male 5 mg/kg PFOA	8.2E-06	8.3E-06	1.9E-04	2.9E-06	2.2E-07
E17.5 Male 1 mg/kg PFOA	>0.05	8.2E-04	>0.05	>0.05	0.03
E11.5 10 mg/kg GenX	1.2E-04	1.6E-09	1.5E-04	0.01	2.7E-04
E11.5 2 mg/kg GenX	0.008	1.3E-05	2.1E-06	0.006	>0.05
E11.5 5 mg/kg PFOA	0.01	5.0E-05	0.02	0.02	>0.05
E11.5 1 mg/kg PFOA	1.2E-10	1.2E-05	2.6E-06	3.1E-06	7.9E-05

Note: A fold-change cutoff of ≥±1.5 was used in these analyses

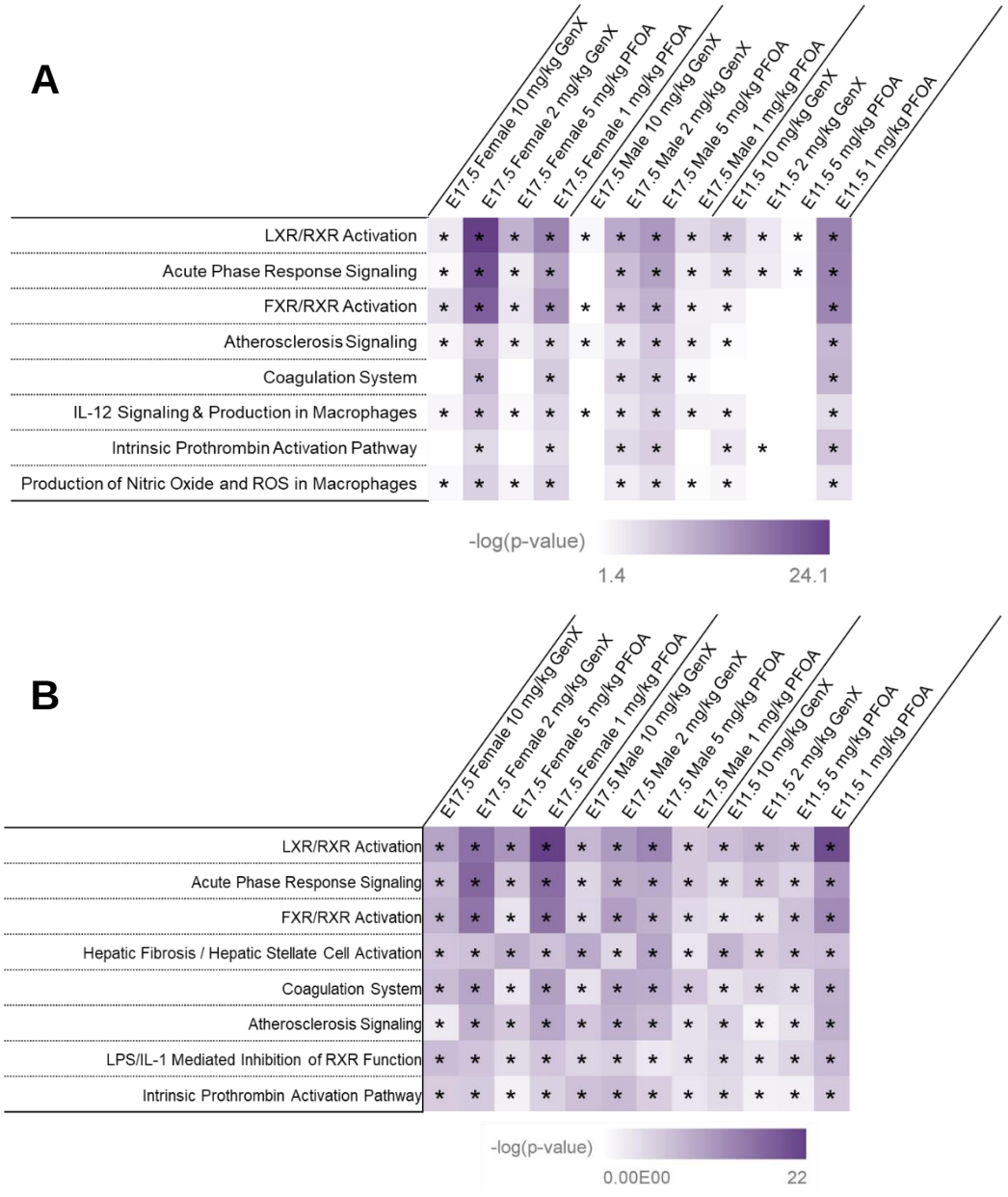

Figure A4-1. Top canonical pathways with differential gene expression in mouse placenta exposed to PFOA or GenX using a ≥±1.5 fold-change cutoff (A) or a ≥±1.2 fold-change cutoff. Heatmap colors correspond to -log(p-values) and asterisks denote p-values < 0.05. Analyses were conducted in Ingenuity Pathway Analysis.

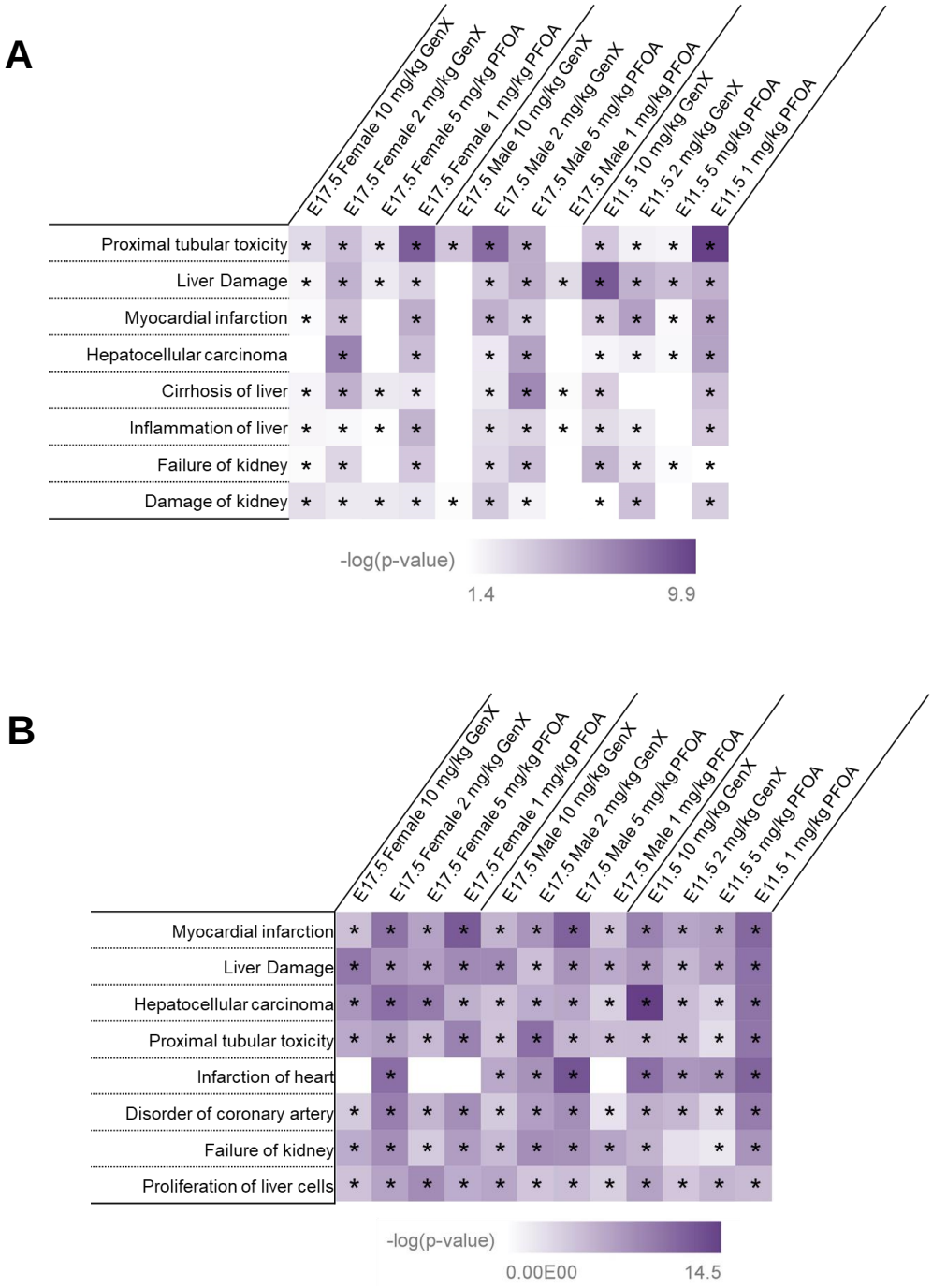

Figure A4-2. Top toxicological pathways with differential gene expression in mouse placenta exposed to PFOA or GenX using a ≥±1.5 fold-change cutoff (A) or a ≥±1.2 fold-change cutoff (B). Heatmap colors correspond to -log(p-values) and asterisks denote p-values < 0.05. Analyses were conducted in Ingenuity Pathway Analysis.

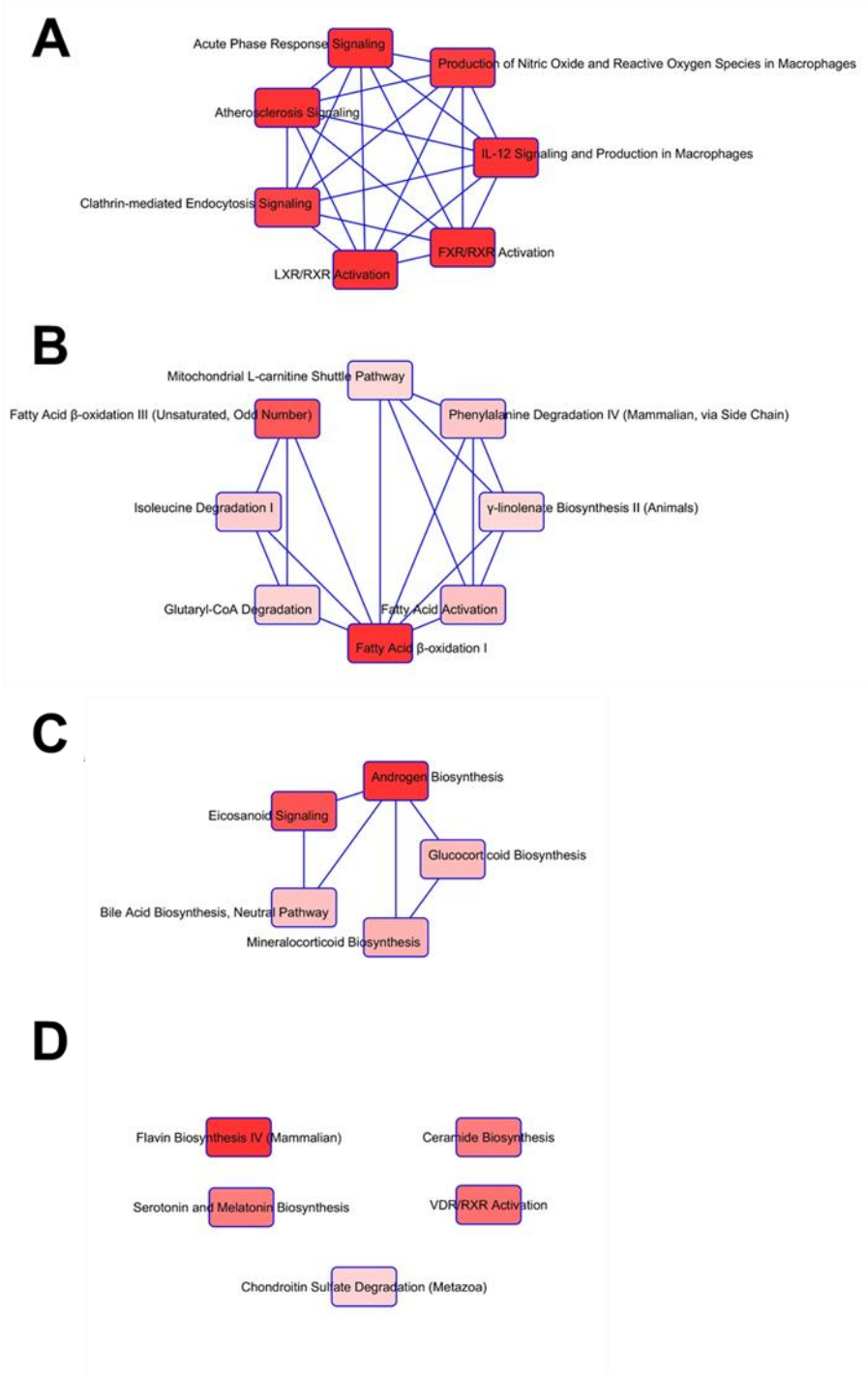

Figure A4-3. Overlap between pathways significantly altered by chemical exposure in placenta. These data are taken from E17.5 Female 10 mg/kg GenX as an illustrative example of overlap between commonly altered pathways. Three different pathway clusters are apparent (A, B, C) as well as "orphan" pathways without any overlap (D). A fold-change cutoff of ≥±1.5 was used in these analyses performed in Ingenuity Pathway Analysis.

REFERENCES

3M 2000. 26-week capsule toxicity study with perfluorooctane sulfonic acid potassium salt (PFOS; T-6295) in cynomolgus monkeys. Administrative Record AR226-0145. URL: https://www.documentcloud.org/documents/4346742-US00004524.html

822-R-16-005 UEJEDN. 2016. Drinking water health advisory for perfluorooctanoic acid (pfoa).

Abbott BD, Wood CR, Watkins AM, Tatum-Gibbs K, Das KP, Lau C. 2012. Effects of perfluorooctanoic acid (pfoa) on expression of peroxisome proliferator-activated receptors (ppar) and nuclear receptor-regulated genes in fetal and postnatal cd-1 mouse tissues. Reproductive Toxicology 33:491-505.

Agency for Toxic Substances and Disease Registry (ATSDR). 2015. Toxicological profile for perfluoroalkyls. Atlanta, GA: Agency for Toxic Substances and Disease Registry, U.S. Department of Health and Human Services, Public Health Service. URL: https://www.atsdr.cdc.gov/toxprofiles/tp.asp?id=1117&tid=237 [acessed July 7, 2019].

Agency for Toxic Substances and Disease Registry (ATSDR). 2017. Perfluoroalkyl and polyfluoroalkyl substances (pfas) in the u.s. population. URL: https://www.atsdr.cdc.gov/pfas/pfas-in-population.html [accessed July 7, 2019].

Agency for Toxic Substances and Disease Registry (ATSDR). 2019. Agency for toxic substances and disease registry: Pfas exposure assessments. Available: https://www.atsdr.cdc.gov/pfas/PFAS-Exposure-Assessments.html [accessed July 7, 2019].

Alexander BH, Olsen GW, Burris JM, Mandel JH, Mandel JS. 2003. Mortality of employees of a perfluorooctanesulphonyl fluoride manufacturing facility. Occupational and Environmental Medicine 60:722-729.

Alexander EK, Pearce EN, Brent GA, Brown RS, Chen H, Dosiou C, et al. 2017. 2017 guidelines of the american thyroid association for the diagnosis and management of thyroid disease during pregnancy and the postpartum. Thyroid 27:315-389.

Apelberg BJ, Witter FR, Herbstman JB, Calafat AM, Halden RU, Needham LL, et al. 2007. Cord serum concentrations of perfluorooctane sulfonate (pfos) and perfluorooctanoate (pfoa) in relation to weight and size at birth. Environmental Health Perspectives 115:1670.

ASDWA. 2020. Per- and polyfluoroalkyl substances (pfas): Per- and polyfluoroalkyl substances (pfas) state drinking water program challenges. Available: https://www.asdwa.org/pfas/ [accessed Jan 01 2020].

Ashley-Martin J, Dodds L, Arbuckle TE, Morisset AS, Fisher M, Bouchard MF, et al. 2016. Maternal and neonatal levels of perfluoroalkyl substances in relation to gestational weight gain. International Journal of Environmental Research Public Health 13:146.

Audette MC, Kingdom JC. 2018. Screening for fetal growth restriction and placental insufficiency. Seminars in Fetal and Neonatal Medicine 23:119-125.

Axmon A, Axelsson J, Jakobsson K, Lindh CH, Jönsson BA. 2014. Time trends between 1987 and 2007 for perfluoroalkyl acids in plasma from swedish women. Chemosphere 102:61-67.

Bach CC, Vested A, Jørgensen KT, Bonde JPE, Henriksen TB, Toft G. 2016. Perfluoroalkyl and polyfluoroalkyl substances and measures of human fertility: A systematic review. Critical Reviews in Toxicology 46:735-755.

Ballesteros V, Costa O, Iñiguez C, Fletcher T, Ballester F, Lopez-Espinosa M-J. 2017. Exposure to perfluoroalkyl substances and thyroid function in pregnant women and children: A systematic review of epidemiologic studies. Environment International 99:15-28.

Bangma J, Szilagyi J, Blake BE, Plazas C, Kepper S, Fenton SE, Fry R. 2020. An assessment of serum-dependent impacts on intracellular accumulation and genomic response of per- and polyfluoroalkyl substances (PFAS) in a placenta trophoblast model. Environmental Pollution. *In review*.

Bao Y, Deng S, Jiang X, Qu Y, He Y, Liu L, et al. 2018. Degradation of pfoa substitute: Genx (hfpo–da ammonium salt): Oxidation with uv/persulfate or reduction with uv/sulfite? Environmental Science & Technology 52:11728-11734.

Barker DJ. 2004. The developmental origins of chronic adult disease. Acta Paediatrica 93:26-33.

Bates D, Mächler M, Bolker B, Walker S. 2014. Fitting linear mixed-effects models using lme4. arXiv preprint arXiv:14065823.

Beesoon S, Martin JW, technology. 2015. Isomer-specific binding affinity of perfluorooctanesulfonate (pfos) and perfluorooctanoate (pfoa) to serum proteins. Environmental Science & Technology 49:5722-5731.

Belet N, Imdat H, Yanık F, Küçüködük Ş. 2003. Thyroid function tests in preterm infants born to preeclamptic mothers with placental insufficiency. Journal of Pediatric Endocrinology & Metabolism 16:1131-1136.

Berg V, Nøst TH, Hansen S, Elverland A, Veyhe A-S, Jorde R, et al. 2015. Assessing the relationship between perfluoroalkyl substances, thyroid hormones and binding proteins in pregnant women; a longitudinal mixed effects approach. Environment International 77:63-69.

Bianco AC, Salvatore D, Gereben B, Berry MJ, Larsen PR. 2002. Biochemistry, cellular and molecular biology, and physiological roles of the iodothyronine selenodeiodinases. Endocrine Reviews 23:38-89.

Bilodeau JF. 2014. Review: Maternal and placental antioxidant response to preeclampsia – impact on vasoactive eicosanoids. Placenta 35:S32-S38.

Bjork JA, Butenhoff JL, Wallace KB. 2011. Multiplicity of nuclear receptor activation by pfoa and pfos in primary human and rodent hepatocytes. Toxicology 288:8-17.

Blake BE, Cope HA, Hall SM, Keys RD, Mahler BW, McCord J, et al. 2020. Evaluation of maternal, embryo, and placental effects in cd-1 mice following gestational exposure to perfluorooctanoic acid (pfoa) or hexafluoropropylene oxide dimer acid (hfpo-da or genx). Environmental Health Perspectives 128:027006.

Blake BE, Pinney SM, Hines EP, Fenton SE, Ferguson KK. 2018. Associations between longitudinal serum perfluoroalkyl substance (pfas) levels and measures of thyroid hormone, kidney function, and body mass index in the fernald community cohort. Environmental Pollution 242:894-904.

Boas M, Main KM, Feldt-Rasmussen U. 2009. Environmental chemicals and thyroid function: An update. Current Opinion in Endocrinology, Diabetes and Obesity 16:385-391.

Brandsma SH, Koekkoek JC, van Velzen MJM, de Boer J. 2018. The pfoa substitute genx detected in the environment near a fluoropolymer manufacturing plant in the netherlands. Chemosphere.220:493-500.

Braun JM, Chen A, Romano ME, Calafat AM, Webster GM, Yolton K, et al. 2016. Prenatal perfluoroalkyl substance exposure and child adiposity at 8 years of age: The home study. Obesity 24:231-237.

Buck RC, Franklin J, Berger U, Conder JM, Cousins IT, De Voogt P, et al. 2011. Perfluoroalkyl and polyfluoroalkyl substances in the environment: Terminology, classification, and origins. Integrated Environmental Assessment and Management 7:513-541.

Buckley JP, Doherty BT, Keil AP, Engel SM. 2017. Statistical approaches for estimating sex-specific effects in endocrine disruptors research. Environmental Health Perspectives 125:067013.

Buhrke T, Kibellus A, Lampen A. 2013. In vitro toxicological characterization of perfluorinated carboxylic acids with different carbon chain lengths. Toxicology Letters 218:97-104.

Burton GJ, Jauniaux EJ. 2004. Placental oxidative stress: From miscarriage to preeclampsia. Journal of the Society for Gynecologic Investigation 11:342-352.

Butenhoff JL, Chang S-C, Olsen GW, Thomford PJ. 2012. Chronic dietary toxicity and carcinogenicity study with potassium perfluorooctanesulfonate in sprague dawley rats. Toxicology 293:1-15.

Butz, GM and Davisson, RL. 2001. Long-term telemetric measurement of cardiovascular parameters in awake mice: a physiological genomics tool. Physiological genomics 5:89-97.

C8 Science Panel. URL:http://www.c8sciencepanel.org/.

Calafat AM, Kuklenyik Z, Reidy JA, Caudill SP, Tully JS, Needham LL. 2007. Serum concentrations of 11 polyfluoroalkyl compounds in the u.S. Population: Data from the national health and nutrition examination survey (nhanes) 1999−2000. Environmental Science & Technology 41:2237-2242.

Centers for Disease Control (CDC). 2013. Fourth national report on human exposure to environmental chemicals. Atlanta (ga): CDC; 2009. URL: https://www.cdc.gov/biomonitoring/pdf/FourthReport_UpdatedTables_Feb2015.pdf

Chaddha V, Viero S, Huppertz B, Kingdom J. Developmental biology of the placenta and the origins of placental insufficiency. In: Proceedings of the Seminars in Fetal and Neonatal Medicine, 2004, Vol. 9 Elsevier, 357-369.

Chan SY, Vasilopoulou E, Kilby MD. 2009. The role of the placenta in thyroid hormone delivery to the fetus. Nature Clinical Practice Endocrinology & Metabolism 5:45-54.

Chang S, Butenhoff JL, Parker GA, Coder PS, Zitzow JD, Krisko RM, et al. 2018. Reproductive and developmental toxicity of potassium perfluorohexanesulfonate in cd-1 mice. Reproductive Toxicology 78:150-168.

Chang SC, Ehresman DJ, Bjork JA, Wallace KB, Parker GA, Stump DG, et al. 2009. Gestational and lactational exposure to potassium perfluorooctanesulfonate (k+pfos) in rats: Toxicokinetics, thyroid hormone status, and related gene expression. Reproductive Toxicology 27:387-399.

Chang, SC, Thibodeaux, JR, Eastvold, ML, Ehresman, DJ, Bjork, JA, Froehlich, JW, Lau, C, Singh, RJ, Wallace, KB, Butenhoff, JL. 2008. Thyroid hormone status and pituitary function in adult rats given oral doses of perfluorooctanesulfonate (PFOS). Toxicology 243:330-339.

Chen F, Yin S, Kelly BC, Liu W. 2017. Chlorinated polyfluoroalkyl ether sulfonic acids in matched maternal, cord, and placenta samples: A study of transplacental transfer. Environmental Science & Technology 51:6387-6394.

Chen F, Yin S, Kelly BC, Liu W. 2017. Isomer-specific transplacental transfer of perfluoroalkyl acids: Results from a survey of paired maternal, cord sera, and placentas. Environmental Science & Technology 51:5756-5763.

Chen MH, Ha EH, Wen TW, Su YN, Lien GW, Chen CY, et al. 2012. Perfluorinated compounds in umbilical cord blood and adverse birth outcomes. PLoS ONE 7:e42474.

Christensen KY, Raymond M, Meiman J. 2019. Perfluoroalkyl substances and metabolic syndrome. International Journal of Hygiene and Environmental Health 222:147-153.

Chung A. 2015. Perfluorooctane sulfonate (pfos) promotes renal injury under diabetic condition in vitro. Hong Kong Journal of Nephrology 17:S3-S4.

Conder JM, Hoke RA, Wolf Wd, Russell MH, Buck RC. 2008. Are pfcas bioaccumulative? A critical review and comparison with regulatory criteria and persistent lipophilic compounds. Environmental Science & Technology 42:995-1003.

Conley JM, Lambright CS, Evans N, Strynar MJ, McCord J, McIntyre BS, et al. 2019. Adverse maternal, fetal, and postnatal effects of hexafluoropropylene oxide dimer acid (genx) from oral gestational exposure in sprague-dawley rats. Environmental Health Perspectives 127:37008.

Consonni D, Straif K, Symons JM, Tomenson JA, van Amelsvoort LG, Sleeuwenhoek A, et al. 2013. Cancer risk among tetrafluoroethylene synthesis and polymerization workers. American Journal of Epidemiology 178:350-358.

Coperchini F, Awwad O, Rotondi M, Santini F, Imbriani M, Chiovato L. 2017. Thyroid disruption by perfluorooctane sulfonate (pfos) and perfluorooctanoate (pfoa). Journal of Endocrinological Investigation 40:105-121.

Coperchini F, Pignatti P, Lacerenza S, Negri S, Sideri R, Testoni C, et al. 2015. Exposure to perfluorinated compounds: In vitro study on thyroid cells. Environmental Science and Pollution Research 22:2287-2294.

Costa G, Sartori S, Consonni D. 2009. Thirty years of medical surveillance in perfluooctanoic acid production workers. Journal of Occupational and Environmental Medicine 51:364-372.

Crisafulli C, Di Paola R, Mazzon E, Paterniti I, Galuppo M, Genovese T, et al. 2010. Liver x receptor agonist treatment reduced splanchnic ischemia and reperfusion injury. Journal of Leukocyte Biology 87:309-321.

Cuffe JSM, Holland O, Salomon C, Rice GE, Perkins AV. 2017. Review: Placental derived biomarkers of pregnancy disorders. Placenta 54:104-110.

Cui L, Zhou Q-f, Liao C-y, Fu J-j, Jiang G-b. 2009. Studies on the toxicological effects of pfoa and pfos on rats using histological observation and chemical analysis. Archives of Environmental Contamination and Toxicology 56:338.

Curran I, Hierlihy SL, Liston V, Pantazopoulos P, Nunnikhoven A, Tittlemier S, et al. 2008. Altered fatty acid homeostasis and related toxicologic sequelae in rats exposed to dietary potassium perfluorooctanesulfonate (pfos). Journal of Toxicology and Environmental Health, Part A 71:1526-1541.

Cushen SC, Goulopoulou S. 2017. New models of pregnancy-associated hypertension. American Journal of Hypertension 30:1053-1062.

D'Amore S, Palasciano G, Moschetta A. 2014. The liver in metabolic syndrome. In: A systems biology approach to study metabolic syndrome, (Orešič M, Vidal-Puig A, eds). Cham:Springer International Publishing, 27-61.

Daniel Z, Swali A, Emes R, Langley-Evans SC. 2016. The effect of maternal undernutrition on the rat placental transcriptome: Protein restriction up-regulates cholesterol transport. Genes & Nutrition 11:27-27.

Darras VM, Hume R, Visser TJ. 1999. Regulation of thyroid hormone metabolism during fetal development. Molecular and Cellular Endocrinology 151:37-47.

Darrow LA, Stein CR, Steenland K. 2013. Serum perfluorooctanoic acid and perfluorooctane sulfonate concentrations in relation to birth outcomes in the mid-ohio valley, 2005-2010. Environmental Health Perspectives 121:1207-1213.

Das KP, Grey BE, Rosen MB, Wood CR, Tatum-Gibbs KR, Zehr RD, et al. 2015. Developmental toxicity of perfluorononanoic acid in mice. Reproductive Toxicology 51:133-144.

Das KP, Wood CR, Lin MT, Starkov AA, Lau C, Wallace KB, et al. 2017. Perfluoroalkyl acids-induced liver steatosis: Effects on genes controlling lipid homeostasis. Toxicology 378:37-52.

de Cock M, de Boer MR, Lamoree M, Legler J, van de Bor M. 2014. Prenatal exposure to endocrine disrupting chemicals in relation to thyroid hormone levels in infants–a dutch prospective cohort study. Environmental Health 13:106.

de Escobar GM, Obregon MJ, del Rey FE. 2004. Maternal thyroid hormones early in pregnancy and fetal brain development. Best Practice & Research: Clinical Endocrinology & Metabolism 18:225-248.

Dhingra R, Winquist A, Darrow LA, Klein M, Steenland K. 2017. A study of reverse causation: Examining the associations of perfluorooctanoic acid serum levels with two outcomes. Environmental Health Perspectives 125:416-421.

Domazet SL, Grøntved A, Timmermann AG, Nielsen F, Jensen TK. 2016. Longitudinal associations of exposure to perfluoroalkylated substances in childhood and adolescence and indicators of adiposity and glucose metabolism 6 and 12 years later: The european youth heart study. Diabetes Care 39:1745-1751.

Domingo JL, Nadal M. 2019. Human exposure to per- and polyfluoroalkyl substances (pfas) through drinking water: A review of the recent scientific literature. Environmental Research 177:108648.

Eckel RH, Grundy SM, Zimmet PZ. 2005. The metabolic syndrome. The Lancet 365:1415-1428.

Edwards TL. 2010a. An oral (gavage) prenatal developmental study of h-28548 in rats. Dupont-18405-1037.

Edwards TL. 2010b. An oral (gavage) reproduction/developmental toxicity screening study of h-28548 in mice. Dupont-18405-1037.

Elcombe CR, Elcombe BM, Foster JR, Chang S-C, Ehresman DJ, Butenhoff JL. 2012. Hepatocellular hypertrophy and cell proliferation in sprague–dawley rats from dietary exposure to potassium perfluorooctanesulfonate results from increased expression of xenosensor nuclear receptors pparα and car/pxr. Toxicology 293:16-29.

Ellinger I, Chatuphonprasert W, Jarukamjorn K. 2018. Physiology and pathophysiology of steroid biosynthesis, transport and metabolism in the human placenta. Frontiers in Pharmacology 9:1027.

Emmett EA, Shofer FS, Zhang H, Freeman D, Desai C, Shaw LM. 2006. Community exposure to perfluorooctanoate: Relationships between serum concentrations and exposure sources. Journal of Occupational and Environmental Medicine/American College of Occupational and Environmental Medicine 48:759.

Environmental Working Group (EWG). 2019. For 50 years, polluters knew pfas chemicals were dangerous but hid risks from public. Environmental Working Group. URL: https://static.ewg.org/reports/2019/pfa-timeline/3M-DuPont-Timeline_sm.pdf

Ervin RB. 2009. Prevalence of metabolic syndrome among adults 20 years of age and over, by sex, age, race and ethnicity, and body mass index: United states, 2003-2006. National Health Statistics Reports:1-7.

European Union (EU). 2017. Commission regulation (eu) 2017/1000 of 13 june 2017 amending annex xvii to regulation (ec) no 1907/2006 of the european parliament and of the council concerning the registration, evaluation, authorisation and restriction of chemicals (reach) as regards perfluorooctanoic acid (pfoa), its salts and pfoa-related substances.

Fei C, McLaughlin JK, Tarone RE, Olsen J. 2007. Perfluorinated chemicals and fetal growth: A study within the danish national birth cohort. Environmental Health Perspectives 115:1677-1682.

Fenton SE, Reiner JL, Nakayama SF, Delinsky AD, Stanko JP, Hines EP, et al. 2009. Analysis of pfoa in dosed cd-1 mice. Part 2. Disposition of pfoa in tissues and fluids from pregnant and lactating mice and their pups. Reproductive Toxicology 27:365-372.

Fernald Community Cohort (FCC) website. URL: https://med.uc.edu/eh/research/projects/fcc.

Filgo AJ, Quist EM, Hoenerhoff MJ, Brix AE, Kissling GE, Fenton SE. 2014. Perfluorooctanoic acid (pfoa)–induced liver lesions in two strains of mice following developmental exposures: Pparα is not required. Toxicologic Pathology 43:558-568.

Fischer, MJ. 2007. Chronic kidney disease and pregnancy: maternal and fetal outcomes. Advances in Chronic Kidney Disease 14:132-145.

Fisher JJ, Bartho LA, Perkins AV, Holland OJ. 2020. Placental mitochondria and reactive oxygen species in the physiology and pathophysiology of pregnancy. Clinical and Experimental Pharmacology & Physiology 47:176-184.

Fisher M, Arbuckle TE, Wade M, Haines DA. 2013. Do perfluoroalkyl substances affect metabolic function and plasma lipids?—analysis of the 2007–2009, canadian health measures survey (chms) cycle 1. Environmental Research 121:95-103.

Fleisch AF, Rifas-Shiman SL, Mora AM, Calafat AM, Ye X, Luttmann-Gibson H, et al. 2017. Early-life exposure to perfluoroalkyl substances and childhood metabolic function. Environmental Health Perspectives 125:481-487.

Fournier T, Handschuh K, Tsatsaris V, Guibourdenche J, Evain-Brion D. 2008. Role of nuclear receptors and their ligands in human trophoblast invasion. Journal of Reproductive Immunology 77:161-170.

Fu J, Gao Y, Cui L, Wang T, Liang Y, Qu G, et al. 2016. Occurrence, temporal trends, and half-lives of perfluoroalkyl acids (pfaas) in occupational workers in china. Scientific Reports 6.

Funderburg AC. 2010. Teflon. American Heritage: Invention and Technology.

Gaballah S, Swank A, Sobus JR, Howey XM, Schmid J, Catron T, McCord J, Hines E, Strynar M, Tal T. 2020. Evaluation of developmental toxicity, developmental neurotoxicity, and tissue dose in zebrafish exposed to GenX and other PFAS. Environmental Health Perspectives, *in press*.

Gagnon R. 2003. Placental insufficiency and its consequences. European Journal of Obstetrics & Gynecology and Reproductive Biology 110:S99-S107.

Gannon SA, Fasano WJ, Mawn MP, Nabb DL, Buck RC, Buxton LW, et al. 2016. Absorption, distribution, metabolism, excretion, and kinetics of 2,3,3,3-tetrafluoro-2-(heptafluoropropoxy)propanoic acid ammonium salt following a single dose in rat, mouse, and cynomolgus monkey. Toxicology 340:1-9.

Gannon SA, Fasano WJ, Mawn MP, Nabb DL, Buck RC, Buxton LW, et al. 2016. Absorption, distribution, metabolism, excretion, and kinetics of 2,3,3,3-tetrafluoro-2-(heptafluoropropoxy)propanoic acid ammonium salt following a single dose in rat, mouse, and cynomolgus monkey. Toxicology 340:1-9.

Gilliland FD, Mandel JS. 1993. Mortality among employees of a perfluorooctanoic acid production plant. Journal of Occupational Medicine 35:950-954.

Gomis MI, Vestergren R, MacLeod M, Mueller JF, Cousins IT. 2017. Historical human exposure to perfluoroalkyl acids in the united states and australia reconstructed from biomonitoring data using population-based pharmacokinetic modelling. Environment International 108:92-102.

Gong X, Yang C, Hong Y, Chung ACK, Cai Z. 2019. Pfoa and pfos promote diabetic renal injury in vitro by impairing the metabolisms of amino acids and purines. Science of The Total Environment 676:72-86.

Gorrochategui E, Pérez-Albaladejo E, Casas J, Lacorte S, Porte C. 2014. Perfluorinated chemicals: Differential toxicity, inhibition of aromatase activity and alteration of cellular lipids in human placental cells. Toxicology and Applied Pharmacology 277:124-130.

Hagenaars A, Vergauwen L, Benoot D, Laukens K, Knapen D. 2013. Mechanistic toxicity study of perfluorooctanoic acid in zebrafish suggests mitochondrial dysfunction to play a key role in pfoa toxicity. Chemosphere 91:844-856.

Han X, Nabb DL, Russell MH, Kennedy GL, Rickard RW. 2011. Renal elimination of perfluorocarboxylates (pfcas). Chemical Research in Toxicology 25:35-46.

Hanssen L, Dudarev AA, Huber S, Odland JØ, Nieboer E, Sandanger TM. 2013. Partition of perfluoroalkyl substances (pfass) in whole blood and plasma, assessed in maternal and umbilical cord samples from inhabitants of arctic russia and uzbekistan. Science of The Total Environment 447:430-437.

Harris MW, Birnbaum LS. 1989. Developmental toxicity of perfluorodecanoic acid in c57bl/6n mice. Fundamental and Applied Toxicology 12:442-448.

Haug LS, Thomsen C, Becher G. 2009. Time trends and the influence of age and gender on serum concentrations of perfluorinated compounds in archived human samples. Environmental Science & Technology 43:2131-2136.

Hayward CE, Lean S, Sibley CP, Jones RL, Wareing M, Greenwood SL, et al. 2016. Placental adaptation: What can we learn from birthweight:Placental weight ratio? Frontiers in Physiology 7.

Hemachandra AH, Klebanoff MA, Duggan AK, Hardy JB, Furth SL. 2006. The association between intrauterine growth restriction in the full-term infant and high blood pressure at age 7 years: Results from the collaborative perinatal project. International Journal of Epidemiology 35:871-877.

Henriksen T, Clausen T. 2002. The fetal origins hypothesis: Placental insufficiency and inheritance versus maternal malnutrition in well-nourished populations. Acta Obstetricia et Gynecologica Scandinavica 81:112-114.

Herrick RL, Buckholz J, Biro FM, Calafat AM, Ye X, Xie C, et al. 2017. Polyfluoroalkyl substance exposure in the mid-ohio river valley, 1991–2012. Environmental Pollution 228:50-60.

Hershman M, Mei R, Kushner T. 2019. Implications of nonalcoholic fatty liver disease on pregnancy and maternal and child outcomes. Gastroenterology & Hepatology 15:221-228.

Heydebreck F, Tang J, Xie Z, Ebinghaus R. 2015. Correction to alternative and legacy perfluoroalkyl substances: Differences between european and chinese river/estuary systems. Environmental Science & Technology 49:14742-14743.

Higgins CP, Luthy RG. 2006. Sorption of perfluorinated surfactants on sediments. Environmental Science & Technology 40:7251-7256.

Hines EP, White SS, Stanko JP, Gibbs-Flournoy EA, Lau C, Fenton SE. 2009. Phenotypic dichotomy following developmental exposure to perfluorooctanoic acid (pfoa) in female cd-1 mice: Low doses induce elevated serum leptin and insulin, and overweight in mid-life. Molecular and Cellular Endocrinology 304:97-105.

Holtcamp W. 2012. Pregnancy-induced hypertension "probably linked" to pfoa contamination. Environmental Health Perspectives 120:a59.

Hopkins ZR, Sun M, DeWitt JC, Knappe DRU. 2018. Recently detected drinking water contaminants: Genx and other per-and polyfluoroalkyl ether acids. Journal of the American Water Works Association 7:13-28.

Hornung RW, Reed LD. 1990. Estimation of average concentration in the presence of nondetectable values. Applied occupational and environmental hygiene 5:46-51.

Hothorn T, Bretz F, Hothorn MT. 2009. The multcomp package.Technical Report 1.0-6, The R Project for Statistical Computing.

Houde M, Martin JW, Letcher RJ, Solomon KR, Muir DC. 2006. Biological monitoring of polyfluoroalkyl substances: A review. Environmental Science & Technology 40:3463-3473.

Hu XC, Andrews DQ, Lindstrom AB, Bruton TA, Schaider LA, Grandjean P, et al. 2016. Detection of poly-and perfluoroalkyl substances (pfass) in us drinking water linked to industrial sites, military fire training areas, and wastewater treatment plants. Environmental Science & Technology Letters 3:344-350.

Huang R, Chen Q, Zhang L, Luo K, Chen L, Zhao S, et al. 2019. Prenatal exposure to perfluoroalkyl and polyfluoroalkyl substances and the risk of hypertensive disorders of pregnancy. Environmental Health 18:5-5.

Huppertz B, Herrler A. 2005. Regulation of proliferation and apoptosis during development of the preimplantation embryo and the placenta. Birth Defects Research Part C: Embryo Today: Reviews 75:249-261.

Hutcheon JA, McNamara H, Platt RW, Benjamin A, Kramer MS. 2012. Placental weight for gestational age and adverse perinatal outcomes. Obstetrics & Gynecology 119:1251-1258.

Interstate Technology and Regulatory Council (ITRC). 2017. Interstate technology and regulatory council: Naming conventions and physical and chemical properties of per-and polyfluoroalkyl substances (pfas). URL: https://pfas-1.itrcweb.org/fact-sheets/

Ishibashi O, Ohkuchi A, Ali MM, Kurashina R, Luo SS, Ishikawa T, et al. 2012. Hydroxysteroid (17-beta) dehydrogenase 1 is dysregulated by mir-210 and mir-518c that are aberrantly expressed in preeclamptic placentas: A novel marker for predicting preeclampsia. Hypertension 59:265-273.

Jaacks LM, Boyd Barr D, Sundaram R, Grewal J, Zhang C, Buck Louis GM. 2016. Pre-pregnancy maternal exposure to persistent organic pollutants and gestational weight gain: A prospective cohort study. International Journal of Environmental Research and Public Health 13:905.

Jain RB, Ducatman A. 2019a. Perfluoroalkyl acids serum concentrations and their relationship to biomarkers of renal failure: Serum and urine albumin, creatinine, and albumin creatinine ratios across the spectrum of glomerular function among us adults. Environmental Research 174:143-151.

Jain RB, Ducatman A. 2019b. Perfluoroalkyl substances follow inverted u-shaped distributions across various stages of glomerular function: Implications for future research. Environmental Research 169:476-482.

Jain RB. 2013. Association between thyroid profile and perfluoroalkyl acids: Data from nhnaes 2007–2008. Environmental Research 126:51-59.

Johnson PI, Sutton P, Atchley DS, Koustas E, Lam J, Sen S, et al. 2014. The navigation guide - evidence-based medicine meets environmental health: Systematic review of human evidence for pfoa effects on fetal growth. Environmental Health Perspectives 122:1028-1039.

Jones PD, Hu W, De Coen W, Newsted JL, Giesy JP. 2003. Binding of perfluorinated fatty acids to serum proteins. Environmental Toxicology and Chemistry 22:2639-2649.

Joshi AA, Vaidya SS, St-Pierre MV, Mikheev AM, Desino KE, Nyandege AN, et al. 2016. Placental abc transporters: Biological impact and pharmaceutical significance. Pharmaceutical Research 33:2847-2878.

Kaboré HA, Duy SV, Munoz G, Méité L, Desrosiers M, Liu J, et al. 2018. Worldwide drinking water occurrence and levels of newly-identified perfluoroalkyl and polyfluoroalkyl substances. The Science of the Total Environment 616:1089-1100.

Kataria A, Trachtman H, Malaga-Dieguez L, Trasande L. 2015. Association between perfluoroalkyl acids and kidney function in a cross-sectional study of adolescents. Environmental Health 14:89.

Kato K, Wong L-Y, Jia LT, Kuklenyik Z, Calafat AM. 2011. Trends in exposure to polyfluoroalkyl chemicals in the us population: 1999− 2008. Environmental Science & Technology 45:8037-8045.

Kennedy GL, Butenhoff JL, Olsen GW, O'Connor JC, Seacat AM, Perkins RG, et al. 2004. The toxicology of perfluorooctanoate. Critical Reviews in Toxicology 34:351-384.

Killough G, Case M, Meyer K, Moore R, Rope S, Schmidt D, et al. 1996. Task 6: Radiation doses and risk to residents from fmpc operations from 1951-1988. Draft report, Radiological Assessments Corporation, Neeses, SC.

Kim H-S, Kwack SJ, Han ES, Kang TS, Kim SH, Han SY. 2011. Induction of apoptosis and cyp4a1 expression in sprague-dawley rats exposed to low doses of perfluorooctane sulfonate. The Journal of Toxicologic Sciences 36:201-210.

Kim MJ, Moon S, Oh B-C, Jung D, Ji K, Choi K, et al. 2018. Association between perfluoroalkyl substances exposure and thyroid function in adults: A meta-analysis. PLOS ONE 13:e0197244.

Kim S, Choi K, Ji K, Seo J, Kho Y, Park J, et al. 2011. Trans-placental transfer of thirteen perfluorinated compounds and relations with fetal thyroid hormones. Environmental Science & Technology 45:7465-7472.

Klaunig JE, Babich MA, Baetcke KP, Cook JC, Corton JC, David RM, et al. 2003. Pparα agonist-induced rodent tumors: Modes of action and human relevance. Critical Reviews in Toxicology 33:655-780.

Klaunig JE, Shinohara M, Iwai H, Chengelis CP, Kirkpatrick JB, Wang Z, et al. 2015. Evaluation of the chronic toxicity and carcinogenicity of perfluorohexanoic acid (pfhxa) in sprague-dawley rats. Toxiocologic Pathology 43:209-220.

Kobayashi S, Azumi K, Goudarzi H, Araki A, Miyashita C, Kobayashi S, et al. 2017. Effects of prenatal perfluoroalkyl acid exposure on cord blood igf2/h19 methylation and ponderal index: The hokkaido study. Journal of Exposure Science & Environmental Epidemiology 27:251-259.

Kolde R, Kolde MR. Package 'pheatmap'. R Package. 2015 Jul 2;1(7).

Koustas E, Lam J, Sutton P, Johnson PI, Atchley DS, Sen S, et al. 2014. The navigation guide - evidence-based medicine meets environmental health: Systematic review of nonhuman evidence for pfoa effects on fetal growth. Environmental Health Perspectives 122:1015-1027.

Kuklenyik Z, Needham LL, Calafat AM. 2005. Measurement of 18 perfluorinated organic acids and amides in human serum using on-line solid-phase extraction. Analytical Chemistry 77:6085-6091.

Kuznetsova A, Brockhoff PB, Christensen RHB. 2017. Lmertest package: Tests in linear mixed effects models. Journal of Statistical Software 82.

Ladics GS, Stadler JC, Makovec GT, Everds NE, Buck RC. 2005. Subchronic toxicity of a fluoroalkylethanol mixture in rats. Drug and Chemical Toxicology 28:135-158.

Laine JE, Ray P, Bodnar W, Cable PH, Boggess K, Offenbacher S, et al. 2015. Placental cadmium levels are associated with increased preeclampsia risk. PloS One 10:e0139341.

Lam J, Koustas E, Sutton P, Johnson PI, Atchley DS, Sen S, et al. 2014. The navigation guide - evidence-based medicine meets environmental health: Integration of animal and human evidence for pfoa effects on fetal growth. Environmental Health Perspectives 122:1040-1051.

Larkin JC, Sears SB, Sadovsky Y. 2014. The influence of ligand-activated lxr on primary human trophoblasts. Placenta 35:919-924.

Lau C, Thibodeaux JR, Hanson RG, Narotsky MG, Rogers JM, Lindstrom AB, et al. 2006. Effects of perfluorooctanoic acid exposure during pregnancy in the mouse. Toxicological Sciences 90:510-518.

Lau C. 2012. Perfluoroalkyl acids: Recent research highlights. Reproductive Toxicology 33:405-409.

Leclerc F, Dubois M-F, Aris A. 2014. Maternal, placental and fetal exposure to bisphenol a in women with and without preeclampsia. Hypertension in Pregnancy 33:341-348.

Leonetti C, Butt CM, Hoffman K, Hammel SC, Miranda ML, Stapleton HM. 2016. Brominated flame retardants in placental tissues: Associations with infant sex and thyroid hormone endpoints. Environmental Health 15:113.

Levey AS, Stevens LA, Schmid CH, Zhang YL, Castro AF, Feldman HI, et al. 2009. A new equation to estimate glomerular filtration rate. Annals of Internal Medicine 150:604-612.

Lewis RC, Johns LE, Meeker JD. 2015. Serum biomarkers of exposure to perfluoroalkyl substances in relation to serum testosterone and measures of thyroid function among adults and adolescents from nhanes 2011–2012. International Journal of Environmental Research and Public Health 12:6098-6114.

Li K, Gao P, Xiang P, Zhang X, Cui X, Ma LQ. 2017. Molecular mechanisms of pfoa-induced toxicity in animals and humans: Implications for health risks. Environment International 99:43-54.

Li M, Huang SJ. 2009. Innate immunity, coagulation and placenta-related adverse pregnancy outcomes. Thrombosis Research 124:656-662.

Lin CY, Chen PC, Lin YC, Lin LY. 2009. Association among serum perfluoroalkyl chemicals, glucose homeostasis, and metabolic syndrome in adolescents and adults. Diabetes Care 32:702-707.

Lin J, August P. 2005. Genetic thrombophilias and preeclampsia: A meta-analysis. Obstetrics & Gynecology 105:182-192.

Lindstrom AB, Strynar MJ, Libelo EL. 2011. Polyfluorinated compounds: Past, present, and future. ACS Publications 45:7954-7961.

Loccisano AE, Longnecker MP, Campbell Jr JL, Andersen ME, Clewell III. 2013. Development of pbpk models for pfoa and pfos for human pregnancy and lactation life stages. Journal of Toxicology and Environmental Health, Part A 76:25-57.

Lou I, Wambaugh JF, Lau C, Hanson RG, Lindstrom AB, Strynar MJ, et al. 2009. Modeling single and repeated dose pharmacokinetics of pfoa in mice. Toxicological Sciences 107:331-341.

Lum KJ, Sundaram R, Barr DB, Louis TA, Buck Louis GM. 2017. Perfluoroalkyl chemicals, menstrual cycle length, and fecundity: Findings from a prospective pregnancy study. Epidemiology 28:90-98.

Lundin JI, Alexander BH, Olsen GW, Church TR. 2009. Ammonium perfluorooctanoate production and occupational mortality. Epidemiology 20:921-928.

Macon MB, Villanueva LR, Tatum-Gibbs K, Zehr RD, Strynar MJ, Stanko JP, et al. 2011. Prenatal perfluorooctanoic acid exposure in cd-1 mice: Low-dose developmental effects and internal dosimetry. Toxicological Sciences 122:134-145.

Maisonet M, Terrell ML, McGeehin MA, Christensen KY, Holmes A, Calafat AM, et al. 2012. Maternal concentrations of polyfluoroalkyl compounds during pregnancy and fetal and postnatal growth in british girls. Environmental Health Perspectives 120:1432-1437.

Maiti K, Sultana Z, Aitken RJ, Morris J, Park F, Andrew B, et al. 2017. Evidence that fetal death is associated with placental aging. American Journal of Obstetrics and Gynecology 217:441.e441-441.e414.

Malik R, Hodgson H. 2002. The relationship between the thyroid gland and the liver. QJM: An International Journal of Medicine 95:559-569.

Mao Q. 2008. Bcrp/abcg2 in the placenta: Expression, function and regulation. Pharmaceutical Research 25:1244-1255.

Marks KJ, Cutler AJ, Jeddy Z, Northstone K, Kato K, Hartman TJ. 2019. Maternal serum concentrations of perfluoroalkyl substances and birth size in british boys. International Journal of Hygiene and Environmental Health 222:889-895.

Marshall SA, Hannan NJ, Jelinic M, Nguyen TPH, Girling JE, Parry LJ. 2017. Animal models of preeclampsia: Translational failings and why. American Journal of Physiology-Regulatory, Integrative and Comparative Physiology 314:R499-R508.

Matilla-Santander N, Valvi D, Lopez-Espinosa MJ, Manzano-Salgado CB, Ballester F, Ibarluzea J, et al. 2017. Exposure to perfluoroalkyl substances and metabolic outcomes in pregnant women: Evidence from the spanish inma birth cohorts. Environmental Health Perspectives 125:117004.

McCord J, Newton S, Strynar M. 2018. Validation of quantitative measurements and semi-quantitative estimates of emerging perfluoroethercarboxylic acids (pfecas) and hexfluoroprolyene oxide acids (hfpoas). Journal of Chromatography A 1551:52-58.

McDowell EM, Trump BF. 1976. Histologic fixatives suitable for diagnostic light and electron microscopy. Archives of Pathology & Laboratory Medicine 100:405-414.

Melzer D, Rice N, Depledge MH, Henley WE, Galloway TS. 2010. Association between serum perfluorooctanoic acid (pfoa) and thyroid disease in the us national health and nutrition examination survey. Environmental Health Perspectives 118:686.

Meng Q, Inoue K, Ritz B, Olsen J, Liew Z. 2018. Prenatal exposure to perfluoroalkyl substances and birth outcomes; an updated analysis from the danish national birth cohort. International Journal of Environmental Research and Public Health 15.

Mistry HD, Kurlak LO, Williams PJ, Ramsay MM, Symonds ME, Broughton Pipkin F. 2010. Differential expression and distribution of placental glutathione peroxidases 1, 3 and 4 in normal and preeclamptic pregnancy. Placenta 31:401-408.

Monroy R, Morrison K, Teo K, Atkinson S, Kubwabo C, Stewart B, et al. 2008. Serum levels of perfluoroalkyl compounds in human maternal and umbilical cord blood samples. Environmental Research 108:56-62.

Morales-Prieto DM, Chaiwangyen W, Ospina-Prieto S, Schneider U, Herrmann J, Gruhn B, et al. 2012. Microrna expression profiles of trophoblastic cells. Placenta 33:725-734.

Munger SC, Natarajan A, Looger LL, Ohler U, Capel B. 2013. Fine time course expression analysis identifies cascades of activation and repression and maps a putative regulator of mammalian sex determination. PLoS Genetics 9:e1003630.

Musso G, Cassader M, Cohney S, De Michieli F, Pinach S, Saba F, et al. 2016. Fatty liver and chronic kidney disease: Novel mechanistic insights and therapeutic opportunities. Diabetes Care 39:1830-1845.

Nader S. Thyroid disease and pregnancy. 2009. Creasy and Resnik's Maternal-Fetal Medicine: Principles and Practice. Sixth edition. Philadelphia, PA: Saunders Elsevier. 995-1014.

National Research Council. 2010. Weight gain during pregnancy: Reexamining the guidelines. National Academies Press. PMID: 20669500.

National Toxicology Program (NTP). 2016. National toxicology program monograph on immunotoxicity associated with exposures to pfoa and pfos. URL: https://ntp.niehs.nih.gov/ntp/ohat/pfoa_pfos/pfoa_pfosmonograph_508.pdf

Nelson JW, Hatch EE, Webster TF. 2010. Exposure to polyfluoroalkyl chemicals and cholesterol, body weight, and insulin resistance in the general us population. Environmental Health Perspectives 118:197.

North Carolina Department of Enviornmental Quality (NC DEQ). 2017. Notice of partial suspension and 60-day notice of intent to partially revoke NPDES permit NC0003573; The Chemours Company, Fayetteville Works. North Carolina Department of Environmental Quality. 16 Nov 2017. URL: https://files.nc.gov/ncdeq/GenX/Letter%20November%2011-16-17.pdf

Nøst TH, Vestergren R, Berg V, Nieboer E, Odland JØ, Sandanger TM. 2014. Repeated measurements of per-and polyfluoroalkyl substances (pfass) from 1979 to 2007 in males from northern norway: Assessing time trends, compound correlations and relations to age/birth cohort. Environment International 67:43-53.

Ohio Environmental Protection Agency (OH EPA). 2019. Ohio per- and polyfluoroalkyl substances (PFAS) action plan for drinking water. Ohio Environmental Protection Agency. Dec 2019. URL: https://epa.ohio.gov/Portals/28/documents/pfas/PFASActionPlan.pdf

Olsen GW, Burlew M, Burris J, Mandel J. 2001. A cross-sectional analysis of serum perfluorooctanesulfonate (pfos) and perfluorooctanoate (pfoa) in relation to clinical chemistry, thyroid hormone, hematology and urinalysis results from male and female employee participants of the 2000 Antwerp and Decatur fluorochemical medical surveillance program, 3M Company. Final Report. October 11, 2001. US EPA Administrative Record, AR-226-1087.

Olsen GW, Burris JM, Ehresman DJ, Froehlich JW, Seacat AM, Butenhoff JL, et al. 2007. Half-life of serum elimination of perfluorooctanesulfonate, perfluorohexanesulfonate, and perfluorooctanoate in retired fluorochemical production workers. Environmental Health Perspectives 115:1298.

Olsen GW, Gilliland FD, Burlew MM, Burris JM, Mandel JS, Mandel JH. 1998. An epidemiologic investigation of reproductive hormones in men with occupational exposure to perfluorooctanoic acid. Journal of Occupational and Environmental Medicine 40:614-622.

Olsen GW, Lange CC, Ellefson ME, Mair DC, Church TR, Goldberg CL, Herron RM, Medhdizadehkashi Z, Nobiletti JB, Rios JA, Reagen WK. 2012. Temporal trends of perfluoroalkyl concentrations in american red cross adult blood donors, 2000–2010. Environmental Science & Technology 46:6330-6338.

Olsen GW, Mair DC, Lange CC, Harrington LM, Church TR, Goldberg CL, Herron RM, Hanna H, Nobiletti JB, Rios JA, Reagen WK. 2017. Per- and polyfluoroalkyl substances (pfas) in american red cross adult blood donors, 2000–2015. Environmental Research 157:87-95.

Olsen GW, Zobel LR. 2007. Assessment of lipid, hepatic, and thyroid parameters with serum perfluorooctanoate (pfoa) concentrations in fluorochemical production workers. International Archives of Occupational and Environmental Health 81:231-246.

Palatini P. 2012. Glomerular hyperfiltration: a marker of early renal damage in pre-diabetes and pre-hypertension, Nephrology Dialysis Transplantation 27(5):1708-1714.

Pan Y, Zhang H, Cui Q, Sheng N, Yeung LW, Sun Y, et al. 2018. Worldwide distribution of novel perfluoroether carboxylic and sulfonic acids in surface water. Environmental Science & Technology 52:7621-7629.

Papadopoulou E, Haug LS, Sabaredzovic A, Eggesbo M, Longnecker MP. 2015. Reliability of perfluoroalkyl substances in plasma of 100 women in two consecutive pregnancies. Environmental Research 140:421-429.

Pavan Lt, Hermouet A, Tsatsaris V, Thérond P, Sawamura T, Evain-Brion Dl, et al. 2004. Lipids from oxidized low-density lipoprotein modulate human trophoblast invasion: Involvement of nuclear liver x receptors. Endocrinology 145:4583-4591.

Pedersen M, Stayner L, Slama R, Sørensen M, Figueras F, Nieuwenhuijsen MJ, et al. 2014. Ambient air pollution and pregnancy-induced hypertensive disorders: A systematic review and meta-analysis. Hypertension 64:494-500.

Pérez F, Nadal M, Navarro-Ortega A, Fàbrega F, Domingo JL, Barceló D, et al. 2013. Accumulation of perfluoroalkyl substances in human tissues. Environment International 59:354-362.

Pijnenborg R, Anthony J, Davey DA, Rees A, Tiltman A, Vercruysse L, van Assche L. 1991. Placental bed spiral arteries in the hypertensive disorders of pregnancy. British Journal of Obsetrics and Gynaecology. 98:648-655.

Pinheiro TV, Brunetto S, Ramos JGL, Bernardi JR, Goldani MZ. 2016. Hypertensive disorders during pregnancy and health outcomes in the offspring: A systematic review. Journal of Developmental Origins of Health and Disease 7:391-407.

Pinney SM, Biro FM, Windham GC, Herrick RL, Yaghjyan L, Calafat AM, et al. 2014. Serum biomarkers of polyfluoroalkyl compound exposure in young girls in greater cincinnati and the san francisco bay area, USA. Environmental Pollution 184:327-334.

Pinney SM, Freyberg RW, Levine GH, Brannen DE, Mark LS, Nasuta JM, et al. 2003. Health effects in community residents near a uranium plant at fernald, ohio, USA. International Journal of Occupational Medicine and Environmental Health 16:139-153.

Pizzurro DM, Seeley M, Kerper LE, Beck BD. 2019. Interspecies differences in perfluoroalkyl substances (pfas) toxicokinetics and application to health-based criteria. Regulatory Toxicology and Pharmacology 106:239-250.

Plösch T, van Straten EME, Kuipers F. 2007. Cholesterol transport by the placenta: Placental liver x receptor activity as a modulator of fetal cholesterol metabolism? Placenta 28:604-610.

Plunkett RJ. 1941. Tetrafluoroethylene polymers. Vol. US223065A. US:Kinetic Chemicals, Inc.

Plunkett RJ. 1986. The history of polytetrafluoroethylene: Discovery and development. In: High performance polymers: Their origin and development. Springer, 261-266.

Pollheimer J, Knöfler M. 2005. Signalling pathways regulating the invasive differentiation of human trophoblasts: A review. Placenta 26:S21-S30.

Porterfield SP. 1994. Vulnerability of the developing brain to thyroid abnormalities: Environmental insults to the thyroid system. Environmental Health Perspectives 102 Suppl 2:125-130.

Preston EV, Webster TF, Oken E, Henn BC, McClean MD, Rifas-Shiman SL, et al. 2018. Maternal plasma per-and polyfluoroalkyl substance concentrations in early pregnancy and maternal and neonatal thyroid function in a prospective birth cohort: Project viva (USA). Environmental Health Perspectives 126:027013.

R Development Core Team. 2011. R: A language and environment for statistical computing. Vienna, Austria. R Foundation for Statistical Computing.

Ramhøj L, Hass U, Boberg J, Scholze M, Christiansen S, Nielsen F, et al. 2018. Perfluorohexane sulfonate (pfhxs) and a mixture of endocrine disrupters reduce thyroxine levels and cause antiandrogenic effects in rats. Toxicological Sciences 163:579-591.

Reiner JL, Nakayama SF, Delinsky AD, Stanko JP, Fenton SE, Lindstrom AB, et al. 2009. Analysis of pfoa in dosed cd1 mice. Part 1. Methods development for the analysis of tissues and fluids from pregnant and lactating mice and their pups. Reproductive Toxicology 27:360-364.

Reynolds CM, Vickers MH, Harrison CJ, Segovia SA, Gray C. 2015. Maternal high fat and/or salt consumption induces sex-specific inflammatory and nutrient transport in the rat placenta. Physiological Reports 3:e12399.

Rhee CM. 2016. The interaction between thyroid and kidney disease: An overview of the evidence. Current Opinions in Endocrinology Diabetes and Obesity 23:407-415.

Rich N. 2016. The lawyer who became dupont's worst nightmare. The New York Times. [Accessed 16 January 2016]. URL: https://www.nytimes.com/2016/01/10/magazine/the-lawyer-who-became-duponts-worst-nightmare.html

Rijs KJ, Bogers RP. 2017. Pfoa and possible health effects: A review of scientific literature. RIVM Report 2017-0086. DOI: 10.21945/RIVM-2017-0086. URL: https://rivm.openrepository.com/handle/10029/620851

Risnes KR, Romundstad PR, Nilsen TI, Eskild A, Vatten LJ. 2009. Placental weight relative to birth weight and long-term cardiovascular mortality: Findings from a cohort of 31,307 men and women. American Journal of Epidemiology 170:622-631.

Ritz C. 2010. Benchmark dose analysis in R. URL: https://cran.r-project.org/web/packages/bmd/bmd.pdf

Roland-Zejly L, Moisan V, St-Pierre I, Bilodeau JF. 2011. Altered placental glutathione peroxidase mrna expression in preeclampsia according to the presence or absence of labor. Placenta 32:161-167.

Rosen MB, Thibodeaux JR, Wood CR, Zehr RD, Schmid JE, Lau CJT. 2007. Gene expression profiling in the lung and liver of pfoa-exposed mouse fetuses. Toxicology 239:15-33.

Rosner R, Warzecha A-K. 2011. Relating neuronal to behavioral performance: Variability of optomotor responses in the blowfly. PloS one 6:e26886.

Rushing BR, Hu Q, Franklin JN, McMahen RL, Dagnino S, Higgins CP, et al. 2017. Evaluation of the immunomodulatory effects of 2, 3, 3, 3-tetrafluoro-2-(heptafluoropropoxy)-propanoate in c57bl/6 mice. Toxicological Sciences 156:179-189.

Russell MH, Nilsson H, Buck RCJC. 2013. Elimination kinetics of perfluorohexanoic acid in humans and comparison with mouse, rat and monkey. Chemosphere 93:2419-2425.

Sagiv SK, Rifas-Shiman SL, Fleisch AF, Webster TF, Calafat AM, Ye X, et al. 2018. Early-pregnancy plasma concentrations of perfluoroalkyl substances and birth outcomes in project viva: Confounded by pregnancy hemodynamics? American Journal of Epidemiology 187:793-802.

Sakr CJ, Kreckmann KH, Green JW, Gillies PJ, Reynolds JL, Leonard RC. 2007. Cross-sectional study of lipids and liver enzymes related to a serum biomarker of exposure (ammonium perfluorooctanoate or apfo) as part of a general health survey in a cohort of occupationally exposed workers. Journal of Occupational and Environmental Medicine 49:1086-1096.

Salafia CM, Charles AK, Maas EM. 2006. Placenta and fetal growth restriction. Clinical Obstetrics and Gynecology 49:236-256.

Sanders JP, Van der Geyten S, Kaptein E, Darras VM, Kuhn ER, Leonard JL, et al. 1997. Characterization of a propylthiouracil-insensitive type i iodothyronine deiodinase. Endocrinology 138:5153-5160.

Savitz DA, Stein CR, Bartell SM, Elston B, Gong J, Shin H-M, et al. 2012. Perfluorooctanoic acid exposure and pregnancy outcome in a highly exposed community. Epidemiology 23:386-392.

Savitz DA, Stein CR, Elston B, Wellenius GA, Bartell SM, Shin HM, et al. 2012b. Relationship of perfluorooctanoic acid exposure to pregnancy outcome based on birth records in the mid-ohio valley. Environmental Health Perspectives 120:1201-1207.

Schindelin J, Arganda-Carreras I, Frise E, Kaynig V, Longair M, Pietzsch T, et al. 2012. Fiji: An open-source platform for biological-image analysis. Nature Methods 9:676.

Seacat AM, Thomford PJ, Hansen KJ, Clemen LA, Eldridge SR, Elcombe CR, et al. 2003. Sub-chronic dietary toxicity of potassium perfluorooctanesulfonate in rats. Toxicology 183:117-131.

Shah S. 2020. Hypertensive disorders in pregnancy. In: Obstetric and gynecologic nephrology: Women's health issues in the patient with kidney disease, (Sachdeva M, Miller I, eds). Cham:Springer International Publishing, 11-23.

Shah-Kulkarni S, Kim B-M, Hong Y-C, Kim HS, Kwon EJ, Park H, et al. 2016. Prenatal exposure to perfluorinated compounds affects thyroid hormone levels in newborn girls. Environment International 94:607-613.

Shankar A, Xiao J, Ducatman A. 2011. Perfluoroalkyl chemicals and chronic kidney disease in us adults. American Journal of Epidemiology 174:893-900.

Shastri S, Sarnak MJ. 2011. Chronic kidney disease: High egfr and mortality: High true gfr or a marker of frailty? Nature Reviews Nephrology 7:680-682.

Shekhawat P, Bennett MJ, Sadovsky Y, Nelson DM, Rakheja D, Strauss AW. 2003. Human placenta metabolizes fatty acids: Implications for fetal fatty acid oxidation disorders and maternal liver diseases. American Journal of Physiology Endocrinology and Metabolism 284:E1098-E1105.

Sills R, Cesta M, Willson C, Brix A, Berrige B. 2019. National toxicology program position statement on informed ("non-blinded") analysis in toxicologic pathology evaluation. Toxicologic Pathology 47:887–890.

Sironi L, Mitro N, Cimino M, Gelosa P, Guerrini U, Tremoli E, et al. 2008. Treatment with lxr agonists after focal cerebral ischemia prevents brain damage. FEBS Letters 582:3396-3400.

Staff AC, Dechend R, Pijnenborg R. 2010. Learning from the placenta: Acute atherosis and vascular remodeling in preeclampsia–novel aspects for atherosclerosis and future cardiovascular health. Hypertension 56:1026-1034.

Stanifer JW, Stapleton HM, Souma T, Wittmer A, Zhao X, Boulware LE. 2018. Perfluorinated chemicals as emerging environmental threats to kidney health: A scoping review. Clinical Journal of American Society of Nephrology 13:1479-1492.

Starling AP, Adgate JL, Hamman RF, Kechris K, Calafat AM, Ye X, et al. 2017. Perfluoroalkyl substances during pregnancy and offspring weight and adiposity at birth: Examining mediation by maternal fasting glucose in the healthy start study. Environmental Health Perspectives 125:067016.

Steenland K, Fletcher T, Savitz DA. 2010. Epidemiologic evidence on the health effects of perfluorooctanoic acid (pfoa). Environmental Health Perspectives 118:1100.

Steenland K, Woskie S. 2012. Cohort mortality study of workers exposed to perfluorooctanoic acid. American Journal of Epidemiology 176:909-917.

Stein CR, Savitz DA, Dougan M. 2009. Serum levels of perfluorooctanoic acid and perfluorooctane sulfonate and pregnancy outcome. American Journal of Epidemiology 170:837-846.

Strynar M, Dagnino S, McMahen R, Liang S, Lindstrom A, Andersen E, et al. 2015. Identification of novel perfluoroalkyl ether carboxylic acids (pfecas) and sulfonic acids (pfesas) in natural waters using accurate mass time-of-flight mass spectrometry (tofms). Environmental Science & Technology 49:11622-11630.

Stubleski J, Salihovic S, Lind PM, Lind L, Dunder L, McCleaf P, et al. 2017. The effect of drinking water contaminated with perfluoroalkyl substances on a 10-year longitudinal trend of plasma levels in an elderly uppsala cohort. Environmental Research 159:95-102.

Suh CH, Cho NK, Lee CK, Lee CH, Kim DH, Kim JH, et al. 2011. Perfluorooctanoic acid-induced inhibition of placental prolactin-family hormone and fetal growth retardation in mice. Molecular and Cellular Endocrinology 337:7-15.

Sun M, Arevalo E, Strynar M, Lindstrom A, Richardson M, Kearns B, et al. 2016. Legacy and emerging perfluoroalkyl substances are important drinking water contaminants in the cape fear river watershed of north carolina. Environmental Science & Technology Letters 3:415-419.

Sun S, Guo H, Wang J, Dai J. 2019. Hepatotoxicity of perfluorooctanoic acid and two emerging alternatives based on a 3d spheroid model. Environmental Pollution 246:955-962.

Sunderland EM, Hu XC, Dassuncao C, Tokranov AK, Wagner CC, Allen JG. 2019. A review of the pathways of human exposure to poly- and perfluoroalkyl substances (pfass) and present understanding of health effects. Journal of Exposure Science & Environmental Epidemiology 29:131-147.

Takahashi M, Ishida S, Hirata-Koizumi M, Ono A, Hirose A. 2014. Repeated dose and reproductive/developmental toxicity of perfluoroundecanoic acid in rats. The Journal of Toxicological Sciences 39:97-108.

Thornburg KL, O'Tierney PF, Louey S. 2010. Review: The placenta is a programming agent for cardiovascular disease. Placenta S54-59.

Tucker DK, Macon MB, Strynar MJ, Dagnino S, Andersen E, Fenton SE. 2015. The mammary gland is a sensitive pubertal target in cd-1 and c57bl/6 mice following perinatal perfluorooctanoic acid (pfoa) exposure. Reproductive Toxicology 54:26-36.

United States Department of Defense (US DOD). 2000. Minutes of the DOD AFFF environmental meeting. URL: https://www.documentcloud.org/documents/4341546-DOC-605.html

United States Environmental Protection Agency (US EPA). 2006. 2010/2015 pfoa stewardship program. URL: https://www.epa.gov/assessing-and-managing-chemicals-under-tsca/fact-sheet-20102015-pfoa-stewardship-program [accessed July 7, 2019].

Vanderlelie J, Venardos K, Clifton V, Gude N, Clarke F, Perkins A. 2005. Increased biological oxidation and reduced anti-oxidant enzyme activity in pre-eclamptic placentae. Placenta 26:53-58.

Villar J, Carroli G, Wojdyla D, Abalos E, Giordano D, Ba'aqeel H, et al. 2006. Preeclampsia, gestational hypertension and intrauterine growth restriction, related or independent conditions? American Journal of Obstetrics and Gynecology 194:921-931.

Wang H, Yang J, Du H, Xu L, Liu S, Yi J, et al. 2018. Perfluoroalkyl substances, glucose homeostasis, and gestational diabetes mellitus in chinese pregnant women: A repeat measurement-based prospective study. Environment International 114:12-20.

Wang H, Zhou L, Gupta A, Vethanayagam RR, Zhang Y, Unadkat JD, et al. 2006. Regulation of bcrp/abcg2 expression by progesterone and 17β-estradiol in human placental bewo cells. American Journal of Physiology-Endocrinology and Metabolism. 290:E798-E807.

Wang Y, Han W, Wang C, Zhou Y, Shi R, Bonefeld-Jørgensen EC, et al. 2019. Efficiency of maternal-fetal transfer of perfluoroalkyl and polyfluoroalkyl substances. Environmental Science and Pollution Research. 26:2691-2698.

Wang Y, Rogan WJ, Chen P-C, Lien G-W, Chen H-Y, Tseng Y-C, et al. 2014. Association between maternal serum perfluoroalkyl substances during pregnancy and maternal and cord thyroid hormones: Taiwan maternal and infant cohort study. Environmental Health Perspectives 122:529-534.

Washington Department of Health (WA DOH). 2020. PFAS. Washington State Department of Health. [Accessed 26 Feb 2020] URL: https://www.doh.wa.gov/CommunityandEnvironment/Contaminants/PFAS

Washino N, Saijo Y, Sasaki S, Kato S, Ban S, Konishi K, et al. 2009. Correlations between prenatal exposure to perfluorinated chemicals and reduced fetal growth. Environmental Health Perspectives 117:660-667.

Watkins AM, Wood CR, Lin MT, Abbott BD. 2015. The effects of perfluorinated chemicals on adipocyte differentiation in vitro. Molecular and Cellular Endocrinology 400:90-101.

Watkins DJ, Josson J, Elston B, Bartell SM, Shin H-M, Vieira VM, et al. 2013. Exposure to perfluoroalkyl acids and markers of kidney function among children and adolescents living near a chemical plant. Environmental Health Perspectives 121:625.

Watson ED, Cross JC. 2005. Development of structures and transport functions in the mouse placenta. Physiology 20:180-193.

Webster GM, Rauch SA, Marie NS, Mattman A, Lanphear BP, Venners SA. 2016. Cross-sectional associations of serum perfluoroalkyl acids and thyroid hormones in us adults: Variation according to tpoab and iodine status (nhanes 2007–2008). Environmental Health Perspectives 124:935.

Webster GM, Venners SA, Mattman A, Martin JW. 2014. Associations between perfluoroalkyl acids (pfass) and maternal thyroid hormones in early pregnancy: A population-based cohort study. Environmental Research 133:338-347.

Weiss JM, Andersson PL, Lamoree MH, Leonards PE, van Leeuwen SP, Hamers T. 2009. Competitive binding of poly-and perfluorinated compounds to the thyroid hormone transport protein transthyretin. Toxicological Sciences 109:206-216.

Wen L-L, Lin C-Y, Chou H-C, Chang C-C, Lo H-Y, Juan S-H. 2016. Perfluorooctanesulfonate mediates renal tubular cell apoptosis through ppargamma inactivation. PLOS ONE 11:e0155190.

Wen L-L, Lin L-Y, Su T-C, Chen P-C, Lin C-Y. 2013. Association between serum perfluorinated chemicals and thyroid function in us adults: The national health and nutrition examination survey 2007–2010. The Journal of Clinical Endocrinology & Metabolism 98:E1456-E1464.

White SS, Calafat AM, Kuklenyik Z, Villanueva L, Zehr RD, Helfant L, et al. 2007. Gestational pfoa exposure of mice is associated with altered mammary gland development in dams and female offspring. Toxicological Sciences 96:133-144.

Wikstrom S, Lin PI, Lindh CH, Shu H, Bornehag CG. 2019. Maternal serum levels of perfluoroalkyl substances in early pregnancy and offspring birth weight. Pediatric Research. 1-8.

Wikström S, Lindh CH, Shu H, Bornehag C-G. 2019. Early pregnancy serum levels of perfluoroalkyl substances and risk of preeclampsia in swedish women. Scientific Reports 9:9179.

Wolak ME, Fairbairn DJ, Paulsen YR. 2012. Guidelines for estimating repeatability. Methods in Ecology and Evolution 3:129-137.

Wolf CJ, Takacs ML, Schmid JE, Lau C, Abbott BD. 2008. Activation of mouse and human peroxisome proliferator− activated receptor alpha by perfluoroalkyl acids of different functional groups and chain lengths. Toxicological Sciences 106:162-171.

Wolf CJ, Zehr RD, Schmid JE, Lau C, Abbott BD. 2010. Developmental effects of perfluorononanoic acid in the mouse are dependent on peroxisome proliferator-activated receptor-alpha. PPAR Research 2010:282896.

Wones R, Pinney SM, Buckholz JM, Deck-Tebbe C, Freyberg R, Pesce A. 2009. Medical monitoring: A beneficial remedy for residents living near an environmental hazard site. Journal of Occupational and Environmental Medicine/American College of Occupational and Environmental Medicine 51:1374.

Wong F, MacLeod M, Mueller JF, Cousins IT. 2014. Enhanced elimination of perfluorooctane sulfonic acid by menstruating women: Evidence from population-based pharmacokinetic modeling. Environmental Science & Technology 48:8807-8814.

Woollett LA. 2011. Review: Transport of maternal cholesterol to the fetal circulation. Placenta 32:S218-S221.

Xu C, Yin S, Liu Y, Chen F, Zhong Z, Li F, et al. 2019. Prenatal exposure to chlorinated polyfluoroalkyl ether sulfonic acids and perfluoroalkyl acids: Potential role of maternal determinants and associations with birth outcomes. Journal of Hazardous Materials 380:120867.

Yahia D, El-Nasser MA, Abedel-Latif M, Tsukuba C, Yoshida M, Sato I, et al. 2010. Effects of perfluorooctanoic acid (pfoa) exposure to pregnant mice on reproduction. The Journal of Toxicological Sciences 35:527-533.

Yang L, Li J, Lai J, Luan H, Cai Z, Wang Y, et al. 2016a. Placental transfer of perfluoroalkyl substances and associations with thyroid hormones: Beijing prenatal exposure study. Scientific Reports 6:21699.

Yang L, Wang Z, Shi Y, Li J, Wang Y, Zhao Y, et al. 2016b. Human placental transfer of perfluoroalkyl acid precursors: Levels and profiles in paired maternal and cord serum. Chemosphere 144:1631-1638.

Yeung LW, Guruge KS, Taniyasu S, Yamashita N, Angus PW, Herath CB. 2013. Profiles of perfluoroalkyl substances in the liver and serum of patients with liver cancer and cirrhosis in australia. Ecotoxicology and Environmental Safety 96:139-146.

Yu WG, Liu W, Jin YH. 2009. Effects of perfluorooctane sulfonate on rat thyroid hormone biosynthesis and metabolism. Environmental Toxicology and Chemistry 28:990-996.

Yu WG, Liu W, Liu L, Jin YH. 2011. Perfluorooctane sulfonate increased hepatic expression of oapt2 and mrp2 in rats. Archives of Toxicology 85:613-621.

Zhang C, Sundaram R, Maisog J, Calafat AM, Barr DB, Louis GM. 2015. A prospective study of prepregnancy serum concentrations of perfluorochemicals and the risk of gestational diabetes. Fertility and Sterility. 103:184-189.

Zhao L, Zhang Y, Zhu L, Ma X, Wang Y, Sun H, et al. 2017. Isomer-specific transplacental efficiencies of perfluoroalkyl substances in human whole blood. Environmental Science & Technology Letters 4:391-398.